Investigation of Multipotent Neural Progenitor Cell to Oligodendrocyte Differentiation including the Transcriptional Activator Protein Pur-alpha by Quantitative Proteomics

Dissertation

zur

Erlangung des Doktorgrades (Dr. rer. nat.)

der

Mathematisch-Naturwissenschaftliche Fakultät

der

Rheinischen Friedrich-Wilhelms-Universität Bonn

vorgelegt von

Carmen Schoor

aus

Koblenz

Bonn, 2018

Angefertigt mit Genehmigung der Mathematisch-Naturwissenschaftlichen Fakultät der Rheinischen Friedrich-Wilhelms-Universit Bonn.

1. Gutachter: Prof. Dr. med. Volkmar Gieselmann

2. Gutachter: Prof. Dr. rer. nat. Gabriele M. König

Tag der Promotion: 29. November 2018

Erscheinungsjahr: 2019

Contents

1. Abstract

Oligodendrocytes are neuroglial cells, localized in the white matter of the central nervous system. They develop from neural stem cells (NSCs), which produce, among others, migrating and proliferating oligodendrocyte precursor cells (OPCs), the progenitors of mature oligodendrocytes. These cells in turn are responsible for the synthesis and maintenance of myelin sheaths of axons to enable fast saltatory signal transduction. Their importance for proper brain function in adults becomes evident in cases where injury-mediated or disease-mediated demyelination of axons occurs, like in multiple sclerosis, where patients display severe neurological deficits. As a consequence, formerly quiescent adult OPCs migrate to the lesion, where they proliferate and differentiate into oligodendrocytes to allow for remyelination of axons. The extent of remyelination however differs between patients and even fails, especially in patients suffering from chronic disorders. On that account, the understanding of molecular mechanisms underlying the differentiation process from neural progenitor cells (NPCs) to oligodendrocytes is crucial to develop appropriate therapeutic strategies.

In the first and second part of this thesis, quantitative large scale mass spectrometry approaches were used to analyze alterations in the oligodendroglial proteome during the in-vitro differentiation of murine neurospheres (mainly consisting of NPCs) to oligospheres (mainly consisting of OPCs) and of rat OPCs to oligodendrocytes. Moreover, cells were analyzed at multiple time points during both processes to allow for the generation of protein kinetics, enabling a much more precised analysis of changes in protein levels compared to approaches with only two time points. In addition, this allows for the determination of early and late upregulated proteins.

Analysis of five biological replicates addressing the differentiation from NPCs to OPCs resulted in the identification of 932 significantly upregulated and 1,184 downregulated proteins. The shift from NPCs to cells committed to the oligodendroglial lineage could be shown by both, immunocytochemistry staining and mass spectrometric analyses. Accordingly, the number of cells expressing the OPC marker chondroitin sulfate proteoglycan NG2 increased and multiple proteins associated with oligodendroglia were upregulated, while proteins involved in the regulation of the mitotic cell cycle were downregulated. Further potential proteins involved in the differentiation process were identified, such as the transcriptional activator protein Pur-alpha (PURA), the transcriptional modulator prohibitin (PHB) and the histone modifier NAD-dependent protein deacetylase sirtuin-2 (SIRT2).

In four biological replicates conducted of the OPC to oligodendrocyte differentiation process 402 significantly upregulated and 485 downregulated proteins were identified. The successful differentiation could be confirmed by increasing numbers of cells expressing the oligodendrocyte marker myelin basic protein (MBP) and by ascending expression levels of proteins synthesizing lipids for myelin sheaths, myelin specific proteins and cytoskeleton organizing proteins. It further became apparent that expression levels of some proteins were altered instantly after exposition to differentiation medium, whereas expression levels of other proteins were altered later on. Early

upregulated or downregulated proteins in the case of differentiation inhibitors, represented potential candidates responsible for the induction of OPC differentiation, including the peptidyl arginine deiminase, type II (PADI2) or the inositol 1,4,5-trisphosphate receptor type 2 (ITPR2).

In the third part, the during NSC to oligodendrocyte differentiation continuously upregulated transcriptional activator protein Pur-alpha was particularly investigated regarding its degradation and interaction partners. It binds to purine-rich parts of single-stranded DNA and RNA, thereby regulating DNA replication and transcription of various genes. Pur-alpha further plays an essential role in synapse formation and development of dendrites, explainable by its function as transporting protein for mRNA to sites of translation in dendrites. Accordingly, Pur-alpha is crucial for proper brain development during early post-natal stages.

In contrary to protein levels, no significant differences in Pur-alpha RNA levels were observed between neurospheres and oligospheres. Several ubiquitination sites were identified within Pur-alpha and the protein possesses multiple anaphase promoting complex/cyclosome (APC/C) recognition sites. We thus assumed that the elevated expression levels of Pur-alpha in oligospheres compared to neurospheres are due to decreased ubqiuitination and thus degradation. Besides, its function as regulator of proliferation regulating proteins, like E2F1, indicated Pur-alpha as a potential factor triggering the differentiation to oligospheres. However, we could not confirm this hypothesis used on *in vitro* degradation and ubiquitination assays. Further conducted interaction partner analyses using two different approaches significantly identified a few subunits of the proteasome complex and one component of the APC/C. Nonetheless, multiple promising Pur-alpha interaction partners were detected, including the La-related protein 1 (LARP1), the polyadenylate-binding protein 1 (PABPC1) or the ATP-dependent RNA helicase DDX3X. Furthermore, the serine protease HTRA1, together with Pur-alpha, might promote the differentiation from NPCs to OPCs. To finally confirm a direct interaction between Pur-alpha and these proteins additional experiments are required.

2. Introduction

2.1. Neural cells

The central nervous system (CNS) is composed of the two structurally and functionally different cell types, neurons and neuroglia. In mammalian cortices both cell types are equally distributed in numbers [Azevedo et al., 2009]. Neuroglial cells can further be classified into four groups, namely astrocytes, microglia, oligodendrocytes and NG2 (chondroitin sulfate proteoglycan NG2) cells [Peters, 2004]. Every cell type undertakes different functions in the CNS while interacting with each other to ensure proper CNS performance. The major function of astrocytes is the trophic and structural support of the neuronal network, while several other roles are postulated such as absorption and release of neurotransmitters or the contribution of astrocytes in the formation of the blood-brain barrier [Araque & Navarrete, 2010]. Microglia are the main immune-competent cells of the CNS, responsible for the removal of cellular debris, arising either from injuries or normal cell turnover [Rubenstein & Rakic, 2013]. Accordingly, one of their main functions is the protection of glial and neuronal cells [Streit, 2002], whereas oligodendrocytes ensure proper function of axons by synthesizing myelin sheaths [Baumann & Pham-Dinh, 2001]. In addition, around 2-9% of total glial cells in the mature CNS consist of the heterogeneous NG2 cell population [Dawson et al., 2003]. So far, their function in the healthy undamaged CNS remains mainly unknown, while they serve as progenitor cells for oligodendrocytes after augmented cell death following injuries or diseases [Levine et al., 2001].

2.1.1. Neural cell development

For a long time, it was assumed that neuronal and glial cells originate from different precursor cell populations, which implies a separation of both cell types early during embryonic development [Kriegstein & Alvarez-Buylla, 2009]. However, based on multiple studies, a new theory has emerged which implies that neurons, oligodendrocytes and astrocytes develop from radial glial (RG) cells in distinct domains of the neural tube, the forebrain and the spinal cord [Anthony et al., 2004] [Malatesta et al., 2000] [Barry & McDermott, 2005].

During embryonic development, neuroepithelial cells, which function as neural stem cells (NSC), first give rise to new daugther cells by symmetric division in the ventricular zone (VZ) of the neural tube [Kriegstein & Alvarez-Buylla, 2009] (Figure 2.1). At embryonic day 10 of murine development, neuroepithelial cells develop into radial glial cells, which function as primary progenitors for neural cells [Kriegstein & Alvarez-Buylla, 2009]. RG cells prominently undergo asymmetric self-renewing divisions to generate neurons, oligodendrocytes and astrocytes. Additionally, a minor population of RG cells reside as NSCs in the VZ during neonatal phase to produce neurons and oligodendrocytes via progenitor cells or convert into adult type B cells, the NSCs of the adult CNS. Upon differentiation, radial glial cells give rise to various neuronal and glial cells, thereby ensuring the cellular and functional diversity of the CNS [Rowitch & Kriegstein, 2010]. This is accomplished by separation of the neuroepithelium into

several but discrete progenitor domains. Accordingly, every region of the neural tube, and at later development stages also regions of the spinal cord and the forebrain, give rise to distinct cell types. Moreover, it was shown that the development of neuronal and glial cells is temporally regulated [Temple, 2001]. Due to their different functions in the CNS, cell types arise from neuroepithelial cells in a distinct chronology, regulated by diverse extrinsic and intrinsic factors (refer to Section 2.2.1). During the early stages of embryonic development mainly neurons are generated, while a switch in the developmental program of radial glial cells occurs at a distinct point, changing from neurogenesis to gliogenesis [Rowitch & Kriegstein, 2010]. The number of oligodendrocytes to be generated depend on the length of axons, so that neurons need to develop first to determine the actual amount of oligodendrocytes to be produced to ensure proper insulation of the entire axon with myelin sheaths [Miller, 2002].

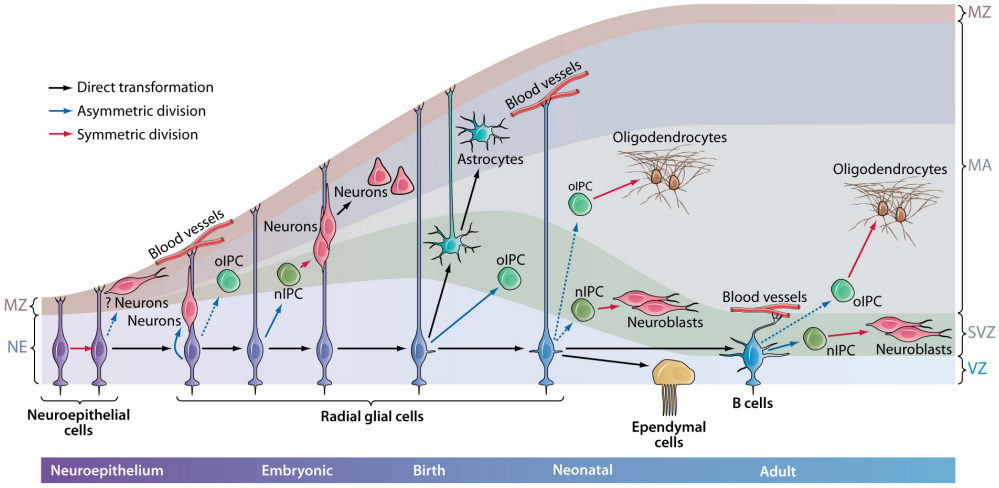

Fig. 2.1.: Neuro-, astro- and oligodendrogenesis during development and in the adult brain. General principle of NSC development and fate. During early development, neuroepithelial cells multiply by symmetric cell division before they convert into RG cells, which in turn generate neurons first. During fetal stage, changes in the cell fate of RG cells occur so that oIPCs and astrocytes are generated. RG cells finally convert into B cells, which function as the NSCs of the adult VZ. The arrow colors depict symmetric and asymmetric division or direct transformation. Solid arrows signify experimental evidence, while dashed arrows signify a hypothesis. MA, mantle; MZ, marginal zone; NE, neuroepithelium; nIPC, neurogenic progenitor cell; NSC, neural stem cell; oIPC, oligodendrocytic progenitor cell; RG, radial glial cell; SVZ, subventricular zone; VZ, ventricular zone. Reproduced from [Kriegstein & Alvarez-Buylla, 2009].

2.2. Oligodendrogenesis

2.2.1. Oligodendrogenesis during early development

The stimulation of radial glial cells to produce OPCs instead of neurons by undergoing asymmetric cell division is regulated by specific signaling molecules. During early embryonic development the morphogen SHH, for example, was shown to strongly affect the behavior and development of neural stem cells [Rowitch & Kriegstein, 2010]. The morphogen promotes oligodendrogenesis by altering the gene expression of several transcription factors, including the oligodendrocyte transcription factor 1 and 2 or the homeobox protein Nkx-2.2 [Tekki-Kessaris et al., 2001]. In

contrary, distinct members of the BMP family were evidenced to inhibit oligodendrogenesis, while they promote neurogenesis and astrogliogenesis [Mabie et al., 1999]. Accordingly, oligodendrogenesis is depending on the timing of neural stem cell exposition to differentiation driving factors and their concentration and simultaneously requires the repression of neurogenesis driving factors. During later stages of embryonic development the generation of oligodendrocyte precursor cells occur independently from SHH [Rowitch & Kriegstein, 2010]. Most likely, the proliferation and generation of oligodendroglial cells is then regulated by the basic fibroblast growth factor (bFGF) [Chandran et al., 2003], but additionally requires the downregulation of BMP family members [Traiffort et al., 2016].

2.2.1.1. OPC migration, proliferation and maturation

In contrary to neurons and astrocytes, the development of oligodendrocytes from radial glial cells occurs in several stages, indicated by the expression of different antigens during oligodendrogenesis (Figure 2.2). In addition, OPCs actively migrate from the VZ to the white matter, the main region where insulation of axons takes place [Baumann & Pham-Dinh, 2001]. While reaching the correct location, OPCs undergo massive proliferation prior to differentiation into mature oligodendrocytes. All steps mentioned underlie distinct regulatory mechanisms.

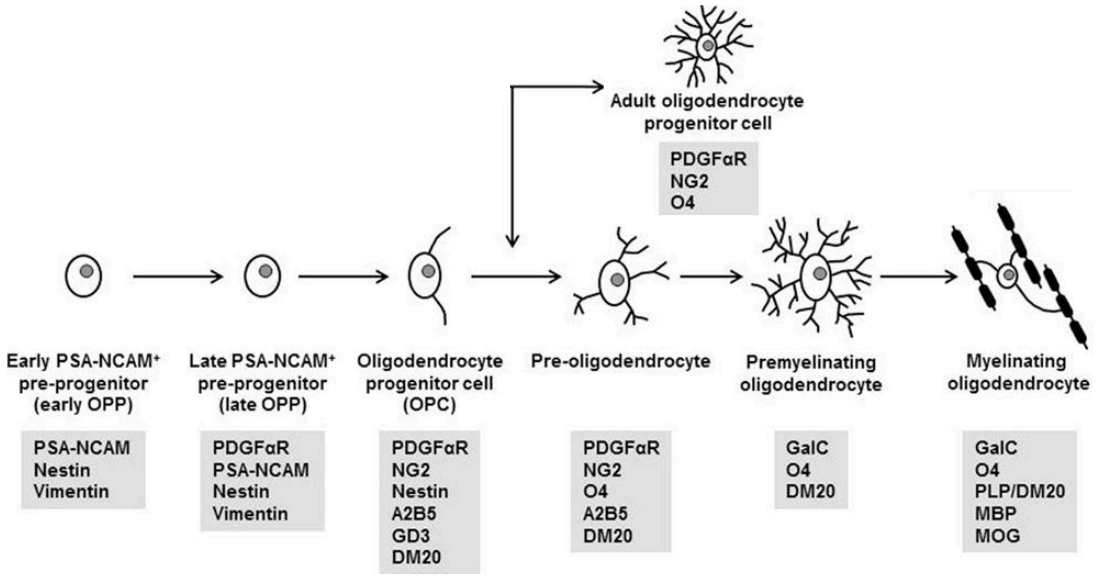

Fig. 2.2.: Oligodendroglial cell lineage. Radial glial cells committed to the oligodendroglial lineage give rise to early oligodendrocyte preprogenitor cells, which then develop into late oligodendrocyte preprogenitors. Thereafter, they differentiate into oligodendrocyte progenitors cells (OPCs) and subsequently migrate into the white and gray matter, where they differentiate into pre-oligodendrocytes or reside in a quiescent state as adult OPCs. Finally, they maturate via premyelinating oligodendrocytes to myelinating oligodendrocytes, thereby expressing multiple specific myelin markers. Adapted from [Schumacher et al., 2012].

OPCs start to migrate away from the VZ to populate the entire CNS at $\sim$ embryonic day 11.5 in mice [Kessaris et al., 2006]. The highly migratory behavior of OPCs was evidenced by transplanting oligodendroglial progenitor cells into the telencephalon of hypomyeli-

nating mice [Warrington et al., 1993]. Several mechanisms are thought to influence migratory processes of OPCs, including migration mediated by secreted molecules or contact-mediated migration [De Castro & Bribián, 2005]. Axonal tracts [Ono et al., 1997], oligodendroglial cell adhesion molecules, like the chondroitin sulfate proteoglycan NG2 [Niehaus et al., 1999], the polysialylated-neural cell adhesion molecule (PSA-NCAM) [Decker et al., 2000] or integrins [Milner et al., 1996] were shown to influence OPC migration by contact-mediated interaction. The secreted mitogens PDGF and bFGF [Milner et al., 1997] and members of the transforming growth factor beta family [Choe et al., 2014] likewise interfere with OPC migration. Reaching their final destination, OPCs start to proliferate due to the local expression of distinct mitogens and chemokines. These factors are mainly consistent with the secreted molecules regulating OPC migration. For instance, the mitogens PDGF [Frost et al., 2009], bFGF [Qian et al., 1997] and neuregulin-1 (NRG1) [Canoll et al., 1996] are known enhancers of OPC proliferation *in vitro*. Growth factor-mediated signaling is usually supported by integrin signaling and both were shown to drive OPC proliferation by altering the transcriptome [O'Meara et al., 2011].

Once a sufficient number of OPCs is generated, a change in the final cell fate program occurs, resulting in cell cycle exit and differentiation to immature and finally myelinating oligodendrocytes (Figure 2.2). In the CNS, the maturation process takes place mainly in early postnatal life and is characterized by radical changes regarding the function and consequently the morphology of OPCs. Accordingly, cytoskeletal reorganization and formation of multiple processes to axons occurs to enable the development and compaction of myelin sheaths [Bauer et al., 2009]. For this purpose, vast amounts of membrane lipids are synthesized and transported to the oligodendroglial extensions, which requires a strongly augmented metabolism in oligodendrocytes [Bauer et al., 2009]. Expectantly, these complex processes require a widespread alteration of the transcriptome. This in turn is accomplished by various extrinsic and intrinsic mechanisms, which most probably act in concert to drive OPC differentiation [Emery, 2010]. It is widely assumed that newly formed or demyelinated axons function as differentiation initiators by releasing glutamate from synaptic-like structures [Etxeberria et al., 2010]. Further extracellular cues originate from neurons, astrocytes and extracellular matrix (ECM) molecules, which in turn activate intracellular signaling cascades within OPCs [Huang et al., 2013]. So far, only few extrinsic factors promoting OPC differentiation are known, including the thyroid hormone triiodothyronine (T_3). Its differentiation promoting function was evidenced *in vitro* [Almazan et al., 1985] and *in vivo* after cuprizone-induced demyelination [Franco et al., 2008].

Although some known extrinsic initiators of differentiation exist, most extracellular signals exhibit inhibitory effects on oligodendrocyte maturation [Emery, 2010]. The mitogen PDGF, for example, triggers OPC migration and proliferation, whereas it prevents further maturation processes [Noble et al., 1988]. This has led to the assumption that the timing of oligodendrocyte differentiation is regulated by PDGF and that differentation is triggered by PDGF withdrawal [Raff et al., 1988] [Tokumoto et al., 1999].

Several indications exist which point towards a downregulation of differentiation inhibitors (derepression model) [Emery, 2010] and an intrinsic nature of differentiation timing (intrinsic cell clock) in OPCs. The remodeling of chromatin by histone deacetylases (HDACs), for example, is assumed to have a strong influence on the differentiation process by interfering with differentiation inhibiting pathways and transcription factors [Shen et al., 2005] [Swiss et al., 2011]. Furthermore, multiple microRNAs act as silencers of gene expression [Zhao et al., 2010]. The

"intrinsic cell clock" hypothesis, in turn, implies a switch in immature OPCs from a proliferative to a differentiated state after exceeding a distinct number of cell divisions by alterations on transcriptional, posttranscriptional and epigenetic levels [Temple & Raff, 1986]. This hypothesis is further consistent with the observation that *in vitro* cultivated OPCs proliferate and differentiate, albeit in the absence of neuronal cells [Dubois-Dalcq et al., 1986].

2.2.2. Oligodendrogenesis in the adult brain

Although most oligodendrocytes are generated during fetal and early perinatal phase, oligodendrogenesis also persists throughout adulthood [Rivers et al., 2008]. So far, studies have evidenced two sources of cells which generate myelinating oligodendrocytes in the adult CNS, namely NSCs and parenchymal NG2 cells. The differentiation of adult NSCs to oligodendrocytes in the SVZ was shown *in vitro* in several studies taking advantage of the neurosphere assay (Section 2.4.1) [Morshead et al., 1994] [Chojnacki & Weiss, 2008]. In addition, the generation of myelinating oligodendrocytes *in vivo* was proven after the occurrence of demyelination and oligodendrocyte cell death [Nait-Oumesmar et al., 1999] [Parent et al., 2006].

2.2.2.1. Oligodendrogenesis in the SVZ and SGZ

In the adult brain, neuro- and gliogenesis takes place in two highly specialized regions, the subventricular zone (SVZ) of the lateral ventricle wall and the subgranular zone (SGZ) of the dentate gyrus [Kazanis et al., 2008]. Adult neurons, astrocytes and oligodendrocytes are generated by three different cell types in the SVZ, namely neural stem cells (type B cells), transit amplifying precursors (type C cells) and neuroblasts (type A cells), whereas in the SGZ mainly neurons develop. Usually, stem cells in the adult brain are maintained in a quiescent state, while some cells undergo self-renewing processes to maintain the stem cell pool or to generate progenitor cells for tissue regeneration purpose [Li & Clevers, 2010] [Fuchs & Chen, 2013].

2.2.2.2. NG2 cells

In the white matter 8-9% and in the gray matter 2-3% of all adult rat cells express the membrane-spanning protein chondroitin sulphate proteoglycan NG2 [Dawson et al., 2003]. This cell population resides ubiquitously in the emerging and the mature CNS and is distinguishable from the other CNS cell types. Accordingly, they are constituted as the fourth major glial cell type in the CNS [Peters, 2004]. NG2 cells proliferate extensively during perinatal phase, while the ability to undergo self-renewing divisions persists throughout life, albeit in a quiescent or moderate way [Rivers et al., 2008]. Those cells arise in the spinal cord and the ventral forebrain during embryonic and perinatal development (Figure 2.2). Initially, progenitor cells do not express NG2, but the transcription factor SOX10 and shortly afterwards PDGFαR. Thereafter, cells start to express NG2 and to migrate outwards into the white and gray matter [Nishiyama et al., 1996].

Due to their multi-extensioned morphology, their ability to generate myelinating oligodendrocytes and the expression of specific oligodendroglial markers, NG2 cells are often also referred to as polydendrocytes and oligodendrocyte precursor cells (OPCs) [Kang et al., 2010] [Dimou et al., 2008]. Although they mainly generate oligodendrocytes, NG2 cells are not completely restricted to the oligodendroglial cell lineage. Several research groups followed the fate of

cells expressing NG2 or PDGFRα by using tamoxifen-inducible NG2-CreER or PDGFRα-CreER mice and revealed that mainly oligodendrocytes, less astrocytes and no neurons were developed [Kang et al., 2010] [Zhu et al., 2011].

So far, NG2 cell functions in the healthy CNS remain unclear. One probable reason for NG2 cell occurrence might be that they function as backup of mature oligodendrocytes to ensure proper function of the adult CNS. This is consistent with the production of oligodendrocytes throughout adulthood to ensure myelin remodeling by either replacing dying oligodendrocytes or intercalating between existing myelin sheaths [Young et al., 2013]. The function of NG2 cells in the pathologic CNS or after brain injuries, is much better known. Within the first 24 hours after demyelination occurred, NG2 cells start to proliferate and differentiate into myelinating oligodendrocytes in affected regions [Watanabe et al., 2002] (Section 2.3.2).

2.3. Oligodendrocytes and myelin sheaths

Oligodendrocytes are the myelinating cells of the CNS and are characterized by the expression of specific myelin proteins, including 2',3'-cyclic-nucleotide 3'-phosphodiesterase (CNP), myelin basic protein (MBP), myelin proteolipid protein (PLP) and myelin-oligodendrocyte glycoprotein (MOG) [Baumann & Pham-Dinh, 2001]. Oligodendrocytes further express specific glycosphingolipids on their cell surface, including galactosylceramides (GalC) and their sulfated derivatives, sulfogalactosylceramides. Myelin forming oligodendrocytes can be found in all white matter regions, whereas the satellite oligodendrocytes prominently reside in gray matter regions and are not associated with myelination [Ludwin, 1979].

Although the support of neurons with neurotrophic factors is one feature of oligodendrocytes, the main function is the insulation of axons by wrapping them with myelin sheaths [Baumann & Pham-Dinh, 2001]. For this purpose, oligodendrocytes possess various extensions, while every extension is connected to one myelin segment, called internode. Adjacent internodes are separated from each other to form parts exposed to the extracellular milieu, the nodes of Ranvier, to provide fast saltatory conduction. In order to achieve this, myelin sheaths posess a specific composition with high proportion of lipids ($\sim$ 70%) and low proportion of myelin proteins ($\sim$ 30%). Remarkably, compared to other membranes, myelin sheaths consist of large amounts of galactolipids, especially cerebrosides and sulfatides [Morell et al., 1999]. Further lipid components are cholesterol and phospholipids.

2.3.1. Demyelinating diseases

The destruction or the loss of myelin sheaths covering axons is called demyelination. This process usually follows the cell death of oligodendrocytes, which in turn is caused by various mechanisms. Demyelination is characterized by a progressive process, due to the onward loss of oligodendrocytes. This is caused by the induction of multiple secondary injury mechanisms within the lesion, such as oxidative stress, glutamate mediated excitotoxicity or the secretion of pro-inflammatory cytokines [Alizadeh et al., 2015]. In general, oligodendrocytes are more vulnerable to cell death compared to other CNS cells. This is a result of both, the complex development oligodendrocytes underlie during maturation (Figure 2.2) and their specific intrinsic functions by exhibiting a unique cell metabolism [El Waly et al., 2014]. Indeed, oligodendrocytes feature high metabolic rates to produce and maintain great amounts of lipid membranes.

Moreover, oligodendrocytes produce less antioxidative substances, such as glutathione, to counteract occurring oxidative stress [Thorburne & Juurlink, 1996].

Disorders causing demyelination are classified into primary and secondary demyelinating diseases, depending on whether oligodendrocytes are directly or indirectly (following on axonal loss) affected [Franklin & Ffrench-Constant, 2008]. The causes are of inflammatoric, genetic, ischemic or viral nature. The most common primary demyelinating disease is multiple sclerosis (MS), an autoimmune neurodegenerative disorder [Hauser & Oksenberg, 2006]. The disease is characterized by a recurring progressive neurodegeneration of the CNS. So far, the loss of axons due to demyelination has been considered as a major reason for neurological deficiencies of MS patients [Bjartmar & Trapp, 2001] [Trapp et al., 1999]. Several hereditary disorders with demyelinating character are known, including the group of leukodystrophies [Kohlschütter & Eichler, 2011]. These diseases directly affect the synthesis and the maintenance of myelin sheaths and are characterized by the degeneration of the white matter and subsequent activation of the CNS immune system [Potter & Petryniak, 2016]. This pertains, for example, to a rarely occurring disease, called metachromatic leukodystrophy (MLD), which is caused by a mutation in the arylsulphatase A (ASA) enzyme. The accumulation of the ASA substrate sulphatide in the degrading compartments of oligodendrocytes, the lysosomes, subsequently leads to a progressive demyelination of the CNS [Gieselmann et al., 2003] [Ramakrishnan et al., 2007]. Furthermore, oligodendrocytes seem to be negatively affected in several other neurodegenerative diseases, such as Alzheimer and Huntington disease. At least, a decrease of the myelin proteins MBP, PLP and CNP is observed in Alzheimer disease [Roher et al., 2002].

2.3.2. Remyelination process

Remyelination is the process where axons are ensheathed with newly synthesized myelin by oligodendrocytes, leading to functional recovery of demyelinated axons. Despite an extensive cell death of most oligodendrocytes within the lesion, spontaneous remyelination can be observed in the injured region [Patrikios et al., 2006]. So far, parenchymal NG2 cells and SVZ derived NSCs (Section 2.2.2) seem to contribute to the remylination process by migrating in the direction of the lesion, following proliferation and differentiation to myelinating oligodendrocytes [El Waly et al., 2014]. The contribution of SVZ-derived progenitors to remyelination could be shown by a four-fold increase of type B cells *in vivo* following on a demyelination [Menn et al., 2006]. Termed cells were observed to migrate to the injured region where they differentiated into proliferating OPCs and mature oligodendrocytes.

Nonetheless, mainly OPCs localized in the neighborhood of developing lesions contribute to the remyelination process [Watanabe et al., 2002]. Those cells were observed to proliferate and generate myelinating oligodendrocytes in neurodegenerated regions of amyotropic lateral sclerosis (ALS) mice *in vivo* [Kang et al., 2010]. In addition, Zawadzka and co-workers have proven the contribution of OPCs to remyelination by confirming the generation of myelinating oligodendrocytes after toxin-induced demylination by following the fate of PDGFRα-CreERT2 mice [Zawadzka et al., 2010]. On the contrary, mature oligodendrocytes do not contribute, since for one thing oligodendrocytes are affected from tissue necrosis and for another thing, they lost their proliferating character upon differentiation [Keirstead & Blakemore, 1997].

2.4. Investigation of oligodendroglial cell development *in vitro*

In order to achieve proper characterization of the oligodendrocyte development process on protein level, *in vivo* studies are recommended. However, the CNS is a complex tissue, making it quite challenging to separate different CNS cell types from each other to determine specifically the oligodendroglial proteome. Although single cell types can be isolated by either laser microdissection or fluorescence-activated cell sorting (FACS) of labeled cells in brain tissue, the isolation resulted in the loss of connected and most remote cellular structures due to highly branched and interconnected cells [Sharma et al., 2015]. Besides, many potential factors involved in the NSCs to oligodendrocyte maturation process were identified using *in vitro* studies [Chaerkady et al., 2011] [Dugas et al., 2006] [Dumont et al., 2007a].

Established *in vitro* systems do not completely reflect the *in vivo* development process from NSCs to oligodendrocytes, but come close to them. Indeed, it could be shown that under cell culture conditions developing oligodendroglial cells express markers specific for different oligodendroglial development stages in the same chronology as cells *in vivo* do [Reynolds & Wilkin, 1988] [Dubois-Dalcq et al., 1986]. Nonetheless, a co-cultivation of oligodendroglial cells with neurons has been shown to enhance myelin gene expression [Macklin et al., 1986]. Nevertheless, despite the absence of axons, oligodendrocytes are able to produce a myelin like membrane *in vitro* [Sarlieve et al., 1983] [Szuchet et al., 1986]. These findings suggest that the maturation program of oligodendroglial cells is intrinsic to the lineage [Temple & Raff, 1986].

2.4.1. *In vitro* system - the neurosphere assay

The neurosphere assay was established by Reynolds and Weiss [Reynolds & Weiss, 1992]. They discovered that cells isolated from the striatum of adult mice proliferate and express the stem cell marker nestin. After growth factor withdrawal, cells developed into all major cell types of the CNS *in vitro* [Reynolds & Weiss, 1996], indicating that these cell aggregates, termed neurospheres, consist of mainly multipotent neural stem cells.

Since then, the cultivation system is used for multiple reasons, including investigations on stem cell properties, neurogenesis and remyelination studies [Jensen & Parmar, 2006]. However, in the last few years a more critical view on the neurosphere assay has developed, especially in the case of stem cell studies [Gil-Perotín et al., 2013]. Multiple factors, such as the number of cell passages, seeding density and culture conditions can influence the composition and the property of neurospheres [Jensen & Parmar, 2006]. Based on the isolation of cortical cells from early postnatal mice (P0 - P1), stem cells, progenitor cells and differentiated cells can be simultaneously present within a sphere [Bez et al., 2003]. The application of the assay to generate large amounts of neurospheres is reasonable, albeit mentioned variabilities have to be considered.

The formation of oligodendroglial progenitors, so called oligospheres, from rat neurospheres using serum-free B104 neuroblastoma conditioned medium and the growth factor EGF was first shown by Zhang and co-workers [Zhang et al., 1998]. Since then, the neurosphere assay has been widely used to generate large amounts of oligospheres [Chen et al., 2007] [Hu et al., 2004]. Upon using B104 neuroblastoma conditioned medium, between 50% [Gibney & McDermott, 2007] and more than 90% [Zhang et al., 1999] [Broughton et al., 2007] of rat cells were positively detected for an oligodendroglial marker. Although fewer studies were performed using murine cells, 89% of total cells were shown to develop into oligodendrocyte progenitor cells [Chen et al., 2007]. Chen

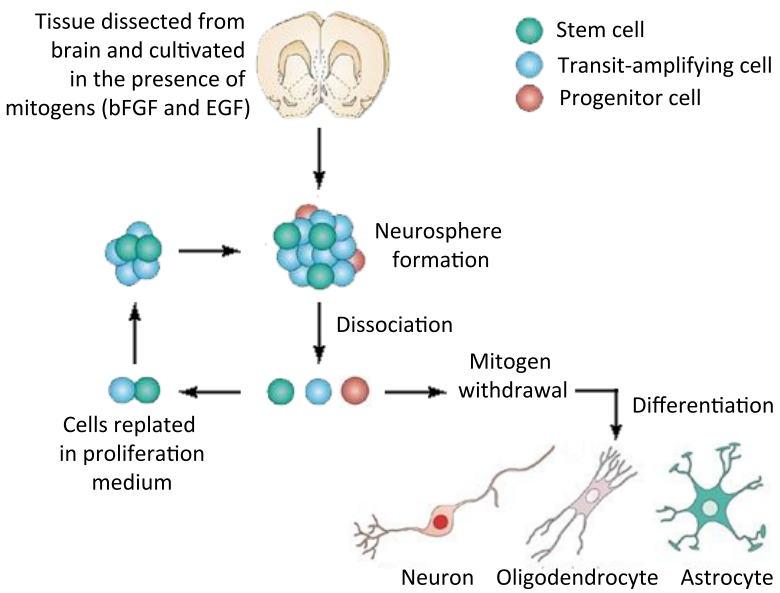

Fig. 2.3.: Neurosphere assay. Cells derived from murine brain tissue are cultivated in proliferation medium containing the epidermal growth factor (EGF) and basic fibroblast growth factor (bFGF). Neurosphere formation results from cell division of neural stem cells or cell aggregation due to highly motile cells, while dissociation lead to the formation of new neurospheres. They consist in varying ratios of stem cells, transit amplifying cells and progenitor cells. Upon exchange to differentiation medium, cells start to develop into either neurons, astrocytes or oligodendrocytes. Adapted from [Chojnacki & Weiss, 2008].

and co-workers further modified the existing differentiation method. The proliferation medium is gradually exchanged for differentiation medium, consisting of B104 neuroblastoma conditioned medium and the growth factors EGF and bFGF, over two weeks. So far, the mitogens PDGF and bFGF within the B104 neuroblastoma conditioned medium seem to be mainly responsible for the development of neurospheres to oligospheres through the activation of distinct signaling cascades, including ERK, PI3K and p38 MAPK [Hu et al., 2012a].

Another possibility to generate OPCs was published by Pedraza and co-workers, who cultivated neurospheres in EGF-containing medium and differentiated them into adherent OPCs on substrate-coated dishes upon changing to PDGF- and bFGF-containing differentiation medium [Pedraza et al., 2008]. Using this protocol, up to 97% of total cells expressed the oligodendroglial marker protein PLP. In contrary to the protocol established by Chen and co-workers, cells are immediately exposed to high concentrations of differentiation inducing factors. Consequently, neurospheres differentiated into oligospheres within four days instead of two weeks.

2.4.2. *In vitro* system for the isolation of rat oligodendrocyte precursor cells

For the isolation of oligodendrocyte precusor cells from mixed glial cell cultures multiple methods are known, including FACS of cell surface labeled antigens or expressed fluorescent proteins [Sugiarto et al., 2011], magnetic activated cell sorting (MACS) [Dincman et al., 2012], immunopanning [Dugas et al., 2006] and the application of shearing forces, the so called shaking method [Szuchet & Yim, 1984] [Chen et al., 2007]. Thereby, OPCs can be separated from other glial cells due to varying adherent properties upon shaking.

In the last decades, transgenic and knockout studies are gaining more and more in importance regarding the study of biological systems and cellular pathways [Picciotto & Wickman, 1998] [Doyle et al., 2012]. Since more techniques for genetic manipulation are available for mice, most of these investigations are performed using mice rather than rats [Ellenbroek & Youn, 2016]. However, genetic manipulation techniques are meanwhile also available for rats and likewise important, the mapping of the complete rat genome was resolved [Gibbs et al., 2004]. Nevertheless, mouse OPCs are more difficult to isolate compared to their rat equivalents, since they used to differentiate *in vitro* in mixed glial cultures and are hard to separate from astroglial cells. Moreover, mouse cells and rat cells do not express the same cell surface proteins, which complicate the isolation via FACS or immunopanning [Duchala et al., 1995] [Fanarraga et al., 1995]. Mouse cells, for example, do not express the cell surface antigen A2B5, which is commonly expressed on oligodendrocyte progenitor cells. The usage of primary cells from wild-type animals only allows for the application of the FACS technique if antigens were labeled prior to measurement. In addition, vast amounts of antibodies are necessary for FACS and immunopanning approaches, which also require long sample processing times. The separation of OPCs from glial cells via MACS on the other side is more expensive than the traditional shaking method.

2.5. Mass spectrometry application

2.5.1. Overview

Within the last decades, the application of mass spectrometry (MS) has become more and more the method of choice to adress questions in the field of proteomics [Kim et al., 2014] [Aebersold & Mann, 2016]. Technical and methodical development providing improved instruments and protocols mainly contributed to its increasing success. Mass spectrometry is used for plenty of applications, including protein identification and quantification analyses, characterizations of post-translational modifications (PTMs), protein interaction studies and imaging mass spectrometry (IMS) [Guerrera & Kleiner, 2005] [Maher et al., 2015]. Moreover, using MS, whole proteomes [Sharma et al., 2015] or phosphoproteoms [Hutchinson et al., 2012] were resolved.

Two main proteomics approaches, the "bottom-up" and the "top-down" technique are in use [Zhang et al., 2013]. Thereby, "top-down" proteomics is used to measure intact proteins or large fragments, while "bottom-up" shotgun proteomics analyzes peptides. A common "bottom-up" workflow includes the cleavage of proteins into a complex mixture of peptides using sequence-specific enzymes, such as trypsin, prior to separation by reversed phase liquid chromatography and subjection to tandem mass spectrometry (MS/MS) [Aebersold & Mann, 2016]. After electrospray ionization of peptides, precursor ions of certain mass-to-charge ratios (m/z) are selected and fragmented into product ions by, for example, collision-induced dissociation (CID), higher-energy collisional dissociation (HCD) or electron transfer dissociation (ETD). The obtained MS/MS spectra are used for the identification of peptides by comparing acquired data to information provided by databases [Aebersold & Mann, 2016] [Wehr, 2006]. Which technique to use depends on multiple factors, such as the complexity or the number of samples. In addition, the kind of application plays an important role. PTM analyses, for example, are more reasonable to approach using the "top-down" technique, since all PTMs available on one protein can be analyzed together using this strategy [Zhang & Ge, 2011]. The characterization and location of

PTMs in turn is reasonable to better understand the biological function of a protein or to determine degradation processes [Sze et al., 2002] [Toby et al., 2016]. Moreover, the higher sequence coverage of "top-down" proteomics minimizes the ambiguities of peptide to protein assignment and enables the determination of distinct protein isoforms [Tran et al., 2011]. However, there are still diverse challenges to cope with, including the fragmentation of large intact protein ions or the separation of proteins from a complex protein mixture [Gregorich & Ge, 2014]. The easier separation, ionization and fragmentation of peptides in turn is the main advantage of the "bottom-up" approach [Zhang et al., 2013]. Accordingly, the "bottom-up" approach features better sensitivity, higher proteome coverage and throughput and is currently more widely used for large-scale proteomic analyses [Catherman et al., 2014]. In addition, especially for "bottom-up" approaches, labeling techniques enabling the quantification of the same protein within up to ten samples (TMT10plex) were developed and protocols improved to analyze and compare protein abundances between different samples [Ong & Mann, 2005] [Rauniyar & Yates III, 2014].

2.5.2. Quantitative large-scale mass spectrometry analysis

2.5.2.1. Overview

The identification of factors involved in the oligodendroglial development process can either be performed on mRNA level or on protein level. Two state of the art techniques are currently primarily used to identify and quantify either mRNA or protein expression levels in complex biological samples, namely high-throughput next generation sequencing [Davey et al., 2011] for transcripts and quantitative mass spectrometry (MS) for proteins [Ong & Mann, 2005]. Recent investigations on the correlation between mRNA and protein levels suggest a poor correlation between both. This difference might be the result of post-transcriptional and translational processes or protein turnover [Vogel & Marcotte, 2012] [Maier et al., 2009]. Accordingly, in order to measure the final and importantly effective protein level, large-scale proteomics studies using mass spectrometry are favored over next generation sequencing approaches.

By using appropriate quantification techniques, MS approaches allow for the identification and quantification of thousands of proteins within one sample in a single experiment. Still, the complexity of samples is a challenging factor, especially if low abundant proteins have to be quantified in shotgun proteomic samples with a high dynamic range (ratio of the largest to smallest detected signal) [Yates et al., 2009]. Thus, peptides belonging to a protein have to be identified in multiple samples among other peptides and further on they have to be quantified in the presence of chemical noise and other peptides [Mallick & Kuster, 2010]. Thus, to approach this problem, a lot of work has been done in the last years regarding sample preparation protocols and instruments, leading to continuous improvements in sample detection and quantification.

To achieve increased proteome coverage, sample complexity is reduced by applying separation techniques prior to measurement. Commonly, two fractionation methods are successively applied (two-dimensional fractionation) [Dowell et al., 2008]. Multiple fractionation techniques are available on both, protein and peptide level, in the first dimension, while the second dimension usually consists of reversed phase liquid chromatography, such as the nano ultra reversed phase high performance liquid chromatography [Motoyama et al., 2006]. Feasible fractionation techniques include isoelectric focusing (IE) [Giorgianni et al., 2003], ion exchange chromatography (IEC) [Opiteck et al., 1997] or one dimensional gel electrophoresis (SDS-Page) [Lee et al., 2003].

2.5.2.2. Quantitative proteomics

Two main strategies are available for the quantitation of protein levels in digested samples, the relative and the absolute quantitation of proteins. For both methods either label-free or stable isotope-labeling approaches are applicable [Yates et al., 2009] [Nikolov et al., 2012]. Most frequently the relative quantitation approach is used, namely to compare protein levels between either differentially treated samples, wild-type and knock-out samples or specimens of a time course. Using stable isotopic labeling approaches in shotgun proteomics, samples are differentially labeled with tags containing heavy and light isotopic atoms, which are distinguishable by a mass shift in the MS/MS spectra for most labeling strategies [Chahrour et al., 2015]. Those labels are introduced on protein or peptide level by either chemical, metabolic or enzymatic reaction [Bantscheff et al., 2007]. A widely used metabolic labeling technique is the stable isotope labeling by amino acids in cell culture (SILAC), while the isobaric tags for relative and absolute quantitation (iTRAQ) technique, the tandem mass tag (TMT) system (Figure 2.4) and the stable isotope dimethyl labeling technique represent common chemical labeling techniques. Which technique to use depends on the issue investigated. For the comparison of more than three samples usually TMT or iTRAQ techniques are applied [Wiese et al., 2007] [Thompson et al., 2003]. Due to the isobaric character, same peptides, although differentially labeled, elute simultaneously from the column and are thus coincidentally measured [Nikolov et al., 2012]. After fragmentation of precursor ions, the reporter ions in the low mass range are used to determine relative peptide abundances, while the higher mass range of MS/MS spectra serves for peptide identification [Rauniyar & Yates III, 2014]. If only up to three different samples have to be compared and appropriate cell culture conditions are given, SILAC is the technique of choice [Ong et al., 2002]. To compare three conditions, cells are differentially treated with natural light amino acids and amino acids labeled with medium and heavy isotopes. Using the proteolytic enzyme trypsin, which cuts after carboxyl-termini of lysine and arginine residues, peptide abundances can be compared due to a mass shift of medium (4 Da) and heavy lysine (8 Da) and medium (6 Da) and heavy (10 Da) arginine to light residues [Olsen et al., 2004] [Geiger et al., 2011]. The advantage of the this approach is that it introduces lowest variability into the system compared to other stable isotope labeling systems, since sample combination follows immediately on cell harvest [Bantscheff et al., 2007]. This is especially noticeable in samples which require extensive sample processing prior to measurement. Dimethyl labeling provides a cheap method for isotopic labeling of samples ranging from sub-micrograms to milligrams [Boersema et al., 2009].

Absolute quantitation approaches use chemically synthesized stable isotope-labeled peptides, which are spiked into the appropriate sample at a known concentration to achieve specific and accurate targeted quantification [Kettenbach et al., 2011]. Targeted proteomics set a focus on a limited number of targets so that liquid chromatography properties and instrument tunings can be specifically optimzed for these targets to allow highest sensitivity and highest throughput [Colangelo et al., 2013]. As targeted quantification methods, selected reaction monitoring (SRM) or multiple reaction monitoring (MRM) are used [Lange et al., 2008]. Thereby, the precursor ion as well as one or more unique fragment ions are analyzed over time to increase accurate quantification. Since synthetic and endogenous peptides are eluted and measured simultaneously, peak areas can be compared with each other and the absolute concentration of the endogenous peptide can be back-calculated [Nikolov et al., 2012]. Therefore, a calibration curve using different amounts of the spiked-in peptide has to be conducted in advance [Keshishian et al., 2007].

Using the label-free strategy, applicable to relative and absolute quantification, every sample is individually measured and results are subsequently compared to each other [Zhu et al., 2009]. Quantitation is thereby achieved by either measuring changes in ion intensities, such as peptide peak areas or heights, or by spectral counting of identified proteins. During the last years, label-free shotgun approaches are growing in popularity, since faster, cleaner and simpler results are possible therewith [Old et al., 2005] [Wang et al., 2006].

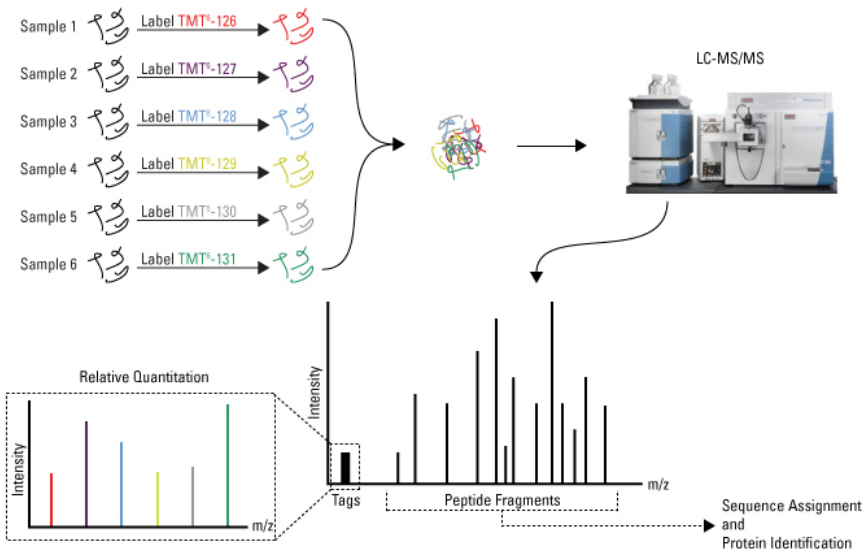

Fig. 2.4.: TMTsixplex labeling. Simplified workflow using TMTsixplex reagents for relative quantification and identification of proteins in up to six samples. All reagents possess same molecular masses, so that identical peptides from different samples co-elute from the liquid chromatography column and are simultaneously ionized and fragmented in the mass spectrometer. Reporter ions can be observed in the low mass region (m/z 126 - 131) of the MS/MS spectrum and are used to compare peptide intensities between samples, while the peptide fragment ions allow for protein identification. Reproduced from the Thermo Fisher homepage (Appendix D: URL1).

2.5.2.3. Large-scale studies of oligodendrocyte precursor cells and oligodendrocytes

So far, only few studies were performed to investigate the molecular mechanisms underlying the differentiation process from neural stem cells (NSCs) to oligodendrocyte precursor cells (OPCs) respectively from OPCs to oligodendrocytes. Additionally, most investigations performed have been focusing on mRNA expression instead of protein expression, such as the analysis of NSC to OPC differentiation by cDNA microarray by Hu and co-workers [Hu et al., 2004]. Only one other study so far exists comparing the protein levels during human embryonic stem cell (ESC) to OPC differentiation by quantitative proteomics [Chaerkady et al., 2011]. Thereby, Chaerkady and co-workers quantified 3,145 unique proteins at a 1% false discovery rate (FDR) cutoff and identified a wide range of differentially expressed proteins in ESCs and OPCs. Some more analyses were conducted focusing on the differentiation from OPCs to oligodendrocytes or simply on oligodendrocytes. Besides several microarray based analyses [Broughton et al., 2007] [Dugas et al., 2006] and analyses on the oligodendrocyte proteome

[Sharma et al., 2015] [Dumont et al., 2007b] [Colello et al., 2002], one study approached the differentiation from OPCs to oligodendrocytes on protein level by identifying target proteins of the mammalian target of rapamycin (mTOR) pathway [Tyler et al., 2011]. The mTOR complex was previously shown to be essential for oligodendrocyte development, especially for the transition from the late oligodendrocyte progenitor cell to the immature oligodendrocyte. Although multiple factors involved in the differentiation process from NSCs to oligodendrocytes were identified in the past, the capability of quantitative large-scale proteomics analyses by mass spectrometry to detect new factors and regulatory networks has been so far rarely used.

2.5.2.4. Identification of interaction partners

Numerous biological processes, such as gene expression, proliferation, metabolism or apoptosis are supported by proteins, which mainly collaborate with other proteins instead of exerting their functions independently [Phizicky & Fields, 1995]. Interactions between proteins are either transient or stable. Stable interactions commonly exist between proteins within multisubunit complexes, such as hemoglobin, while transient protein interactions commonly occur during signal transduction or hormone-receptor binding processes [Nooren & Thornton, 2003] [Valdar & Thornton, 2001]. Interaction partner studies become increasingly important in identifying functional protein complexes and in better understanding protein functions within the cell, indicated by the continuously increasing number of methods suitable for interaction partner analyses and the vast amounts of large-scale protein-protein interaction (interactom) studies [Xing et al., 2016]. Interaction partner analyses are usually performed using protein microarrays [Popescu et al., 2007], yeast two-hybrid systems [Ito et al., 2001], affinity purification systems [Gavin et al., 2002] and mass spectrometry (MS) [Ho et al., 2002] [Trinkle-Mulcahy et al., 2008].

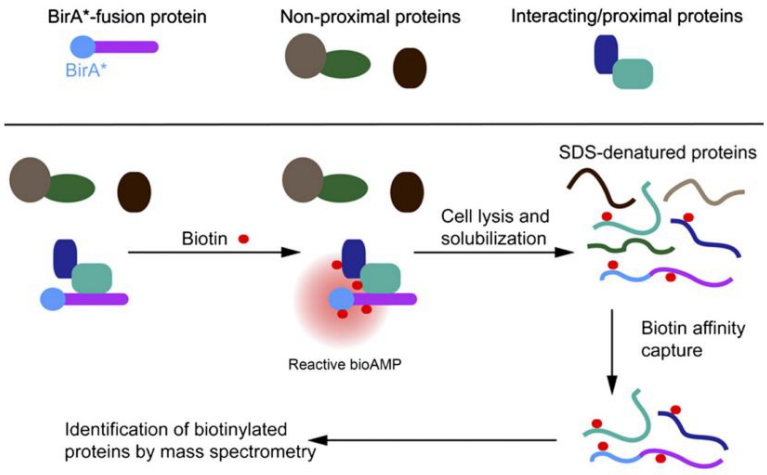

Fig. 2.5.: Schematic model of the BioID workflow. The protein of interest is expressed in mammalian cells fused to a promiscuous biotin ligase (BirA*), thereby selectively biotinylating nearby proteins. After cell lysis and solubilization, biotin-labeled proteins are selectively isolated, digested to peptides and identified by MS. Image is taken from: The Journal of cell biology. A promiscuous biotin ligase fusion protein identifies proximal and interacting proteins in mammalian cells. Reproduced from [Roux et al., 2012].

Multiple approaches using MS for interaction partner analysis are in use, whereof the affinity pull-down (immunoprecipitation) [Free et al., 2009], the proximity-dependent biotin identifica-

tion (BioID) method [Roux et al., 2012] and the protein correlation profiling (PCP) approach [Kristensen et al., 2012] are most frequently applied. Using the BioID method (Figure 2.5), cells are transfected with a construct, containing the information for a constitutively active E.coli biotin ligase (BirA mutant R118G = BirA*) and the protein of interest. The addition of biotin then leads to the biotinylation of lysine residues and N-termini of proteins, which are located in the vicinity of the protein of interest. Biotinylated proteins can thereafter be selectively isolated by, among others, NeutrAvidin affinity purification and subsequently identified by MS analysis.

Identification and validation of protein-protein interactions by co-immunoprecipitation (co-IP) is another common technique, which is based on the physiological interaction of proteins with the bait protein and simultaneously on the interaction of the bait protein and the appropriate antibody [Phizicky & Fields, 1995]. By using non-denaturing lysis buffer, intracellular protein-protein interactions can be retained and interacting proteins can be captured using the appropriate antibody affinity column. Although several ways are conceivable to perform co-immunoprecipitation, the principle of this technique, explained in Figure 2.6, remains the same.

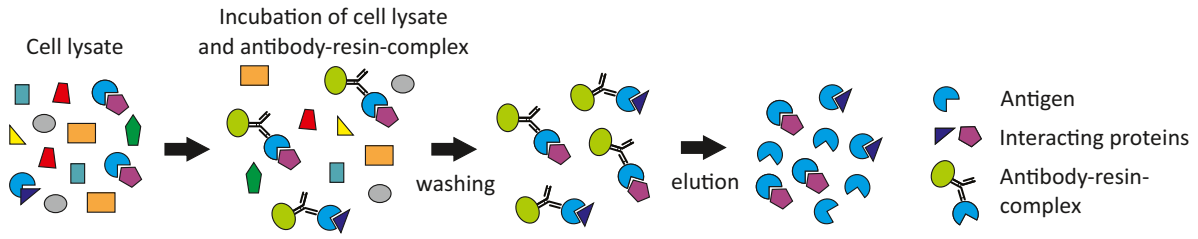

Fig. 2.6.: Schematic model of the co-immunoprecipitation workflow. Cell lysate and resin-coupled antibody against the bait protein are incubated together to form a complex, consisting of the resin-bound antibody, the bait protein and interacting proteins. After several washing steps to eliminate nonspecific bound proteins, the bait protein is eluted together with the interacting proteins and antibody. The image is adapted from Thermo Scientific Pierce - Protein interaction technical handbook (01/2017).

2.6. Transcriptional activator protein Pur-alpha

2.6.1. Overview

The murine transcriptional activator protein Pur-alpha (PURA), also known as the purine-rich single-stranded DNA-binding protein alpha, consists of 321 amino acids and has a mass of $\sim$ 35 kDa. The protein belongs to the purine-rich element binding protein family, a group of three proteins, namely Pur-alpha, Pur-beta and Pur-gamma. An interesting feature of the protein is its ability to regulate its own gene expression (autoregulation) by binding to GC/GA-rich sequences next to the Pur-alpha transcription start site [Muralidharan et al., 2001]. Pur-alpha is ubiquitously expressed in various organs and cells of humans, but mainly in cortical and endocrine tissue (www.proteinatlas.org; [Uhlén et al., 2015]). In addition, depending partly upon the cell cycle stage, Pur-alpha is more frequently localized in the cytoplasm and rather in the nucleus. During mitosis the highest protein levels are observed, while levels drop to a minimum at the onset of late G_1 respectively early S phase [Itoh et al., 1998]. This is especially important regarding the differential molecular functions of cytoplasmic and nuclear Pur-alpha.

2.6.2. Function

The Pur-alpha protein was first identified because of its ability to bind the c-myc gene [Bergemann & Johnson, 1992]. Meanwhile, many investigations were performed on the molecular function of Pur-alpha, thereby identifying three highly conserved PUR domains. Domain I and II are most probably responsible for the binding of Pur-alpha to guanine-rich parts, also known as the PUR element, of single-stranded DNA or RNA [Weber et al., 2016]. Domain III is assumed to be responsible for the dimerization of Pur-alpha molecules. In addition, Pur-alpha possesses local helix-unwinding capacity which enables the displacement of the complementary strand and thus enables the binding of double strand molecules as well [Darbinian et al., 2001a].

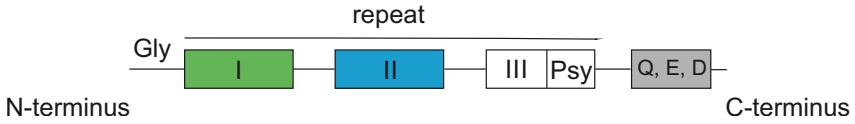

Fig. 2.7.: Pur-alpha protein structure. The 321 amino acid long murine Pur-alpha protein consists at the N-terminus of 18 glycine residues, also termed "glycine-rich domain" and a C-terminal glutamine-rich (Q), glutamic acid-rich (E) and aspartic acid-rich (D) domain. In between the glycine- and glutamine-rich sequences three PUR domains and the psycho domain, implicated in binding to the tumor suppressor protein retinoblastoma-associated protein (Rb), are localized.

Due to the presence of PUR elements at eukaryotic origins of DNA replication, Pur-alpha is involved in DNA replication processes in multiple species [Bergemann & Johnson, 1992]. Using Pur-alpha knockout mice (Pura^{-}/$^{-}$), the implication of Pur-alpha in replication initiation was investigated. In mice lacking Pur-alpha expression, almost no replication in hippocampal and cerebellar neuronal precursor cells was detected during early postnatal phase [Khalili et al., 2003]. By contrast, wild type mice, located at same development states, exhibited increased DNA replication rates. In addition, Pur-alpha was evidenced to interact with viral origins of replications and promoter regions, including the ones of the John Cunningham virus (JCV) and the human immunodeficiency virus (HIV). Moreover, several studies have revealed that Pur-alpha is capable of binding to the JCV early gene promoter and to the single-stranded DNA binding protein YB-1, thereby stimulating viral gene expression in a synergistic way [Safak et al., 1999].

So far, viral promoter regions are not the only target site of Pur-alpha. The protein was found to bind to the promoter regions of genes responsible for the expression of the endothelial transcription factor GATA-2 [Penberthy et al., 2004], VSM α-actin [Kelm et al., 1997], PDGF-A [Zhang et al., 2005] and MBP [Muralidharan et al., 1997]. Conclusively, the transcriptional regulation of diverse proteins is another main function of Pur-alpha, which has earned it the name transcriptional activator protein Pur-alpha. Moreover, the wide range of genes affected shows that Pur-alpha is involved in many biological processes, reaching from brain development via myeloid cell development and muscle development to cellular proliferation [Johnson et al., 2013]. It further proves that Pur-alpha is expressed in oligodendrocytes, indicated by the binding to the promoter region of the *Mbp* gene and by the involvement of the transcription factor E2F1 (E2F-1) in the transition of OPCs from proliferation to differentiation [Magri et al., 2014].

Moreover, Pur-alpha was shown to associate with several cyclin-dependent kinases and the retinoblastoma protein pRb in the nucleus, which implicates a role of Pur-alpha in the cell cycle [Liu et al., 2005]. The assumption is further fortified by either the protein's ability to inhibit the proliferation of glioblastoma cells [Darbinian et al., 2001b] and, as already mentioned, by the transcriptional regulation of the two cell proliferation regulators E2F-1 and GATA2 by Pur-alpha. Furthermore, after microinjection of Pur-alpha into NIH3T3 cells, around 80% of total cells displayed a cell cycle arrest, which further strengthens its cell cycle regulatory function [Stacey et al., 1999]. Thereby, most cells were prevented from entering mitosis or were blocked upon entering S phase, depending on the time of Pur-alpha injection. On the contrary, injection with a Pur-alpha mutant protein, which included the pRb binding site and the glutamine-rich domain, did not affect cell cycle progression.

As already mentioned, Pur-alpha expression is strongly increased during early postnatal phase when neuronal development takes places. However, Pur-alpha levels stay constantly elevated after developmental processes are accomplished, stronlgy suggesting an implication of Pur-alpha beyond regulation of transcription, replication and progress through the cell cycle [Khalili et al., 2003]. This implies other major functions for Pur-alpha in the cytoplasm. Several studies have proven the binding of Pur-alpha to RNA transcripts of distinct genes in neurons and have indicated a function of Pur-alpha in the transport of specific mRNAs to dendrites and in mRNA translation processes taking place at their final destination [Ohashi et al., 2002]. The essential function of Pur-alpha in dendrites becomes evident by the failure of $Pura^{-}/^{-}$ mice to form synapses and by an impaired development of dendrites [Johnson et al., 2006]. Immunohistochemical analyses further confirmed the crucial role of Pur-alpha in the formation of neurofilaments in dendrites and in the formation of synapses in the hippocampus [Khalili et al., 2003].

2.6.3. Pur-alpha associated diseases

Pur-alpha seems to be essential for proper brain development in mice during early post-natal stages. This is further consistent with the observation of human patients with *de novo* mutations in the *Pura* gene, exhibiting moderate to severe neurodevelopmental delays and learning disabilities as well as seizures, neonatal hypotonia and feeding difficulties [Hunt et al., 2014].

Pur-alpha is further implicated in the pathology of two neurodegenerative disorders, fragile X mental retardation syndrome (FXS) respectively fragile X-associated tremor/ataxia syndrome (FXTAS) and amyotrophic lateral sclerosis (ALS). The assumption is based on the interaction of Pur-alpha with proteins responsible for the diseases. The pathology of FXS and FXTAS derive from mutations in the synaptic functional regulator (*Fmr1*) gene, leading to differently long expansions of a trinucleotide CGG repeat. Pur-alpha was identified together with FMR1 (FMRP) in mRNP complexes, which regulate the transport of mRNA to translation sites in dendritic cells [Jin et al., 2007]. In addition, the binding of overexpressed Pur-alpha to lengthy rCGG repeats was shown to suppress the neurodegenerative pathology of the disease. The association of Pur-alpha and the disorder ALS is based on an investigation, indicating that Pur-alpha worsens neurodegenerative processes in drosophila *in vivo* [Di Salvio et al., 2015].

3. Material and Methods

The material part gives an overview of the equipment, cells and animal strains used, while the method part describes all methods and techniques utilized in this thesis.

3.1. Material

3.1.1. Instruments

Table 3.1.: Alphabetical instrument list

Application	Name/Type	Manufacturer
General equipment		
	V700 Photo Scanner	Epson
	37°C incubator	Heraeus Instruments
	761 pH-Meter Calimatic	Knick
	Analytic scale CP 124-OCE	Sartorius
	Axiovert 100M (Software: Axio Vision 4)	Zeiss
	Axiovert 200M (Software: Axio Vision 4)	Zeiss
	BD FACSCanto II	BD Bioscience
	Bioimager Screen Scanner BAS-1800 II	Fujifilm
	Digital pH-Meter 751 Calimatic	Knick
	Dry block heater	STAR LAB
	FLA-5000 Imaging System	Fujifilm
	Freezer -20°C	Siemens
	Freezer -80°C (Ultra low)	Sanyo
	Galaxy MiniStar	VWR
	Gel dryer Model 583	BioRad
	GENios Microplate reader (Software: XFluor4)	TECAN
	Heating and magnetic stirrer ARE	Velp Scientifica
	Heating-ThermoMixer MHR 23	HLC
	Ice machine	Ziegra
	Labtherm Heater	Liebisch
	LS 6500 Liquid Scintillation Counter	Beckman Coulter
	Lyovac GT2	Amsco/Finn-Aqua
	Mini incubator INCU-line	VWR
	Model P-2000 Puller	Sutter Instruments
	Nanopure Ultra Pure Water System	Barnstead
	PC 4400 scale	Mettler
	Polymax1040 orbital shaker	Heidolph
	Refrigerator	AEG
	Rotamax 120 orbital shaker	Heidolph
	Rotamix RM1	Elmi
	RS-TR05 roller mixer	Phoenix Instruments

	Scan Speed 40 vacuum concentrator	SCANVAC
	SpeedVac SC100	Savant
	ThermoMixer C	Eppendorf
	ThermoMixer Comfort 1.5 ml	Eppendorf
	Ultrasonic bath 2510	Branson
	Ultrasonic homogenizer UP 50 H	Hielscher
	Vortex Genie2	Scientific Industries
Centrifuges		
	5810 R, 5415D, 5417R, 5424R	Eppendorff
	Allegra X-15R	Beckman Coulter
	Labofuge 400e	Heraeus Instruments
	Mikro 200R	Hettich
	Z 216 MK	Hermle
Nucleic acid handling		
	7300 Real Time PCR system (Software: SDS version 1.4)	Applied Biosystems
	Agarose gel casting system	Peqlab
	DU® 640 Spectrophotometer	Beckman
	Electrophoresis gel system	Peqlab
	NanoDrop 2000 spectrophotometer	Thermo Scientific
	T3 Thermocycler	Biometra
	UV-imaging system	Biometra
Protein electrophoresis	and Western blotting	
	FUSION Solo (Software: FUSION-Capt Advance Solo 4)	Peqlab/Vilber Lourmat
	G3100A OFFGEL Fractionator	Agilent Technologies
	Mini PROTEAN 3 electrophoresis system	BioRad
	Mini-PROTEAN® Tetra Cell electrophoresis system	BioRad
	PerfectBlue™ Doppel-Gelsystem Twin ExW S	Peqlab
	PerfectBlue™ 'Semi-Dry'-Electroblotter, Sedect™	Peqlab/Vilber Lourmat
	Power Pac 300 power supply	BioRad
	Trans-Blot® Cell Wet/Tank blotting system	BioRad
Mass spectrometers and	chromatographic instruments	
	Autoflex III smartbeam MALDI TOF/TOF	Bruker Daltonics
	Easy-nLC 1000	ThermoScientific
	LTQ Orbitrap Velos	Thermo Scientific
Cell culture		
	37°C incubator	New Brunswick Scientific
	EVE Automatic cell counter	NanoEntek
	Laminar flow workbench	Clean Air
	Light microscope Axio Vert A1	Zeiss
	Light microcope Stemi SV 6	Zeiss
	Water bath	GFL

3.1.2. Software

Table 3.2.: Alphabetical software list

Name	Producer	URL
AIDA Image Analyzer	Raytest	https://www.raytest.com/
BiNGO 3.0.3	Gent University (Gent, Belgium)	https://www.psb.ugent.be/cbd/papers/BiNGO/Home.html

Cytoscape 3.0.3	Institute for Systems Biology (Seattle, USA)	http://www.cytoscape.org/
GOrilla (Gene Ontology enRIchment anaLysis and visuaLizAtion tool)	Weizmann Institute of Science (Tel-Aviv, Israel)	http://cbl-gorilla.cs.technion.ac.il
Limma	Walter and Eliza Hall Institute of Medical Research (Parkville, Australia)	http://bioinf.wehi.edu.au/limma/
MaxQuant 1.3.0.5 and 1.5.2.8	Max Planck Institute of Biochemistry (Martinsried, Germany)	http://MaxQuant.org
PANTHER Classification System 11.1	University of Southern California (Los Angeles, USA)	http://www.pantherdb.org
Perseus 1.5.5.3	Max Planck Institute of Biochemistry (Martinsried, Germany)	http://www.perseus-framework.org
Mascot	Matrix Science Limited	http://www.matrixscience.com/
Rank product	Breitling and colleagues (University of Glasgow, UK)	https://bioconductor.org/packages/release/bioc/html/RankProd.html
REViGO	Ruđer Bošković Institute (Zagreb, Croatia)	http://revigo.irb.hr/

3.1.3. Chemicals / Solutions / Buffers / Consumables

Every chemical, reagent, solution, buffer and consumable used, but not mentioned in the table, was ordered from the companies Merck (Darmstadt, Germany), Roche (Mannheim, Germany), Carl Roth (Karlsruhe, Germany), Sarstedt (Nümbrecht, Germany), Sigma-Aldrich (Taufkirchen, Germany), AppliChem (Darmstadt, Germany) and Thermo Scientific (Darmstadt, Germany).

Table 3.3.: Alphabetical list of chemicals, solutions, buffers and consumables used

Application	Name / Type	Supplier	Contents
General			
	Amersham Nitrocellulose blotting membrane 0.45µm	GE Healthcare	
	Cell strainer 40 and 70 µm	Corning	
	Coverslips	VWR	
	CryoBoxes™	Nalgene	
	Filter paper	Whatman	
	Microtubes 1.5 ml and 2 ml	Sarstedt	
	Microtubes MCT-150-L-C	Maxymum Recovery	
	Parafilm® M	Pechiney Plastic Packaging	
	Pasteur pipettes 15 and 20 cm	Brand	
	Pierce™ Micro-Spin Columns	Thermo Scientific	
	Pierce™ Spin Columns	Thermo Scientific	
	Plastic tubes 15 and 50 ml	Greiner	
	PVDF blotting membrane	Merck Millipore	
	Slides	Engelbrecht	
	Sterile filter	Sarstedt	
Agarose gel electrophoresis			
	10X TAE pH 8.0		400 mM Tris base 200 mM acetic acid 12.7 mM EDTA
	Agarose UltraPure™	Life Technologies	
	Ethidium bromide solution		5 mg/ml

Bacterial culture			
	Ampicillin stock solution		100 mg/ml
	LB-agarose plates		1.5% agar in LB-medium
	LB-medium		1% (w/v) NaCl 0.5 - 1% yeast extract 1% (w/v) Trypton pH 7.2 (autoclaved)
BioID Assay			
	Neutravidin washing buffer I		0.1% (w/v) sodium deoxycholat 1% (v/v) Triton X-100 0.5 M NaCl 1 mM EDTA 50 mM Hepes pH 7.5
	Neutravidin washing buffer II		250 mM LiCl 0.5% (v/v) Tergitol™ NP-40 0.5% (w/v) sodium deoxycholat 1 mM EDTA 10 mM Tris-HCl pH 8.1
	Neutravidin washing buffer III		50 mM NH_4HCO_3 50 mM NaCl
Cell culture			
	Forskolin	Sigma-Aldrich	100 mM in DMSO
	Laminin	Sigma-Aldrich	50 µg/ml in 1x PBS
	Nocodazol	Sigma-Aldrich	5 mg/ml in DMSO
	Phenylmethylsulfonyl fluoride	Sigma-Aldrich	
	Poly L-lysine	Sigma-Aldrich	4 mg/ml in 1x PBS
	Poly L-ornithine	Sigma-Aldrich	4 mg/ml in 1x PBS
	Soybean trypsin inhibitor	Thermo Scientific	
	Stempro Accutase	Thermo Scientific	
	Thymidine	Applichem	200 mM in 1x PBS
	TurboFect	Thermo Scientific	
Chromatography			
	Acetonitrile MS-grade	Biosolve BV	
	Formic acid MS-grade	Sigma-Aldrich	
	Trifluoro acetic acid MS grade	Sigma-Aldrich	
	Water MS-grade	Biosolve BV	
Cell lysis			
	BioID-lysis buffer		50 mM Tris-HCl pH 7.4 0.5 M NaCl 2% (v/v) Triton X-100 0.4% (w/v) SDS 5 mM EDTA 1 mM DTT 1x protease inhibitor
	Non-denaturating lysis buffer (IP)		20 mM Tris-HCl 137 mM NaCl 5% (v/v) glycerol 1% (v/v) Tergitol™ NP-40 2 mM EDTA 1x protease inhibitor

	NP40 lysis buffer		50 mM Hepes pH 7.8 150 mM KCl 1 mM $MgCl_2$ 1 mM EGTA 10% (v/v) glycerol 0.5% (v/v) Tergitol™ NP-40 0.5 mM DTT 1x protease inhibitor
	RIPA buffer		0.1% (w/v) SDS 0.5% (w/v) sodium deoxycholate 1% (v/v) Tergitol™ NP-40 150 mM NaCl 50 mM Tris pH 8.0 1x protease inhibitor
	SDS cell lysis buffer		4% (w/v) SDS 0.1 M Hepes pH 7.6 1x protease inhibitor
	Swelling lysis buffer		20 mM Hepes pH 7.7 5 mM KCl 5 mM MgCl2 1 mM DTT 1x protease inhibitor
	cOmplete™ Protease Inhibitor	Roche	
Cloning & Genotyping			
	GeneRuler™ 1 kb Plus DNA Ladder	Fermentas	
	GeneRuler™ 50 bp DNA Ladder	Fermentas	
	Genotyping lysis buffer		150 mM NaCl 2mM EDTA 1% (w/v) SDS 20 mM Tris pH 8.0
	HiPure Plasmid Midiprep Kit	Thermo Scientific	
	MiniPrep Kit	Qiagen	
	QIAquick PCR Purification Kit	Qiagen	
	Phenol:Chloroform:Isoamyl Alcohol 25:24:1	Carl Roth	
	Phusion HF DNA Polymerase Kit	Thermo Scientific	
	Proteinase K		10 mg/ml in ddH_2O
	PureLink Quick Gel Extraction Kit	Thermo Scientific	
	REDTaq Ready Mix	Sigma-Aldrich	
	Restriction enzymes incl. buffers	Fermentas; New England BioLabs	
	RNase-free DNase Kit	Qiagen	
	RNeasy Mini Kit	Qiagen	
	saturated NaCl		5 M NaCl in ddH_2O
	T4-DNA ligase	Thermo Scientific; New England BioLabs	
	Taq DNA Polymerase	Thermo Scientific	
	TRIzol™ Reagent	Life Technologies	
Degradation assay			
	TnT® Coupled Wheat Germ Extract System	Promega	
	TnT® Coupled Rabbit Reticulocyte Lysate System	Promega	

	Rabbit Reticulocyte Lysate System	Promega	
	Bioimager Screen	Fujj/Raytest	
	EasyTag™ EXPRESS35S Protein Labeling Mix, [35S]-, 2mCi	PerkinElmer	
	His6-UbcH10	Boston Biochem	
	His6-Ube2S	Boston Biochem	
	MG132	Calbiochem	100 mM in DMSO
	Regneration Mix		0.1 µg cyclo 0.1 µg ubiquitin 20 mM ATP 150 mM creatine phosphate 2 mM EGTA pH 8.0 20 mM MgCl2
FACS			
	Propidium iodide	Fluka	1 mg/ml in ddH_2O
	RNAse	Sigma-Aldrich	10 mg/ml in ddH_2O
	Polystyrene tube (12x75 mm)	Sarstedt	
Immunofluorescence	staining		
	1000X 4',6-diamidino-2-phenylindole (DAPI) solution		1 mg/ml in ddH_2O
	4% PFA solution		4% (w/v) PFA in 1x PBS
	Blocking solution		2% (v/v) NGS in 1x TBS
	Permeabilization solution		0.2% (v/v) Triton X-100 in 1x TBS
	ProLong™ Gold	Molecular Probes	
	ProLong™ Diamond	Molecular Probes	
Mass spectrometric	sample preparation		
	Empore™ Anion Exchange-SR Extraction Disks	Thermo Scientific	
	Empore™ SPE Disks Octadecyl C18	Thermo Scientific	
	Immobiline DryStrip Gels	GE Healthcare	
	IPG-Buffer, pH 3-10	GE Healthcare	
	Microcon-30kDa Centrifugal Filter Unit	Merck Millipore	
	Oasis HLB cartridges	Waters	
	Pierce™ NeutrAvidin™ Agarose	Thermo Scientific	
	RapiGest surfactant	Waters	
	ReproSil-Pur 120 C18-AQ	Dr.Maisch	
	Silac Aminoacids	Cambridge Isotope Lab	
	TMTsixplex™ Isobaric Label Reagent	Thermo Scientific	
	Trypsin from porcine pankreas (proteomics grade)	Sigma-Aldrich	
Miscellaneous			
	1x PBS pH 7.4		137 mM NaCl 2.7 mM KCl 10 mM Na_2HPO_4 2 mM KH_2PO_4
	1x TBS pH 8.0		100 mM Tris 150 mM NaCl
	CS-Fused-Silica-Capillary column (length 15-20cm, ID 100 µm)	selfpacked	containing Bruker-Michrom Magic C18 5 µm particles
	DC™ Protein Assay	BioRad	
	Pierce™ Protein A Agarose	Thermo Scientific	
	Tris buffer pH 7.0 / 8.0 / 9.0		0.1 M Tris-HCl in ddH2O

RNA	DNase I (RNase-free)	Roche Diagnostics	
	RiboLock RNAse Inhibitor	Thermo Scientific	
	RiboRuler High Range RNA Ladder	Fermentas	
	SuperScript® II Reverse Transcriptase	Invitrogen	
	SYBR® Select Master Mix	Applied Biosystems	
Recombinant protein	production		
	B-PER™ Bacterial Protein Extraction Reagent	Thermo Scientific	
	Affi-Gel 15 Gel	BioRad	
	Amicon Ultra 15 (10K)	Millipore	
	DNAse	Sigma-Aldrich	2500 Units/ml
	Lysozyme	Sigma-Aldrich	50 mg/ml
	Pierce™ Glutathione Agarose	Thermo Scientific	
	Poly-Prep® Chromatography Columns	BioRad	
	ZelluTrans dialysis membrane	Carl Roth	
SDS-PAGE & Western	blotting		
	10X SDS running buffer		0.25 M Tris-Base 14.5% glycerol 1% (w/v) SDS
	4X Sample buffer (Laemmli buffer)		8% (w/v) SDS 40% glycerol 240 mM Tris-HCl pH 6.8 4% (w/v) bromphenolblue 4% (v/v) ß-mercaptoethanol
	Acidic stripping buffer (pH 2.2)		200 mM glycine 0.1% (w/v) SDS 1% (v/v) Tween 20
	Blotting buffer pH 8.3		48 mM Tris-Base 39 mM glycine 0.037% (w/v) SDS 20% (v/v) methanol
	PageBlue Protein Staining Solution (Coomassie)	Thermo Scientific	
	PageRuler™ Prestained Protein Ladder	Thermo Scientific	
	Pierce™ ECL Western Blotting	Thermo Scientific	
	Ponceau S solution		0.2% (w/v) Ponceau S 3% (w/v) trichloroacetic acid
	Running gel buffer		1.5 M Tris-HCl pH 8.8 0.4% (w/v) SDS
	Stacking gel buffer		0.5 M Tris-HCl pH 6.8 0.4% (w/v) SDS
	TBS-T		1x TBS in 0.05% (v/v) Tween 20

3.1.4. Eukaryotic cells and cell lines

Media were provided by Life Technologies (Carlsbad, USA) and Euroclone (Pero, Italy), while reagents were purchased from Sigma-Aldrich (Taufkirchen, Germany), Applichem (Darmstadt, Germany), Invitrogen (Darmstadt, Germany) and PeproTech (Hamburg, Germany).

Table 3.4.: Eukaryotic cells and cell lines used in this thesis

Name	Description	Culture conditions
Primary rat cells		
	DMEM20S	DMEM 4 mM L-glutamine 1 mM sodium pyruvate 20% FCS 50 U/ml penicillin 50 µg/ml streptomycin
	BDM	DMEM 4 mM L-glutamine 1 mM sodium pyruvate 0.1% (w/v) BSA 50 µg/ml apo-transferrin 5 µg/ml insulin 30 nM sodium selenite 10 nM D-biotin 10 nM hydrocortisone 100 U/ml penicillin 100 µg/ml streptomycin
	Proliferation medium OPC medium	BDM plus 20 ng/ml PDGF-AA 20 ng/ml bFGF
	Oligodendrocyte differentiation medium	BDM plus 10 ng/ml CNTF 5 mg/l NAC
Primary mouse cells		
	Neural culture medium (NCM)	DMEM/F12 25 µg/ml insulin 100 µg/ml apo-transferrin 20 nM progesterone 60 mM putrescine 30 nM sodium selenite 100 U/ml penicillin 100 µg/ml streptomycin
	Proliferation medium Neurospheres growth medium (NGM)	NCM plus 20 ng/ml EGF 20 ng/ml bFGF
	Differentiation medium (Oligospheres medium)	NCM plus B104 neuroblastoma conditioned medium (B104 CM) (ratio 7:3)
Cell lines		
B104 rat neuroblastoma cells	neuronal progenitor cells (Schubert et al.)	DMEM/ F12 10% FCS
FNS	Fetal neural stem cell; neurospheres, derived from E14 foetal brain and maintained for 40 passages in EGF and FGF-2 containing medium (adapted from Conti et al., 2005)	Euromed N 1/10 (v/v) DMEM/F-12 1x N2 supplement 100 U/ml penicillin 100 µg/ml streptomycin
HEK293T	Derivative of HEK293 cells; stably transfected with SV40 Large T-antigen	DMEM 100 U/ml penicillin 100 µg/ml streptomycin 10% FCS (heat inactivated)
HeLa	Immortalized cell line isolated from cervical cancer Henrietta Lacks	DMEM 100 U/ml penicillin 100 µg/ml streptomycin 10% FCS (heat inactivated)

HeLa S3	Derivative of HEK293 cells; cells have been adapted to grow in suspension culture	DMEM 100 U/ml penicillin 100 µg/ml streptomycin 10% FCS (heat inactivated)
Oli-Neu	Oligodendroglial precursor cell line SATO medium	DMEM 1X N-2 supplement 5 mg/l insulin 0.5 µM TIT 0.5 µM L-thyroxine 2 mM L-glutamine 1% horse serum 10 mM Hepes pH 7.4 100 U/ml penicillin 100 µg/ml streptomycin

3.1.5. Mice, rat and bacterial strain

All animals were obtained from our in-house animal facility. The wildtype and EYFP-knockin mice used in all experiments had a C57BL/6 genetic background. The wildtype rats used in all OPC experiments had a Sprague Dawley genetic background. All animals were raised in accordance with the instructions of local and state authorities regarding animal welfare.

The only bacterial strain used was the E.coli XL1 blue strain.

3.1.6. Antibodies

Table 3.5.: Antibodies used for immunocytochemistry staining and western blots

Type	Target name	Host species	Manufacturer	Product No.	Application	Dilution	Miscellaneous
Primary							
	Biotin		Pierce	21126	WB	1:10,000	Streptavidin HRP conjugate
	F4/80	rat	selfmade		ICC	1:100	
	GFAP	mouse	Abcam	ab10062	ICC	1:200	
	GFAP	rabbit	Abcam	ab7260	ICC	1:100	
	GST	mouse	Santa Cruz	sc138	WB	1:200	
	MBP	rat	Abcam	ab7349	ICC	1:100	
	MYC1	mouse	selfmade		WB	1:700	
	Nestin (rat-401)	mouse	BD Pharmingen	556309	ICC	1:100	
	NG2	rabbit	Millipore	ab5320	ICC	1:100	
	NG2	rat	selfmade		ICC	1:25	
	PDGFRα	rabbit	Abcam	ab96806	ICC	1:100	
	PURA	rabbit	Abcam	ab79936	WB	1:700	
	PURA	guineapig	selfmade		WB	1:150	affinity purified
	TUBA4A	mouse	Sigma Aldrich	T5168	WB	1:5,000	
	TUBB3	mouse	Dianova	T-1315	ICC	1:100	
	Ubiquitin (P4D1)	mouse	Cell signalling	3936S	WB	1:1,000	
Secondary							
	α-rabbit-Cy3	goat	Dianova	111-165-144	ICC	1:600	
	α-rat-Dylight488	goat	Dianova	112-485-167	ICC	1:800	
	α-mouse-Alexa488	goat	Invitrogen	A11017	ICC	1:600	

α-mouse-Alexa546	goat	Invitrogen	A11018	ICC	1:400
α-guineapig-Cy3	goat	Dianova	106-165-003	ICC	1:500
α-rabbit-Alexa488	goat	Molecular Probes	A-11008	ICC	1:400
α-rat-Alexa488	goat	Molecular Probes	A-11006	ICC	1:200
α-mouse-HRP	goat	Dianova	115-035-068	WB	1:5,000
α-rabbit-HRP	goat	Dianova	111-035-003	WB	1:5,000
α-guineapig-HRP	goat	Dianova	106-035-003	WB	1:5,000

3.1.7. Oligonucleotides and plasmids

Table 3.6.: Oligonucleotides used for PCR, qPCR and genotyping

Application	Name	Internal number	Sequence (5' → 3')
PCR			
	BioID_FWD_NsiI		AAA-ATGCAT-ATGGAACAAAAACTCATCTCAGAAG
	BioID_REV_HindIII		AAA-AAGCTT-CTCTGCGCTTCTCAGGGA
	BioID_REV_SalI		TTT-GTCGAC-CTACTTCTCTGCGCTTCTCAGG
	Pura (BamHI) FWD	A64	AAA-GGATCC-ATGGCGGACCGAGACA
	Pura (XbaI) REV	A76	AAA-TCTAGA-TCAATCTTCTTCCCCTTCTTCC
	PurA_EcoRI_FWD	A78	AAA-GAATTC-GCGGACCGAGACAGCG
	Pura_HindIII_FWD	B02	AAA-AAGCTT-ATGGCGGACCGAGACA
	PurA_NsiI_FWD	A77	AAA-ATGCAT-ATGGCGGACCGAGACA
	PurA_XhoI_Rev	A79	AAA-CTCGAG-TCAATCTTCTTCCCCTTCTTCC
qPCR			
	GPDH_FWD	A28	ACAACTTTGGCATTGTGGAA
	GPDH_REV	A29	GATGCAGGGATGATGTTCTG
	Pura_qPCR_FWD	B04	ACCTACCGCAACTCCATC
	Pura_qPCR_REV	B05	CCGCTTCTCCCTCTGTTTC
	qUbc-F1	L-3981	AGGCAAGACCATCACCTTGGACG
	qUbc-R1	L-3982	CCATCACACCCAAGAACAAGCACA
	Zf_Pura_qPCR_F1	C1	AGGCACAGGACGAGCCACG
	Zf_Pura_qPCR_R1	C2	TCTGGCCCTGCGTGGAGC
genotyping (NG2-eYFP)			
	69-for(NG2-p5)	2901	CGCTGAACTTGTGGCCGTTTA
	70-rev(NG2-p7)	2881	TGACCTTGGATTCTGAGC
	71-R-NG2-p6	2882	ACAGCTTTCCTTCCAGAC

Table 3.7.: List of plasmids used for cloning

Name	Insert	Source	Remarks
G0656pFIV3.2RSV-myc-BioID	myc-taged E-coli biotin-ligase		mycBioID-PCR copied from G0656pFIV3.2 RSV-myc-BioID-Pura; Ligated into vector via NsiI & SalI
G0656pFIV3.2RSV-myc-BioID-Pura	Fusion protein of myc-taged E-coli BirA* and murine PURA		Pura-PCR copied from pBluescript-SK-Pura and mycBioID-PCR from pcDNA3.1.-myc-BioID; triple ligation via NsiI, HindIII & XbaI
pBluescript-SK-Pura	murine PURA		Pura-PCR of murine tissue; Ligated into vector via BamHI & XbaI
pGEX-5X-1-GST-Pura	murine PURA		PCR copied from pBluescript-SK-Pura; Ligated into vector via EcoRI & XhoI
G0656pFIV3.2RSV		Kindly provided by the University of Iowa	RSV promoter containing lentiviral vector

pBluescript-SK (-)		Kindly provided by Prof. Odermatt (University of Bonn)
pcDNA3.1.-myc-BioID	myc-taged E-coli biotin-ligase	Kindly provided by Kyle Roux (Roux et al., 2012)
PCS2-Securin-His8-Sp6	his-taged human Securin	Kindly provided by the Harvard Medical School
pGEX-5X-1-GST		Amersham

3.2. Methods

3.2.1. Primary cell culture technique

3.2.1.1. Cultivation of murine oligodendrocyte precursor cells

Oligodendrocyte precursor cells (OPCs) were isolated according to Chen and co-workers [Chen et al., 2007]. The protocol was modified by using P0 or P1 mice instead of E14.5–17.5 mice. In this thesis, the protocol was used for cells derived from NG2 wildtype (WT) mice and NG2-EYFP-knockin mice.

Generation of neurospheres First, cortices of P0 or P1 old mice were dissected and cut into smaller pieces. Cortical tissue was transferred into a 15 ml tube containing ice cold neurospheres growth medium (NGM) and homogenized by pipetting suspension up and down for 35 times with a fire-polished pasteur pipette. The suspension was kept on ice for 2 min and then passed through a 40 µm cell strainer to restrain cell agglomerates. Numbers of cells were determined with a hemocytometer and cells were plated at a density of $2 \cdot 10^6$ cells per 4 ml NGM per well of a six-well plate. Cells were then incubated at 37 ℃ in a tissue culture incubator, supplied with 5% CO_2, while replacing half of the medium every 2nd or 3rd day.

Production of B104 neuroblastoma conditioned medium (B104 CM) B104 neuroblastoma conditioned medium was obtained according to Chen and co-workers [Chen et al., 2007]. Correspondingly, B104 neuroblastoma cells [Schubert et al., 1974] were cultivated in B104 growth medium (DMEM/F-12 supplemented with 10% FCS and antibiotics) until confluency, washed with 1X Puck's BSS (80 g NaCl, 4 g KCl, 0.9 g $Na_2HPO_4 \times 7\ H_2O$, 0.4 g KH_2PO_4 and 10 g glucose in 1 liter ddH_2O) and fed for 4 days with N2 medium (DMEM/F-12 supplemented with 1X N2 supplements). Subsequently, medium was collected and phenylmethylsulfonyl fluoride was added to a final concentration of 1 µg/ml and quickly mixed by swirling the suspension. After centrifugation at 2,000 g at 4 ℃for 30 min in a swinging bucket, the pellet was discarded and the supernatant was filtered using a 0.22 µm sterile filter and stored at -80 °C prior to usage.

Generation of oligospheres After ∼7 days, developed cell clusters (neurospheres) were transferred into a 50 ml tube and centrifuged down for 1 min at 95 g. The supernatant was thereafter transferred into a new 50 ml tube and filtered with a 0.22 µm sterile filter. The loose cell pellet was resuspended in medium containing 3 parts NGM (reused) and 1 part B104 CM and NCM (oligosphere medium) (ratio 30:70) by pipetting the solution slowly up and down with a 25 ml plastic pipette. Afterwards, neurospheres were distributed equally into each well of a new six-well plate. Cells were further incubated at 37 ℃ in a tissue culture incubator with 5% CO_2 while replacing one fourth of the medium with oligosphere medium every 2nd day.

Cell harvest of neurospheres and oligospheres Cells were transferred into a 15 ml or 50 ml tube, centrifuged for 1 min at 72 g and washed once with ice cold 1X PBS buffer. After an additional centrifugation step, the supernatant was discarded and samples were frozen immediately in liquid nitrogen and stored at -80 ℃.

3.2.1.2. Genotyping

Genotyping of mice derived from breedings between homozygous NG2-WT species and homozygous NG2-EYFP-knockin species was performed via polymerase chain reaction (PCR) using genomic DNA, which was extracted from a very small tissue sample of the tail tip or the ear. First, the tissue was digested in 750 µl genotyping lysis buffer containing 4 µl Proteinase K (20 mg/ml) in a ThermoMixer® at 500 rpm and 55 ℃ overnight. The next day, 250 µl saturated sodium chloride (NaCl) solution was added for 5 min to precipitate proteins from the solution, which could subsequently be removed from the sample by centrifugation at 12,000 g and 4 ℃ for 10 min. In the following step, 750 µl of the supernatant was transferred to a new microtube and precipitation of DNA was achieved by the addition of 500 µl isopropanol.

Table 3.8.: Genotyping: PCR reaction mixture composition and PCR thermocycling program

Component	20 µl Reaction	Final concentration
Genomic DNA	1 µl	
2X REDTaq® ReadyMix™ PCR	10 µl	1X
10 µM Sense Primer	0.2 µl	0.1 µM
10 µM 1st Antisense Primer	0.2 µl	0.1 µM
10 µM 2nd Antisense Primer	0.2 µl	0.1 µM
ddH_2O	ad 20 µl	

Step	Temperature	Time
Initial Denaturation	94°C	5 minutes
33 Cycles	94°C	30 seconds
	52°C	30 seconds
	72°C	1 minute
Final Extension	72°C	3 minutes
Hold	4°C	

Afterwards, genomic DNA was pelleted by centrifuging samples at 18,000 g and 4 ℃ for 30 min. Ensuing, a washing step with 500 µl 70% (v/v) ethanol and a centrifugation step at 18,000 g and 4 ℃ for 10 min were performed, before air-drying the DNA pellet at room temperature (RT) for 10 min. Finally, genomic DNA was resuspended in 100 - 200 µl ddH_2O and incubated at 37 ℃ for 1 - 2 h or at 4 ℃ overnight. Thereafter, 1 µl of the DNA sample was mixed with the appropriate primers and DNA polymerase according to the PCR mixture composition mentioned in Table 3.8 and subsequently PCR was proceeded according to the PCR program depicted in Table 3.8. Thereafter, the amplified PCR products were separated via agarose gel electrophoresis and visualized using ethidium bromide (refer to Section 3.2.9.7).

3.2.1.3. YFP imaging of intact neurospheres

The Axiovert 200 M microscope, connected to a AxioCam HRc camera, was used to detect the yellow fluorescent protein (YFP), expressed by cells derived from the NG2-EYFP-knockin mouse. Therefore, brightfield illumination was used to focus on one single sphere, followed by application of a filter set which detects the YFP protein. The filter set consisted of an excitation filter covering an excitation range of 500/20, an emission filter covering a range of 535/30 and a dichroic beam-splitter of 515 nm.

3.2.1.4. Cultivation of rat oligodendrocytes

The cultivation of primary rat OPCs and subsequent differentiation to oligodendrocytes was conducted according to Chen and co-workers [Chen et al., 2007].

Generation of rat OPCs First, cortices of P1 or P2 rats were exposed and meninges were removed with special dissecting forceps. Afterwards, the cortices were cut into small pieces with a sterilized razor blade and tissue digestion with 0.25% (w/v) trypsin and 0.2 mg/ml DNase solution in HBSS was performed at 37 ℃ for 15 min. The tissue was collected in a 50 ml tube, 5 ml DMEM20S was added and following centrifugation at 95 g for 5 min, the supernatant was discarded and 20 ml medium was added. By triturating the tissue with a 10 ml glass pipette several times, a homogeneous suspension was received. The tissue was then incubated for 10 min on ice, before passing the cell suspension through a 70 µm cell strainer to collect the flow-through. The remaining pellet was again titruated and the homogeneous suspension was passed through the same 70 µm cell strainer and filled up with 10 ml medium. Finally, the combined flow-through was filled in multiple T75 flasks, which were previously coated with poly-D-lysine (PDL) (refer to Section 3.2.2.2) for 1 - 2 h at 37 ℃. Cells were afterwards incubated for 10 days at 37 ℃ in a tissue culture incubator with 5% CO_2 while replacing the whole medium every 2nd or 3rd day with fresh DMEM20S.

After 10 days, a confluent culture of mixed glial cells was obtained. Separation of the different cell types was achieved by shaking flasks on a horizontal orbital shaker for a varying length of time. First, flasks were preshaken at 200 rpm and 37 ℃ for 1 h to remove microglial cells together with the supernatant. After addition of 10 ml of fresh DMEM20S to each flask, the caps were thoroughly tightened and wrapped with plastic foil to provide low oxygen level, which allowed OPCs to detach easily from the astrocyte layers below. Cells were then shaken at 200 rpm for around 18 - 20 h in the incubator, providing 37 ℃ and 5% CO_2. The next day, the complete supernatant including mainly OPCs was transferred to an untreated cell culture plate and incubated at 37 ℃ for 30 - 60 min. Remaining microglia and astrocytes attach more efficiently to the bottom of the cell culture plate, whereby cell suspension including OPCs was separated from the contaminating cells by gently swirling flasks. After centrifugation at 100 g for 10 min in a swinging bucket, almost the whole supernatant was exchanged with 1 ml of fresh OPC medium and cell pellet was resuspended. Before plating, the amount of living cells was determined with a hemocytometer. Finally, the cell suspension was diluted with OPC medium and plated onto poly-D-ornithine (PDO) coated cell culture plates (refer to Section 3.2.2.2) at a density of $1 \cdot 10^4$ cells per cm^2 and incubated at 37 ℃ for 7 - 10 days, while exchanging half of the medium with fresh OPC medium every 2nd day. Mixed glial cell cultures can be cultivated and shaken a second time. Therefore, fresh medium was added to the cells and cultivation for an additional week was performed, before shaking the OPCs off the other glial cells again.

Generation of oligodendrocytes Around 7 - 10 days post-isolation of OPCs from mixed glial cell cultures, differentiation of OPCs to oligodendrocytes was performed by changing to oligodendrocyte differentiation medium, containing 15 nM triiodothyronine (T3), 10 ng/ml ciliary neurotrophin factor (CNTF) and 1X n-acetyl l-cystein (NAC). Differentiation was performed for 9 days while exchanging the whole medium with fresh medium every 2nd day.

3.2.2. Eukaryotic cell line culture techniques

3.2.2.1. Cell maintenance

Cells were maintained under sterile conditions using laminar airflow workbenches and autoclaved or heat-sterilized cell culture material. Incubation of cells was performed in standard cell culture vessels in a water-saturated atmosphere at 37 ℃, supplemented with 5% CO_2.

3.2.2.2. Coating plates with poly-ornithine, poly-lysine and laminin

Cell culture vessels were incubated with the appropriate amount (complete coverage of the cell culture plate surface) of 20 µg/ml poly-D-ornithine or 100 µg/ml poly-D-lysine solution for at least 60 min at 37 ℃ in the incubator. Thereafter, the solution was removed and cell culture vessels were either washed 3x with 1X PBS prior to immediate usage or storage at 4 ℃ for a maximum of two weeks or rinsed with sterile ddH_2O and coated with laminin. The laminin solution was slowly thawed at 4 ℃ and diluted to a final concentration of 5 µg/ml, before incubating cell culture plates at 37 ℃ for 60 min in the incubator. Cell culture plates were either stored at 4 ℃ for a maximum of one week by wrapping a plastic foil around them or rinsed 3x with to 37 ℃ - prewarmed 1X PBS prior to usage. It should be noted that with increasing reuse of laminin working solution, the coating properties seemed to worsen, indicated by an ineffective attachment of cells to the cell culture vessels. The PDO and PDL solutions were reused up to 5x and the laminin working solution up to 3x, while avoiding repeated freezing-thawing cycles.

3.2.2.3. Cell passaging

First, adherent cells were washed once with 37 ℃ - prewarmed 1X PBS. Thereafter, an appropriate amount of 0.05% (w/v) trypsin solution was added to cover the complete cell culture vessel and trypsinization was performed for 3 - 5 min in the incubator. For trypsin-sensitive cells, like fNS cells, the incubation time was limited to 3 min plus subsequent addition of soybean trypsin inhibitor (ratio 1:1), while human cell lines were treated for 5 min with trypsin solution. Cell suspension was afterwards transferred into a 15 ml tube by adding 37 ℃ - prewarmed medium and subsequently centrifuged at max. 500 g for 5 min to discard the supernatant. Cells were resuspended in the appropriate medium, before plating them in the desired cell number on new cell culture plates. For simple cell maintenance, cells were usually splitted in a range of 1/5 to 1/10, while for seeding of exact amounts cells were counted with a hemocytometer beforehand. Thereafter, cells were again cultivated in the incubator at 37 ℃ and 5% CO_2. Oli-neu were splitted into new cell culture flasks by washing cells once with 37 ℃ - prewarmed 1X PBS, adding fresh medium and pipetting the suspension several times against the wall of the flask to detach cells from the bottom. Cell suspension was centrifuged at max. 500 g for 5 min, supernatant was discarded, cells were resuspended and plated onto new cell culture vessels.

3.2.2.4. Cell harvest

Trypsinization Prior to cell harvesting by trypsinization, medium was discarded and cells were washed once with 37 ℃ - prewarmed 1X PBS. Solution was removed and exchanged to the appropriate amount of 0.05% (w/v) trypsin solution to completely cover the surface of the cell culture plate. fNS cells were incubated for 3 min, whereas all other cells were incubated for 5 - 10

min at 37 ℃ in the humidified incubator, before adding 37 ℃ - prewarmed medium to the cells. After transferring cell suspension into a new 15 ml tube, cells were pelleted by centrifugation at 500 g for 5 min and the supernatant was discarded. Cells were washed once with ice-cold 1X PBS and centrifuged once again, before discarding supernatant by application of vacuum. Finally, cell pellets were shock frozen in liquid nitrogen and stored at -80 ℃.

Scraping cells Prior to cell harvesting, medium was discarded and cells were washed once with 37 ℃ - prewarmed 1X PBS. After removal of washing solution, 5 ml of 1X PBS was added and cells were detached from the cell culture vessels by scraping thoroughly. Cell suspension was then filled into a 15 ml tube, centrifuged at 500 g for 5 min to discard the supernatant. Finally, cells were washed again with 10 ml ice-cold 1X PBS and centrifuged, before discarding supernatant by application of vacuum. Finally, cell pellets were shock frozen in liquid nitrogen and subsequently stored at -80 ℃.

3.2.2.5. Cryopreservation

For long-term storage, cells were maintained in DMSO-containing medium in a liquid nitrogen tank to be revitalized at any time point, when needed. First, adherent cell cultures were trypsinized (refer to Section 3.2.2.3), while suspension cell culture systems were directly transferred into a 15 ml tube and centrifuged at 500 g for 5 min to discard the supernatant. Trypsinized cells were washed once with 37 ℃ - prewarmed 1X PBS and centrifuged again. Cells were thereafter resuspended in medium, transferred into a cryovial and DMSO was added in a dropwise manner to a final concentration of 15%. Thereafter, cryovials were immediately stored for 24 h in a polystyrene box in the -80 ℃ freezer to ensure slow pre-freezing of cells. The next day, cells were transferred into the liquid nitrogen tank for long-term storage.

3.2.2.6. Revival of cells after cryopreservation

Cryovials were thawed for around 10 min at RT, before transferring cell suspension into a 15 ml tube by adding 1X PBS. Cells were then pelleted by centrifugation to remove DMSO-containing supernatant. Following this, cells were resuspended in 37 ℃ - prewarmed medium and plated onto appropriate cell culture vessels. Thereafter, cells were cultivated as usual.

3.2.2.7. Transient transfection

Transfection of eukaryotic cells was performed using the transfection reagent TurboFect™ to improve the delivery of the expression vector into the nucleus of cells. The day before transfection, cells were seeded in appropriate amounts to ensure a cell confluency of around 70% at the time of transfection. 24 h later, the transfection solution was prepared by diluting 1 µg of plasmid DNA in 100 µl of serum-free medium and mixing it with 2 µl TurboFect reagent by vortexing. The mixture was subsequently incubated at RT for 15 to 20 min to allow formation of the DNA-polymer-complex, before adding the solution drop wise onto the cells. Immediately afterwards, cell culture plates were shaken gently to achieve complete distribution of the transfection solution within the medium. Transfection and subsequent expression of the protein were performed for 24 h in the humidified incubator at 37 ℃.

3.2.2.8. Cell cycle synchronization

Cell cycle synchronization of HeLa S3 cells HeLa S3 cells were cultivated in spinner flasks containing DMEM, supplemented with 10% FCS and antibiotics at 37 ℃ and 5% CO_2. Counting 2.5 - 3.5 million cells per ml, synchronization of cells in S phase was performed by adding 200 mM thymidine in 1X PBS to a final concentration of 2 mM and subsequent incubation for 24 h. The next day, cells were released by transferring the flask content into fresh 50 ml tubes, centrifuging them at 300 g and 4 ℃ for 5 min, discarding the supernatant and resuspending each pellet in 37 ℃ - prewarmed medium. Cells were again centrifuged and medium discarded, before changing to fresh medium without adding any cell cycle influencing additives to enable cell cycle progress. Following 3 h of incubation, nocodazole stock solution (5 mg/ml in DMSO) was added for 11 h to the medium to a final concentration of 110 ng/µl. After preventing cells to undergo mitosis, cells were released for 4 h, before harvesting samples at G_1 stage. Therefore, the supernatant was first transferred into a 50 ml tube, centrifuged at 300 g and 4 ℃ for 5 min to discard the supernatant, following resuspension of the cell pellet in fresh medium. Cells were finally harvested by spinning tubes 3x at 300 g and 4 ℃ for 5 min, while resuspending the cell pellet in 1X PBS in between. After three washing steps, cell pellets were resuspended in ice-cold 1X PBS and centrifuged again to completely remove the supernatant.

Cell cycle synchronization of fNS cells The established protocol for cell cycle synchronization in G1 phase was adjusted for a cell division time of 24 h for adherent fNS cells. First, fNS cells were plated at a density of $3.5 \cdot 10^6$ cells per 10 cm cell culture plate, coated with laminin and PLO. The next day, at a confluency of ∼60%, medium was exchanged and cells were treated with 2 mM thymdine (stock solution 100 mM thymidine in 1X PBS) for 22 h. The day after, cells were released by washing 2x with 37 ℃ - prewarmed 1X PBS and exchanging to fresh EuroMed-N medium containing the growth factors EGF and bFGF. Cells were allowed to recover and to undergo the cell cycle for 3 h, before adding 5 mg/ml nocodazole in DMSO to a final concentration of 100 ng/µl to synchronize all cells in mitosis. After 16 h, the mitosis block was terminated by changing to fresh medium and cells were allowed to further undergo the cell cycle. During mitosis, cells were just loosely attached to the cell culture plate surface, resulting in many detached cells. Thus, the supernatant including detached cells was transferred into a fresh microtube, centrifuged at 500 g for 5 min, washed once with 1X PBS, before resuspending cells in fresh medium and plating them again onto laminin and PLO coated cell culture vessels. 4 h later, all cells were harvested by trypsinization, washed two times with ice-cold 1X PBS and samples were shock frozen with liquid nitrogen and stored at -80 ℃.

3.2.2.9. Fixation of cells for flow cytometry

Approximately 1 million cells were harvested per sample for flow cytometric analyses. Therefore, cells cultivated in adherent cell cultures were trypsinized, whereas cells cultivated in suspension cultures were directly transferred into a tube, centrifuged for 5 min at 500 g to discard the supernatant and washed once with 37 ℃ - prewarmed 1X PBS. After an additional centrifugation step and removal of supernatant, cells were resuspended in 0.3 ml of ice-cold 1X PBS. Then, 0.7 ml of 100% methanol was added drop wise under continuous but gentle vortexing. Samples were incubated for 60 min on ice, before storing them at -20 ℃ for up to two weeks.

3.2.3. Bacterial culture techniques

3.2.3.1. Cell maintenance

Liquid media was used for the growth of bacteria cultures, whereas for the isolation of single colonies solidified growth medium was used. Accordingly, bacteria were incubated in a glass flask containing lysogeny broth (LB) medium and ampicillin on an orbital shaker at 200 rpm and 37 ℃ overnight. To obtain single colonies, for example after transformation, the cell suspension was distributed onto LB-agarose-plates containing ampicillin and incubated at 37 ℃ overnight.

3.2.3.2. Transformation of chemical competent bacteria

Transformation of bacteria describes the uptake and incorporation of exogenous genetic material, like plasmid DNA, into bacterial cells to enable the amplification of plasmids or the expression of recombinant proteins in larger amounts. In the first step, 100 µl of chemical competent E. coli XL-1 Blue cells were thawed on ice, gently mixed with the ligation composite and afterwards incubated for 30 min on ice. Thereafter, cells were heat shocked for 45 s at 42 ℃ in a ThermoMixer®, before placing cells immediately on ice for 2 min. Next, 900 µl prewarmed LB medium was added to the cell suspension and incubated in the ThermoMixer® at 225 rpm and 37 ℃ for 60 min. Finally, 100 µl of the suspension was spread onto LB-agarose plates containing ampicillin, before incubating them at 37 ℃ overnight. The next day, plates were checked for the formation of colonies, followed by picking some colonies for mini preparation to determine clones, which had incorporated the plasmid of interest.

3.2.3.3. Recombinant protein expression and cell lysis

E.coli cells, containing the plasmid of interest, were grown in LB-medium containing ampicillin at 37 ℃ until mid-log phase, indicated by an OD600 of 0.6 - 1.0. Protein expression was initialized by adding 1 M isopropyl β-D-1-thiogalactopyranoside (IPTG) to a final concentration of 0.1 mM and subsequent incubation at 29 ℃ for 4 h. Prior to induction, IPTG concentrations and incubation times were tested to determine the best conditions yielding in highest protein expression. Next, bacteria were lyzed and proteins extracted according to the manufacturers protocol with the B-PER® Bacterial Protein Extraction Reagent, supplemented with 2 µl lysozyme (50 mg/ml) and 2 µl DNase I (2,500 units) per ml of reagent and the appropriate amount of protease inhibitor. Following a 15 min' incubation time at RT, samples were centrifuged at 15,000 g for 5 min and the supernatant was transferred into a new plastic tube.

3.2.4. Protein techniques

3.2.4.1. Cell lysis

The volume of lysis buffer used equaled approximately 10X the volume of the cell pellet. After addition of the desired ice-cold buffer solution (refer to 3.3) including 1X Protease Inhibitor Cocktail, cells were immediately resuspended by pipetting the suspension up and down. Thereafter, cells were incubated for 30 minutes in an overhead shaker at 25 rpm and centrifuged for 30 min at 18,000 g and 4 ℃. Upon using the BioID lysis buffer (refer to 3.3), samples were additionally homogenized using an ultrasonic homogenizer for 3x 30 s at cycle 3 and an amplitude of 50% in the cold room. The supernatant was separated from the remaining cell pellet,

transferred to a fresh microtube and either used for subsequent experiments or stored at -20 ℃.

Upon using the SDS lysis buffer (refer to 3.3), resuspended cells were incubated at 95 ℃ for 5 min. After cooling the sample down to RT, cells were centrifuged at 5,000 g for 1 min. Samples were sonicated 3x with an ultrasonic homogenizer for 30 s with an amplitude of 60 - 80% in the cold room, followed by an additional incubation step at 95 ℃ for 5 min. Finally, samples were centrifuged at 20,000 g and RT for 30 min.

Immunoprecipitation (IP) cell lysis method First, cells were washed with ice-cold 1X PBS and harvested by adding 1 ml of lysis buffer and scrape cells thoroughly off the cell culture plate. The IP lysis buffer consisted of 20 mM Tris-HCl, 137 mM NaCl, 5% (v/v) glycerol, 1% (v/v) Tergitol™ NP-40, 2 mM EDTA and 1X protease inhibitor (cOmplete™). The cell suspension was further incubated at 4 ℃ for 15 min in an overhead shaker and thereafter centrifuged at 18,000 g and 4 ℃ for 15 min. Finally, the supernatant was transferred into a new microtube and the protein concentration was determined.

Degradation assay cell lysis method The appropriate amount of ice-cold swelling buffer (for recipe refer to Table 3.3), which equaled 75% of the cell pellet volume, was added to the cells. Next, the regeneration mix was added at a ratio of 1 µl to 21 µl swelling buffer and cells were subsequently lyzed by physical disruption. For this purpose, cells were sheared 10X using a 26 gauge needle attached to a 1 ml (fNS) or a 3 ml (HeLa S3) syringe, followed by 3 repeated freeze-thaw cycles in liquid nitrogen and 37 ℃ - prewarmed waterbath. Thereafter, cell suspension was centrifuged at 5,000 g and 4 ℃ for 5 min and the supernatant was collected in new mircrotubes. An additional centrifugation step at 14,000 g and 4 ℃ was performed for 60 min and the supernatant including suspended proteins was finally collected in new microtubes.

3.2.4.2. Protein assay

The colorimetric *DC* Protein Assay (Bio-Rad) was used according to the manufacturers protocol to determine the protein concentration of a sample relative to the bovine serum albumine (BSA) standard calibration solution. Eight dilutions with known concentrations of BSA (0, 0.0156, 0.0313, 0.0625, 0.1250, 0.2500, 0.5000 and 1.0000 µg/µl) and appropriate dilutions of the sample (commonly 1:2, 1:5 and 1:10) were prepared. The solution used for diluting standards and samples equaled the cell lysis buffer. A volume of 5 µl of each standard and sample dilution was pipetted in triplicates into the wells of a 96 well-plate. Next, 25 µl of a mixture of 1 ml Reagent A and 5 µl Reagent S was added per well and filled up with 200 µl Folin's reagent solution. After 15 min, absorption at 750 nm was measured with the GENios microplate reader and protein concentration of samples were calculated using the equation of the standard regression line.

3.2.4.3. Protein precipitation

The chloroform/methanol precipitation method was used to concentrate proteins and to eliminate contaminants. All precipitation steps were performed on ice. First, sample volume was increased to 200 µl with lysis buffer, followed by the addition of 1 ml of 2 parts chloroform and 1 part methanol. The mixture was vortexed vigorously for 30 s and proteins were thereafter centrifuged at 20,000 g and 4 ℃ for 30 min. Since proteins used to be concentrated in a layer

between the lower organic and aqueous phase in the microtube, the organic phase was carefully removed by using a Hamilton syringe, thereby avoiding the destruction of the protein layer. Thereafter, the upper aqueous phase was removed so that only the protein layer remained in the microtube. Subsequently, a washing step with 1 ml 100% methanol was performed, thereby vortexing the microtube vigorously for 30 s. Afterwards, cells were centrifuged at 20,000 g and 4 ℃ for 30 min, the liquid phase was removed and the pellet was dried by vacuum centrifugation.

3.2.4.4. Protein electophoresis

The sodium dodecyl sulfate polyacrylamide gel electrophoresis (SDS-PAGE) was used to separate proteins according to their size in an electric field. In this thesis, the Mini-PROTEAN® systems from BioRad were used. Usually 1 mm and after immunoprecipitation 1.5 mm gels were produced by adding the compounds listed in Table 3.9. First, the separating gel was poured and allowed to polymerize, followed by the stacking gel and the application of the appropriate comb. Sample conditioning included a 5 min incubation step at 95 ℃ with 4X Lämmli buffer and the subsequent incubation at RT until samples reached ambient temperature. Optionally, samples assigned to MS were additionally incubated with acrylamide at a final concentration of 1% (w/v) at RT for 30 min. Finally, samples were loaded together with a protein molecular weight marker (PageRuler Prestained Protein Marker) into the pockets of the gel. Usually, gels were run for 10 - 15 min at 80 V, before increasing the current to 120 - 150 V to achieve protein separation.

Table 3.9.: Composition of SDS-Polyacrylamide gels

Compound	stacking gel	separating gel 7.5%	separating gel 10%	separating gel 12.5%	separating gel 15%
total volume	1 ml	5 ml	5 ml	5 ml	5 ml
H_2O	0.604 ml	2.707 ml	2.395 ml	2.082 ml	1.770 ml
40% acrylamide	0.125 ml	0.938 ml	1.250 ml	1.563 ml	1.875 ml
Tris-HCl	0.250 ml (pH 6.8)	1.250 ml (pH 8.8)	1.250 ml (pH 8.8)	1.250 ml (pH 8.8)	1.250 ml (pH 8.8)
10% SDS	10 µl	50 µl	50 µl	50 µl	50 µl
APS	10 µl	50 µl	50 µl	50 µl	50 µl
TEMED	1 µl	5 µl	5 µl	5 µl	5 µl

3.2.4.5. Vacuum drying of SDS-PAGE gel

The SDS-PAGE gel containing ^{35}S-methionine labeled proteins was washed for 5 min with water, followed by two washing steps with 5% (v/v) glycerol for 10 min. The gel preconditioning was performed to avoid gel rupture during the drying procedure. Meanwhile, the gel dryer temperature was adjusted to 80 ℃. Onto the gel dryer plate consecutively two layers of Whatman filter papers, soaked with 5% (v/v) glycerol, and the gel were placed and everything was finally covered with plastic foil. Vacuum was applied and the gel was dried for 2 h at 80 ℃.

3.2.4.6. Western blot

Western blots were conducted using a semi-dry blotter and nitrocellulose membranes. The first layer of the ”sandwich technique” was arranged on the blotter’s anode and consisted of 3 Whatman papers, followed by a nitrocellulose membrane, the SDS-PAGE gel and additional 3

Whatman papers. All layers were soaked with blotting buffer and the arrangement was finally covered with the blotter's cathode lid. Transfer of proteins onto the membrane was subsequently performed for 90 - 110 min at 60 mA per SDS-PAGE gel. Afterwards, the membrane was incubated for 60 min at RT in blocking solution, containing 5% filtered skim milk in TBS-T to minimize unspecific binding of antibodies, followed by two washing steps with TBS-T for 5 min. Next, antibody staining was performed, which was accomplished by incubating the membrane either at 4 ℃ overnight or at RT for 2 h with the appropriate primary antibody, diluted to the appropriate concentration with blocking solution. Before adding the diluted secondary antibody solution (usually 1:5,000 - 1:10,000) for 60 min at RT to the membrane, the blot was washed 3x with TBS-T for 5 min. The blot was washed 2x with blotting solution and 1x with TBS-T and subsequently detection of proteins was conducted by incubating the membrane with ECL Western Blotting Substrate. The secondary antibodies were conjugated to a horseradish peroxidase (HRP) enzyme, which allowed for the visualization of bands using a CCD-camera system from Peqlab. The FUSION CAPT ADVANCE software was used to quantify signals.

3.2.4.7. Proximity-dependent biotinylation and identification of proteins (BioID)

For the BioID assay SILAC-labeled HEK293T cells were used. First, cells were grown in medium without biotin, before transfecting cells with the constructs containing the BirA*-fusion protein for 24 h using TurboFect™. The next day, biotin was added to the medium to a final concentration of 50 µM and biotinylation was enabled for additional 24 h.

3.2.4.8. NeutrAvidin affinity purification

In this thesis, NeutrAvidin™ Agarose was used to selectively purify biotinylated proteins after the BioID assay. For this purpose, NeutrAvidin-agarose beads (supplied as 50% slurry) were washed 3x with 1 bead volume of lysis buffer. Then cleared beads were mixed with cell lysate in a ratio of 200 µl bead slurry per confluent 15 cm cell culture plate. The incubation step was performed at 4 ℃ in an overhead shaker at 20 rpm overnight. The next day, samples were washed thoroughly with four different washing buffers. The washing steps were always carried out in the same way, by first incubating samples with 1 ml washing buffer for 5 min in the ThermoMixer® at 800 rpm and subsequent centrifugation at 500 g for 1 min to remove solution. Samples were washed 2x with 2% (w/v) SDS in ddH_2O, then 1x with a buffer consisting of 0.1% (w/v) sodium deoxycholat, 1% (v/v) Triton X-100, 0.5 M NaCl, 1 mM EDTA, 50 mM HEPES, pH 7.5, afterwards 1x with a buffer containing 250 mM LiCl, 0.5% Tergitol™ NP-40, 0.5% (w/v) sodium deoxycholat, 1 mM EDTA, 10 mM Tris-HCl, pH 8.1 and finally 2x with 50 mM NH_4HCO_3 and 50 mM NaCl. Afterwards, disulfide bonds were reduced by incubating samples at 800 rpm and 56 ℃ for 30 min with 300 µl 10 mM DTT in 0.1 M NH_4HCO_3 and resulting -SH groups were modified with acrylamide (final concentration: 56 mM) by incubating samples at 800 rpm and RT for 30 min.

3.2.4.9. Immunopreciptiation (IP) and co-immunoprecipitation (co-IP)

Immunoprecipitation was performed with two different batch sizes. The IP approach was used to check for Pur-alpha ubiquitinylation, while the co-IP approach was used for interaction partner analysis. For the IP approach 0.5 mg and for the co-IP approach 3 mg of cell lysate was incubated

together with 20 µl (IP) or 500 µl (co-IP) self-made guinea pig serum against Pur-alpha (protein concentration ∼1.1 mg/ml) in an overhead shaker at 20 rpm and 4 ℃ overnight. The control sample consisted of 0.5 mg (IP) or 3 mg (co-IP) cell lysate, incubated with 5 µl (IP) or 100 µl (co-IP) guinea pig preimmune serum and 15 µl (IP) or 400 µl (co-IP) lysis buffer using same conditions. The availability of only a small aliquot of preimmune serum limited its application to the mentioned volumes. The second incubation step was subsequently performed in an overhead shaker at 20 rpm at 4 ℃ for 3 h with the cell-lysate-serum mixture and 20 µl (IP) or 140 µl (co-IP) of Pierce™ Protein A Agarose, previously washed two times with a solution consisting of lysis buffer and 1X protease inhibitor. Afterwards, the mixture was washed 3x with ice-cold lysis buffer and 1X protease inhibitor and 3x with ice-cold 1X PBS. For the IP approach beads remained in the microtube, while for the co-IP approach each sample was transferred to two Micro-Spin columns, washed with the appropriate buffer and centrifuged at 4 ℃ and 1,000 g for 1 min. Thereafter, the IP samples were incubated in 4X Lämmli buffer and the co-IP sample mixture with 2X Lämmli buffer at 95 ℃ for 5 - 10 min. IP samples were centrifuged at 10,000 g for 1 min prior to SDS-PAGE. Co-IP samples were centrifuged at 1,000 g for 1 min, while sample heating and elution was repeated two times. Eluates were stored at -80 ℃.

3.2.4.10. Dissociation of spheres for immunocytochemistry analysis

Neurospheres and oligospheres were transferred into a 15 ml tube, centrifuged at 95 g for 1 min and washed once with 37 ℃ - prewarmed 1X DPBS buffer (PBS, lacking calcium and magnesium). Thereafter, an incubation step of 10 min with 1 ml 37 ℃ - prewarmed StemPro® Accutase® was performed at RT to loosen the cell cluster. Thereafter, cells were mechanically titruated by pipetting cell suspension 40x up and down while pushing the suspension against the wall of the plastic tube using a blue pipette tip. Cells were resuspended in 2 ml of fresh medium (NGM or oligospheres medium) and centrifuged at 437 g for 5 min. The supernatant was discarded and fresh medium containing 20 µM forskolin was added. Cells were finally plated at a density of $3 \cdot 10^5$ to $4 \cdot 10^5$ cells per coated glass coverslip (⌀ 13 mm). To achieve a more efficient attachment of cells, a drop of around 50 µl was first added onto the coverslip and after additional 30 min, medium was added to a final volume of 500 µl. Coating of coverslips was performed for 2 h at 37 ℃ with 20 µg/ml poly-L-ornithine, followed by two washing steps with 1X PBS and a drying step of ∼15 min.

3.2.4.11. Immunocytochemistry staining and microscopy of cells

Fixation of cells was performed with 4% (w/v) paraformaldehyd (PFA) in 1X PBS at RT for 10 min. Coverslips were washed 2x with 1X PBS and stored at 4 ℃ for a maximum of 7 days in 1X PBS. All incubation steps took place in a humid chamber. For this purpose, a wet Whatman paper was arranged on the bottom of the chamber, followed by a layer of Parafilm® M. 20 µl of incubation solution was added onto the Parafilm® M and the coverslips were put the other way round onto the solution to reduce the amount of reagents used. Fixed cells were incubated for 10 min with 0.2% (v/v) Triton X-100 in 1X TBS, except the coverslips used for staining of the cell surface protein NG2. Afterwards, coverslips were washed 2x with 1X TBS for 5 min and blocked with 2% NGS in 1X TBS for 30 min. Washing steps were repeated and incubation with primary antibody in 2% NGS and 1X TBS was performed either at RT for 2 h or at 4 ℃ overnight. Thereafter, coverslips were washed 3x with 1X TBS for 5 min and then incubated

with the appropriate secondary antibody and 4',6-diamidino-2-phenylindole (DAPI), diluted in 2% NGS and 1X TBS, for approximately 90 min at RT in the dark. Again, coverslips were washed 3x with 1X TBS for 5 min and then shortly rinsed 3x with water and finally 1x with 100% ethanol. Coverslips were dried for 10 min at RT in the dark and mounted with Prolong® Gold or Prolong® Diamond antifade reagent on specimen slides. Slides were stored at RT in the dark overnight and thereafter at 4 °C.

Images of immunocytochemistry staining were taken using either the Axiovert 100M (Zeiss) equipped with an AxioCamHR or the Axiovert 200M (Zeiss) equipped with an AxioCamMR3. All pictures were taken using the Plan Apochromat 20x/0.8 objective. The following filter sets were applied using the Axiovert 100M: filter set 01 (excitation BP 365/12, beam splitter FT 395, emission LP 397); filter set 10 (excitation BP 450-490, beam splitter FT510, emission BP 515-565); filter set 15 (excitation BP 546/12, beam splitter FT 580, emission LP 590). The following filter sets were used for the Axiovert 200M: filter set 38 (excitation BP 470/40, beam splitter FT 495, emission BP 525/50); filter set 43 HE (excitation BP 550/25 (HE), emission FT 570 (HE), beam splitter BP 605/70 (HE)); filter set 49 (excitation G 365, beam splitter FT 395, emission BP 445/50).

3.2.4.12. RNA *In vitro* synthesis

The mMESSAGE mMACHINE® kit was used to *in vitro* transcribe plasmids containing a SP6 promoter, like the PCS2-Securin-His8-Sp6 plasmid. First, using restriction enzymes the plasmid was linearized (refer to Section 3.18) and DNA was precipitated by adding 1/20th volume 0.5 M EDTA, 1/10th volume 3 M sodium acetate and 2 volumes of ethanol. The mixture was incubated for 20 min at -20 °C and centrifuged thereafter at 20,000 g and 4 °C for 15 min. The supernatant was removed, the pellet air-dried and finally resuspended in 20 µl ddH_2O. Concentration was determined by NanoDrop and *in vitro* transcription using the compounds mentioned in Table 3.10 was performed according to the manufacturers protocol.

Table 3.10.: Reaction composition for *in vitro* RNA synthesis using the mMESSAGE mMACHINE® kit

Compound	Amount
2X NTP/CAP	10 µl
Enzyme Mix	2 µl
10X Reaction buffer	2 µl
RNasin® Ribonuclease Inhibitor (40 U/µl)	2 µl
linear template DNA	0.1-1.0 µg
Nuclease-Free water	ad 20 µl

At RT, water and ribonucleotides were combined in a microtube prior to the addition of the 10X Reaction Buffer and the remaining compounds. After sample mixing by gently pipetting the reaction mixture up and down, it was incubated in a ThermoMixer® at 37 °C for at least 2 h. Then, 1 µl Turbo DNAse was added and incubated for additional 15 min to remove the remaining template DNA, followed by RNA precipitation using 30 µl lithium chloride solution and 30 µl nuclease-free water at -20 °C over night. The next day, the sample was centrifuged at 20,000 g and 4 °C for 15 min and the remaining pellet was washed once with 1 ml 70% (v/v)

ethanol, followed by an additional centrifugation step. After removing the supernatant, the RNA pellet was air-dried at RT and finally resuspended in 10 - 20 µl and stored at -80 °C.

3.2.4.13. *In vitro* synthesis of ^{35}S-methionine-labeled-protein

Radioactive labeled proteins were *in vitro* synthesized using the three systems, the TnT® Coupled Wheat Germ Extract System, the TnT® Coupled Rabbit Reticulocyte Lysate System and the Rabbit Reticulocyte Lysate System, to evaluate protein degradation in an APC/C-active environment. Using the TnT® Coupled Transcription and Translation Systems, DNA served as template and transcription and translation reaction was concatenated in one reaction. Since the Pur-alpha sequence was expressed under a T7-promoter, the plasmid was linearized prior to synthesis using the restriction enzyme OliI, which cut almost immediately after the Pur-alpha sequence. Subsequently, the DNA fragment was purified by phenol-chloroform-isoamylalcohol purification (refer to Section 3.2.9.7). Securin was expressed under a SP6-promoter, which requires no plasmid linearization. Using the Rabbit Reticulocyte Lysate System, translation of *in vitro* synthesized RNA (refer to Section 3.2.4.12) was performed to obtain radioactive labeled proteins. Prior to synthesis, RNA was incubated for 3 min at 65 °C.

Table 3.11.: Reaction mixture composition for *in vitro* protein synthesis

(a) TnT® Coupled Transcription and Tranlsation System

Compound	Amount
TNT® Coupled Wheat Germ Extract or TNT® Coupled Rabbit Reticulocye Lysate	25 µl
TNT® Reaction Buffer	2 µl
TNT® RNA Polymerase (SP6 or T7)	1 µl
Amino Acid Mixture Minus Methionine, 1mM	1 µl
[^{35}S]methionine	2–4 µl
RNasin® Ribonuclease Inhibitor (40 U/µl)	1 µl
DNA template (0.2 - 2.0 µg/µl)	1 µg
Nuclease-Free water	ad 50 µl

(b) Reticulocyte Lysate System

Compound	Amount
Rabbit Reticulocyte Lysatem Extract	35 µl
Amino Acid Mixture Minus Methionine, 1mM	1 µl
[^{35}S]methionine	2 µl
RNasin® Ribonuclease Inhibitor (40 U/µl)	1 µl
RNA template (1.0 µg/µl)	1 µg
Nuclease-Free water	ad 50 µl

Usually, 1 µg DNA or RNA was incubated together with the radioactive compound (final concentration 0.6 µCi/µl), provided by the EXPRESS ^{35}S-protein labeling mix, and other components mentioned in Table 3.11, according to the manufacturers protocol. The reaction was performed at 30 °C for 90 min for Pur-alpha synthesis, respectively 120 min for Securin synthesis using the Coupled Transcription and Translation Systems and 90 min for both proteins using the Rabbit Reticulocyte Lysate System.

3.2.4.14. Degradation assay

The *in vitro* degradation of Pur-alpha and Securin was performed with a protein extract of synchronized G_1 stage cells from either Hela S3 cells or fNS cells (refer to Section 3.2.4.1), which i. a. provided the active APC/C and the proteasome complex. Additional additives represented ubiquitin conjugating enzyme H10 (UbcH10), ubiquitin-conjugating enzyme E2 S (Ube2S), the regeneration mix (for recipe refer to Table 3.3) and the *in vitro* translated ^{35}S-labeled target. Moreover, either 100 mM carbobenzoxy-Leu-Leu-leucinal (MG132), an inhibitor

of the proteasome, or 1X PBS to adjust the samples reaction volume, was added. The exact composition can be found in Table 3.12. The degradation assay was performed at 300 rpm and 30 ℃ for usually 2 h. Thereafter, samples including 4X Lämmli buffer were incubated at 95 ℃ for 5 min and stored at -20 ℃.

Table 3.12.: Reaction composition for degradation assay

Compound	Degradation reaction	Control reaction
	Volume / Concentration	Volume / Concentration
G1 lysate	20 µl	20 µl
UbCH10 (1 mg/ml)	1 µl	1 µl
Ube2S (1 mg/ml)	1 µl	1 µl
Regeneration Mix	1 µl	1 µl
1X PBS	Volume adjustment	
MG132 (100 mM)	-	10 mM
^{35}S-labeled substrate	depending on its radioacitivity	

3.2.4.15. Detection of radioactive-labeled proteins

Radioactive signals were detected by exposing samples to a phosphorimaging screen. Therefore, the dried SDS-PAGE (refer to Section 3.2.4.5) was attached to a bioimaging plate, which possesses a phosphor layer on a flexible support, and placed into an imaging cassette for usually 24 h. Signals were visualized using the Bioimaging Analysis System from Fuji and were quantitatively evaluated using the AIDA software.

3.2.4.16. Recombinant protein purification and dialysis

GST-fusion proteins were purified from the protein extract (refer to Section 3.2.3.3) by using glutathione agarose beads according to the manufacturers protocol for purification of GST-tagged proteins using the batch method. For this purpose, 500 µl of equilibrated resin was incubated together with the protein extract and the appropriate amount of equilibration/wash buffer in a 50 ml plastic tube in an overhead shaker at 25 rpm and 4 ℃ for 1 h. Thereafter, samples were centrifuged at 700 g for 2 min and washed with 5 ml of equilibration/wash buffer. Both steps were repeated once. Subsequently, absorption of eluted fractions was photometrically assessed at 280 nm against the elution buffer to check for protein containing fractions.

Protein fractions were collected in an equilibrated ZelluTrans (MWCO: 6 - 8 kDA) dialysis membrane device and dialyzed overnight against 1.5 l 10 mM NH_4HCO_3, pH 7.9 to remove contaminating reagents. Buffer exchange was performed 3x with increasing dialysis periods. The next day, volume reduction of the dialysate was achieved by shock freezing samples with liquid nitrogen, followed by a vacuum centrifugation step at RT for 22 h.

3.2.4.17. Purification of Pur-alpha antiserum

In order to specifically isolate antibodies targeting Pur-alpha from the complex immune serum of a guinea pig, immunized with the GST-Pur-alpha fusion protein (done by Pineda antibody service), the immunoaffinity support reagent Affi-Gel 15 was used according to the manufactures

instructions. The reagent consists of an agarose gel bead support, crosslinked to a neutral 15-atom spacer arm with an N-hydroxysuccinimide ester, which reacts spontaneously with free alkyl or aryl amino groups by forming a stable amide bond. Every step of the purification procedure was performed in the cold room and additionally ice-cold solutions were used. First, the appropriate amount of Affi-Gel was transferred into a microtube, washed 2x with ddH_2O and centrifuged in between at 3,000 g for 30 s. Subsequently, the slurry was resuspended in dialysis buffer (10 mM NH_4HCO_3, pH 7.9), mixed with the purified target protein and incubated for 4 h in an overhead shaker at 25 rpm. Following this, a small volume of the reaction mixture was collected by centrifugation to check for successful coupling of protein to the immunoaffinity support by SDS-PAGE and subsequent Coomassie Blue staining. After confirming that almost all protein molecules were bound to the column, 0.1 ml of 1 M ethanolamine pH 8 were added per 1 ml of Affi-Gel and the reaction mixture was incubated for an additional hour to saturate all reactive groups of the immunoaffinity column. Thereafter, the mixture was transferred onto 10 ml Poly-Prep® chromatography columns to wash and equilibrate the agarose gel beads. Therefore, the appropriate amount of dialysis buffer was added onto the column, which in turn was placed in a tube to collect the flow-through. Further washing steps consisted of 10 ml 1X PBS buffer, 10 ml elution buffer (100 mM glycin pH 2.4, 150 mM NaCl) and again 10 ml 1X PBS. Meanwhile the immune serum was heat inactivated at 56 °C for 30 min to destroy complement factors, before adding the solution to the conditioned column for 5 min. By removing the stopper on the opening on the bottom of the column, the solution was collected in a tube by gravity-flow and was again transferred onto the column to perform an additional incubation step for 5 min. Next, column was washed with the appropriate amount of 1X PBS, before eluting antibodies 10X with 1 ml of an acidic buffer, consisting of 100 mM glycin pH 2.4 and 150 mM NaCl, into microtubes containing 200 µl 1 M Tris-HCl buffer pH 8. Fractions containing the Pur-alpha antibody were determined by SDS-PAGE and subsequent Coomassie blue staining of heavy and light antibody chains. Finally, positive fractions were supplemented with 0.02% (w/v) sodium azide for preservation and stored at 4 °C for further usage.

3.2.5. Sample preparation for mass spectrometry analyses

3.2.5.1. In-gel digestion

First, proteins were stained with Coomassie Blue, before excising gel regions or protein bands of interest with a sharp scalpel and cut them into small pieces of around 1x1 mm. Next, gel pieces were destained with 500 µl 30% (v/v) acetonitrile (ACN) and 0.07 M NH_4HCO_3 in a ThermoMixer® at 800 rpm and RT for 30 min, followed by liquid removal. Destaining was repeated several times until gel pieces were free of blue color. Thereafter, gel pieces were incubated in 500 µl ACN at 800 rpm and RT for 15 min and dehydrated gel pieces turned white. Solution was completely evaporated in a vacuum centrifuge at 60 °C and in-gel digestion was performed. Therefore, 10 µl trypsin solution (50 ng/µl in 0.1 M NH_4HCO_3) was added to every sample, shortly incubated, before filling samples up with 0.1 M NH_4HCO_3 to 50 µl. After 10 min, gel pieces were finally completely covered with 0.1 M NH_4HCO_3 and incubated at 37 °C overnight. The next day, solution including peptides was transferred into a new microtube and remaining peptides were extracted from the gel matrix. This was accomplished by three extraction steps, proceeded at RT for 15 min in the ThermoMixer® at 800 rpm. First, peptides were extracted with 50 µl 0.1% (v/v) trifluoroacetic acid (TFA) and 50% (v/v) ACN. After

transferring the extracts into a new microtube, gel pieces were first incubated with 50 µl 0.1 M NH_4HCO_3 for 15 min and then with additional 100 µl ACN for 15 min. Samples containing the combined peptide extracts were evaporated in a vacuum centrifuge at 60 ℃.

3.2.5.2. On-bead digestion

The on-bead digestion protocol was used after NeutrAvidin affinity purification of Bio-ID samples (Subsection 3.2.4.8). For this assay, the beads-protein mixture, already washed with a buffer suitable for digestion with trypsin (BioID lysis buffer (Subsection 3.2.4.1)), was first incubated with 10 mM DTT in 0.1 M NH_4HCO_3 at 56 ℃ for 30 min under constant agitations at 800 rpm to achieve reduction of disulfide bonds. The resulting sulfhydryl groups were thereafter alkylated with acrylamide at a final concentration of 56 mM at RT for 30 min, under constant agitation. On-bead digestion was performed at 37 ℃ overnight by adding 5 µg of trypsin, diluted in 300 µl 0.1 M NH_4HCO_3, to the samples. The next day, solutions containing peptides were transferred into fresh microtubes and extraction of residual bound peptides was performed with 2x 300 µl 5% ACN and 0.1% FA in the ThermoMixer® at 800 rpm and RT for 15 min. Finally, solutions containing peptides were combined in one microtube for further processing.

3.2.5.3. In-solution digestion of precipitated proteins with *Rapi*Gest™

Digestion of precipitated proteins was performed with trypsin in 0.1% *Rapi*Gest™ SF Surfactant, a reagent which facilitates the enzymatic digestion of proteins. First, the protein pellet (130 µg protein) was resuspended in 65 µl 0.1% (v/v) *Rapi*Gest™ in 100 mM triethylammonium bicarbonate (TEAB) pH 8.5 and incubated at 900 rpm and 37 ℃ in the ThermoMixer® for 15 min. Subsequently, 0.6 µg of trypsin was added to the sample, followed by an incubation period of 90 min at 900 rpm and 37 ℃. Disulfide bonds were cleaved by adding 8 µl 50 mM DTT to the reaction mixture at 56 ℃ for 45 min, followed by alkylation of the formed sulfhydryl groups with 10 µl 450 mM acrylamide in 100 mM TEAB pH 8.5 at RT for 30 min. Subsequently, a second digestion reaction was performed with 1.5 µg of trypsin in 100 mM TEAB pH 8.5 at a final volume of 130 µl. In-solution digestion was carried out at 37 ℃ overnight.

3.2.5.4. In-solution digestion of proteins by FASP method

Initially, the appropriate amount of 1 M DTT stock solution in 0.1 M HEPES pH 7.6 was added to 100 µg of protein to obtain a final concentration of 0.1 M DTT. Samples were then incubated at 95 ℃ for 5 min and cooled down to RT. 30 kDa cut-off filters (Microcon® 30K devices) were used for filter aided sample preparation (FASP). Samples were loaded and washed with 2x 200 µl 8 M Urea in 0.1 M HEPES pH 8.5 (UA) and centrifuged at 14,000 g for 15 min in between. Following centrifugation steps to elute UA were always performed at 14,000 g for 15 min, since it was determined to be the optimal time to ensure the complete flow through of UA without risking sample drying. Afterwards, 100 µl 0.05 M acrylamide in UA solution was added onto the filter and incubation of samples was first performed for 1 min at RT and 600 rpm in a ThermoMixer® and then for 20 min without agitation. Samples were centrifuged at 14,000 g for 10 min and washed with 3x 100 µl of UA and centrifuged in between. Thereafter, 3x 100 µl 0.05 M HEPES pH 8 buffer was passed through the filters by centrifuging devices at 14,000 g for 10 min. Digestion with trypsin was performed in 60 µl 0.05 M HEPES pH 8, at a ratio of 1 µg of

trypsin per 100 µg of protein. After incubation of samples at 600 rpm in a ThermoMixer® for 1 min, samples were stored at 37 ℃ in a wet chamber overnight to ensure complete digestion of proteins in a humid ambiance. The next day, filters were transferred into new collection tubes.

3.2.5.5. Labeling with TMTsixplex™

The Tandem Mass Tag™ technique is a common method to quantify proteins in multiple samples in a single experiment using mass spectrometry. TMT label reagents were removed from the freezer and immediately equilibrated to RT and dissolved in 41 µl 100 % ACN for 5 min under occasional vortexing. Vials were briefly centrifuged and each TMT label reagent was combined with one sample (corresponding to 25 - 100 µg protein digest). The labeling reaction was carried out at RT for 90 min (60 min for samples prepared with the FASP method), before adding 8 µl 5 % (w/v) hydroxylamine in 0.1 M TEAB pH 8.5 (0.1 M HEPES pH 8.5 for FASP) to the sample, mixing and incubating for additional 15 min to quench the reaction. Using the FASP method, some additional steps were performed, including the addition of 40 µl 0.1 M HEPES pH 8.5, incubation of samples in the ThermoMixer® at 600 rpm and RT for 1 min and a final centrifugation step at 14,000 g for 10 min. Another washing step with 40 µl 0.1 M HEPES pH 8.5 and centrifugation step was performed, before eluting samples with 50 µl 0.5 M NaCl solution from the filter units by centrifugation at 14,000 g for 10 min.

Up to six samples, all labeled with a different TMT label reagent, were combined at equal amounts and reduced to ∼200 µl in a vacuum centrifuge at 60 ℃. Finally, the concentration of ACN was minimized to ensure binding of peptides to the reversed-phase material (Section 3.2.5.7). Therefore, 200 µl 0.1% (v/v) TFA were added and samples were thoroughly mixed and again concentrated to 200 µl using a vacuum centrifuge. The last steps were repeated several times until the final concentration of ACN in the sample dropped below 5%.

It should be noted that TMT-labeling of immunoprecipitation samples was performed after in-gel digestion and peptide extraction. Since in solution TMT-labeling interacts with primary amines, it was necessary to remove the NH_4HCO_3 buffer by resuspending samples in 50 µl 0.1% (v/v) FA and evaporating samples until dryness in a vacuum centrifuge at 60 ℃. Samples were afterwards desalted on Oasis HLB cartridges (Section 3.2.5.7), again vacuum dried and finally resuspended in 100 µl 0.1 M HEPES pH 8 prior to TMT-labeling.

3.2.5.6. *Rapi*Gest removal

*Rapi*Gest removal was accomplished by adding 100% TFA to a final concentration of 5%. The reaction was carried out in the ThermoMixer® at 1,000 rpm and 37 ℃ for 45 min. After sample centrifugation at 20,000 g for 30 min, the supernatant was carefully collected, while avoiding to touch the pellet on the bottom of the microtube.

3.2.5.7. Sample cleanup by solid phase extraction (SPE)

Oasis HLB cartridges were used to remove salts, detergents and certain acids from samples. First, cartridges were activated by applying 4x 1 ml of 70% ACN, 0.1% FA, followed by equilibration with 4x 1 ml of 0.1% FA. Next, the acidified sample was passed slowly through the cartridges. This procedure was repeated two times with the collected sample flow-through, followed by ten washing steps with 1 ml of 0.1% FA. The sample was subsequently eluted, first with 500

µl 30% ACN, 0.1% FA, followed by 500 µl 50% ACN, 0.1% FA and finally 300 µl 70% ACN, 0.1% FA. Every step was repeated two times by passing the flow-through again through the cartridges before applying the next solution containing higher ACN content. Finally, eluates were combined and the sample was completely dried in a vacuum centrifuge at 60 ℃.

3.2.5.8. Isoelectric fractionation of peptides (OFFGEL)

A 3100 OFFGEL fractionator from Agilent was used for isoelectric focusing in immobilized pH gradient (IPG) gel strips. Based on the sample complexity either fractionation into 12 fractions or 24 fractions was performed. First, the IPG gel strip (pH 3 - 10, 13 cm or 24 cm) was assembled into the tray and fixed with a 12 or 24-well plastic frame as described in the instruction manual. Rehydration of the strip was performed with 20 µl IPG buffer pH 3 - 10 for at least 30 min while not exceeding 2 h. Likewise, the dried sample was conditioned with 3.6 ml of IPG buffer, before adding equal sample volumes into each well of the tray. A high voltage was applied to the ends of the gel strips, accomplishing the separation of peptides into 12 or 24 fractions overnight. Detailed instrument settings are given in Table 3.13. The next day, each fraction was transferred into a new microtube. For complete extraction of peptides 150 µl 0.1% TFA was added into every well of the tray, incubated for 15 min and extracts were finally combined with the corresponding fractions and dried in a vacuum centrifuge at 60 ℃.

Table 3.13.: Offgel program for 12 and 24 fractions

12 well	Volt Hour (kVh)	Voltage (V)	Current (µA)	Power (mW)	Time (h)
Focussing	20	4500	50	200	100
Hold	-	500	20	50	-

24 well	Volt Hour (kVh)	Voltage (V)	Current (µA)	Power (mW)	Time (h)
Focussing	50	4500	50	200	100
Hold	-	500	20	50	-

3.2.5.9. Strong Anion exchange (SAX) chromatrography

Adapted from [Wiśniewski et al., 2009], the chromatography was performed with Britton and Robinson Elution Buffers of different pH-values. Therefore, 5X stock solutions of 0.1 M acetic acid (AcOH), 0.1 M phosphoric acid and 0.1 M boric acid were prepared and titrated with NaOH to a pH-value of 11, 8, 6, 5, 4 and 3. Afterwards, buffers were diluted with H_2O to 1X and NaCl was added in a final concentration of 0.25 M to the buffer pH = 3 to achieve complete elution of peptides. In this thesis, self-made SAX StageTips were used. Accordingly, for every experiment one SAX tip containing 12 layers of 3M™ Empore™ Anion Exchange-SR disks in a 200 µl pipette tip and six StageTips containing C18-sorbents (Section 3.2.5.10) were produced. Before sample loading, activation and conditioning of StageTips was performed by washing tips with first 100 µl methanol, followed by 100 µl 1 M NaOH and 2x 100 µl buffer 11 with centrifugation steps in between at 500 g for 3 min. SAX tips were also conditioned, using first 100 µl methanol, then

100 µl 80% ACN, 0.5% AcOH and finally 100 µl 0.5% AcOH with 1 min centrifugation steps at 500 g in between. Meanwhile, samples were conditioned by diluting dried samples with 200 µl buffer pH = 11 so that all peptides were negatively charged. Next, the SAX tip was placed into a C18 StageTip, which in turn was fixed in a hole in the lid of a microtube. The sample was loaded onto the SAX tip and centrifuged at 5,000 g for 3 min. Elution of peptides was performed with buffers of different pH-values, by starting with buffer pH = 11. and ending with buffer pH = 3. The solutions were always eluted from the SAX tip by centrifugation at 5,000 g for 3 min into an equilibrated C18 StageTip, before proceeding to the next C18 StageTip and eluting with a buffer of lower pH-value. Finally, peptides were eluted from the C18 StageTips with 2x 10 µl 80% ACN, 0.5% AcOH and dried in a vacuum centrifuge at 60 ℃.

3.2.5.10. Peptide cleanup with StageTips

Sample cleanup using self-made stop-and-go-extraction tips (StageTips) was performed according to Rappsilber and co-workers [Rappsilber et al., 2007]. Six layers of C18 mesh material were placed in 200 µl tips, which in turn were placed in self-made adapters fitting into 1.5 ml microtubes. By centrifuging the devices at 3,000 g for 1 min, solutions were eluted into the microtubes. Two buffers were used in this experiment, consisting of the washing buffer A (0.5% AcOH in H_2O) and the elution buffer B (0.5% AcOH in 80% ACN).

Prior to sample loading, StageTips were equilibrated by first adding 20 µl methanol, followed by 20 µl buffer B and finally 20 µl buffer A. Meanwhile, dried samples were dissolved in 100 µl of 1% ACN, 1% FA in the ultrasonic water bath for 5 min and subsequently loaded onto the StageTips. After centrifugation, retained peptides were washed by adding 100 µl buffer A onto the columns and eluted into a fresh microtube with 2x 20 µl elution buffer B. Next, samples were evaporated by vacuum centrifugation to remove the organic solvent excess, before dissolving peptides in 20 µl 5% ACN, 5% FA. Following centrifugation at 18,000 g for 15 min, peptide solution was finally applied to LC-MS/MS system.

3.2.6. Mass spectrometric measurements

Mass spectrometric analyses of peptides were conducted using a LC-MS/MS system, composed of an Easy-nLC 1000 nano liquid chromatography device, coupled to a LTQ Orbitrap Velos mass spectrometer. Following LC/MS grade solvents were used for system maintenance and sample measurement: solvent A, consisting of 0.1% FA in H_2O and solvent B, consisting of 0.1% FA in ACN. Self-made fused silica capillaries with an outside diameter (OD) of 360 µm and an inside diameter (ID) of 100 µm were generated with a P2000 laser tip puller and packed with C18-reversed phase material (5 µm ReproSil-Pur 120 C18-AQ particles) to achieve separation of peptides. Furthermore, a linear gradient of 60 min was applied at a flowrate of 400 nl/min, followed by two short column flushes at 95% solvent B and a column equilibration of 10 min at the end of every sample. Refer to the Table 3.14 for more detailed gradient information.

Orbitrap survey spectra, covering a mass range of 400 - 1,200 m/z, were acquired with a resolution of 30,000 at m/z 400. MS/MS spectra, obtained by collision-induced dissociation (CID) of peptides, were measured with the LTQ ion trap, set to a minimal signal required of 5,000, an isolation width of 2 m/z and a normalized collision energy of 35%. In contrast, MS/MS spectra, obtained by higher-energy collisional dissociation (HCD) of peptides, were analyzed in the Orbitrap, adjusted to a minimal signal required of 5,000, an isolation width of

Table 3.14.: Profile of a 60 min gradient LC-MS/MS run

Gradient	Time (min)	Solvent B (%)
60 min	0	1
	60	35
	61	95
	64	1
	67	95
	70	1
	80	1

2 m/z, a normalized collision energy of 42% and a resolution of 7,500 at 400 m/z. The lowest mass value for Orbitrap MS/MS was set to 100 m/z. The system was set to select the 10 most abundant peaks from each survey scan for following fragmentation analysis, independent of CID or HCD fragmentation. In order to reduce repeated fragmentation reactions of the same peptides, dynamic exclusion was enabled (repeat count: 1, repeat duration: 30 s, excl. list size: 500, excl. duration: 30 s, excl. mass width relative to mass, excl. mass width relative to low/high: 10.00 ppm, expiration count: 1, expiration S/N threshold: 3.0).

3.2.7. Mass spectrometry data analysis

3.2.7.1. Protein identification and quantification with MaxQuant

Analyses of the raw MS files from the neurosphere experiment were conducted using the quantitative proteomics software package MaxQuant version 1.3.0.5 [Cox & Mann, 2008] [Cox et al., 2011] against a murine UniProtKB/TrEMBL database (50,850 entries, ipi.MOUSE.v3.87.fasta from 07/2013). All acquired raw files (five replicates and two technical replicates) were included in one single search. The MaxQuant default settings were used for data analysis.

Alternatively, MaxQuant version 1.5.2.8 was used to analyze data sets acquired from BioID- and co-IP experiments. Default settings were applied with the following modifications: Top MS/MS peaks per 100 Da (FTMS) = 12, Top MS/MS peaks per 100 Da (ITMS) = 8, PSM FDR = 0.01, Min. delta score for modified peptides = 6, disabled: Re-quantify and Match between runs. Both analyses were conducted against the reviewed Swissprot database, either based on human species (20,129 entries, from 12/2016) or murine organism (16,839 entries, from 12/2016). For SILAC-quantification (BioID) the standard method with two labeling states was selected. While for the light channel no isotope labels were selected, the heavy channel was set to Arg+10 and Lys+8. The quantification parameters were the following ones: Use only unmodified peptides = True, Modifications included in protein quantification = Acetyl (Protein N-term), Oxidation (M), Biotinylation (Protein N-term, K), Peptides used for protein quantification = Razor, Discard unmodified counterpart peptides = True, Min. ratio count =2.

3.2.7.2. Protein identification and quantification with Proteom Discoverer

The OPC differentiation experiment was analyzed using the Proteome Discoverer™ 2.1 software with the in-house Mascot search engine [Cottrell & London, 1999]. All raw files (four

biological and one technical replicate) were included in one single search against the rat UniProtKB/TrEMBL database (25,841 entries, from 05/2015). The Spectrum Selector Node was used with default settings. Top MS/MS peaks per 100 Da was set to 12. The following Mascot search parameters were applied: Precursor mass tolerance 10 ppm, Fragment mass tolerance: 20 mmu, Maximum missed cleavage sites: 1, fixed modification: propionamide, dynamic modification: oxidation (M); acetylation (N-term protein); pyro-Glu (N-term E); pyro-Glu (N-term Q) and additionally for the labeling experiment: TMT6plex (N-term and lysine residues). The false discovery rate calculation on PSM level was performed using the Percolator node with following decoy database search parameters: Target FDR (Strict): 0.01, Target FDR (Relaxed): 0.05, Validation based on: PEP. Based on the TMT 6-plex derived reporter ion intensities relative quantification was performed using the Reporter Ions Quantifier Node with default settings.

3.2.8. Bioinformatic analysis

3.2.8.1. Limma

Processed data of the neurospheres and OPC experiments were analyzed using the moderated t-test method, which is implemented in the software package limma in R/Bioconductor (http://bioinf.wehi.edu.au/limma/) [Ritchie et al., 2015].

3.2.8.2. Rank product

With the rank product software package, also implemented in R/Bioconductor a second approach was used to determine significant differences in protein expression (https://bioconductor.org/packages/release/bioc/html/RankProd.html) [Hong et al., 2011].

3.2.8.3. Perseus

The Perseus version 1.5.5.3 (http://www.perseus-framework.org, Cox & Mann) was used to statistically analyze the acquired data from BioID and co-IP experiments. For this purpose the evidence files, compiled by MaxQuant, were used. The evidence file consists of all identified amino acid sequences with their measured intensities and the assigned protein. First, potential contaminants and reverse hits were removed from the data list. For the co-IP experiments, target versus control ratios of each protein and experiment were computed, followed by the removal of all proteins which did not exhibit valid values in at least two of three replicates. Afterwards, target to control ratios of every peptide belonging to the same leading razor protein were combined by calculating the median. Thereafter, the expression ratios were log2 transformed, followed by data normalization to the median of all ratios belonging to one experiment. For the SILAC-BioID experiment, SILAC heavy to light ratios (bait/control) were calculated for every protein and replicate. Thereafter, all ratios belonging to the same leading razor protein were combined by determining the median, followed by removing all proteins without valid values in at least two of three replicates. Thereafter, log2 transformation and normalization of the H/L ratios to the median of all ratios within one experiment was performed. Calculated expression ratios were finally statistically evaluated using the one-sample T-test in combination with the Benjamini Hochberg correction for multiple hypotheses.

3.2.8.4. Gorilla

The GOrilla tool (http://cbl-gorilla.cs.technion.ac.il, [Eden et al., 2009]) was used to accomplish large scale gene function analyses to identify enriched GO terms in ranked lists of genes. In this thesis, analyses were performed with two unranked lists, consisting of a target and a background list. Significantly enriched proteins were thereby implemented in form of their identifiers, the leading razor proteins and were searched against all conceivable proteins of the appertaining experiments, identified using MaxQuant or Proteome Discoverer (background list). Finally, enriched GO terms were identified using the standard Hyper Geometric testing, which calculates a p-value for every GO term, indicating the degree of enrichment within the target list. By setting the significance threshold to the default p-value of 0.001, every GO term was filtered out which exhibited a higher p-value.

3.2.8.5. BiNGO

The BiNGO 3.0.3 tool (https://www.psb.ugent.be/cbd/papers/BiNGO/Home.html) was used on the Cytoscape software platform to perform overrepresentation analyses of GO terms [Maere et al., 2005]. In this thesis, the tool was used to determine which GO categories were statistically overrepresented in the OPC dataset by analyzing all up- and downregulated proteins against the whole GO annotation set for the rat proteome provided by UniProt (from 06/2015). Further, GO term lists implemented in the go-basic.obo file, provided by the Gene Ontology Consortium, were used for assignment.

3.2.8.6. REViGO

After complex GO term enrichment analyses, the REViGO tool (http://revigo.irb.hr/) was used to facilitate the interpretation of obtained results [Supek et al., 2011]. The software processes a long GO term list, together with the calculated p-values by summarizing the input and removing redundant GO terms, dependent on the chosen similarity level. In this thesis the default settings were used, with exception of the database, which was adjusted to the appropriate species.

3.2.8.7. qPCR data analysis: ΔΔCt method

The ΔΔCt method is a common method to perform comparative quantification of expression level of a gene of interest, relative to a control sample (calibrator), which could be an untreated or a wild-type sample. The method further includes the normalization to a house keeping gene (normalizer), to increase the reliability of the determined values. This also includes that the normalizer gene is validated beforehand, individually for every sample type and sample workflow. The exact formula of the ΔΔCt method is shown below, using the housekeeping gene glyceraldehyde-3-phosphate dehydrogenase (GAPDH) exemplarily. In the first step, the target threshold cycle (Ct) value of every sample was subtracted from the normalizer Ct value of the same sample, following the subtraction of the calculated value of the gene of interest from the calculated value of the calibrator. The relative expression level is then simply determined by calculating 2 to the power of -ΔΔCt.

$$\Delta\Delta C_t = (C_{t,\text{target}} - C_{t,\text{GAPDH}})_{\text{day}>0} - (C_{t,\text{target}} - C_{t,\text{GAPDH}})_{\text{day}\,0}$$

$$\text{relative expression level} = 2^{-\Delta\Delta C_t}$$

3.2.9. Nucleic acid and cloning techniques

3.2.9.1. RNA isolation

Cell lysis and sample homogenization was performed with 0.75 ml Trizol® Reagent per $5-10\cdot10^6$ cells by passing the cell suspension 10X through a 21 G needle, attached to a 1 ml syringe. The homogenized sample was incubated for 5 min at RT to facilitate complete nucleoprotein complex dissociation, before adding 100 µl of the phase separation reagent 1-bromo-3-chloropropane (BCP) per 1 ml of sample. After vortexing microtubes for 30 s and incubating samples at RT for additional 5 min, samples were centrifuged at 12,000 g and 4 ℃ for 15 min. The upper aqueous phase, containing RNA molecules, was transferred into a new tube, without touching the interphase. RNA was precipitated by adding 500 µl isopropanol per 1 ml of Trizol, vortexing and incubating samples for 10 min at RT. After centrifugation at 12,000 g and 4 ℃ for 10 min, the RNA pellet was isolated and washed with 0.5 ml 75% (v/v) ethanol. An additional centrifugation step at and 12,000 g and 4 ℃ for 10 min was appended and the supernatant discarded and the RNA pellet air-dried. Finally, RNA was resuspended in 40 µl diethyl pyrocarbonate (DEPC)-treated water and incubated for 10 min at RT, followed by 15 min at 55 - 60 ℃ in the waterbath. RNA concentration was determined using the NanoDrop 2000 UV-Vis spectrophotometer.

3.2.9.2. RNA purification

Isolated RNA was purified using the RNeasy Mini Kit (Qiagen) and the RNase-free DNase Kit (Qiagen). All steps were performed and solutions prepared according to the manufactures protocol. The sample volume was adjusted to 100 µl with DEPC-treated water, 350 µl RLT buffer plus β-mercaptoethanol was added and samples were thoroughly mixed. Subsequently, RNA was precipitated with 250 µl ethanol, thoroughly mixed by pipetting up and down and loaded onto a RNeasy mini column. All following centrifugation steps were performed at 8,000 g for 15 s. After the first centrifugation step, the flow-through was discarded and the sample was washed with 350 µl RW1 buffer, followed by a second centrifugation and removal of the flow-through. Since genomic DNA was probably isolated together with RNA, samples were treated for 15 min at RT with DNase I working solution, composed of DNase I stock solution and buffer RDD, followed by a washing step with 350 µl RW1 buffer plus centrifugation. After discarding the flow-through, the column was transferred to a fresh collection tube and samples were washed with 2x 500 µl RPE buffer and the flow-through was removed in between by centrifugation. Next, columns were centrifuged at 8,000 g for 2 min and subsequently at 12,000 g for 1 min after exchanging to a fresh collection tube. Finally, RNA was eluted with 30 - 50 µl DEPC-treated water into a fresh microtube by centrifugation at 8,000 g for 1 min and RNA concentration and purity was estimated with the NanoDrop photometer and/or an agarose gel.

3.2.9.3. Polymerase chain reaction (PCR)

The polymerase chain reaction is a common technique to amplify a DNA template, which only exists in single or few copies. For the amplification of the Pur-alpha-constructs and the myc-BioID-construct almost the same thermocycling conditions and reaction mixtures were used. The exact composition can be found in Table 3.15. For the myc-BioID reaction HF-buffer was used, whereas for the Pur-alpha reaction the GC-buffer was used in combination with DMSO, because of the high content of guanine and cytosine nucleotides. The PCR was conducted on a Biometra

T3 Thermocycler with a heated lid, applying the adjusted program shown in Table 3.15. The effective annealing temperatures of the primers amounted 62 °C for the amplification of myc-BioID and 67 °C for the amplification of Pur-alpha. After PCR reaction, samples were separated by agarose gel electrophoresis (Subsection 3.2.9.7) and DNA was subsequently extracted using the PureLink® Quick Gel Extraction Kit (Subsection 3.2.9.8) according to the manufactures instructions. Alternatively, samples were purified and recovered for subsequent reaction steps using the QIAquick PCR Purification Kit (Qiagen), according to the manufacturers protocol.

Table 3.15.: PCR reaction mixture composition and PCR thermocycling program

Component	20 µl Reaction	Final conc.
	Volume / amount	
Template DNA	10 - 20 ng	
5X GC / HF Buffer	4 µl	1X
2 mM dNTPs	2 µl	0.2 mM
10 µM Forward Primer	1 µl	0.5 µM
10 µM Reverse Primer	1 µl	0.5 µM
DMSO	0.6 µl	3%
Phusion DNA Polymerase	0.2 µl	0.4 Units
ddH_2O	ad 20 µl	

Step	Temperature	Time
Initial Denaturation	98°C	120 seconds
30 Cycles	98°C	30 seconds
	67°C / 62°C	30 seconds
	72°C	60 seconds
Final Extension	72°C	180 seconds
Hold	4°C	

3.2.9.4. cDNA synthesis by reverse transcription polymerase chain reaction (RT-PCR)

The synthesis of first-strand cDNA from RNA was performed with the SuperScript™ II Reverse Transcriptase kit. The synthesis was set up and proceeded in a thermocycler passing a defined cycling program, based on the manufactures protocol for the enzyme. As template, up to 5 µg of RNA was used, diluted with DEPC-treated water to a final volume of 10 µl. First, samples were placed in the thermocycler and preheated to 65 °C. Next, 1 µl of oligo(dT)-primer was added to each sample and reaction was performed at 65 °C for additionally 10 min to ensure the existence of single stranded RNA. The reaction was then cooled down to 4 °C for 2 min. Thereafter, the first strand master mix (exact composition is listed in Table 3.16) was added to every sample, followed by an incubation step at 42 °C for 2 min. The reaction mixture was again cooled down to 4 °C and reverse transcription was initiated by adding 1 µl of the enzyme SuperScript II Reverse Transcriptase to the reaction mixture. The reaction was performed at 42 °C for 1 h, before increasing the temperature to 70 °C for 15 min and finally decreasing it to 4 °C. The obtained cDNA samples were diluted in a ratio of one volume cDNA to ten volumes of water and a test PCR with different primers was performed to check for successful reversed transcription. Samples were afterwards stored at -20 °C for real-time PCR (qPCR) analyses.

Table 3.16.: RT-PCR reaction mixture composition

Compound	Volume
First-Strand-Buffer (5x)	4 µl
DTT (100 mM)	2 µl
dNTP (10 mM)	1 µl
ddH_2O	ad 1 µl

3.2.9.5. Quantitative real-time polymerase chain reaction (qPCR)

In this thesis the quantitative RT-PCR was performed using the SYBR® Select Master Mix (Applied Biosystems), which provided the reporter molecule SYBR Green I dye. The composition of the reaction mixture is shown in Table 3.17. In a 96-well plate 5 µl cDNA samples or water (control) were mixed together with 1 µl of the appropriate forward and reverse primer (10 µM), 10 µl SYBR® Select Master Mix and 3 µl ddH_2O. The reaction was afterwards conducted with the Applied Biosystems 7300 RT PCR System, using the amplification program shown in Table 3.17. Data analysis was performed using the SDS version 1.4 software and Ct values were manually assessed by adjusting the baseline and Ct value threshold according to the manual from Applied Biosystems (Data analyses on the ABI PRISM® 7700 Sequence Detection System: Setting Baselines and Thresholds, 2002). Every target and control sample was measured in triplicates and Ct values were finally used to calculate the mean Ct value.

Table 3.17.: qPCR reaction mixture composition and program

Compound	Volume
cDNA	5 µl
SYBR® Select Master Mix	10 µl
Forward primer (10 µM)	1 µl
Reverse primer (10 µM)	1 µl
ddH2O	3 µl

Stage	Step	Cycles	Temperature [°C]	Time [min]
1	Activation UDG	1	50	02:00
2	Activation DNA Polymerase	1	95	02:00
3	Denature	40	95	00:15
	Anneal & Extend		60	01:00
4	Dissociation (4 steps)	1	95	00:15
			60	00:20
			95	00:15
			60	00:15

3.2.9.6. Restriction digest

Restriction endonucleases, recognizing stereotypical sequences within the DNA, from either ThermoScientific or NEB were used to cleave the DNA phosphodiester bounds. The digestion reaction usually took place at 37 °C for 2 h with the following composition (Table 3.18).

Table 3.18.: Reaction mixture composition for restriction digest

Compound	Volume/amount
10X restriction buffer	2 µl
DNA	1 - 2 µg
Restriction enzyme (10 units/µl)	1 µl
ddH_2O	ad 20 µl

3.2.9.7. DNA purification

Phenol-Chloroform-Isoamylalcohol extraction First, DNA sample volumes were increased to 100 µl with ddH_2O. Subsequently, DNA was extracted with 100 µl phenol-chloroform-isoamylalcohol (25:24:1), samples were vortexed thoroughly for 30 s and centrifuged at 18,000 g and RT for 20 min. The upper aqueous layer, containing the DNA molecules, was transferred into a new tube and another purification step was performed. For this purpose, 100 µl chloroform was

added to the samples, vortexed and centrifuged at 18,000 g for 20 min. Optionally, this step was repeated once again, before precipitating nucleic acids with 1/10 volume of 3 M sodium acetate solution, 1/20 volume of EDTA and 2 volumes of ethanol. Samples were incubated overnight at -80 ℃ and centrifuged at 18,000 g and 4 ℃ for 20 min. Finally, the DNA pellet was washed 1x with 70% (v/v) ethanol and dried at RT before resuspending it in 20 µl ddH_2O.

Agarose gel electrophoresis The agarose gel electrophoresis method was used to separate DNA or RNA fragments according to their length. It was applied either to confirm the expected size of a PCR product, after minipreparation to determine positive clones or after restriction digest to separate and purify certain DNA fragments out of a nucleotide mixture.

The agarose gels were prepared in 1X Tris-acetate-EDTA (TAE) buffer, supplemented with ethidium bromide (1:200 from 5 mg/ml stock solution), with a final agarose concentration of 1% for the separation of nucleic acid fragments with a size of 500 - 10,000 bp or 2% for nucleic acid fragments with a size smaller than 200 bp. Samples were mixed with 10X loading dye (FastDigest Green Buffer from Thermo Scientific) and separated in parallel to a DNA marker (e.g. GeneRuler 1 kb DNA Ladder) at 120 - 140 V for 45 - 60 min. Visualization of nucleotides was achieved by UV-excitation of the supplemented ethidium bromide, which intercalated into DNA strands. Images were finally taken using a CCD-based camera system.

3.2.9.8. Nucleotide-extraction from agarose gels

The extraction of nucleotides after agarose gel elecrophoresis was performed with the PureLink® Quick Gel Extraction Kit (Thermo Scientific), according to the manufacturers protocol. First, the DNA fragment was excised from the gel using a sharp razor blade, thereby reducing the amount of contaminating agarose gel to a minimum. Next, one volume of the DNA-containing agarose gel was dissolved in three volumes Gel solubilization buffer and incubated at 50℃ for 15 min in the ThermoMixer®. In between, the microtube was manually inverted for several times. After complete solubilization, the solution was added onto the Quick Gel Extraction Column and centrifuged at 12,000 g for 1 min. Subsequently, 500 µl washing buffer was added, followed by two centrifugation steps at 12,000 g for 1 min, with exchange of the collection tube in between. Finally, elution of nucleotides was performed with 50 µl ddH_2O by centrifugation.

3.2.9.9. DNA-concentration determination via spectrophotometry

The NanoDrop 2000 UV-Vis spectrophotometer was used to determine the concentration of DNA and RNA solutions and to verify the purity of a sample. The measured absorbance is proportional to the DNA or RNA amount (50 ng/µl dsDNA or 40 ng/µl RNA and 1 cm light path = 1 absorbance unit). For every measurement 1 µl of DNA or RNA solution was used.

3.2.9.10. DNA-ligation

The ligation of DNA fragments, generated by PCR or excised from other DNA templates, into a plasmid was used to combine sequences with different information or functions to a functional construct. The enzyme T4 DNA ligase was used to catalyze the formation of a phosphodiester bond between a 5' phosphate and 3' hydroxyl termini. Therefore, it was necessary that insert and plasmid possessed either the same cohesive end termini or blunt ends, achievable by the

digestion of both templates with same restriction enzymes. The reaction was set up according to Table 3.19 with an incubation time of either 2 h at RT or overnight at 16 ℃.

Table 3.19.: Reaction mixture composition for ligation

Compound	Volume / amount
10x T4 DNA ligase buffer	1.5 µl
10x T4 DNA ligase (1 unit/µl)	1 µl
Linear vector DNA	20 ng
Insert DNA	1:5 or 1:7 molar ratio over vector
ddH_2O	ad 15 µl

3.2.9.11. Isolation of plasmid DNA

Depending on the size of the bacterial starting material, mini- or midi preparations were performed for plasmid isolation. First, a single bacterial colony was picked from the LB-agarose plate, transferred into a glass tube containing 5 ml LB-medium for mini preparation or 20 - 50 ml for midi preparation plus ampicillin and incubated at 200 rpm and 37 ℃ in a horizontal shaker overnight. For the isolation of small amounts of DNA, the Qiagen MiniPrep Kit was used, according to the manufacturers protocol. Therefore, the bacterial suspension was centrifuged at 10,000 g for 5 min and the supernatant was discarded. The cell pellet was then resuspended in 250 µl resuspension buffer including RNase A and transferred to a new tube. First, 250 µl of an alkaline lysis buffer containing SDS was added, mixed and incubated for 5 min, before proteins were precipitated by adding 350 µl neutralization buffer and inversion of microtubes for several times. Cells were centrifuged at 17,000 g for 10 min and the supernatant was transferred onto a QIAprep spin column. Samples were washed with 750 µl of the provided washing buffers and centrifuged again at maximum speed to remove any solution. Finally, using 50 µl ddH_2O, the plasmid was eluted by centrifugation at maximum speed for 1 min.

For midi preparation, the PureLink® HiPure Plasmid Midiprep Kit was used, according to the manufacturers protocol. For this purpose, the bacterial suspension was transferred into a tube and centrifuged at 4,000 g for 10 min. The provided columns were equilibrated with the equilibration buffer and meanwhile the pellet was resuspended in resuspension buffer, containing RNase A. Bacteria were incubated with cell lysis buffer for 5 min and thereafter with precipitation buffer, thereby inverting the tube several times. The solution was added onto the column, followed by two washing steps using the provided washing buffers. Elution of the plasmid DNA was performed with 5 ml elution buffer, followed by the precipitation of DNA with isopropanol. The suspension was centrifuged at 12,000 g and 4 ℃ for 30 min. Thereafter, the supernatant was almost completely removed and after drying the pellet for 10 min at RT, it was resuspended in 100 µl ddH_2O. The concentration and purity of the resuspended plasmid DNA was determined using the NanoDrop spectrophotometer, before storing the plasmid at -20 ℃.

3.2.9.12. Propidium iodide staining of DNA

Fixed samples (Section 3.2.2.9) were first centrifuged at 1,200 g for 5 min. Subsequently, samples were washed 2x with 1X PBS to completely clear cells from methanol. Thereafter, cells were

resuspended in a 1X PBS buffer containing 100 µg RNAse and 50 µg propidium iodide and incubated in a ThermoMixer® at 800 rpm and 37 ℃ for 60 min. Samples were stored on ice and measured in the FACS facility as soon as possible.

3.2.9.13. Flow cytometric analysis

Flow cytometric analyses were performed using the BD FACSCanto II to detect the DNA content of propidium iodide labeled cells. For this purpose, the blue laser with an excitation wavelength of 488 nm was used in combination with the band pass optical filter 695/40 and the red fluorescence emission detector. In the first step, unstained cells were used to identify the population of interest and by adjusting the voltages for forward scatter (FSC) and side scatter (SSC) they could be distinguished from cell debris and cell doublets. Subsequently, PI-stained cells were measured to adjust the voltages for PI in order to cover a wide detection range. Based on the PI area (PI-A) values it is possible to determine the amount of chromosome sets within one cell. A quantitative conclusion was achieved by measuring more than 10,000 cells per sample.

4. Results

4.1. Differentiation of neural progenitor cells (NPCs) to oligodendrocyte precursor cells (OPCs)

The differentiation process from multipotent neural progenitor cells (NPCs) to oligodendrocyte precursor cells (OPCs) was investigated regarding alterations of protein expression levels using quantitative mass spectrometry. For the *in-vitro* cultivation of OPCs from brain tissue a widely used and well established approach was applied. The so called neurosphere assay was used to cultivate large numbers of neural progenitor cells as neurospheres in suspension cell cultures [Reynolds & Weiss, 1992]. For the generation of oligospheres, which mainly consisted of oligodendrocyte precursor cells (OPCs), medium conditioned by the neuroblastoma cell line B104 was used [Zhang et al., 1998]. Specific factors within this medium, including the growth factors platelet-derived growth factor (PDGF), insulin-like growth factor (IGF) and basic fibroblast growth factor (bFGF) promote the generation of cells committed to the oligodendroglial cell lineage *in-vitro* [Hu et al., 2012a] [Hu et al., 2012b].

According to Figure 4.1, cortical cells of P0 or P1 C57BL/6 mice were isolated and cultivated *in-vitro* in suspension cultures. The serum-free proliferation medium consisted of several mitogens, including bFGF and the epidermal growth factor (EGF). After around seven days in proliferation medium, cell clusters containing a heterogeneous mixture of NPCs, so called neurospheres, developed by symmetric and asymmetric cell division. Reaching a size of 200 - 300 µm, neurospheres were differentiated to oligospheres by gradually changing from proliferation medium to B104-conditioned medium-containing differentiation medium. Differentiation to OPCs was performed for 15 days. In the meantime, cells of different development stages were used for immunocytochemistry (ICC) and quantitative mass spectrometry (MS) analyses.

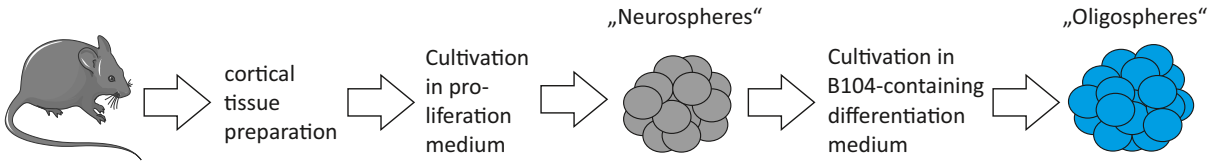

Fig. 4.1.: Workflow used for the *in-vitro* cultivation of oligospheres (oligodendrocyte precursor cells). Cortical cells, derived from P0 or P1 mice, were cultivated in basic fibroblast growth factor- and epidermal growth factor-containing proliferation medium. After around seven to ten days, cell aggregates with a size of 200 - 300 µm, so called neurospheres (mainly consisting of neural progenitor cells), were formed and subsequently differentiated to oligospheres (mainly consisting of oligodendrocyte precursor cells) by gradually changing from proliferation to differentiation medium. Among others the differentiation medium consisted of medium conditioned by the neuroblastoma cell line B104, which has been evidenced to induce the generation of oligodendroglial cells.

4.1.1. Monitoring of neurosphere differentiation by YFP imaging and immunocytochemistry (ICC) analysis

Differentiation from neurospheres to oligospheres was first studied using cells derived from NG2-EYFP-knockin mice [Karram et al., 2008]. Accordingly, YFP is expressed under the NG2 promoter, which allowed to follow the differentiation process to NG2-expressing OPCs by monitoring the amount of YFP (yellow fluorescent protein)-fluorescence. The NG2 protein in turn represents a cell surface marker, specifically expressed by OPCs [Dawson et al., 2003]. Thus, the expression of YFP was evaluated for a period of 17 days by fluorescence microscopy. An exemplary course of YFP expression after differentiation initiation is shown in Figure 4.2.

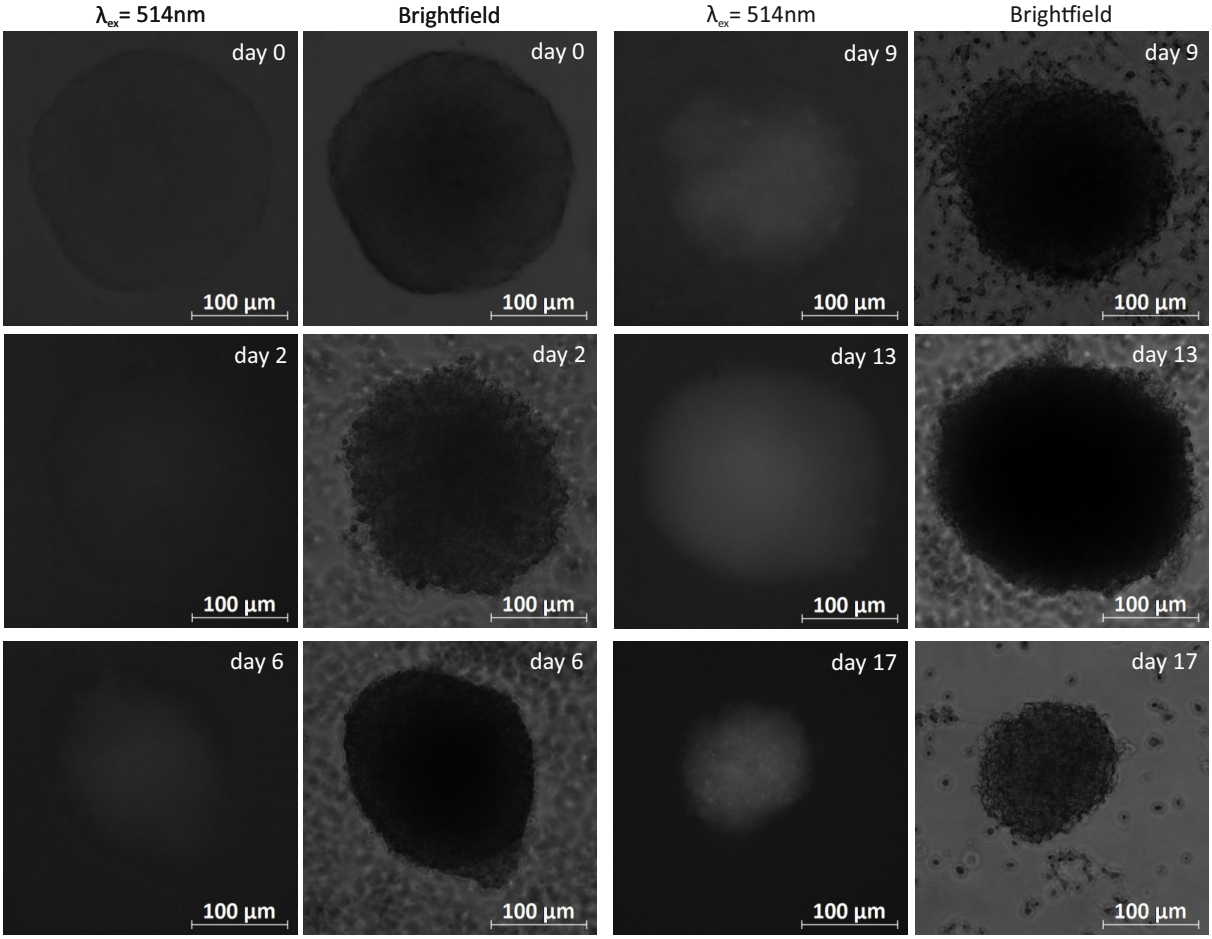

Fig. 4.2.: YFP expression of single spheres during neurosphere differentiation. Cortical cells derived from NG2-EYFP-knockin mice were cultivated for 7 - 10 days in proliferation medium. Differentiation from neurospheres to oligospheres was started by gradual exchange to differentiation medium, mainly consisting of medium conditioned by the neuroblastoma cell line B104. Images were taken at day 0, 2, 6, 9, 13 and 17 of differentiation with the Axiovert 200 M, using a 20X objective. After focusing on one sphere under brightfield illumination, special filters were applied, covering the excitation and emission range of the yellow fluorescent protein (excitation filter: 500/20, emission filter: 535/30, dichroic beam-splitter: 515 nm). Images were taken with an exposure time of 1,500 ms.

Two days after starting the differentiation process no YFP expression was detectable within the sphere. However, a light YFP expression was visible at day 6, which indicated that some cells expressed the NG2 protein. With prolonged exposure of spheres to differentiation medium, the YFP signal further increased so that after 13 days a distinct expression was visible within the sphere which stayed consistent until day 17. The chosen size of spheres for comparison of expression ranged from 200 to 300 µm, with exception of the sphere detected at day 17. It should be noted that with enduring cultivation of cells in differentiation medium, spheres began to become more diffuse and cells started to migrate out of the cluster, making it more difficult to take sharp images of intact spheres.

For more precise and quantifiable results of the cell development process, ICC staining of antigens was performed in biological triplicates. Neurons and glial cells arising from multipotent NPCs were detected by staining antigens, specific for the different cell types. Accordingly, neurons were stained using an antibody against β3-tubulin protein [Sullivan, 1988], microglia against the adhesion G protein-coupled receptor E1 (F4/80) [Perry et al., 1985], astrocytes against the glial fibrillary acidic protein (GFAP) [Sofroniew & Vinters, 2010], OPCs against the NG2 protein and oligodendrocytes against the myelin basic protein (MBP) [Sternberger et al., 1978]. Furthermore, the stem cell and progenitor cell marker nestin was used to monitor the development from NPCs to differentiated cells [Hockfield & McKay, 1985]. For proper quantitation of different cell types the dissociation of spheres into single cells using StemPro® Accutase® including a short recovery period to ensure attachment of cell to coverslips was an indispensable step prior antigen staining. It should be noted that just a differentiation period of nine days was covered, due to the fact that with enduring differentiation time dissociated cells started to die. ICC staining of cells with only secondary antibodies was performed to determine the background fluorescence of each dye (pictures not shown). Consequently, the exposure time for all images taken were adjusted to the exposure time where no background signal was observed. Representative ICC images from one of three replicates are shown in Figure 4.3.

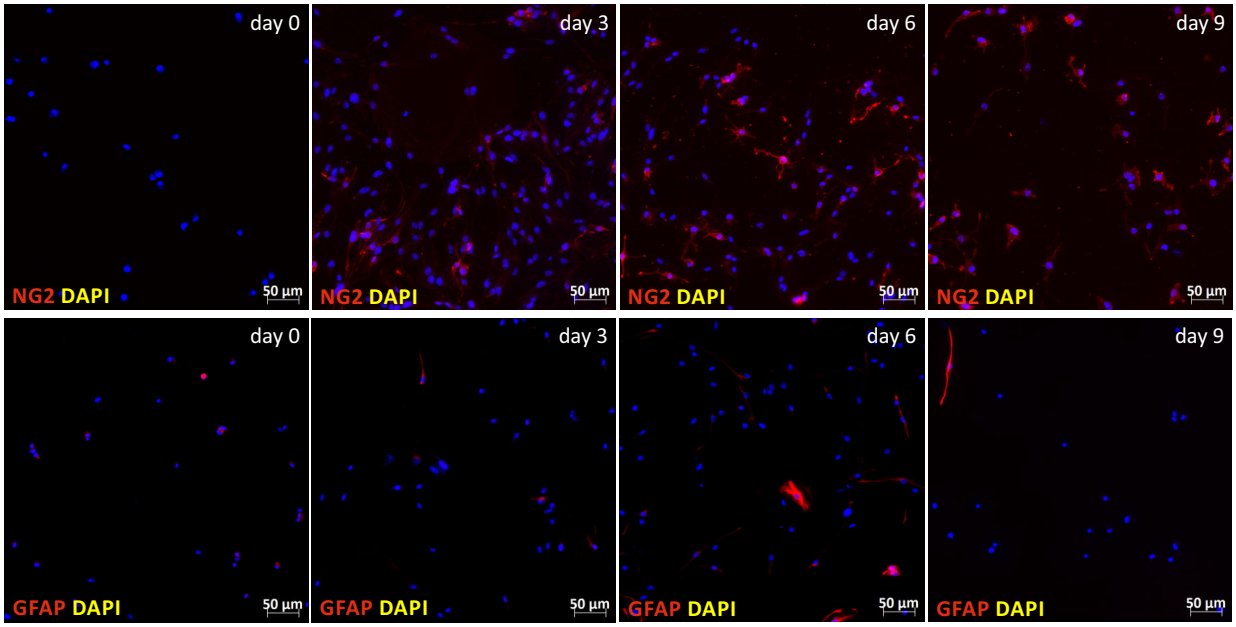

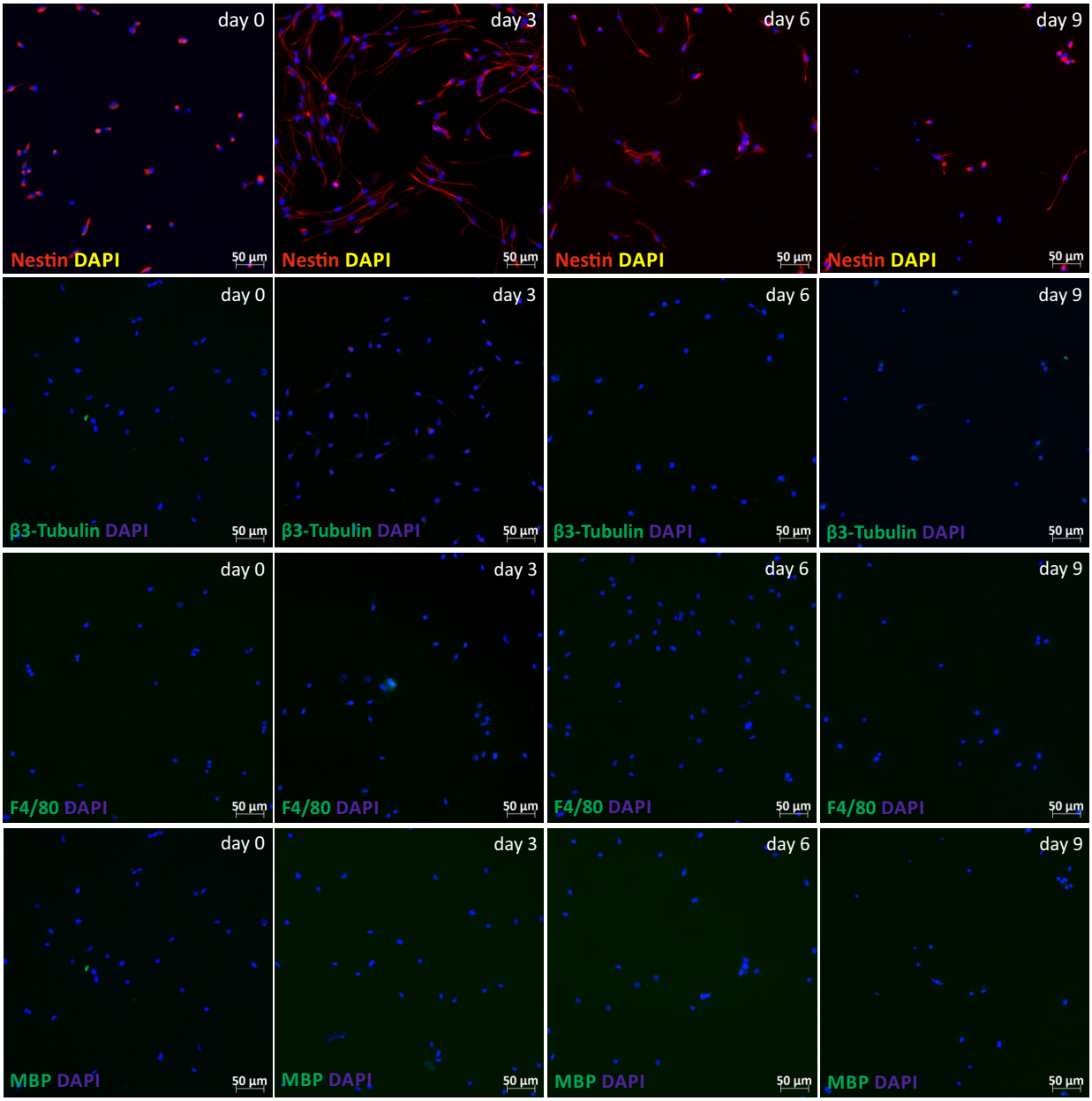

Fig. 4.3.: Immunocytochemistry staining during neural progenitor cell to oligodendrocyte precursor cell differentiation for nine days. Cortical cells of P0 / P1 mice were cultivated for 7 - 10 days to neurospheres and differentiated for nine days by gradual exchange to differentiation medium. Spheres were dissociated at day 0 and every third day, $\sim 3 \cdot 10^5$ cells were plated per poly-L-ornithine-coated coverslip and incubated overnight in proliferation- (day 0) or differentiation medium (day 3 - 9), supplemented with 20 µM forskolin. Cells were fixed with 4% paraformaldehyde, permeabilized with Triton X-100 (except NG2-stained specimen) and blocked with normal goat serum. Staining with primary antibodies was performed overnight at 4 °C and with secondary antibodies and 4',6-diamidino-2-phenylindole for 90 min at room temperature. Oligodendrocyte precursor cells were stained with anti-NG2 antibody (ab) and α-rabbit-Cy3 ab, astrocytes with anti-GFAP ab and α-mouse-Alexa546 ab, stem and progenitor cells with anti-nestin ab and α-mouse-Alexa546 ab, neurons with anti-beta III tubulin ab and α-mouse-Alexa488 ab, microglia with anti-F4/80 ab and α-rat-Dylight488 ab and oligodendrocytes with anti-MBP ab and α-rat-Dylight488 ab. Images were taken using the Axiovert 100 M and 200 M.

According to Figure 4.3, OPCs and astrocytes develop from neurospheres upon differentiation, while the number of stem and progenitor cells decreased. Neither neurons, microglia nor oligodendrocytes were detected within the first nine days of the differentiation experiment. As already mentioned, staining with the anti-NG2 and the anti-GFAP antibody was performed in triplicates, whereas staining with the anti-nestin antibody was only conducted in duplicates. In order to determine the number of cells belonging to OPCs, astrocytes and stem and progenitor cells, between three and seven images per antigen and time point were taken using the AxioVert 100 M or 200 M microscope. Subsequently, positive labeled cells were counted and the ratio of positive labeled cells to unstained cells was determined by using the nucleus staining marker 4',6-diamidino-2-phenylindole (DAPI) as control. Results are shown in Figure 4.4.

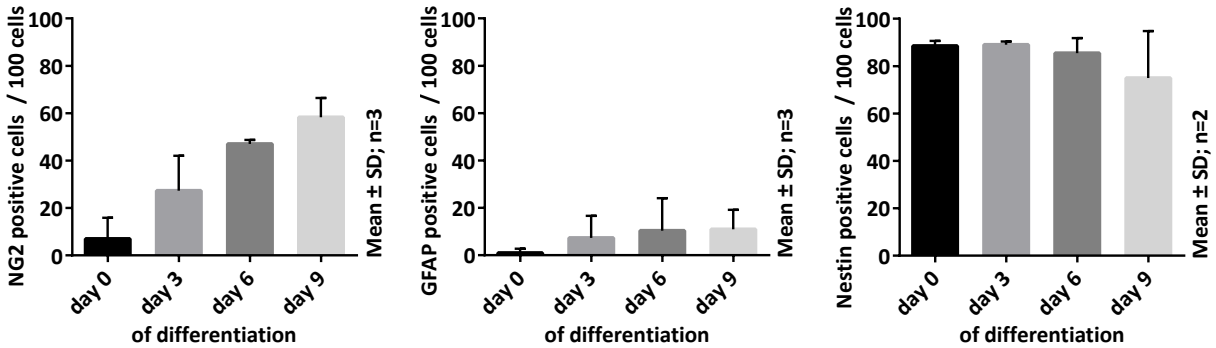

(a) NG2-positive cells (b) GFAP-positive cells (c) Nestin-positive cells

Fig. 4.4.: Number of NG2-, GFAP- and nestin-positive cells at day 0, 3, 6 and 9 of neural progenitor cell differentiation. Neurosphere to oligosphere differentiation over nine days was performed in biological triplicates regarding the staining of the NG2 and GFAP protein, respectively in duplicates in terms of nestin staining. Spheres were dissociated at day 0, 3, 6 and 9 and single cells were cultivated on coverslips overnight. Cells were fixed and stained with primary and secondary antibodies for oligodendrocyte precursor cells (NG2), astrocytes (GFAP) and neural stem and progenitor cells (Nestin). Between 3 - 7 images were taken per time point and replicate using the AxioVert 100 M or 200 M and positively labeled cells were counted. For every cell type the average of cells positive for the antigen was determined and plotted proportionally to 4',6-diamidino-2-phenylindole (DAPI)-positive cells. All images considered in this analysis can be found in the electronic supplement (Folder: Supplementary Images S1).

The nestin staining of single cells derived from neurospheres revealed that 89% of all cells expressed the intermediate filament protein nestin at day 0 of the differentiation process (Figure 4.4). Nestin was detected in neuroepithelial stem cells, CNS stem cells and in proliferating CNS progenitor cells, but not in differentiated cells of the CNS [Messam et al., 2000]. At the earliest, six days after differentiation initiation a slight reduction of cells expressing nestin (86%) was detected, which further continued until day 9 of differentiation, where 75% of total cells were positively stained for nestin. Accordingly, some cells have undergone differentiation during the experiment. Based on the observation made by evaluating ICC images of major neural cell types, most probably GFAP-expressing astrocytes represented the part of nestin negative cells. This assumption is based on the fact that no neurons, microglia or oligodendrocytes were detected at any time point during the differentiation process. In addition, OPCs have been shown to express both, the NG2 and the nestin protein [Kerr et al., 2010] [Zhang et al., 2006b].

Astrocytes themselves were not present in neurospheres (day 0), but developed after three

days in differentiation medium. The number of cells which differentiated into astrocytes further increased until day 6 and stayed almost constant afterwards. In numbers this means that the mean of GFAP stained cells raised from 1% at day 0, via 7% at day 3 and 10% at day 6 to finally 11% at day 9. As anticipated, most of the cells cultivated in neurospheres finally differentiated into NG2-expressing OPCs. NG2-positive cells in turn were partly detectable in neurospheres at day 0 of the differentiation process, while the number further increased with prolonged exposure time to differentiation medium. The mean percentage of NG2-stained cells increased from 7% at day 0, via 27% at day 3 and 47% at day 6 to finally 58% at day 9. It should be further noted that the morphology of NG2-positive cells changed with prolonged differentiation time and thus prolonged developmental progress while forming augmented and more branched extensions.

Altogether, nine days after differentiation initiation around 70% of total cells were detectable with antibodies against either the NG2 or the GFAP protein. In addition, no MBP-positive, nor F4/80-positive, nor β3-tubulin-positive cells were detected at any time point. Accordingly, around one third of cells were not assignable to any cell type, assuming that after nine days of differentiation one third of total cells were still at the development stage of multipotent progenitor cells. This is consistent with the finding, that nine days after differentiation initiation still 75% of all cells expressed the nestin protein, while only 58% expressed the NG2 protein. Further evidence therefore was given by the YFP-neurosphere differentiation experiment, which indicated a progressive YFP expression, also after nine days of differentiation.

4.1.2. Analysis of proteome level alterations during the differentiation to oligodendrocyte precursor cells by large scale mass spectrometry

For quantitative large scale mass spectrometry analyses neurospheres were cultivated as mentioned before (Figure 4.1). After seven days, differentiation was induced and cells were harvested every third day, starting at day 0 while covering a period of fifteen days. Thus, each experiment consisted of six samples (time points). Each sample was labeled with a different TMTsixplex™ reagent [Thompson et al., 2003] (isobaric labeling). Samples were thereafter combined to one sample to determine the relative abundance of proteins per time point. Accordingly, identical peptides, although labeled with different isobaric tags, possess the same mass and thus co-elute from the liquid chromatography column. Upon fragmentation during tandem mass spectrometry (MS/MS), the isobaric tags are cleaved and six reporter ions of different masses are observed that can be assigned to the samples. For more accurate results, the same differentiation experiment was performed in five biological replicates. All generated raw-files were afterwards combined and analyzed using the quantitative proteomics software MaxQuant [Cox & Mann, 2008]. The MS/MS spectra obtained were used for identification of peptides, while the unique reporter ion intensities were utilized for relative quantitation of peptides in each sample.

Combining the analyses of five biological and two technical replicates of the differentiation process in one search using MaxQuant, altogether 6,150 proteins were identified, based on 292,868 peptide spectrum matches (PSMs) (false discovery rate (FDR) = 0.01). The exact numbers of identified proteins per replicate are depicted in the bar chart in Figure 4.5 (a). In the bar chart, the technical replicates (applies to replicate 1 and 2) are already concatenated. Sample preparation and measurement of multiple experiments introduced variance into the data set,

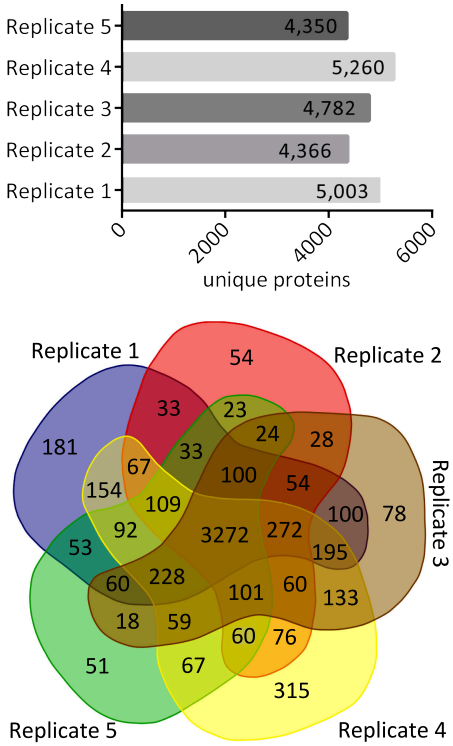

(a) MaxQuant protein identification

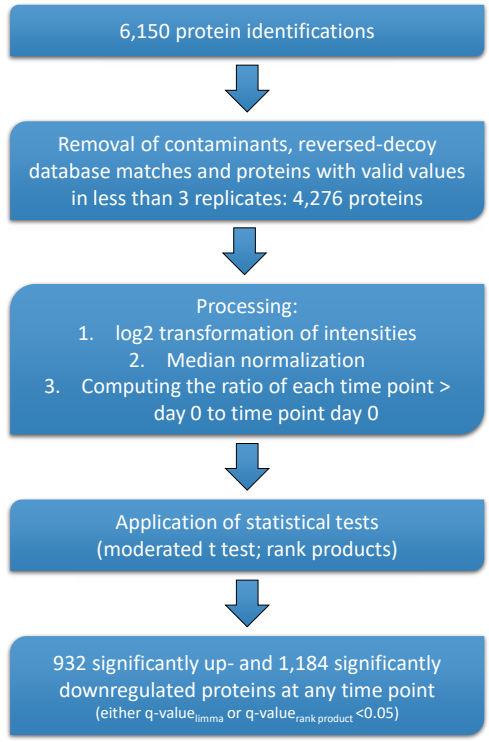

(b) Data processing workflow

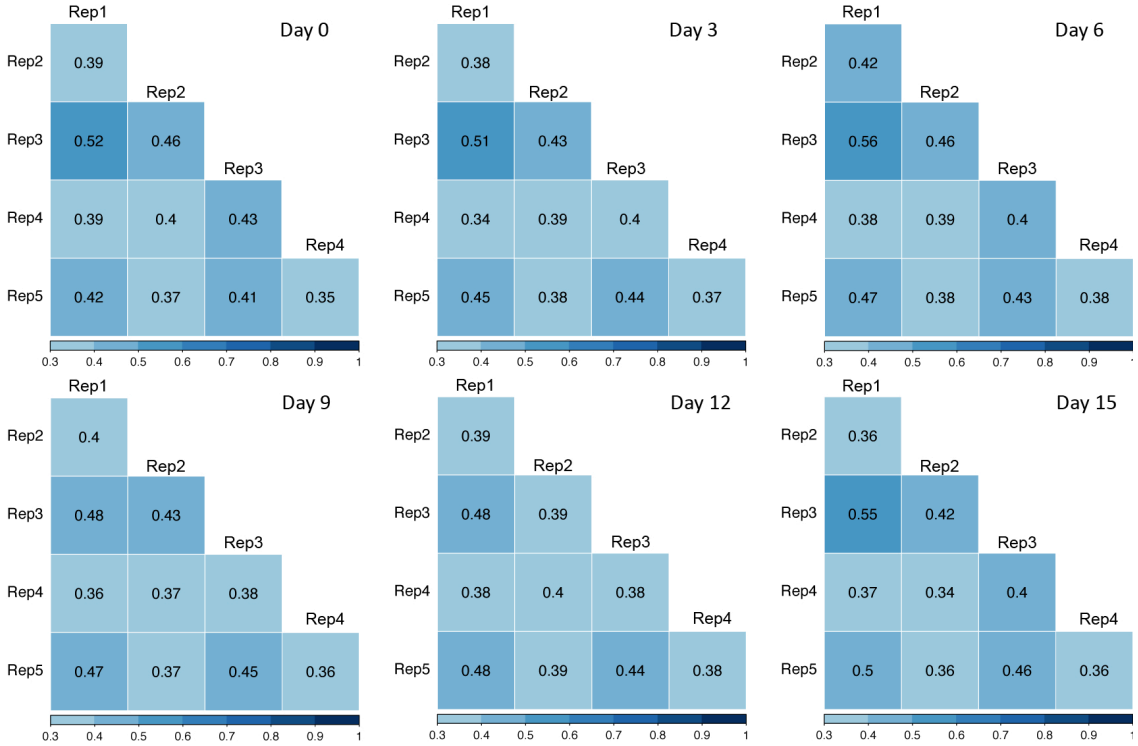

(c) Pearson correlation

Fig. 4.5.: MaxQuant analysis of neurosphere differentiation data and subsequent data processing steps. Neurosphere differentiation samples, labeled with TMTsixplex™, were measured using a LTQ-Orbitrap Velos mass spectrometer and analyzed using MaxQuant. The analysis of data acquired from five biological and two technical replicates against the murine UniProtKB/TrEMBL database at 1% false discovery rate resulted in the identification of 6,150 unique proteins (a) The table shows the number of identified proteins per replicate, whereas the Venn diagram indicates the overlap of proteins between all replicates (replicate 1 and 2 consist of concatenated technical replicates). (c) The heat maps indicate the Pearson's correlation coefficients of median-normalized intensities between all replicates for each time point. The higher the Pearson's correlation values, the more intense the blue color. (b) The data processing workflow was applied after MaxQuant analysis. After concatenating technical replicates, removing contaminants and reversed-decoy database matches, filtering, processing and applying statistical tests, proteins with a q-value (FDR adjusted p-value) < 0.05 were considered as significantly regulated proteins. The computational data processing was done by the bioinformatician Dr. Nahal Brocke-Ahmadinejad.

which became apparent by investigating the correlation between each replicate and time point using Venn diagrams (UGent Bioinformatics & Evolutionary Genomics, Appendix D: URL2) and Pearson's correlation coefficients (Figure 4.5 (c)). The Venn diagram (Figure 4.5 (a)) depicts all 6,150 proteins identified. Numbers in overlapping areas thereby indicate the amount of proteins shared between the respective replicates. With in total 3,272 proteins more than 50% of identified proteins were detected in all five replicates. Besides this, 4,082 proteins were found in four and 4,786 proteins in three replicates. Based on the Pearson's correlation coefficients of normalized intensities, a statement could be made regarding the reproducibility between all replicates. While some replicates, especially experiment one and three and one and five correlated better, some replicates showed a worse Pearson's correlation. In summary, it can be stated that most replicates showed a correlation coefficient of ~ 0.4, indicating a moderate correlation according to Evans [Evans, 1996].

For the purpose of relative quantification and subsequent determination of significantly regulated proteins, MaxQuant data was further processed. In the first step, contaminants as well as peptides which were detected by the decoy database (contains the original amino acid sequences of proteins in reversed order) were removed from the original 6,150 proteins. Thereafter, the data set was filtered for proteins which were detected with valid reporter ion intensity values in at least three replicates, so that finally 4,276 proteins were considered for further analysis. Subsequent processing steps included for every protein the log2 transformation of the median reporter ion intensity (based on all intensities belonging to the same protein), followed by the normalization to the median intensity of each reporter ion group (each TMT label). Finally, computation of the ratio between each time point greater day 0 and time point day 0 was performed. Expression ratios were evaluated using statistical tests (moderated t-test (Limma) and Rank product) [Ritchie et al., 2015] [Hong et al., 2011] to identify differential abundant proteins at each time point. The analysis resulted in 932 significantly (q-value (FDR adjusted p-value) < 0.05) up- and 1,184 downregulated proteins at any time point (at one or more time points). Due to the high numbers of regulated proteins, it was further useful to determine whether proteins were mainly regulated at earlier or later time points of the differentiation experiment. For this purpose, the amount of significantly regulated proteins at each time point was plotted in the histograms (Figure 4.6). It should be noted that the sum of all proteins plotted in both histograms is larger than the already mentioned 932 up- and 1,184 downregulated

proteins. These numbers only depict the total number of regulated proteins, while the histograms depict the number of proteins significantly regulated at a particular time point.

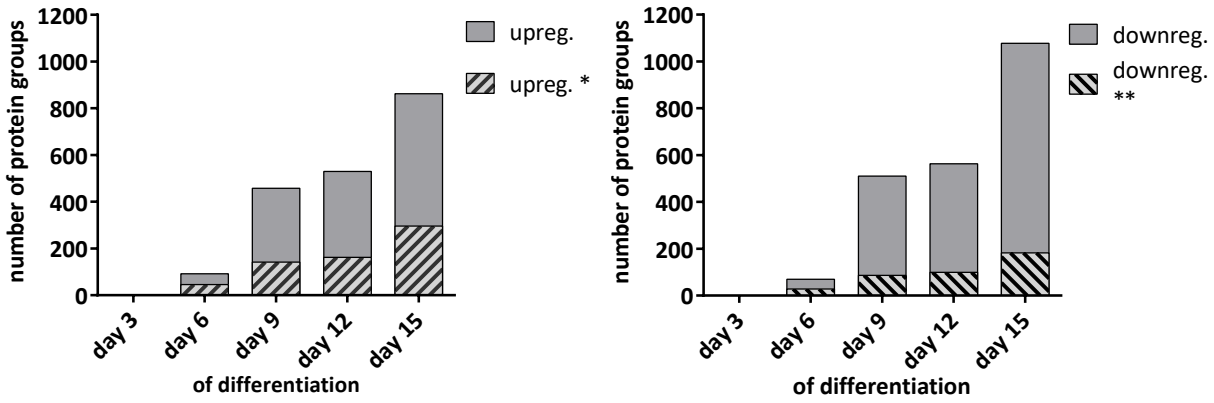

(a) Significantly upregulated proteins

(b) Significantly downregulated proteins

Fig. 4.6.: Significantly (a) up- and (b) downregulated proteins during neurosphere differentiation. TMTsixplex™-labeled Neurosphere differentiation samples (five biological and two technical replicates) were measured using a LTQ-Orbitrap Velos. Raw MS-data was searched against the murine UniProtKB/TrEMBL database at 1% false discovery rate using MaxQuant. The log2 transformed and normalized reporter ion intensities of proteins detected in $\geq$ three replicates were used to compute the expression ratio of day 3, 6, 9, 12 and 15 to day 0. Two statistical tests were applied and proteins, showing a q-value < 0.05 in either Limma- or Rank product-test, were determined as significantly regulated. Proteins showing a log2 fold change ≥ 1 (upreg. *) or $\leq$ -1 (downreg. **) are shaded in grey / black. The algebraic sign was considered to determine whether a protein is up- or downregulated at a particular time point (irrespective of any fold change value). upreg. = upregulated; downreg. = downregulated.

The longer cells were exposed to differentiation medium, the more proteins were significantly up- or downregulated. Since the exchange from proliferation to differentiation medium occurred step wise so that OPCs developed gradually, an augmented number of regulated proteins at the end of the experiment was expected. After three days in differentiation medium no significant changes in protein expression level was observed for any protein in comparison do undifferentiated cells (Figure 4.6). However, after six days in differentiation medium, already 92 proteins were significantly upregulated, whereof 46 proteins were more than two fold upregulated. On the other side, 70 proteins exhibited a decrease in expression levels, whereof 40% exhibited a downregulation of more than two fold after six days. Interestingly, within three days, from day 6 to day 9, a strong increase in numbers of regulated proteins occurred, indicated by ∼500 up- and downregulated proteins nine days after differentiation initiation. The amount of regulated proteins further increased from day 12 until day 15, especially in the group of downregulated proteins. The percentage of more than two fold up- or downregulated proteins stayed almost constant at day 9, 12 and 15 with ∼30% respectively 17%.

To further get a general idea of the expression course of every significantly regulated protein during the differentiation process, Venn diagrams, shown in Figure 4.7, were compiled. Only few proteins were already upregulated six days after differentiation initiation, albeit almost all of them were found to be upregulated in all following time points. In numbers this means that 83

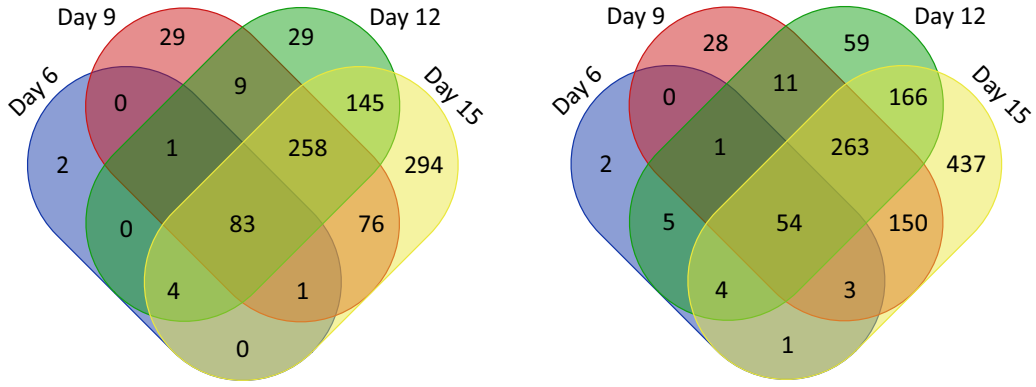

(a) upregulated proteins

(b) downregulated proteins

Fig. 4.7.: Venn diagram of (a) upregulated and (b) downregulated proteins during neurosphere differentiation. TMTsixplex™-labeled Neurosphere differentiation samples (five biological and two technical replicates) were measured using a LTQ-Orbitrap Velos and analyzed using MaxQuant. The log2 transformed and normalized reporter ion intensities of proteins detected in at least three replicates were used to compute for each protein the expression ratio of day 3, 6, 9, 12 and 15 to day 0. Two statistical tests, Limma and Rank product, were applied and proteins featuring q-values < 0.05 were determined as significantly regulated. Finally, all regulated proteins were analyzed using the Venn diagram tool, provided by UGent Bioinformatics & Evolutionary Genomics. The diagrams show the distribution of all proteins that were significantly regulated at day 6, 9, 12 and 15 compared to day 0. The comparison with regulated proteins at day 3 is missing because no significantly regulated proteins were identified.

(9%) of in total 932 significantly upregulated proteins showed a regulation in all four time points (except day 3), while still a large number of 258 proteins (28%) were only upregulated at more progressed differentiation stages, from day 9 until day 15 (Figure 4.7 (a)). Moreover, most of the regulated proteins at day 9 and 12 of the experiment were likewise upregulated in subsequent time points. However, with 32% (294 proteins) of total significantly identified proteins most were found to be only upregulated at day 15. The Venn diagram of downregulated proteins (Figure 4.7 (b)) shows almost the same distribution pattern of proteins over time. A downregulation during all four time points was observed for 54 (5%) proteins, while 263 (22%) showed a constant downregulation from day 9 until day 15. However, proteins which were only downregulated at day 15 represented the largest group, counting in total 437 (37%) proteins.

4.1.2.1. Time dependent alterations of the proteome during neurosphere differentiation: Data analysis strategies

The next steps approached the question of changes in protein expression levels during the differentiation experiment. Possible candidates involved in the differentiation process investigated were determined by using different analysis strategies, due to high data complexity. In the first approach, hierarchical clustering of proteins was performed, resulting in the classification of proteins based on their time dependent changes in expression during the differentiation process. The hierarchical clustering technique was used since it segments objects into optimally homogeneous clusters based on empirical measurement of similarity between the objects [Johnson, 1967]. Hierarchical clustering analyses are widely used for gene expression and protein expression analyses

to get a first impression of the expression patterns of genes or proteins in large-scale data sets [Sørlie et al., 2001] [Meunier et al., 2007]. In addition, a second approach was used to consider only the significantly regulated proteins and their expression patterns over time, based on the log2 expression ratios (log2 fold changes) calculated. The combination of data from multiple biological replicates, subsequent normalization of acquired data and application of statistical tests (moderated t-test or rank product) enhanced the probability of finding true regulated proteins and improved quantification results. Due to the gradual exchange of proliferation to differentiation medium a moderate development to OPCs was achieved, indicated by immunocytochemistry staining (Figure 4.3). Significantly upregulated proteins were first detected after six days of neurosphere differentiation (Figure 4.6). The focus was thus set on a) proteins significantly upregulated in all time points from day 6 - day 15 (Table 4.1) and on b) proteins significantly upregulated from day 9 - day 15 (Table 4.2), respectively day 12 - day 15 (Table 4.3). In addition, gene ontology (GO) enrichment analyses to identify enriched biological processes (BPs) and cellular components (CCs) were performed.
Expectably, proteins involved in initial steps of cell differentiation are upregulated at the beginning of the experiment. However, no proteins were significantly regulated at day 3 and besides this only few proteins were regulated only at day 6 or day 6 and 9 (Figure 4.7). Regarding the experiment, this implies that proteins involved in differentiation initiation can not be detected with a q-value ≤ 0.05 in cells prior cultivation of cells for six days in differentiation medium. This is probably due to the fact that differentiation did not occur in all cells simultaneously, but rather that cells committed individually to the oligodendroglial cell fate. Therefore, all regulated proteins were grouped into protein classes that feature similar molecular functions. Since usually distinct protein classes, like receptors or transcription factors, are involved in initiating cellular differentiation, proteins belonging to these protein classes were investigated regarding their expression behavior.

4.1.2.2. Hierarchical clustering

In the first approach, the neurosphere data set was analyzed without focusing on the significance of proteins, but on changes in intensities over time. The hierarchical clustering analysis was performed on the protein mean intensities across all replicates, grouping proteins with same expression patterns over time into same clusters. As a result, the analysis of the large data set can be simplified and groups of proteins which display interesting expression patterns over time can be investigated in particular. Altogether, 4,276 proteins, featuring valid values in at least three replicates, were considered. The amount of clusters can be defined manually. The cluster dendrogram including the line graphs of every cluster is depicted in Figure 4.8 (a). Each line thereby represents the intensity profile of a protein from day 0 until day 15 of neurosphere differentiation.

According to Figure 4.8, all clusters consisted of different amounts of proteins displaying differential expression patterns over time. In this experiment the number of clusters was set to seven since therewith a group consisting of 179 proteins was observed that showed an increasing expression pattern between day 0 and day 15 (Cluster 4, Figure 4.8 (b)). The complete list of proteins available in cluster 4 including their mean intensities can be found in the electronic supplement (Supplementary Data S1). In case of the other clusters, no distinct expression pattern can be observed. Upon increasing the number of clusters most probably protein groups showing more distinct expression patterns should be discernible.

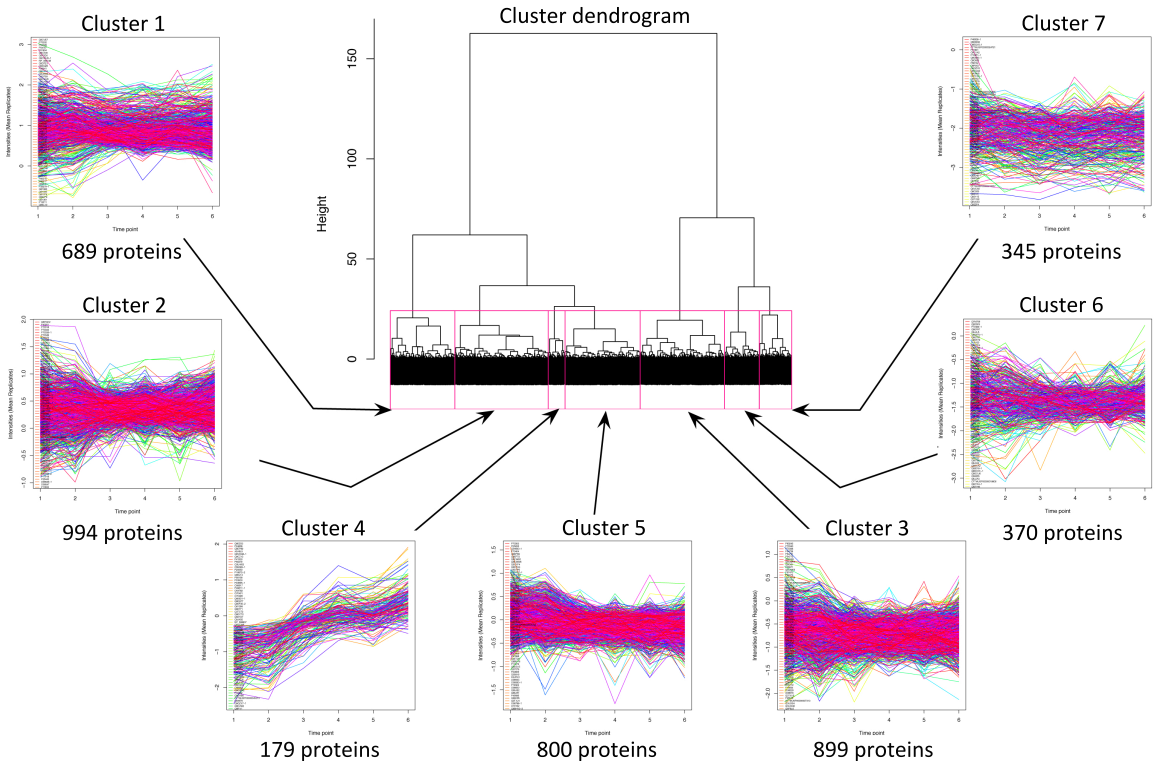

(a) Hierarchical clustering

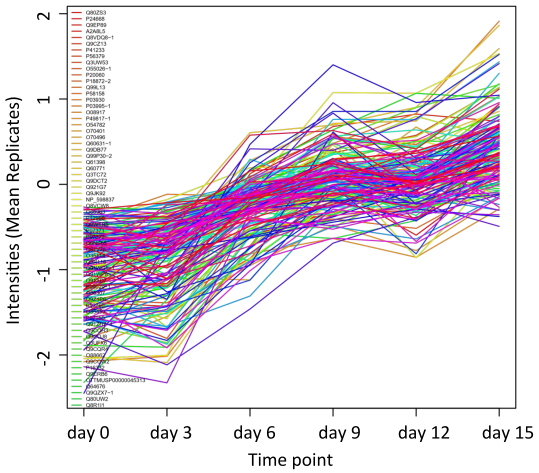

(b) Cluster 4

Fig. 4.8.: (a) Hierarchical clustering of proteins identified during neurosphere differentiation. The log2 transformed and median normalized intensities across each time point of proteins, detected with valid values in at least three replicates (4,276 proteins) using MaxQuant, were considered. Based on intensity distances, initially each object was assigned to its own cluster (agglomerative strategy). Thereafter, the algorithm proceeded iteratively, at each stage joining the two most similar clusters. The final number of seven clusters was defined manually, ensuring a good distribution of upregulated proteins into one cluster (Cluster 4) (b). The initial distances were computed using the distance measure "euclidean". The Ward's minimum variance method served as linkage criterion, aimed at finding compact, spherical clusters [Ward Jr, 1963]. **(b) Cluster 4**, including 179 proteins featuring increasing expression patterns. In the histograms the six time points (x-axis) are plotted against the mean intensity of all replicates. The analysis was performed by Dr. Brocke-Ahmadinejad.

Proteins belonging to cluster 4 were thus considered for Gene Ontology (GO) enrichment analysis [Ashburner et al., 2000] [Huang et al., 2008] to gain a general impression of the biological meaning and the cellular localization of these proteins. The GOrilla (Gene Ontology enRIchment anaLysis and visuaLizAtion) tool [Eden et al., 2009] was used to search for enriched GO terms in cluster 4 against a background list, consisting of all identified proteins using MaxQuant. The results obtained in the categories "biological process" and "cellular component" were finally depicted in the bar charts shown in Figure 4.9.

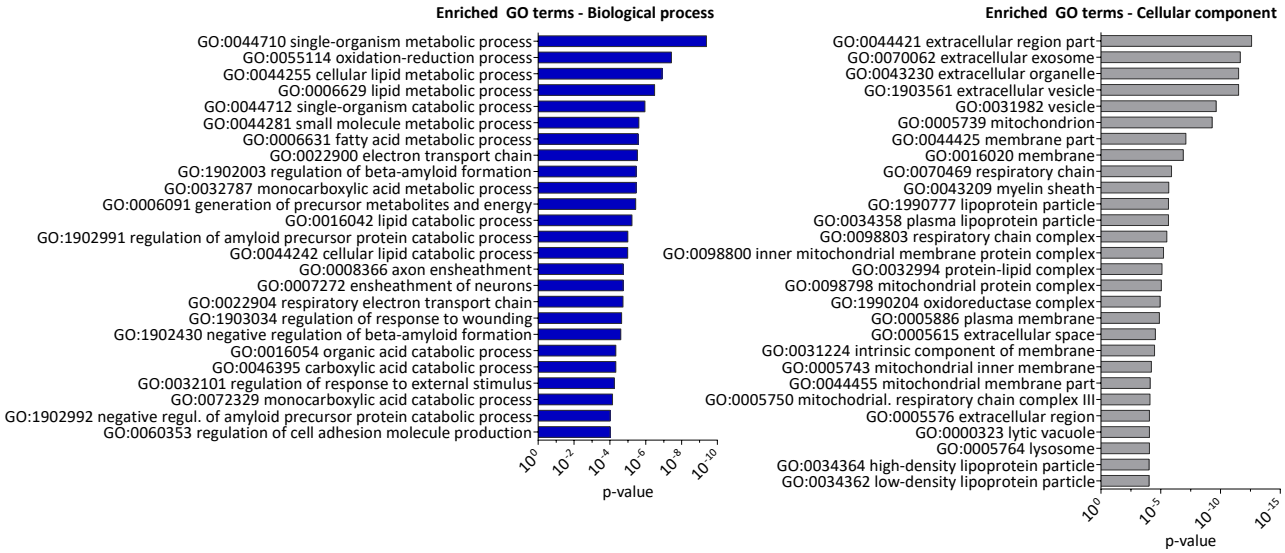

Fig. 4.9.: GO term enrichment analysis of cluster 4 containing proteins regarding the ontologies (a) biological process and (b) cellular component. The GOrilla tool was used to search for enriched GO terms in the target list (cluster 4; 179 proteins), against the background list (all identified proteins within the neurosphere differentiation experiment). The leading razor protein (in case of multiple assignments, best scoring protein where a peptide can be linked to) thereby functioned as identifier. Only proteins associated with a GO term were considered for GO term enrichment analysis (altogether 5,254 target and background proteins). Enriched GO terms were determined using the standard hyper geometric testing by calculating an enrichment p-value (x-axis) for each GO term. The p-value threshold was set to 0.001. The diagram depicts only those GO terms which feature an enrichment p-value < 0.0001 together with their p-values in descending order, represented as bar-charts. The complete list of enriched GO terms can be found in the electronic supplement (S2a and S2b). The calculated p-values did not include the multiple hypothesis correction on the number of tested GO terms. GO = gene ontology.

According to Figure 4.9, the GO term enrichment analysis of proteins included in cluster 4 identified many enriched GO terms in both ontology categories. The most interesting biological processes represented the ones exhibiting lowest enrichment p-values. Especially GO terms associated with lipid metabolism and energy supply were overrepresented in cluster 4, indicated by the low enrichment p-values of the GO terms "lipid metabolic process", "fatty acid metabolic process" and "oxidation-reduction process". Moreover, the GO terms "lipid homeostasis" and the associated GO terms "sterol and cholesterol homeostasis" were augmented. Besides metabolic processes, also GO terms related to myelination were enriched, including the "ensheathment of neurons" and "myelination".
Likewise, clusters of enriched GO terms were identified within the category of cellular compo-

nents, whereof many proteins can be assigned to the "extracellular region part". It seems that cluster 4 classified proteins were especially localized within extracellular exosomes, which belong to the group of extracellular organelles [Mathivanan et al., 2010]. Furthermore, many proteins can be assigned to intracellular membrane-bound organelles, such as lysosomes, peroxisomes and mitochondria. In addition, proteins associated with "myelin sheaths" were already enriched during the differentiation process from NPCs to OPCs. Moreover, the GO term "protein-lipid complex" was enriched, which in turn is connected to the enriched GO term "lipoprotein particle". The complete list of enriched GO terms, including associated proteins, can be found in the electronic supplement (Supplementary Data S2a and S2b).

4.1.2.3. Proteins significantly upregulated from day 6 until day 15 of the neurosphere differentiation process

Using hierarchical clustering analysis, a first exploration of the neurosphere data set regarding constantly upregulated proteins was achieved. However, no statistical test was applied during hierarchical analysis. For that reason another approach investigating only significantly regulated proteins (q-value ≤ 0.05, determined by either moderated t-test or rank product) was considered. According to Figure 4.6 no significant changes in protein expression levels were detectable for any protein three days after differentiation initiation compared to time point day 0, while at later time points changes became evident for many proteins. The most promising group represented the group of proteins showing a significant upregulation from day 6 until day 15 (Table 4.1) of neurosphere differentiation.

Overall, 83 of total 932 proteins (Figure 4.6) were significantly upregulated from day 6 until the end of the differentiation experiment. Table 4.1 only depicts the top 40 upregulated proteins, while the complete protein list can be found in the electronic supplement (Supplementary Data S3). Although many proteins implicated in neural cell adhesion were significantly upregulated (green-labeled), only for the neural extracellular matrix protein TNR (tenascin-R) a connection to oligodendrocytes is so far known. The protein is expressed chronologically before other common myelin proteins, like PLP (proteolipid protein), and consistent with this, TNR is assumed to play a role in controlling the timing of oligodendrocyte differentiation [Pesheva et al., 1997]. Besides this, many continuously upregulated proteins play a role in lipid metabolic processes and lipid and cholesterol transport processes (red-labeled). So far, the expression of the three proteins APOE (apolipoprotein E), PSAP (prosaposin) and ABCA1 (ATP-binding cassette sub-family A member 1) is confirmed in oligodendrocytes. APOE and ABCA1 are known target genes of the liver X receptors LXR-α and LXR-β, which in turn are responsible for the regulation of cholesterol homeostasis in oligodendrocytes [Nelissen et al., 2012], while PSAP has been evidenced to promote myelin lipid synthesis and to prolong cell survival in oligodendrocytes [Hiraiwa et al., 1997]. Most of the proteins depicted showed a continuous upregulation. This for example applies to the proteins GFAP (glial fibrillary acidic protein), SRGAP3 (SLIT-ROBO Rho GTPase-activating protein 3), serine protease HTRA1 and for proteins assigned to the lipid metabolism, like phospholipase ABHD3 and PECI (enoyl-CoA delta isomerase 2, mitochondrial). Although MS-based analysis revealed a prominent increase of the astroglial-specific protein GFAP during neurosphere differentiation, the ICC staining showed that in average only 10% of total cells expressed the GFAP protein at day 9 (Figure 4.4). Consequently, it seems that only few astrocytes expressed high amounts of GFAP.

Table 4.1.: Top 40 proteins significantly upregulated from day 6 until day 15 of neurosphere differentiation. MS-data of five biological and two technical replicates of neurosphere differentiation was searched against the murine UniProtKB/TrEMBL database (50,850 entries) at 1% false discovery rate using MaxQuant. The log2 transformed, normalized intensities of proteins detected in ≥ 3 replicates were used to compute the expression ratios of day 3, 6, 9, 12 and 15 to day 0. Two statistical tests were applied and proteins showing a q-value < 0.05 in either Limma- or Rank product-test were determined as significantly regulated. The table depicts the top 40 upregulated proteins (day 6 - 15), arranged according to the log2 expression ratios of day 15/0. Low values are colored in red, high values in blue (color scale at the bottom of the table). Proteins related to lipid metabolism and cholesterol transport are colored in red, while cell adhesion molecules are colored in green (according to GOrilla).

No	Gene	Accession	$\log_2$ day 6/0	$\log_2$ day 9/0	$\log_2$ day 12/0	$\log_2$ day 15/0
1	Gfap	P03995	1.3588	2.5579	2.9107	3.9910
2	Hspb8	Q9JK92	1.9664	3.1185	3.1103	3.5761
3	Edil3	O35474	2.3591	2.3410	2.7119	3.3588
4	Pvalb	P32848	1.6356	1.7759	1.6188	3.2136
5	Pcolce	Q61398	1.9476	2.0376	2.2454	3.2056
6	Abhd3	Q91ZH7	1.7061	2.3512	2.7228	2.9916
7	Apoe	P08226	1.5433	2.1456	2.1446	2.8135
8	Nudt7	Q99P30	1.4210	1.8569	1.8860	2.7351
9	Ahnak2	OTTMUSP00000043398	1.8720	1.9254	1.7084	2.4109
10	Abca1	P41233	1.1897	1.5992	1.8064	2.3629
11	Aqp4	P55088	0.9371	1.3585	1.4702	2.3569
12	Srgap3	Q812A2	0.6280	1.3013	1.6446	2.2741
13	Rac3	P60764	2.1236	2.2161	2.0350	2.2443
14	Htra1	Q9R118	0.9196	1.1890	1.5993	2.1729
15	Ttyh1	Q9D3A9	1.1349	1.2442	1.5773	2.1279
16	Scarb2	O35114	1.0577	1.3935	1.5474	2.1249
17	Moxd1	Q9CXI3	1.8454	1.9481	1.9877	2.1149
18	Cd63	Q8BT06	1.1272	1.4609	1.5086	2.0990
19	Dpp7	Q9ET22	1.5092	2.1746	1.4518	1.9956
20	Tagln3	Q9R1Q8	0.8306	1.1130	1.2912	1.9797
21	Tst	P52196	1.1729	1.6234	1.2128	1.9380
22	Plec	NP_001157012	0.9991	1.4317	1.4744	1.9182
23	Hexb	P20060	1.0141	1.4133	1.3232	1.8904
24	Gpr17	Q6NS65	1.2977	1.7330	2.1375	1.8794
25	Pygb	Q8CI94	0.9526	1.4470	1.2833	1.8454
26	Dcx	Q8C852	1.8130	1.8865	2.0541	1.8343
27	Shisa4	Q8CA71	1.0157	1.3390	1.4142	1.8323
28	Gsn	P13020	1.2513	1.5419	1.7483	1.8170
29	Naga	Q9QWR8	0.8739	1.4377	1.2402	1.8152
30	Glul	P15105	1.1323	1.2159	1.6521	1.7972
31	Srr	Q9QZX7	1.9059	2.0372	1.9031	1.7832
32	Tnr	Q8BYI9	1.2046	1.8126	1.8864	1.7432
33	Sepw1	P63300	1.1045	1.2234	1.2485	1.7299
34	Glud1	P26443	0.9758	1.0650	1.2191	1.6930
35	Peci	Q9WUR2	1.0225	1.1423	1.4040	1.6760
36	Aldh1l2	Q8K009	1.0940	1.3963	1.3135	1.6745
37	Scrg1	O88745	1.0972	1.4033	1.4756	1.6676
38	Pcsk1n	Q9QXV0	1.2885	1.6959	1.2864	1.6511
39	Cav1	P49817	1.1193	1.2981	1.0789	1.6456
40	Nrbp2	Q91V36	1.1000	1.6443	1.8572	1.6251
		Fold change color scale	0.6000	1.7000	2.8000	4.0000

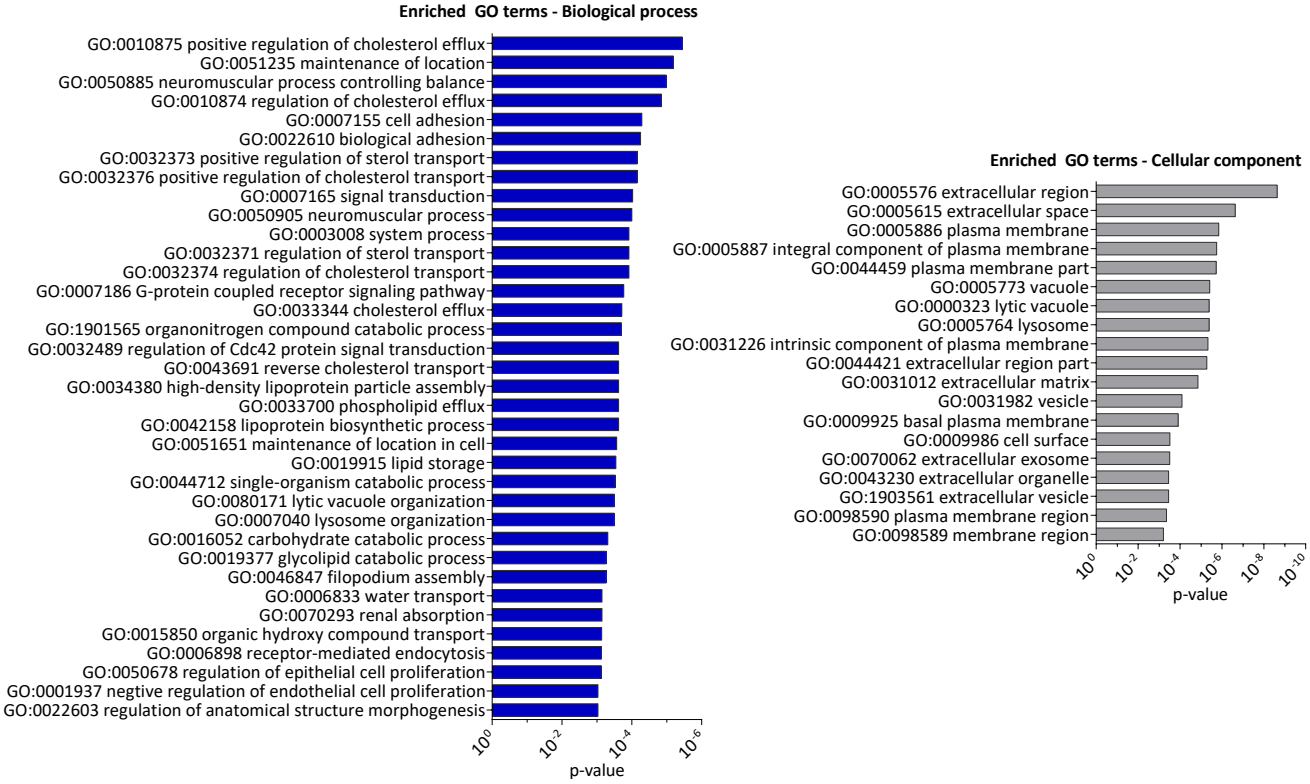

Fig. 4.10.: Gene ontology enrichment analysis of proteins significantly upregulated from day 6 - 15 of neurosphere differentiation. The GOrilla tool was used to search for enriched (a) biological processes and (b) cellular components within the group of 83 significantly upregulated proteins against all proteins that were identified in five biological and two technical replicates using MaxQuant. The leading razor protein thereby functioned as identifier. Only proteins associated with a GO term were considered for GO term enrichment analysis (5,254 target and background proteins). Enriched GO terms were determined using the standard hyper geometric testing by calculating an enrichment p-value (x-axis) for each GO term. The diagram depicts those GO terms which feature an enrichment p-value < 0.001 together with their p-values in descending order, represented as bar-charts. The calculated p-values did not include the multiple hypothesis correction on the number of tested GO terms. GO = gene ontology.

Another group of proteins displayed increasing expression levels until day 12 of the differentiation process and thereafter lower expression levels. Thus, a probable assumption for the proteins GPR17 (uracil nucleotide/cysteinyl leukotriene receptor) and NRBP2 (nuclear receptor-binding protein 2) might be their involvement in differentiation initiation and progress. Actually, an elevated expression of the protein NRBP2 during neural progenitor differentiation has already been shown. Its upregulation is consistent with its function as regulator of neural precursor cell apoptosis during the differentiation process [Larsson et al., 2008]. Additionally, investigations concerning the GPR17 protein revealed its expression in OPCs, where it is assumed to promote OPC migration and terminal cell fate determination [Coppi et al., 2013].

Although some proteins known to be involved in OPC development were identified among the significantly upregulated proteins, the function of many other proteins remained unknown. Thus, GO enrichment analysis of significantly upregulated proteins (day 6 - 15) was carried out using

the GOrilla tool. According to Figure 4.10 (a), particularly proteins involved in sterol transport were constantly upregulated, indicated by the enriched GO terms "positive regulation of cholesterol efflux" and "reverse cholesterol transport". The same proteins were also responsible for the enrichment of the GO terms "high-density lipoprotein particle assembly" and "lipoprotein biosynthetic process". Moreover, catabolic processes, necessary for energy recovery and subsequent usage in anabolic pathways, like lipid biosynthetic processes, were enriched, indicated by the GO terms "carbohydrate catabolic process" and "glycolipid catabolic process". As already mentioned, proteins involved in "cell adhesion" were enriched.
GO term analysis further revealed that basically three groups of related cellular components were enriched (Figure 4.10 (b)). The first group consisted of GO terms related to "plasma membrane", while the second group can be assigned to components localized in the extracellular region, like "extracellular matrix" and "extracellular organelles", including "exosomes". Finally, the group of intracellular enriched organelles consisted of vacuoles, particularly lysosomes, which are commonly responsible for the degradation of intracellular material [Cooper & Hausman, 2000].

4.1.2.4. Proteins significantly upregulated from day 9 until day 15 respectively from day 12 until day 15 of neurosphere differentiation

According to Figure 4.7, a large group among the significantly upregulated proteins, namely 28% respectively 16%, were upregulated from day 9 until day 15 respectively day 12 until day 15 of the differentiation process. Conclusively, many proteins seemed to be highly expressed towards the end of the differentiation experiment. Respective proteins are depicted in Table 4.3, together with the statistically evaluated log2 expression ratios. The complete list can be found in the electronic supplement (Supplementary Data S4 and S5).

Proteins involved in the formation of myelin sheaths were prominently upregulated towards the end of the differentiation process. This is consistent with myelination as a specific process of oligodendroglial cells and developed OPCs or descendants of OPCs at the end of the differentiation experiment. Some regulated proteins that can be assigned to the myelination process are labeled with red color in the tables (Figure 4.2 and 4.3), while some more proteins can be found in the electronic supplement (Supplementary Data S4 and S5). This includes for example the proteins CLDN11 (claudin-11), PLP1 (proteolipid protein 1), MBP (myelin basic protein) [Baumann & Pham-Dinh, 2001], UGT8A (2-hydroxyacylsphingosine 1-beta-galactosyltransferase, also known as cerebroside synthase) [Honke et al., 2002] and SIRT2 (NAD-dependent protein deacetylase sirtuin-2) [Tang & Chua, 2008]. Although these proteins were significantly upregulated nine days after differentiation initiation they mainly reached their expression peak towards the end of the differentiation experiment. The immunocytochemistry staining however did not reveal any mature oligodendrocytes within the first nine days of the experiment (Figure 4.3). While the proteins CLDN11 [Tiwari-Woodruff et al., 2001], SIRT2 [Li et al., 2007] and PLP1 [Werner et al., 2007] have been shown to already exert functions in OPCs or to be expressed in OPCs, MBP and UGT8A are specifically expressed in oligodendrocytes [Aston et al., 2005]. According to the MS analysis, MBP and UGT8A expression was first detected in cells differentiated for nine days. It can thus be assumed that some precursor cells developed into oligodendrocytes towards the end of the differentiation experiment.
Moreover, many proteins known to have an impact on fatty acid metabolism were strongly expressed at more progressed stages of the differentiation process. These proteins are labeled

Table 4.2.: Top 40 proteins significantly upregulated from day 9 until day 15 of neurosphere differentiation. The log2 transformed and normalized intensities of proteins detected in at least three replicates of the neurosphere differentiation experiment were used to compute the log2 expression ratios of all time points to day 0. Two statistical tests were applied and proteins showing a q-value < 0.05 in either Limma- or Rank product-test were determined as significantly regulated. The table depicts the top 40 upregulated proteins (day 9 - 15) arranged according to the log2 expression ratios of day 15/0. Not significantly regulated expression ratios are not shown (day 3, 6). The log2 expression ratios are distributed in a colored scale, with low values colored in a strong red and higher values colored in a strong blue. Proteins affecting myelination are labeled in red, while proteins regulating fatty acid metabolisms are labeled in green (determined by GOrilla).

No	Gene	Accession	$\log_2$ day 9/0	$\log_2$ day 12/0	$\log_2$ day 15/0
1	S100a4	P07091	1.9528	2.4174	3.1494
2	Tppp3	Q9CRB6	2.4268	2.3082	3.0661
3	S100a1	OTTMUSP00000024891	2.5364	2.8374	2.9993
4	Cldn11	Q60771	2.0832	2.5140	2.8739
5	Vgf	NP_001034474	3.1286	2.4785	2.8671
6	Plp1	P60202	2.0772	2.0733	2.7518
7	Cd36	Q08857	1.8874	1.4338	2.6451
8	S100a6	P14069	1.9159	2.1381	2.6411
9	Ugt8a	Q64676	2.1926	2.6206	2.5625
10	Lgals3	P16110	1.2544	1.3297	2.5492
11	Clu	Q06890	1.5932	1.6568	2.5162
12	Padi2	Q08642	1.9790	1.9327	2.4558
13	Brd2	Q7JJ13	1.4043	1.4110	2.4449
14	Ugt1a6a	Q64435	1.5027	1.8315	2.3186
15	Entpd2	O55026	1.4945	1.5053	2.2970
16	Mgll	Q3UFX6	1.3014	1.7903	2.1640
17	Sirt2	Q8VDQ8	2.0553	2.2013	2.1158
18	Ust	Q8BUB6	1.5385	1.7680	2.0562
19	S1pr1	O08530	1.6027	1.9347	2.0119
20	Ech1	O35459	1.4532	1.2820	1.9702
21	Bcas1	Q80YN3	2.3208	1.8787	1.9647
22	Pttg1ip	Q8R143	0.9979	1.3242	1.9360
23	Enpp6	Q8BGN3	1.6896	1.8247	1.9159
24	Hsdl2	Q2TPA8	1.3358	1.4931	1.8998
25	Acsf2	Q8VCW8	0.8936	1.2664	1.8707
26	Mgst1	OTTMUSP00000033598	1.2443	1.5743	1.8636
27	Cd9	P40240	1.2657	1.3385	1.8611
28	Atp11b	OTTMUSP00000024745	1.2266	1.5767	1.8395
29	Aldh6a1	Q9EQ20	1.1231	1.4203	1.8389
30	Mbp	P04370	1.6843	1.6690	1.8310
31	Tuba4a	P68368	1.1306	1.2244	1.7980
32	Adhfe1	Q8R0N6	1.2961	1.1970	1.7784
33	Fuca2	Q99KR8	1.0714	1.3039	1.7493
34	Sez6l	Q6P1D5	1.2603	1.3508	1.7144
35	Ephx2	P34914	1.3686	1.1309	1.7141
36	Lsamp	Q8BLK3	1.5932	1.3681	1.7075
37	Abat	P61922	1.0915	1.1208	1.7050
38	Acad10	Q8K370	1.0650	1.1082	1.6889
39	Ass1	P16460	1.5935	1.5451	1.6825
40	S100a13	P97352	1.2732	1.1343	1.6729

Table 4.3.: Top 40 proteins significantly upregulated from day 12 until day 15 of neurosphere differentiation. The log2 transformed and normalized intensities of proteins detected in at least three replicates of the neurosphere differentiation experiment were used to compute the log2 expression ratios of all time points to day 0. Two statistical tests were applied and proteins showing a q-value < 0.05 in either Limma- or Rank product-test were determined as significantly regulated. The table depicts the top 40 upregulated proteins (day 12 - 15) arranged according to the log2 expression ratios of day 15/0. Not significantly regulated expression ratios are not shown (day 3, 6 and 9). The log2 expression ratios are distributed in a colored scale, with low values colored in a strong red and higher values colored in a strong blue. Proteins regulating fatty acid metabolisms are labeled in green (determined by GOrilla).

No	Gene	Accession	$\log_2$ day 12/0	$\log_2$ day 15/0
1	Sts	P50427	1.5485	1.8274
2	Trappc6a	Q78XR0	1.6774	1.7195
3	Sorbs2	Q3UTJ2	1.1569	1.5974
4	Fahd2a	Q3TC72	0.9989	1.5469
5	Enpp4	Q8BTJ4	0.9166	1.4718
6	Opcml	OTTMUSP00000028915	1.0463	1.4639
7	Acox3	Q9EPL9	0.6844	1.3326
8	N/A	Q3UNZ8	1.1014	1.2813
9	Hibch	Q8QZS1	0.7166	1.2547
10	Brp44	Q9D023	0.9602	1.2442
11	Hadh	Q61425	0.8273	1.2369
12	Serpinb6a	OTTMUSP00000000666	1.2455	1.2278
13	Decr2	Q9WV68	1.3209	1.2270
14	Mp68	P56379	0.7031	1.2138
15	Plcd1	Q8R3B1	0.9445	1.1654
16	Prkcdbp	Q91VJ2	0.8979	1.1477
17	Aco2	Q99KI0	0.7377	1.1357
18	Nebl	OTTMUSP00000012207	0.7460	1.1256
19	Acad11	Q80XL6	1.0452	1.0662
20	Slc25a18	Q9DB41	0.6114	1.0479
21	Atp6v0a2	P15920	1.1848	1.0416
22	Parvb	Q9ES46	1.2443	1.0381
23	Acot2	Q9QYR9	0.9229	1.0319
24	Crat	P47934	0.9014	1.0060
25	Tspyl4	Q8VD63	1.1253	0.9960
26	Atp1a1	Q8VDN2	0.6828	0.9947
27	Ndufa2	Q9CQ75	0.6697	0.9924
28	Cyc1	Q9D0M3	0.7786	0.9910
29	Cyb5r1	Q9DB73	0.8071	0.9477
30	Uqcrc1	Q9CZ13	0.6028	0.9433
31	Uqcrc2	Q9DB77	0.6091	0.9409
32	Dock4	P59764	1.1746	0.9384
33	Coro1b	Q9WUM3	0.8972	0.9338
34	Fam82b	Q9DCV4	0.7813	0.9211
35	B3gat3	P58158	0.9069	0.9201
36	Vdac1	Q60932	0.6058	0.9129
37	Slc25a22	Q9D6M3	0.7339	0.9019
38	Ndufb5	Q9CQH3	0.6864	0.9006
39	Spns1	Q8R0G7	0.6864	0.8947
40	Slc4a4	OTTMUSP00000031585	0.9032	0.8925

with green color in both tables (Figure 4.2, 4.3). This is for example applicable to the proteins CD36 (platelet glycoprotein 4) [Febbraio et al., 1999], ACSF2 (acyl-CoA synthetase family member 2, mitochondrial) [Watkins et al., 2007] and MGLL (monoglyceride lipase) [Karlsson et al., 1997]. Although some proteins involved in the fatty acid metabolism were upregulated after nine days of differentiation, most proteins involved in this process were mainly upregulated after twelve days (Figure 4.3). This is consistent with an augmentation of the lipid metabolism upon differentiation of OPCs to oligodendrocytes.

Similar to former approaches, GO term enrichment analyses were performed to identify biological processes and cellular components enriched towards the end of the differentiation experiment. For this purpose, proteins significantly upregulated from day 9 until day 15 and from day 12 until day 15 were combined and analyzed using GOrilla. Histograms depicting the top 40 enriched GO terms in both ontologies can be found in the Appendix (Figure A.1). The complete list of enriched GO terms featuring a p-value < 0.001, namely 70 biological processes and 68 cellular components, can be found in the electronic supplement (Supplementary Data S6a and S6b). Several enriched GO terms were already detected in former GO term analyses. Nevertheless, the enrichment p-values were noticeably lower in this GO term analysis compared to former analyses (Figure 4.9 and Figure 4.10), indicating a stronger overrepresentation of distinct GO terms towards the end of the differentiation experiment. Since only proteins regulated at later time points were considered in this analysis, identified enriched GO terms could be very likely associated with oligospheres and rather with neurospheres.

Most of the upregulated proteins were involved in single-organism metabolic processes or more specifically in ”oxidation-reduction processes”, including the contribution in the ”electron transport chain”, as well as in ”lipid metabolic processes” (Figure A.1). Regarding the lipid metabolism, mainly catabolic processes, such as ”cellular lipid catabolic process”, ”lipid oxidation” and ”fatty acid beta-oxidation” were enriched. GO term analysis in addition revealed that proteins assigned to myelination were present in the group of proteins significantly upregulated towards the end of the differentiation experiment.
Within the ontology of cellular component, many proteins upregulated at later time points of the differentiation process could mainly be assigned to organelles, such as ”lysosomes”, ”endosomes”, ”exosomes” and the ”mitochondrion”. Regarding the mitochondrion, most upregulated proteins can be assigned to the ”inner mitochondrial membrane protein complex” and the ”respiratory chain”. In addition, the GO term ”myelin sheath” was enriched.

Comparison of GO term results, obtained by either analysis of proteins upregulated from day 6 on (Figure 4.10) or analysis of proteins upregulated towards the end of the experiment (Figure A.1), revealed that mainly the sterol and especially the cholesterol metabolism and lipoproteins were affected at earlier stages, while myelination, transport processes and lipid metabolism, especially the fatty acid metabolism, were affected during later stages of neurosphere differentiation.

4.1.2.5. Investigation of distinct protein classes

In this approach, proteins were characterized based on their affiliation to protein classes responsible for cell differentiation, including receptors, transcription regulating factors and kinases using the UniProt and AmiGO 2 protein search engines. These classes were chosen, since cell fate de-

termination and subsequent cellular differentiation is mainly affected by transcription regulating proteins, like transcription factors and histone modifiers, that enhance or repress the gene expression of proteins responsible for cellular development. However, activation of transcriptional regulatory proteins often depends on extrinsic signaling mediated by substrate binding to the respective cell surface receptors and activation of downstream signaling pathways via kinases. First, a murine protein class was searched in the UniProtKB database [Apweiler et al., 2004] (for example: transcription factor and mus musculus), following verification and specification using the GO database AmiGO 2 [Carbon et al., 2008]. Transcription regulating factors for example were additionally filtered for the GO terms "DNA binding" and "regulation of transcription, DNA dependent". The second filtering step was necessary to obtain more specific results due to the wide range of proteins associated with the respective term (e.g. transcription factor). Finally, proteins showing positive results in both searches were assembled in tables for each protein class and depicted in line charts and tables containing the top regulated proteins.

Transcription regulating factors Altogether, 123 proteins regulating transcription were identified within the neurosphere differentiation experiment. The line graph (Figure 4.11) depicts the expression pattern of all transcription regulating factors, while the top 10 (based on the day 6 to day 0 log2 expression ratio) up- and downregulated transcription regulating factors are additionally differentially labeled. The complete list of regulated proteins that regulate transcription can be found in the electronic supplement (Supplementary Data S7). The expression of most transcription regulating factors, namely 104 proteins, decreased from day 0 until day 6 of the differentiation experiment, indicated by the log2 expression ratios. It should be noted that not all proteins were continuously upregulated during the differentiation period, but rather some outliers were present. Compared to the category of receptors or kinases, changes in protein levels over time were less evident among transcription regulating factors.

Most regulated transcription regulating factors exhibited almost same expression levels at day 0 and day 3, indicating that little regulation occurred during the first days of the differentiation experiment. For some transcription regulating factors a change in protein levels was visible three or six days after differentiation initiation, while thereafter changes were less evident or expression levels even decreased (Figure 4.11). This for example applies to the protein TCEAL5 (transcription elongation factor A protein-like 5), AHCTF1 (protein ELYS), ARNT2 (aryl hydrocarbon receptor nuclear translocator 2) and STAT3 (signal transducer and activator of transcription 3). TCEAL5, AHCTF1 and ARNT2 have been so far not connected to oligodendroglia or to NPC differentiation, while STAT3 is an effector protein within the fibroblast growth factor pathway [Hart et al., 2001], which in turn was evidenced to promote differentiation to oligodendroglial cells [Hu et al., 2012b]. The protein SIRT2 (NAD-dependent protein deacetylase sirtuin-2) was expressed at high levels after six days, while the highest upregulation was observed after nine days of differentiation. SIRT2 has already been evidenced to regulate oligodendroglial cell differentiation [Ji et al., 2011]. For two additional proteins a relation to oligodendroglia was previously shown. The protein PURA (transcriptional activator protein Pur-alpha) was evidenced to positively regulate the expression of the myelin basic protein [Tretiakova et al., 1999], whereas its interference with the transcription factor E2F1 results in decreased cellular proliferation [Darbinian et al., 2004]. Likewise, PHB (prohibitin) was shown to negatively regulate E2F1 activity [Wang et al., 1999]. The evidenced detection of PHB in oligodendroglial cells suggests its involvement in the regulation of cell proliferation [Bernstein et al., 2012].

Depending on the target gene, transcription regulating factors can either activate or repress gene transcription. Moreover, target proteins can either have inducing or repressing effects on NPC differentiation. The downregulation of a transcription activator, regulating the expression of a negative regulator of the differentiation process, would accordingly promote cellular differentiation. In addition, downregulation of a transcription regulating factor can also be an indication for its involvement in NPC specific processes, like the cell cycle. For most downregulated transcription regulating factors a change in protein expression was evident six days after differentiation initiation, which continued until day 15 of the differentiation process, where lowest expression values were detected (Figure 4.11). Compared to the group of upregulated transcription regulating factors, changes in expression levels over time were more evident. The downregulation of some transcription regulating factors can be explained by their biological functions. The highly downregulated protein RCOR2 (REST corepressor 2) is a component of the REST complex, which in turn has been shown to regulate self-renewal and pluripotency mechanisms in ESCs [Abrajano et al., 2009]. The strongly downregulated transcription factor SOX3 is a member of the SoxB1 family and its expression has been evidenced in NPCs, where it maintains cells in an undifferentiated state [Bylund et al., 2003]. The strongly downregulated protein KDM3A (lysine-specific demethylase 3A) is likewise implicated in stem cell maintenance. At least a reduction of KDM3A has been shown to result in cell differentiation of embryonic stem cells [Loh et al., 2007]. The protein ZEB1 (transcriptional repressor protein zinc finger E-box-binding homeobox 1), an enhancer of neuronal differentiation [Ravanpay et al., 2010], showed the strongest downregulation among all transcription regulating proteins.

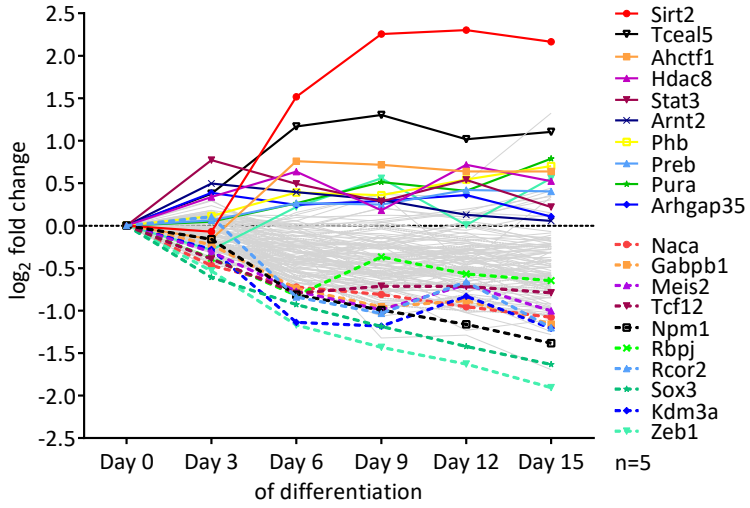

Fig. 4.11.: Changes in log2 expression ratios of transcription regulating factors during neurosphere differentiation. The evidence file, generated by MaxQuant, was filtered for contaminants, positive reverse database matches, peptides featuring values > 0 in all reporter ion channels and proteins detected in ≥ 3 biological replicates. Log2 transformed peptide intensities were normalized to the median per reporter ion channel, combined on protein level by calculating the median and replicates were combined by calculating the mean of all protein intensities. Obtained data was filtered for "transcription factor" using UniProt and for "DNA binding", "regulation of transcription" using AmiGO 2. The line graphs depicts the log2 transformed day > 0 / day 0 expression ratios of proteins present in both searches. The top 10 up- and downregulated transcription regulating factors (day 6/0) are differentially labeled.

Receptors proteins and proteins interacting with receptors In total, 93 receptors and proteins interacting with receptors were detected in the neurosphere differentiation data set. These proteins are plotted in Figure 4.12, while the complete list can be found in the electronic supplement (Supplementary Data S8). Based on the log2 transformed expression ratios of day 6 to day 0, 48 proteins were up- and 45 proteins were downregulated. The expression levels increased in a continuous way with only a few outliers. Compared to the class of transcription regulating factors, the differences in protein expression ratios were more pronounced.

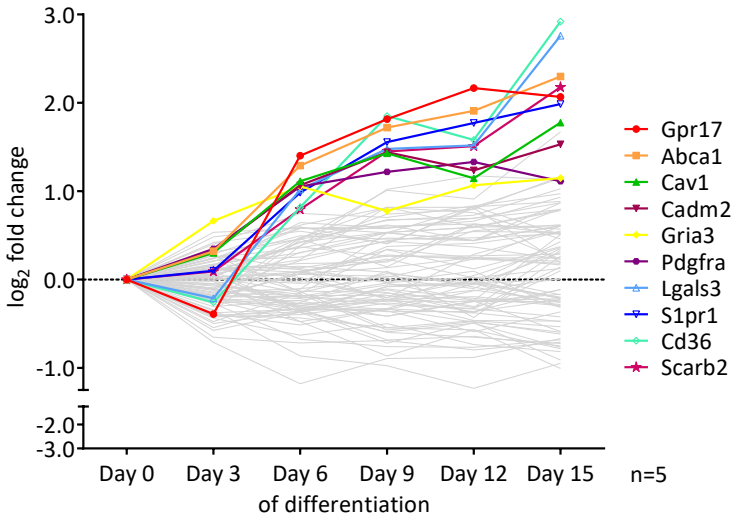

Fig. 4.12.: Changes in log2 expression ratios of receptors and proteins interacting with receptors during neurosphere differentiation. The evidence file, generated by MaxQuant, was filtered for contaminants, positive reverse database matches, peptides featuring values > 0 in all reporter ion channels and proteins detected in ≥ 3 biological replicates. Log2 transformed peptide intensities were normalized to the median per reporter ion channel, combined on protein level by calculating the median and finally replicates were combined by calculating the mean of all protein intensities. Obtained data was filtered for "receptors" using UniProt and "receptor activity" using AmiGO 2. The line graphs depicts the log2 transformed day > 0 / day 0 expression ratios of proteins present in both searches. The top 10 upregulated proteins (day 6/0) are differentially labeled.

While most proteins within this protein class were constantly upregulated during the differentiation process, only few proteins, including the proteins PDGFRA (platelet-derived growth factor receptor alpha) and GRIA3 (glutamate receptor 3), displayed almost same expression ratios from day 6 until day 15. The protein PDGFRA was evidenced to activate the downstream PDGF signaling pathway, responsible for differentiation of neural stem cells to OPCs [Hu et al., 2012a]. With S1PR1 (sphingosine 1-phosphate receptor 1) another receptor was upregulated, whose expression was shown to be positively regulated by the mitogen PDGF [Jung et al., 2007].
Some of the continuously upregulated proteins have already been assigned to oligodendrocytes. The proteins CAV1 (caveolin-1) [Cheli et al., 2015] and GPR17 (uracil nucleotide/cysteinyl leukotriene receptor) [Coppi et al., 2013], for example, are either involved in OPC differentiation initiation and maturation upon ligand binding or in OPC migration. This is consistent with their increasing expression pattern during NPC to OPC differentiation. Moreover, the likewise early upregulated protein ABCA1 (ATP-binding cassette sub-family A member 1) has

already been detected in oligodendrocytes [Kim et al., 2006]. The highest upregulated receptor at day 15, the protein CD36 (platelet glycoprotein 4), has been postulated to promote peripheral nerve remyelination [Eto et al., 2008]. The, especially towards the end of the experiment, highly upregulated protein LGALS3 (galectin-3) represents an extracellular binding partner for the NG2 proteoglycan [Fukushi et al., 2004]. Its detection in the neurosphere differentiation data set might result from its interaction with the NG2 protein, expressed on OPCs. In addition, with SCARB2 (lysosome membrane protein 2), also known as the lysosomal integral membrane protein type 2 (LIMP-2), a lysosomal receptor for the lysosomal enzyme glucosylceramidase showed continuous upregulation during neurosphere differentiation.

Kinases The class of protein kinases investigated counts in total 131 regulated proteins, whereof 62 proteins were up- and 69 proteins were downregulated after six days of neurosphere differentiation (for complete list refer to the electronic supplement (Supplementary Data S9)). This includes also transmembrane receptors containing a tyrosine kinase domain, like PDGFRA. Most of the kinases showed a continuous increase in protein expression until day 15 of the differentiation process (Figure 4.13), like the proteins NRBP2 (nuclear receptor-binding protein 2), DCLK1 (serine/threonine-protein kinase DCLK1) and CAMK2G (calcium/calmodulin-dependent protein kinase type II subunit gamma). The protein NRBP2 is implicated in the survival of neural progenitor cells upon differentiation [Larsson et al., 2008]. In addition, only for the protein CDK5 (cyclin-dependent-like kinase 5) a connection to oligodendrocytes is known so far. CDK5 was shown to positively regulate differentiation of OPCs [Miyamoto et al., 2008].

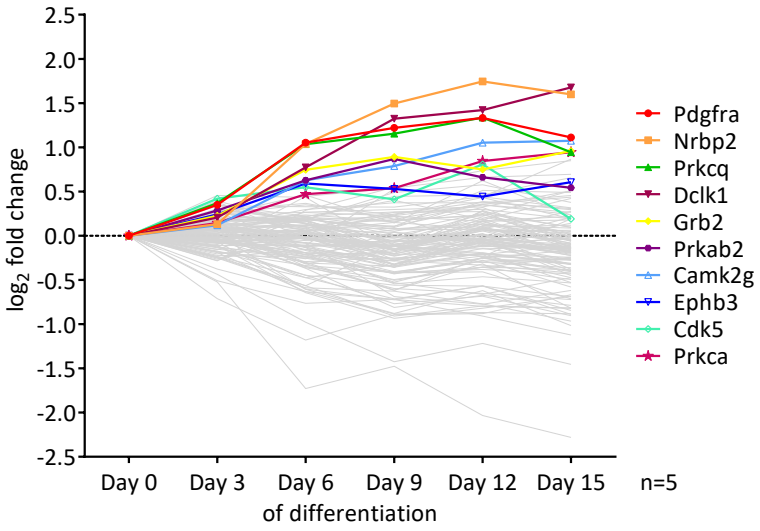

Fig. 4.13.: Changes in log2 expression ratios of kinases during neurosphere differentiation. The evidence file (MaxQuant) was filtered for contaminants, positive reverse database matches, peptides featuring values > 0 in all reporter ion channels and proteins detected in ≥ 3 biological replicates. Log2 transformed peptide intensities were normalized to the median per reporter ion channel, combined on protein level by calculating the median and finally replicates were combined by calculating the mean of all protein intensities. Obtained data was filtered for "protein kinases" using UniProt and "protein kinase activity" using AmiGO 2. The line graph depicts the log2 transformed day > 0 / day 0 expression ratios of proteins present in both searches. The top 10 upregulated kinases (day 6/0) are differentially labeled.

4.1.2.6. Significantly downregulated proteins (day 6 until day 15)

Compared to proteins showing a time dependent upregulation, more proteins displayed a downregulation during the differentiation process. Most likely, these proteins are involved in processes taking place in NPCs, like the maintenance or the regulation of the cell cycle or the self-renewal process. These proteins might lose their function while undergoing cell differentiation into OPCs. Thus, proteins exhibiting a continuous drop in expression levels might be worth investigating. According to Figure 4.7, 54 proteins were significantly downregulated from day 6 until day 15 of the differentiation experiment. The top 40 proteins, based on the log2 expression ratios of day 15 to day 0, together with their corresponding log2 expression ratios, are listed in Table 4.4. The complete list of proteins significantly downregulated from day 6 until day 15 can be found in the electronic supplement (Supplementary Data S10).

According to Table 4.4, many proteins were already strongly reduced in their expression after a cultivation period in differentiation medium of six days. This for example applies to the protein NES (intermediate filament structural protein nestin), which is responsible for proper survival and self-renewal of NSCs [Park et al., 2010] or POLA1 (DNA polymerase alpha catalytic subunit), responsible for the initiation of DNA replication [Rytkönen et al., 2006]. Moreover, some proteins (red-labeled) can be assigned to cell cycle processes, either being part of the complex accomplishing mitosis or possessing regulatory functions, including the proteins TIMELESS (protein timeless homolog) [Yoshizawa-Sugata & Masai, 2007], TOP2A (DNA topoisomerase 2-alpha) [Downes et al., 1994], MAD2L1 (mitotic spindle assembly checkpoint protein MAD2A) [Luo et al., 2000] or CCNA2 (cyclin-A2) [Pagano et al., 1992].

Only one gene ontology enrichment analysis was performed, based on all proteins significantly downregulated from day 6 until day 15, from day 9 until day 15 and from day 12 until day 15. This approach was chosen since the GO term analysis of proteins significantly downregulated from day 6 until day 15 resulted in any enriched GO terms (p-value < 0.001). The GO term analysis of downregulated proteins was conducted to obtain an indication for overrepresented biological processes and cellular components in neurospheres compared to oligospheres.
In total, 135 enriched biological processes and 45 enriched cellular components were identified, listed in the electronic supplement (Supplementary Data S11a and S11b). The histograms depicting only the top 40 GO terms can be found in the Appendix (Figure A.2). Mainly, DNA and RNA related processes were enriched, indicating their importance in neurospheres and rather in oligospheres. This is consistent with our expectation that during the differentiation experiment rather cell differentiation instead of cell proliferation occurs. This finding is further strengthened by the enrichment of GO terms related to DNA and RNA metabolic processes, including "DNA replication" and "mRNA splicing and processing" (Figure A.2 (a)). In addition, GO terms related to regulation of particularly metabolic processes, including the GO terms "regulation of RNA biosynthetic process", or "regulation of DNA metabolic process" were enriched. Moreover, proteins involved in cell cycle processes were prominently enriched in neurospheres, consistent with the enrichment of several cell cycle regulated GO terms, like the "mitotic cell cycle process". On the other hand, less enriched GO terms were identified with a p-value < 0.001 in the ontology of cellular components (Figure A.2 (b)). However, almost all downregulated proteins were localized in the nucleus, the nucleoplasm or the nucleolus. Moreover, GO terms related to the "spliceosomal complex" and the "spliceosomal snRNP complex" were enriched.

Table 4.4.: Top 40 significantly downregulated proteins from day 6 until day 15 of neurosphere differentiation. MS-data of five biological and two technical replicates of neurosphere differentiation was searched against the murine UniProtKB/TrEMBL database (50,850 entries) at 1% false discovery rate using MaxQuant. The log2 transformed, normalized intensities of proteins detected in $\geq$ 3 replicates were used to compute the expression ratios of day 3, 6, 9, 12 and 15 to day 0. Two statistical tests were applied and proteins showing a q-value < 0.05 in either Limma- or Rank product-test were determined as significantly regulated. The table depicts the top 40 (day 6 - 15), arranged according to the log2 expression ratios of day 15/0. High values are colored in red, low values in blue (color scale at the bottom of the table). Proteins, implicated in the cell cycle or DNA replication are colored in red.

No	Gene	Accession	$\log_2$ day 6/0	$\log_2$ day 9/0	$\log_2$ day 12/0	$\log_2$ day 15/0
1	Timeless	Q9R1X4	-1.7044	-2.0791	-1.7478	-2.4583
2	Car3	P16015	-1.2692	-2.1259	-2.2301	-2.3644
3	Sall3	Q62255	-1.2293	-1.7742	-1.5330	-2.3278
4	Nes	Q6P5H2	-1.4476	-2.0088	-2.0071	-2.1110
5	Ccna2	P51943	-1.6138	-1.4410	-1.8674	-2.0910
6	Tyms	P07607	-1.4039	-1.8714	-1.6394	-1.9082
7	Slc1a5	E9PXK5	-1.2246	-1.9086	-1.4898	-1.8802
8	Pola1	P33609	-1.6540	-1.9328	-1.6778	-1.7939
9	Hat1	OTTMUSP00000014193	-1.3509	-1.6237	-1.3758	-1.7772
10	Top2a	Q01320	-1.8196	-1.7130	-2.0214	-1.7485
11	Mad2l1	Q9Z1B5	-1.1844	-1.4907	-1.5707	-1.6561
12	Hmgcs1	Q8JZK9	-1.2102	-1.3287	-1.4141	-1.6333
13	Ncaph	Q8C156	-1.2494	-1.1806	-1.2257	-1.5925
14	Chaf1b	Q9D0N7	-1.4978	-1.8891	-1.6469	-1.5621
15	Mcm6	P97311	-1.1056	-1.4365	-1.1333	-1.5202
16	Stmn2	Q9CZ46	-0.8812	-0.9059	-1.3709	-1.4871
17	Rab3d	P35276	-0.8840	-1.6541	-1.5488	-1.4806
18	Tagln	P37804	-1.2442	-1.3306	-1.3331	-1.4570
19	Ubap2	Q91VX2	-1.2336	-1.1199	-1.3341	-1.3875
20	Rab3b	Q9CZT8	-0.9108	-1.2014	-1.2172	-1.3477
21	Pola2	P33611	-1.0762	-1.6271	-1.2381	-1.3078
22	Haus5	Q9D786	-0.9079	-1.2785	-0.9964	-1.2974
23	Prim2	P33610	-1.0063	-1.2253	-0.9541	-1.2784
24	Stmn1	P54227	-0.7771	-0.9608	-1.2242	-1.2770
25	Gls	OTTMUSP00000023770	-1.2011	-1.5253	-1.0787	-1.2330
26	Zcchc8	Q9CYA6	-0.9158	-0.7888	-0.6819	-1.1681
27	Tbl3	Q8C4J7	-2.3503	-0.9982	-1.0168	-1.1404
28	Smc4	Q8CG47	-0.8022	-0.9543	-0.9885	-1.1184
29	Scd2	P13011	-0.8268	-1.1288	-0.7261	-1.0750
30	Tia1	P52912	-0.8036	-0.7410	-0.7879	-1.0679
31	Metap2	Q3UI33	-0.9311	-1.0579	-1.2826	-1.0585
32	Dut	OTTMUSP00000016347	-1.1516	-1.1816	-1.3232	-1.0273
33	Klhdc4	ENSMUSP00000134361	-1.3417	-1.0252	-1.2301	-1.0179
34	Hip1	Q8VD75	-0.6205	-0.9219	-0.8219	-0.9873
35	Nfib	P97863	-0.6595	-0.6682	-0.8068	-0.9315
36	Nap1l1	NP_001140179	-0.6780	-0.8680	-0.9177	-0.9212
37	Tsen34	Q8BMZ5	-0.6535	-0.8232	-0.5807	-0.8974
38	Pbxip1	Q3TVI8	-0.9257	-1.0627	-1.0107	-0.8884
39	Serbp1	Q9CY58	-0.6927	-0.7115	-1.0715	-0.8579
40	Psme3	P61290	-0.5991	-0.7839	-0.7395	-0.8455
		Fold change color scale	-0.3000	-1.0000	-1.7000	-2.4000

4.2. Differentiation of rat oligodendrocyte precursor cells (OPCs) to oligodendrocytes

In a second approach, changes in protein abundance during differentiation from oligodendrocyte precursor cells (OPCs) to oligodendrocytes were investigated. Commonly, investigation of biological systems are performed using mouse models and rather rat models. Although the mapping of the complete rat genome was achieved in 2004 [Gibbs et al., 2004], still more information is available on murine proteins compared to rat proteins (UniProtKB/TrEMBL: 50,850 entries for mouse proteins (07/2013) and 25,841 for rat proteins (05/2015) [Apweiler et al., 2004]). However, due to the following facts, cells derived from P1 or P2 rats were used to generate OPCs. There are two common methods used for the cultivation of OPCs. The first one, the neurospheres assay, was used in the former investigation of neural progenitor cell to OPC differentiation. However, the requirement of a pure and large culture of OPCs would have made the dissection of many mouse cortices and the application of fluorescence-activated cell sorting (FACS) necessary. Moreover, the subsequent differentiation of OPCs, derived from the neurospheres assay, to oligodendrocytes has been turned out to be difficult, since murine cells show a higher incidence of apoptosis mediated by the intrinsic pathway [Horiuchi et al., 2010]. Although this issue can be overcome by using the adenylyl cyclase activator forskolin, not enough cells can be obtained for mass spectrometric purpose. The second common method to cultivate OPCs is the widely used shaking method [Szuchet & Yim, 1984] [Chen et al., 2007]. However, in comparison to rat OPCs, mouse OPCs are more difficult to isolate and they tend to differentiate *in vitro* in mixed glial cultures, where they are harder to separate from astrocytes compared to rat OPCs. Conclusively, rat cells were separated from mixed glial cultures using the shaking method. Separation was achieved by shaking flasks on an orbital shaker for a varying length of time. Due to different adhesion properties of cell types, OPCs can be isolated from microglia and astrocytes. Differentiation of OPCs to mature oligodendrocytes was performed for nine days by changing the complete cell culture medium every second day with fresh differentiation medium, containing triiodothyronine (T3) [Baas et al., 1997], a known promoter of oligodendrocyte maturation, ciliary neurotrophin factor (CNTF) [Talbott et al., 2007] and n-acetyl l-cystein (NAC) [Mayer & Noble, 1994], which both have been shown to increase OPC survival.
Cells were harvested at different time points for either performing immunocytochemistry (ICC) analysis to confirm differentiation of OPCs into oligodendrocytes or large scale proteomic analysis for the purpose of investigating time-dependent alterations in the oligodendroglial proteome during differentiation.

4.2.1. Monitoring of oligodendrocyte precursor cell differentiation by microscopy

First, the protocol for preparation and separation of OPCs was tested by performing ICC staining of chondroitin sulfate proteoglycan 4 (NG2)-expressing OPCs, GFAP-expressing astrocytes, beta III tubulin-expressing neurons, F4/80-expressing microglia and MBP-expressing oligodendrocytes, cultivated for three days in differentiation medium.
The evaluation of immunofluorescence images (Figure 4.14 (a)) revealed that three days after differentiation initiation most isolated cells were NG2 positive, indicating the quality of the shaking method for separation of OPCS from other cell types. Furthermore, some cells were already differentiated into oligodendrocytes, while only a few cells were GFAP- or beta III

tubulin-positive and none were positive for F4/80. Cells of the oligodendroglial lineage express the NG2 protein during a distinct period of their development, particularly during progenitor and pre-oligodendrocyte stage. Accordingly, after confirming an almost pure OPC culture, cells were differentiated into oligodendrocytes and fixed on coverslips every third day for nine days. Representative immunofluorescent images are shown in Figure 4.14 (b).

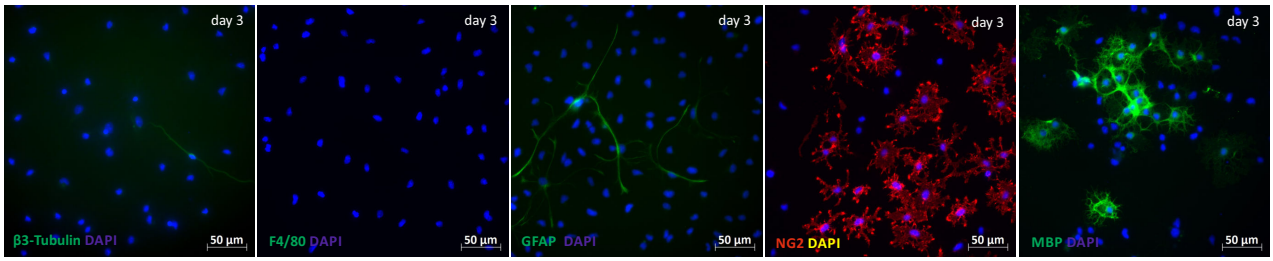

(a) Immunocytochemistry staining - Day 3

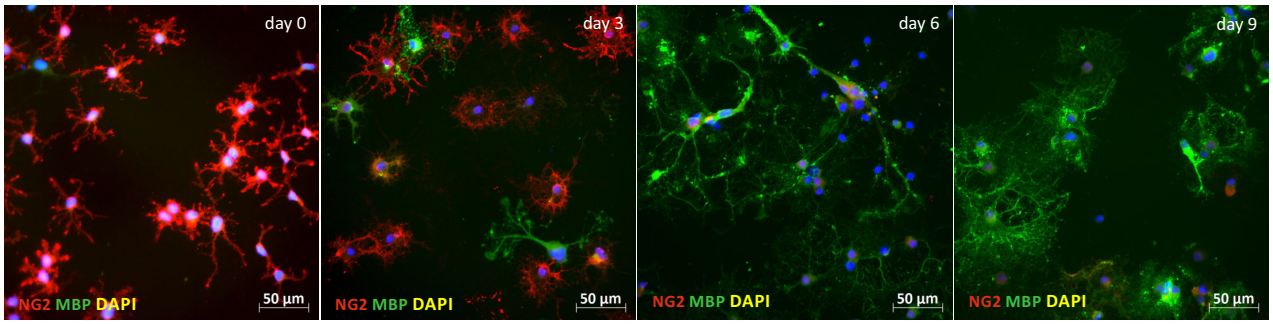

(b) Immunocytochemistry staining - Day 0 until day 9

Fig. 4.14.: Immunocytochemistry staining of differentiating oligodendrocyte precursor cells. OPCs from rat cortical cells (P1 or P2), cultivated for 10 or 20 days (depending on whether cells derived from the 1st or 2nd shaking off batch) were isolated from mixed glial cell culture by the shaking method, seeded onto poly-L-ornithine-coated coverslips, cultivated for seven to ten days in proliferation medium and thereafter in differentiation medium for nine days. ICC staining (a) was performed at day 3 against neurons (anti-beta III tubulin ab, α-mouse-Alexa488 ab), microglia (anti-F4/80 ab, α-rat-Dylight488 ab), astrocytes (anti-GFAP ab and α-mouse-Alexa546 ab), OPCs (anti-NG2 antibody and α-rabbit-Cy3 ab) and oligodendrocytes (anti-MBP ab, α-rat-Dylight488 ab). (b) ICC staining against OPCs and oligodendrocytes from day 0 until day 9 of differentiation. For both approaches, cells were fixed with paraformaldehyde, permeabilized with Triton X-100, blocked with normal goat serum, stained with primary antibodies overnight at 4 ℃ and with secondary antibodies and DAPI for 90 minutes at room temperature. Coverslips were washed and mounted on slights using antifade reagents. Images were taken using the Axiovert 100 M microscope (20x objective). ab = antibody; OPCs = oligodendrocyte precursor cells; ICC = immunocytochemistry; P1/P2 = perinatal day 1 or 2

The ICC staining covering nine days of the OPC differentiation process (Figure 4.14 (b)) indicated that at the beginning of the differentiation experiment (day 0) an almost pure NG2-expressing cell population existed. Only a few cells could not be detected with neither the NG2 nor the MBP antibody, indicating that they did not belong to the oligodendroglial cell lineage. After three days in differentiation medium, some cells still expressed NG2 on their cell surface, whereas a small population already started to differentiate into MBP-expressing oligodendro-

cytes. Moreover, the morphology of NG2-expressing cells changed during the differentiation process, indicated by the formation of more widespread extensions. With prolonged cultivation of cells in differentiation medium, the amount of MBP-expressing cells increased, while the number of NG2-expressing cells decreased noticeably. However, some cells were only stained with the nucleus-marker DAPI.

4.2.2. Analysis of time dependent protein level alterations during oligodendrocyte precursor cell differentiation by large scale mass spectrometry

After ensuring that most of the cells were NG2-positive at the beginning of the differentiation experiment and that differentiation to oligodendrocytes is achieveable with the differentiation medium used, the focus was laid on proteins and their changes in expression during the differentiation from OPCs to oligodendrocytes. Therefore, cells were cultivated in larger numbers and according to the ICC experiment, cells were differentiated for nine days and subsequently harvested at the beginning of the experiment and every third day. Accordingly, the experiment counted four samples (four time points). For relative quantification purpose, every time point was labeled with isobaric reagents (four TMTsixplex™ reagents) [Thompson et al., 2003]. Altogether, four biological replicates of OPC differentiation were generated. It should be noted that for three biological replicates the chloroform/methanol protein precipitation method was used, followed by in solution digestion with Rapigest, whereas the digestion and isobaric labeling steps of the forth replicate were performed on filter aided sample preparation (FASP) devices (Microcons) [Wiśniewski et al., 2009]. Both sample preparation methods represented common approaches in the mass spectrometric field [Feist & Hummon, 2015]. Samples were applied to a nanoflow ultra-high performance liquid chromatography (UHPLC), coupled to a LTQ-Orbitrap Velos mass spectrometer and the raw data of four biological and one technical replicate was combined and analyzed with the Proteome Discoverer™ 2.1 software and the database search algorithm Mascot [Cottrell & London, 1999].

Using Mascot, altogether 3,876 unique proteins, based on 120,000 peptide spectrum matches (PSMs) were identified (false discovery rate (FDR) = 0.01). Analyzing the Venn diagram (UGent Bioinformatics & Evolutionary Genomics, Appendix D: URL2) shown in Figure 4.15, it is discernible that not all proteins were found in every replicate, but at least 1,903 proteins were present in all replicates. Moreover, 2,593 proteins were detected in at least three biological replicates. The Pearson correlation of normalized intensities between the replicates are depicted in a scatterplot (Figure 4.15) to allow for easier identification of outliers. Accordingly, for every time point the correlation coefficients between two replicates (based on the normalized intensities) were calculated to verify the reproducibility between the runs. The Pearson's correlation coefficient, which attains values between -1 and 1, amounted between 0.4 and 0.6 for two considered replicates, which indicated a moderate correlation of intensities according to Evans [Evans, 1996]. For the two technical replicates 3a and 3b the Pearson's correlation coefficients amounted around 0.62. Replicate 4 correlated less well with the other replicates and especially at day 6 of the differentiation process outliers were observed. Accordingly, the Pearson's correlation coefficient amounted around 0.3 (weak correlation).
For the purpose of relative quantification of significantly regulated proteins data was further processed, according to the workflow shown in Figure 4.15. In the first step, the 3,876 proteins

Replicate	Protein IDs
1	2,915
2	2,802
3	3,191
4	2,628
total	3,876

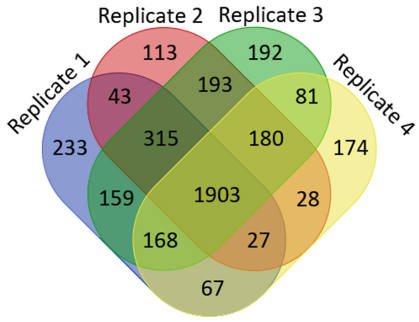

(a) Proteome Discoverer output

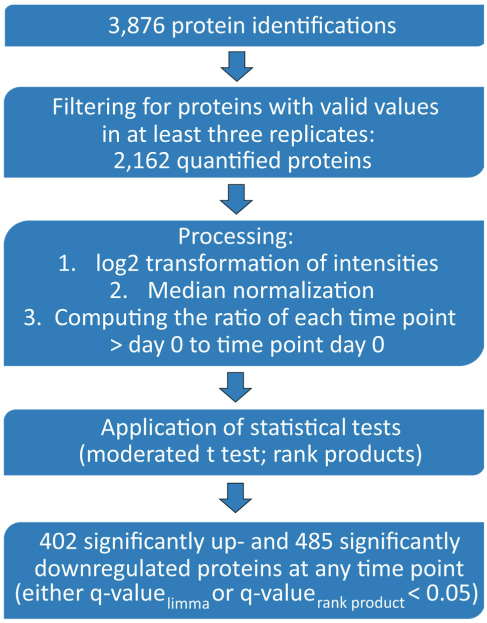

(b) Data analysis workflow

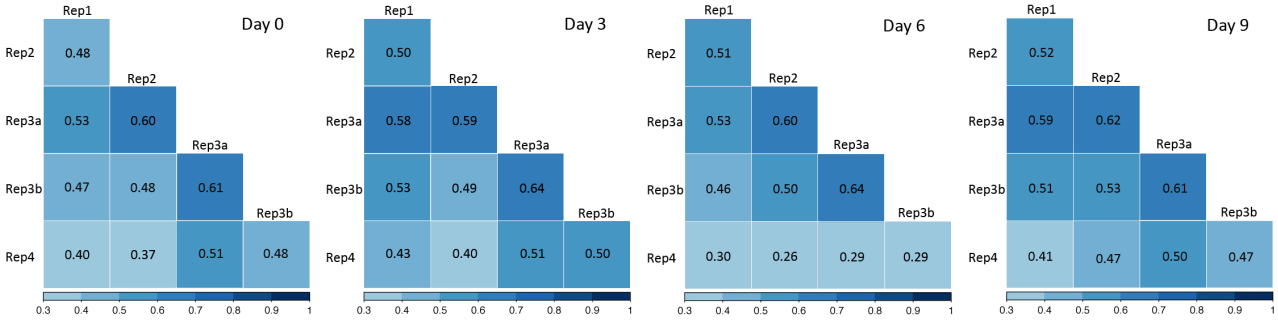

(c) Pearson correlation

Fig. 4.15.: Mascot analysis of oligodendrocyte precursor cell differentiation and subsequent data processing steps. Oligodendrocyte precursor cell differentiation samples were harvested at day 0, 3, 6 and 9, labeled with TMTsixplex™, measured using a LTQ-Orbitrap Velos mass spectrometer and analyzed using Mascot. Raw data analysis of four biological and one technical replicate against the rat UniProtKB/TrEMBL database (25,841 entries) lead to the detection of 3,876 proteins (1% false discovery rate). (a) The table shows the number of identified proteins per replicate, whereas the Venn diagram indicates the overlap of proteins between all replicates (replicate 3 consists of concatenated technical replicates). (c) The heat maps indicate the Pearson's correlation coefficients of median-normalized intensities between all replicates at each time point. The higher the value, the more intense the blue color. (b) The data processing workflow was applied after Mascot analysis and removal of proteins without unique quantification values. After concatenating technical replicates, filtering, processing applying statistical tests, proteins with a q-value (FDR adjusted p-value) < 0.05 were considered as significantly regulated proteins. The computational data processing was done by the bioinformatician Dr. Nahal Brocke-Ahmadinejad. The first three replicates were processed using chloroform/methanol protein precipitation, while the forth replicate was processed on filter aided sample preparation devices.

identified were filtered for proteins that featured unique quantification results, namely 3,595 proteins, and thereafter for proteins that were detected with valid intensity values in at least three replicates, so that finally 2,162 proteins were considered for further analysis. The intensities of the reporter ions were further log2 transformed, normalized to the median of each reporter ion channel (each TMT label) and the ratios of the intensities of each time point to the time point of day 0 were finally determined. Expression ratios were evaluated using statistical tests (moderated t-test (limma) or versus null distribution method (rank product)) [Ritchie et al., 2015] [Hong et al., 2011] to identify differential abundant proteins at each time point. Altogether, 402 significantly (q-value (FDR adjusted p-value) < 0.05) up- and 485 downregulated proteins at any time point (at either one or more time points of the differentiation process) were identified. Proteins were determined as upregulated by featuring any positive log2 fold change value and downregulated by featuring any negative log2 fold change value. Accordingly, from the 3,876 proteins detected, 10% of total proteins were significantly upregulated and 13% were significantly downregulated. Because of the high numbers of regulated proteins, it was further useful to determine whether proteins were mainly regulated at earlier or later time points of the differentiation experiment. Accordingly, significantly regulated proteins at each time point were plotted in the histograms, shown in Figure 4.16. To further get a general idea of the expression course of every significantly regulated protein during the differentiation process, Venn diagrams, shown in Figure 4.17, were compiled.

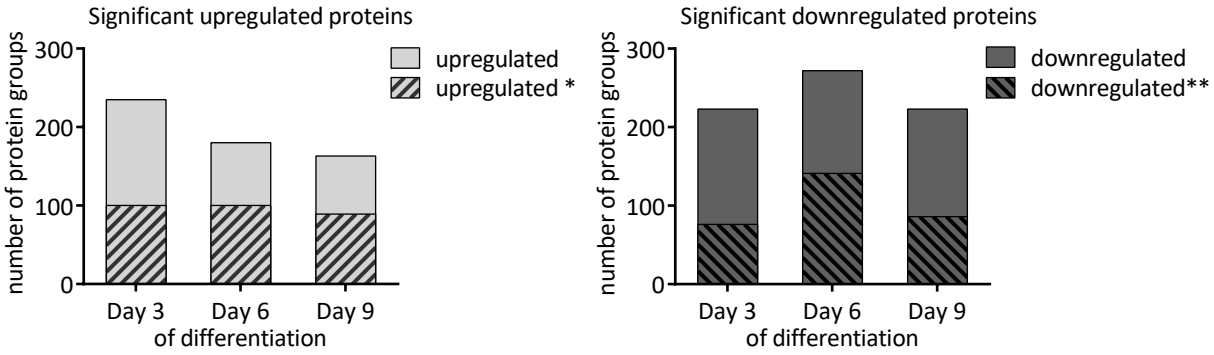

Fig. 4.16.: Significantly up- and downregulated proteins during the differentiation from oligodendrocyte precursor cells to oligodendrocytes. Four biological and one technical replicate of oligodendrocyte precursor cell differentiation were conducted. Samples were harvested at day 0, 3, 6 and 9, labeled with TMTsixplex™, measured using a mass spectrometer and analyzed using Mascot against the rat UniProtKB/TrEMBL database at 1% false discovery rate. The log2 transformed and normalized reporter ion intensities of proteins detected with valid values in at least three replicates were used to compute the expression ratios of day 3, 6, and 9 to day 0. Expression ratios were statistically evaluated and proteins showing a q-value < 0.05 using either limma or rank product were determined as significantly regulated. The histogram depicts all significantly regulated proteins per time point, irrespective of any fold change value (only the algebraic sign was considered for up- or downregulation). Proteins showing a log2 expression ratio (fold change) of * ≥ 1 or a log2 fold change of ** $\leq$ -1 are additionally shaded.

The histograms (Figure 4.16) display all significantly regulated proteins for every time point separately so that the protein numbers finally amount more than the previously mentioned 402 up- respectively 485 downregulated proteins. Most upregulated proteins were detected three

days after differentiation initiation. Altogether, 235 proteins were significantly upregulated at day 3 of the differentiation process, whereof 100 proteins featured a log2 fold change (log2FC) greater than 1. In contrary, only 180 proteins were upregulated at day 6, whereof 100 proteins were upregulated more than two fold and 89 at day 9, whereof 163 displayed a log2 fold change value greater than 1.
Regarding the significantly downregulated proteins, a population of 223 proteins were regulated three days after differentiation initiation, whereas 76 proteins exhibited a downregulation of more than two fold (Figure 4.16). With progressed differentiation time the number of downregulated proteins further increased to 272, whereof 141 proteins showed a downregulation of more than two fold. After nine days of OPC differentiation, the number of downregulated proteins detected accounted 223 proteins, whereof 86 proteins were more than two fold downregulated.

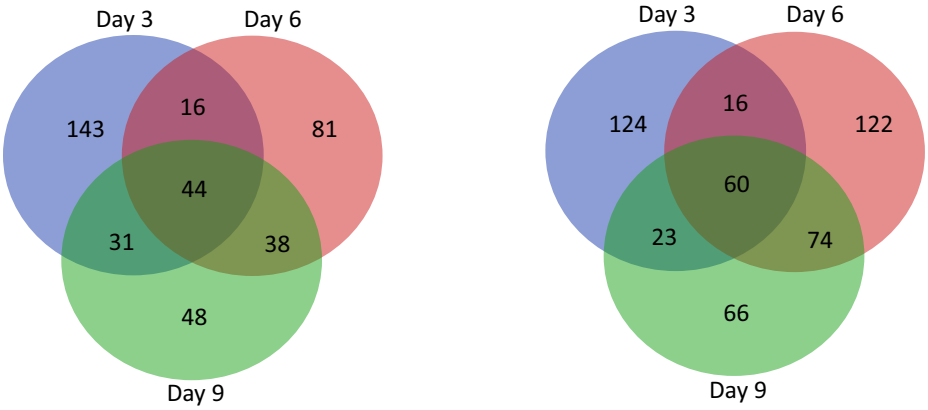

(a) upregulated proteins (b) downregulated proteins

Fig. 4.17.: Venn diagram of (a) significantly upregulated and (b) significantly downregulated proteins. TMTsixplex™ labeled oligodendrocyte precursor cell differentiation samples (day 0, 3, 6 and 9) of four biological and one technical replicate were measured using a LTQ-Orbitrap Velos. Data analysis was performed against the rat UniProtKB/TrEMBL database (25,841 entries) at 1% false discovery rate using Mascot. The log2 transformed and normalized reporter ion intensities of proteins detected with valid values in at least three replicates were used to compute the expression ratios of day 3, 6, and 9 to day 0. Expression ratios were statistically evaluated and proteins showing a q-value < 0.05 using either limma or rank product were determined as significantly regulated. All regulated proteins were analyzed using the Venn diagram tool, provided by UGent Bioinformatics & Evolutionary Genomics. The diagrams depict all proteins which were significantly regulated at day 3, 6 and 9 compared to day 0.

In addition, Venn diagrams were conducted in order to simplify the comparison of significantly upregulated respectively downregulated proteins between the three time points (Figure 4.17). In the diagram every circle represents one replicate. The numbers in the overlapping regions indicate the amount of proteins shared between the replicates. Proteins upregulated at one single time point constituted the largest population among all groups. Altogether, more than half of total proteins were regulated in one time point. Nevertheless, showing a permanent upregulation over the entire differentiation experiment applied to 44 proteins (11%). Additionally, 16 proteins (4%) were upregulated at the beginning of the experiment (day 3 and 6), while 38 proteins (9%) were upregulated towards the end of the experiment (day 6 and 9). Finally, 32 proteins showed

an upregulation at day 3 and 9 (8%) but not at day 6, most probably due to quantification errors, leading to q-values greater 0.05 at time point day 6.
Regarding the downregulated proteins, similarly, most proteins were only regulated at one time point during the differentiation experiment (Figure 4.17 (b)). In addition, many proteins were downregulated at later time points of the differentiation process, namely at day 6 and day 9, which applied to 74 proteins (16%). In contrary, only 16 proteins (3%) were downregulated at earlier stages of the experiment, thus at day 3 and day 6. Nonetheless, with 60 (12%) proteins the group of permanent downregulated proteins still constituted a large population.

4.2.2.1. Time dependent alterations of the proteome during OPC differentiation

Data acquired from four biological and one technical replicate of the OPC differentiation process resulted in the detection of 3,876 proteins, whereof 10% were significantly up- and 13% were downregulated. To facilitate the analysis of the complex data set, different approaches were considered that either specifically focused on groups of similar regulated proteins or on distinct protein classes. One of the most promising groups included the permanently upregulated proteins (day 0 until day 9) (Section 4.2.2.2). The expression values of proteins belonging to this group were evaluated using statistical tests (q-value ≤ 0.05). Remaining proteins are most probably involved in the differentiation process from OPCs to oligodendrocytes. In addition, gene ontology (GO) enrichment analyses were conducted to gain a general impression of the biological meanings and the cellular localization of these proteins [Ashburner et al., 2000] [Huang et al., 2008]. In order to identify proteins that might initialize OPC differentiation and which might thus only be upregulated at the beginning of the experiment, specific protein classes were analyzed in particular, including receptors, kinases, transcription factors and histone modifiers (Section 4.2.2.3). Usually, the binding of extrinsic factors to specific receptors lead to the activation of intracellular signaling pathways, resulting in subsequent activation or repression of gene expression. Moreover, intrinsic factors are involved in the cellular differentiation process by modifying DNA or histones (chromatin remodeling) in a way that affects gene expression, also referred as epigenetic modulation [Liu & Casaccia, 2010]. On the other hand, continuously downregulated proteins were investigated to detect proteins affecting OPC specific processes as well as factors negatively affecting the differentiation process (Section 4.2.2.4).

4.2.2.2. Significantly and permanently upregulated proteins (day 0 until day 9)

First, the permanently upregulated proteins were examined. The expression of some proteins was already confirmed in OPCs respectively oligodendrocytes and in addition, for some proteins a function in OPCs respectively oligodendrocytes is already known. For some other proteins the potential role these proteins might occupy within the differentiation process has to be still determined. For this purpose, proteins were analyzed regarding their log2 expression ratios and their regulation pattern displayed over time. Accordingly, proteins exhibiting same expression patterns might be effected by similar regulator proteins or are responsible for similar biological processes during the differentiation process. Therefore, expression ratios of time point day 3, 6 and 9 to time point day 0 were calculated for the 44 continuously upregulated proteins.

According to Table 4.5, which depicts the log2 transformed expression ratios of day 3, 6 and 9 to day 0, proteins affecting myelination were significantly upregulated. This pertained, among oth-

Table 4.5.: Proteins, significantly upregulated in all time points during oligodendrocyte precursor cell differentiation. MS-data of four biological and one technical replicate of oligodendrocyte precursor cell differentiation was searched against the rat UniProtKB/TrEMBL database at 1% false discovery rate using Mascot. The log2 transformed, normalized intensities of proteins detected in ≥ 3 replicates were used to compute the expression ratios of day 3, 6 and 9 to day 0. Proteins, showing a q-value < 0.05 in either Limma or Rank product test were determined as significantly regulated and plotted in the table, arranged according to the log2 expression ratios of day 9/0. Low values are colored in red, high values in blue (color scale at the bottom of the table). Proteins involved in myelination are labeled with red color (according to gene ontology analysis (BiNGO).

No	Gene	Accession	$\log_2$ day 3/0	$\log_2$ day 6/0	$\log_2$ day 9/0
1	Gfap	A1E251	1.9539	2.2641	2.5786
2	Plp1	A0A097BVK2	1.6900	1.4773	2.1859
3	Rras2	Q5BJU0	1.9261	1.5659	2.1741
4	Enpp6	D3ZRI1	1.9902	1.5030	2.0609
5	Aqp4	Q8CIY8	1.5525	2.1006	1.9721
6	Sept5	A0A096MJN4	0.9247	1.7748	1.7122
7	Cnp	A0A097BVJ5	1.9461	1.7271	1.6832
8	Dpysl4	F1LNT0	1.2845	1.7683	1.6779
9	App	Q6P6Q5	0.6907	1.8243	1.6219
10	Rhog	Q32PX6	1.2238	1.2915	1.5558
11	Fabp5	Q2XTA4	0.8789	0.7771	1.5257
12	Cd81	Q6P9V1	0.6419	1.8872	1.4951
13	Plcl1	F1LP62	1.4714	2.2123	1.4787
14	Gjc3	F1LPT0	1.4376	1.7454	1.4091
15	Cldn11	Q6IRG7	1.0923	1.5037	1.3806
16	Stxbp3	Q99PV2	0.8251	1.2639	1.3658
17	Man1a1	G3V9N9	1.6150	1.7017	1.3526
18	Bin1	Q5HZA7	1.4111	1.0117	1.3477
19	Nfasc	D3ZW56	1.1904	0.9665	1.3323
20	Pgk2	Q5XIV1	0.8934	0.8886	1.3071
21	Cystm1	D3ZR95	1.7255	1.5582	1.2987
22	Serinc5	G3V9U9	1.2539	1.4377	1.2670
23	Ldha	B5DEN4	1.2368	0.8510	1.2116
24	Ero1l	F8WFP9	0.7762	1.5131	1.1912
25	Fam177a1	D3ZIM7	1.2843	0.9357	1.1703
26	RGD1563349	F1M4B6	0.8368	1.3797	1.1641
27	Dgka	F1M956	1.0380	1.3759	1.1512
28	Gamt	G3V960	1.4912	1.6992	1.1440
29	Tpi1	M0R4U4	0.6916	0.8852	1.0569
30	Pfkl	Q6P783	1.4535	1.2829	1.0442
31	Eprs	Q6TXE9	0.4405	1.1136	1.0189
32	Pgk1	A0A096MJL6	0.6974	0.8558	1.0131
33	Ust	D3ZPB6	1.9413	1.7252	1.0060
34	Dip2b	F1M8R8	0.6377	0.8742	0.9958
35	Rap1gds1	F1M7Y3	1.2199	0.8975	0.9690
36	Ctsl	I2FHN3	0.6141	1.0128	0.8542
37	Aldoart2	Q6AY07	0.9136	0.8030	0.8397
38	Rap2c	D3ZK56	0.9385	0.9848	0.8286
39	Acss2	G3V9U0	2.0770	1.1324	0.8185
40	Gca	D3ZYI0	1.9047	1.3839	0.7798
41	Shisa4	A0MV40	1.0631	1.0536	0.7659
42	Idh1	Q0QER8	0.9705	0.5517	0.7430
43	Iars	F1LS86	0.5033	0.9849	0.6717
44	Auh	F1LU71	0.4691	0.6451	0.6508
	Fold change color scale		0.5000	1.5000	2.5000

ers, to the high abundant myelin proteins PLP1 (proteolipid protein 1) [Sidman et al., 1964] and CNP (2',3'-cyclic-nucleotide 3'-phosphodiesterase) [Lappe-Siefke et al., 2003] and to the protein ENPP6 (ectonucleotide pyrophosphatase/phosphodiesterase family member 6). ENPP6 expression in oligodendrocytes has already been shown [Greiner-Tollersrud et al., 2013]. It is assumed to play a role in sphingomyelin signaling, due to its ability to hydrolyze lysosphingomyelin. For the proteins PLP1, ENPP6 and RRAS2 (Ras-related protein R-Ras 2), a slight decrease in expression ratios was detectable six days after differentiation initiation, while the highest expression levels were constituted after nine days of cultivation. This suggests that the lower expression ratios observed at day 6 were due to quantification errors. Additional strongly upregulated proteins related to myelination represented the protein CLDN11 (claudin-11), which is responsible for the generation of cell tight junctions in myelin sheaths [Gow et al., 1999] and the protein GJC3 (gap junction channel protein) [Altevogt et al., 2002]. However, the astrocytes-specific protein GFAP (glial fibrillary acidic protein) was detected as the most abundant upregulated protein, showing a permanent upregulation at high fold change values (Figure 4.5).
Some proteins displayed a strong increase in expression in the initial days of differentiation, while reaching their maximum after a cultivation period of six days. This was, among others, applicable to the proteins APP (amyloid beta A4 protein), PLCL1 (phosphoinositide phospholipase C), CD81 (tetraspanin) and GAMT (guanidinoacetate N-methyltransferase). Although CD81 is expressed in oligodendrocytes [Sullivan & Geisert, 1998], little is known about its function in these cells. Besides CD81, also APP [Skaper et al., 2009], PLCL1 [Cahoy et al., 2008] and GAMT [Takasaki et al., 2010] were already detected in oligodendrocytes.
Furthermore, another group of proteins, including CYSTM1 (cysteine-rich transmembrane module-containing 1), BIN1 (myc box-dependent-interacting protein 1), ACSS2 (cytoplasmic acetyl-coenzyme A synthetase) and UST (uronyl-2-sulfotransferase) exhibited the highest expression levels three days after differentiation initiation, while at later stages a reduction in expression was detectable. In the CNS, BIN1 is mainly expressed in oligodendrocytes. In addition, an increase in expression levels was observed for BIN1 during OPC to oligodendrocyte differentiation, while the loss of BIN1 is associated with demyelination in multiple sclerosis patients [De Rossi et al., 2016]. Among the other proteins mentioned only the protein ACSS2 was aldready detected in oligodendrocytes [Ariyannur et al., 2010].
Immunofluorescence analyses revealed a small myelin basic protein (MBP)-expressing population beneath a large NG2-expressing population at day 3, whereas at day 6 the majority of cells expressed MBP. Accordingly, proteins showing highest expression ratios either at day 3 or day 6 might be promising candidates for accomplishing early differentiation processes.

Gene ontology (GO) enrichment analysis was performed, aiming the identification of biological processes and cellular components that were mainly affected by the continuously (day 3 until day 9) upregulated proteins. The analyses were performed with the Biological Network Gene Ontology (BiNGO) 3.3.0 tool [Maere et al., 2005], a plugin used on the software platform Cytoscape [Shannon et al., 2003] in order to calculate and depict overrepresented GO categories. The BiNGO tool was used this time, since it allows the implementation of every annotation database and GO term file. Moreover, the Gene ontology annotation database [Barrell et al., 2008]) was used as source for gene annotations, since the annotation file for the species rattus norvegicus provided by the GO consortium, the PANTHER and the GOrilla database contain less gene annotations. The enrichment analysis of significantly upregulated

proteins was performed for every time point (day 3, 6 and 9) separately. This was necessary, since the analysis of the permanently upregulated 44 proteins resulted in insufficient detection of enriched GO terms, caused by the small number of proteins implemented. However, many enriched GO terms were identified in the separate analyses, making it necessary to reduce data complexity by concatenating related GO terms using REViGO [Supek et al., 2011]. The REViGO tool summarizes long lists of GO terms by determining one GO term which represents related GO terms. A similarity of 0.7 was set as default, meaning that GO terms with larger values than 0.7 were removed by merging them into the cluster represented by the term possessing a more significant p-value. The 25 most enriched GO terms in the ontology of biological processes and cellular components, determined by enrichment p-values, are depicted in Figure 4.18 (a), (b) and (c) for each analyzed day separately. The complete list can be found in the electronic supplement (Supplementary Data S12 (day 3), S13(day 6) and S14 (day9)).

GO enrichment analysis of OPCs treated for three days with differentiation medium resulted in the detection of 49 biological processes and 32 cellular components, after removal of redundant proteins by REViGO. Regarding the number of GO terms, enriched in the analysis performed with proteins significantly upregulated after six days, a remarkable drop in both ontologies was detectable. Altogether, 27 enriched GO terms assigned to biological processes and 17 enriched GO terms assigned to cellular compartments were observed, after application of REViGO. Analysis performed with proteins upregulated after nine days of differentiation lead to the detection of 35 GO terms within the category of biological processes and 17 GO terms within the category of cellular components (after REViGO application).

The comparison of enriched biological processes between the three GO analyses (day 3, 6 and 9) revealed that several GO terms were enriched within all three analyses, although varyingly strong (different log10 p-values). Prominently, metabolic processes were enriched from the beginning until the end of the differentiation process. Thereto belonged, for example, the highly abundant GO term "carboxylic acid metabolic processes" as well as the GO term "pyridine-containing compound metabolic process". In addition, the GO term "carbohydrate catabolic process" was permanently overrepresented. Released energy and molecules are probably used for the generation of lipids, indicated by the enriched GO terms "lipid biosynthetic process" and "isoprenoid biosynthetic process" at day 3 (Figure 4.18 (a)). Furthermore, another group of continuously enriched GO terms belonged to the parent GO term "nervous system development", including "glial cell differentiation" and "axon ensheathment". Although these GO terms were enriched in all three analyses, lowest log10 p-values and thus highest enrichment was observed in the analysis conducted of significantly upregulated proteins at day 9 (Figure 4.18 (c)).
Besides, some GO terms were only enriched in the analysis of proteins significantly upregulated at day 3 of the differentiation process (Figure 4.18 (a)). These GO terms are associated with "intracellular signal transduction", like the GO terms "small GTPase mediated signal transduction" and "ras protein signal transduction". Besides this, another assembly of enriched GO terms was formed by proteins relevant for the organization of the cytoskeleton, like "actin cytoskeleton organization" or "cell-cell junction organization". Further, proteins accomplishing "vesicle-mediated transport" and "intracellular protein transport" represented enriched GO terms at the beginning of the differentiation process.

With regard to cellular components, mainly same GO terms were enriched in all three GO

term analyses. Prominently, the GO term "extracellular organelles" and especially the GO term "extracellular exosomes" displayed the lowest log10 p-values and were thus highly enriched during the complete differentiation process (Figure 4.18). Likewise, the cellular components "myelin sheath" and "main axon" were enriched during all stages. Besides this, another group of matching overrepresented GO terms was constituted of the terms "actin filament" and "cytoskeleton", which were closely related to a second group consisting of the terms "cell junction" and "apical junction complex". These GO terms however were only enriched in the analysis of proteins regulated at day 3 of the differentiation process, while the GO term "cell junction" was overrepresented in the analysis of proteins regulated at day 9.

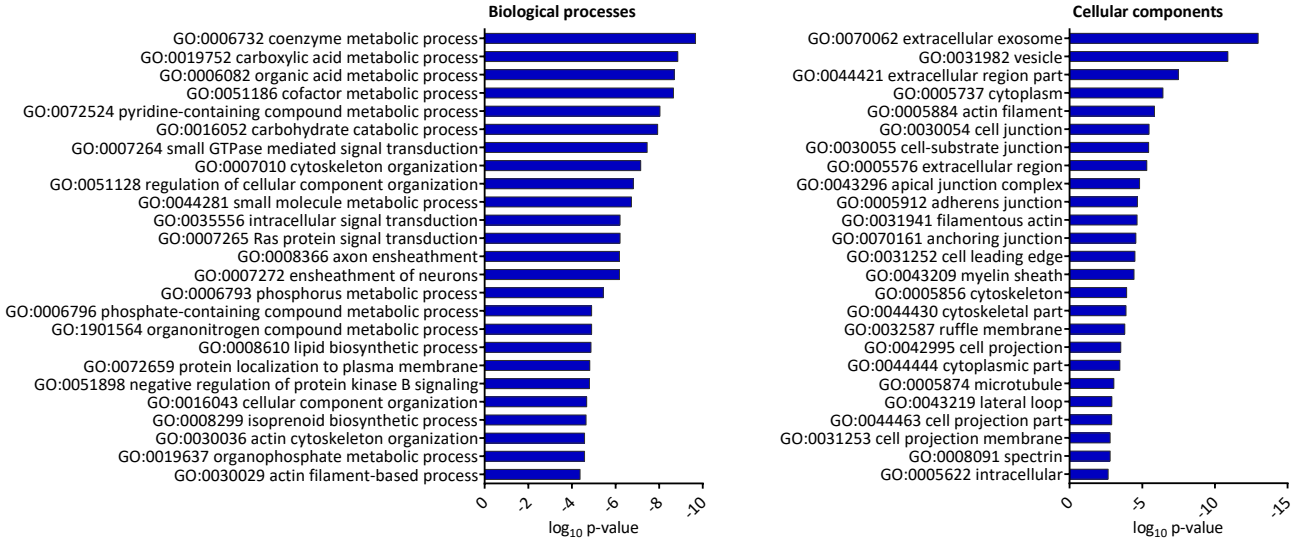

(a) Day 3 - Enriched biological processes and cellular components

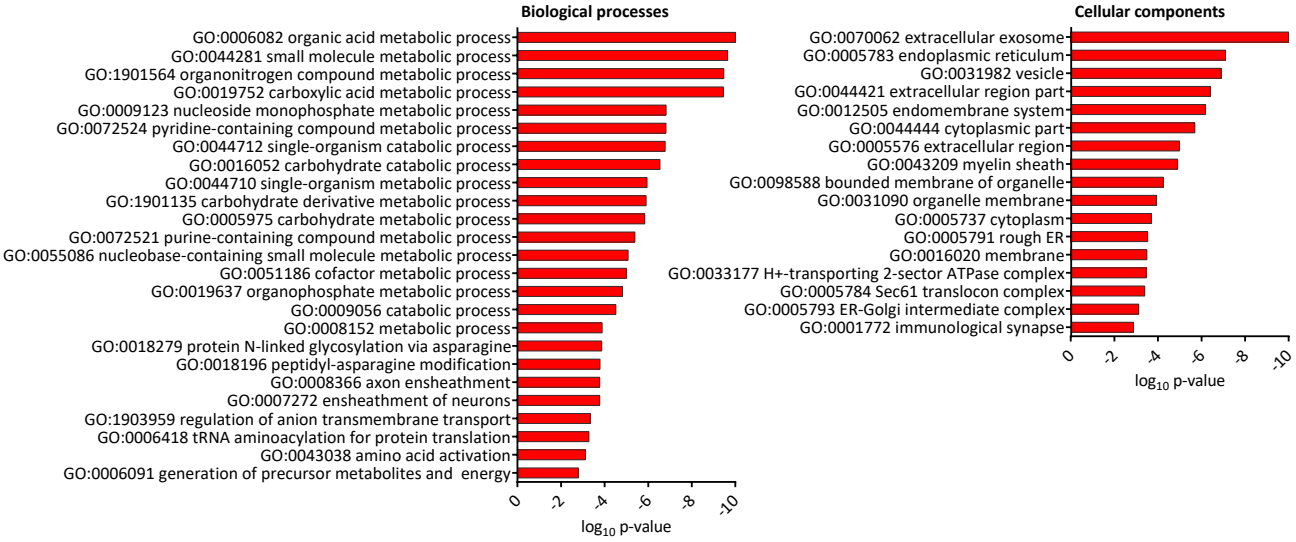

(b) Day 6 - Enriched biological processes and cellular components

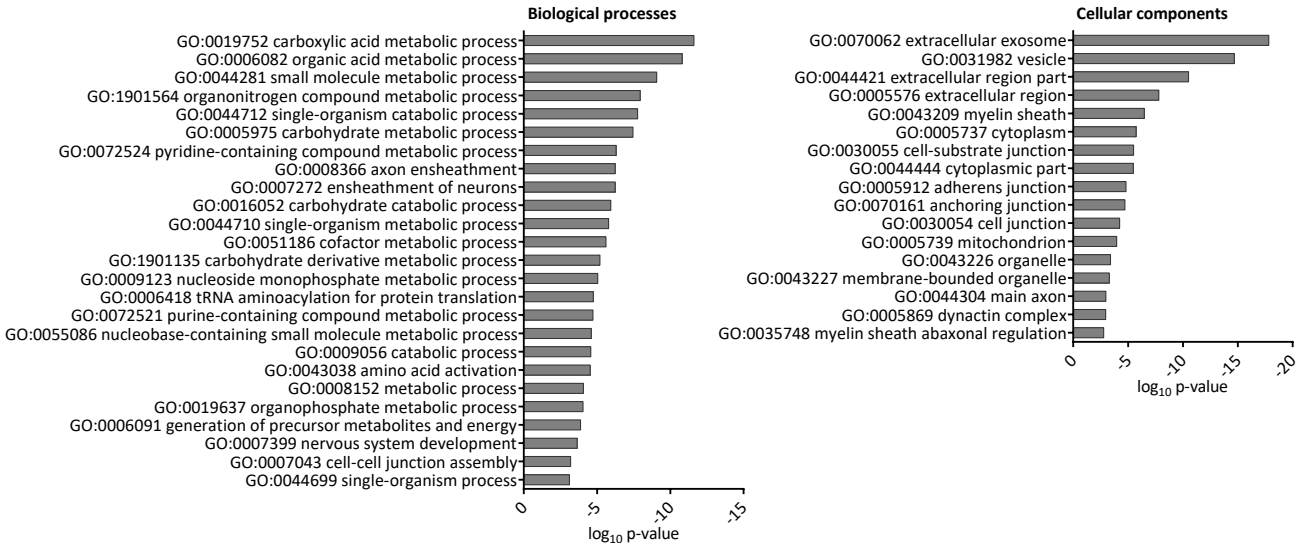

(c) Day 9 - Enriched biological processes and cellular components

Fig. 4.18.: Enriched GO terms of upregulated proteins at (a) day 3, (b) day 6 and (c) day 9 of oligodendrocyte precursor cell differentiation. GO enrichment analyses of significantly upregulated proteins during OPC differentiation were performed against all proteins from the species rattus norvegicus, provided by the gene ontology annotation database (gene association.goa uniprot.142.gz, released on 27.04.2015) using BiNGO. For matching of regulated proteins to GO terms the Go-basic.obo (Gene Ontology consortium, 04/2015) [Ashburner et al., 2000] was applied. As statistical test the hypergeometric test was used and as multiple test correction the Benjamini & Hochberg False Discovery Rate (FDR) was computed from the p-values. The significance level was set to 0.05. Proteins were then applied to REViGO, which summarized the input by removing redundant GO terms. A similarity of 0.7 was set as default. For every time point either the 25 most abundant or all enriched biological processes and cellular components are plotted together with their computed log10 p-values in the graphs. The lower the log10 p-values, the higher the enrichment of the GO term in the data set. GO = gene ontology.

4.2.2.3. Investigation of distinct protein classes

In the second approach, the data set was searched for transcription regulating factors, like transcription factors and histone modifiers, receptors and kinases. For this purpose, appropriate GO terms were applied to ensure the immediate relation of proteins to specific processes. For example, the group of kinases was determined by filtering all detected proteins within the data set (2,162 proteins, featuring valid values in at least three replicates) for protein kinases in the organism "rattus norvegicus" using the UniProtKB search interface [Apweiler et al., 2004] and for the GO term "protein kinase activity" using the GO database AmiGO 2 [Carbon et al., 2008]. Finally, the expression ratios of day 3, 6 and 9 to day 0 (based on median normalized and log2 transformed intensities) were blotted separately for every protein class in line graphs. Additionally, the top up- and downregulated proteins (according to day 3 to day 0 log2 fold changes) were labeled with different colors and mentioned in the legend. Based on the expression pattern proteins exhibited, assumptions regarding their function can be made. Proteins, initially upregulated (day 3) might be responsible for differentiation initiation, while proteins which are upregulated towards the end of the experiment (day 9) might be involved in biological processes taking place in mature oligodendrocytes.

Transcription regulating factors Transcriptional regulation is mainly mediated by transcription factors, activating or repressing gene transcription, proteins interacting with enhancers or promoters and histone modifiers which alter the chromatin structure. Histone modifiers regulate the access of the RNA polymerase and transcription factors to the DNA promoter by either methylating or demethylating, acetylating or deacetylating, citrullinating, phosphorylating or ubiquitinylating histones [Bannister & Kouzarides, 2011]. Histone modification might have effects on gene expression or the chromosome packaging and according to Nielsen and co-workers [Nielsen et al., 2002] considerable nuclear and chromatin reorganization takes place during OPC differentiation. In the last decade, multiple factors, expressed by OPCs, were identified which inhibit the maturation to oligodendrocytes [Liu & Casaccia, 2010] [Copray et al., 2009]. The expression of transcription inhibiting factors needs to be suppressed prior to OPC maturation, whereas the expression of activators of maturation or genes responsible for myelin synthesis needs to be enhanced in order to accomplish differentiation and to ensure their functionality.

Altogether, 60 proteins regulating transcription were quantitatively detected within the OPC differentiation experiment, whereof 13 proteins showed positive day 3 to day 0 log2 fold change values. Moreover, towards the end of the differentiation experiment only 11 proteins exhibited positive expression ratios. In addition, the expression levels of downregulated proteins dropped considerably compared to the slightly increasing expression levels of upregulated proteins. The complete list of regulated transcription regulating factors can be found in the electronic supplement (Supplementary Data S15).
Three days after differentiation initiation, RPS6KA5 (ribosomal protein S6 kinase A5) exhibited more than three times higher expression levels compared to time point day 0 (Figure 4.19). RPS6KA5 is a serine/threonine-protein kinase that also acts as a histone modifier. It regulates transcription by phosphorylating histones [Soloaga et al., 2003]. Moreover, the proteins PADI2 (peptidyl arginine deiminase, type II), which citrullinates the arginine residues of histones [Zhang et al., 2012a], and the transcriptional repressor protein ARHGAP35 (rho GTPase-activating protein 35) showed highest log2 fold changes at time point day 3 [LeClerc et al., 1991]. In addition, some proteins showed highest expression levels at day 6, including the proteins MGEA5 (protein O-GlcNAcase) and PURA (transcriptional activator protein Pur alpha), which expression levels were three times higher at day 6 compared to the starting point. PURA has already been evidenced to positively regulate the expression of the MBP protein [Tretiakova et al., 1999]. The expression of PURA likewise increased during the differentiation from neural precursor cells (NPCs) to OPCs (Subsection 4.1.2.5), indicating its importance as a transcription factor for the oligodendroglial development.

Regarding the downregulated proteins regulating transcription (Figure 4.19), the expression levels of several proteins dropped noticeably at the beginning of the differentiation process. Proteins, particularly downregulated at earlier stages included the protein DNMT1 (DNA (cytosine-5)-methyltransferase) and the transcriptional regulator protein CBFB (core-binding factor, beta subunit). DNMT1 binds to histones, like HDAC2, and has been shown to inhibit ESC differentiation [Jackson et al., 2004]. The upon differentiation downregulated protein ELP3 (elongator complex protein 3) was detected in oligodendrocytes and its depletion has been shown to result in increased oligodendrocyte specific proteins after an demyelinating event [Dion et al., 2015]. Furthermore, the transcription factor NFIA (nuclear factor 1 A-type) was strongly downregulated at day 3 and day 9. The elevated protein levels observed at day 6 most probably resulted

from quantification errors. NFIA is necessary for both, oligodendroglial and astroglial progenitor cell generation. Upon terminal differentiation the proastrocytic function of NFIA dominates [Deneen et al., 2006]. Thus, its downregulation during OPC differentiation might inhibit the differentiation of progenitor cells into astrocytes *in vitro*.

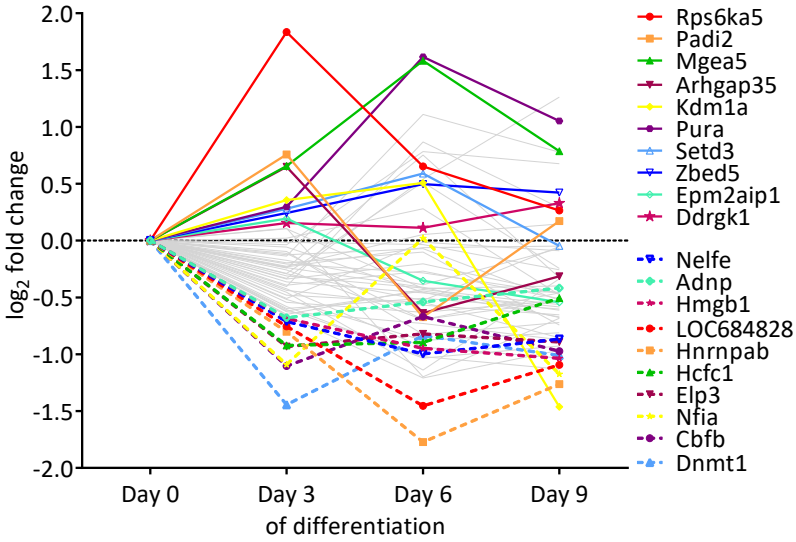

Fig. 4.19.: Changes in log2 expression ratios of transcription regulating factors during oligodendrocyte precursor cell differentiation. The PSM file (Proteome Discoverer) was filtered for peptides featuring unique quantification results, featuring values > 0 in all reporter ion channels and for proteins detected in ≥ 3 biological replicates. Peptides were summarized to protein level by calculating the median for every channel and each replicate separately. Log2 transformed peptide intensities were normalized to the median per reporter ion channel, combined on protein level by calculating the median and finally replicates were combined by calculating the mean of all protein intensities. Obtained data was filtered for "transcription factor" (UniProt) and for the GO terms "DNA binding" and "regulation of transcription" (AmiGO 2). Histone modifiers were searched using the terms "histone acetylation", "histone deacetylation", "histone methylation", "histone demethylation", "histone phosphorylation" and "histone citrullination" using AmiGO 2. The line graph depicts the log2 transformed day > 0 / day 0 expression ratios of proteins present in the searches. The top 10 up- and downregulated transcription regulating factors (day 3/0) are differentially labeled.

Protein receptors and proteins interacting with receptors Altogether, 29 receptors and receptor-interacting proteins were identified, whereof 12 proteins were up- and 17 proteins were downregulated three days after differentiation initiation. The whole protein list can be found in the electronic supplement (Supplementary Data S16), while the top 10 upregulated receptors and proteins interacting with receptors are depicted in Figure 4.20. CADM4 (cell adhesion molecule 4), the most upregulated protein at the beginning of the experiment, is a member of the cell adhesion molecule family which has been implicated in myelination and axon–glia interaction [White & Krämer-Albers, 2013]. Moreover, with CADM2 (cell adhesion molecule 2) another member of the family and with NECTIN1 (nectin cell adhesion molecule 1) another protein which functions as a cell adhesion molecule were upregulated. These three proteins were prominently upregulated at early stages of the experiment, while the expression levels decreased thereafter, suggesting an involvement in differentiation initiation. On the other hand, some re-

ceptors and receptor-interacting proteins showed highest expression levels towards the end of the experiment, suggesting their involvement in oligodendrocyte differentiation or in oligodendocyte-specific processes. Indeed, the proteins APP (amyloid beta A4 protein) [Skaper et al., 2009], CHN2 (beta-chimaerin) [Dugas et al., 2006] and ITRP2 (inositol 1,4,5-trisphosphate receptor type 2) [Marques et al., 2016] were already detected in oligodendrocytes.

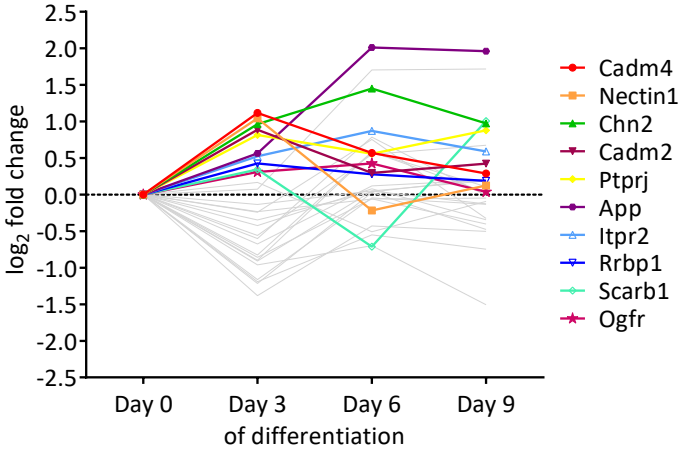

Fig. 4.20.: Changes in log2 expression ratios of receptors during oligodendrocyte precursor cell differentiation. The PSM file, generated by Proteome Discoverer, were filtered for peptides featuring unique quantification results, featuring values > 0 in all reporter ion channels and for proteins detected in ≥ 3 biological replicates. Peptides were summarized to protein level by calculating the median for every channel and each replicate separately. Log2 tran sformed peptide intensities were normalized to the median per reporter ion channel, combined on protein level by calculating the median and finally replicates were combined by calculating the mean of all protein intensities. Obtained data was filtered for "receptor" (UniProt) and for the GO term "receptor activity" (AmiGO 2). The line graph depicts the log2 transformed day > 0 / day 0 expression ratios of proteins present in both searches. The top 10 upregulated receptors (day 3/0) are differentially labeled.

Kinases Altogether, 29 protein kinases were identified. Based on the log2 fold change values at the beginning and three days after differentiation initiation, 14 proteins were up- and 15 proteins were downregulated. The top 10 upregulated kinases are shown in Figure 4.21, while the complete list can be found in the electronic supplement (Supplementary Data S17).
For the protein FYN (tyrosine-protein kinase Fyn), which was two fold upregulated at time point day 3, a direct association to oligodendrocytes was already evidenced [Liang et al., 2004]. The protein has been shown to have an impact on morphological changes during oligodendrocyte differentiation and on transcription of myelin-specific genes. The protein PRKCA (protein kinase C) displayed constant expression levels during the complete differentiation process. This is consistent with former investigations performed, suggesting a function of PRKCA in facilitating process extensions and expression of myelin proteins during later stages of OPC differentiation [Syed et al., 2008]. Moreover, MAP3K3 (mitogen-activated protein kinase kinase kinase 3) exhibited a steady and strong increase in expression over time, implying the importance of this kinase for the differentiation and maturation of oligodendrocytes. Indicated as a mediator of NF-κB transcription activation and signal transduction cascade [Ellinger-Ziegelbauer et al., 1997] [Bouwmeester et al., 2004], MAP3K3 might additionally have supporting functions on axon survival and axon function via activation of NF-κB signaling cascade [Blank & Prinz, 2014].

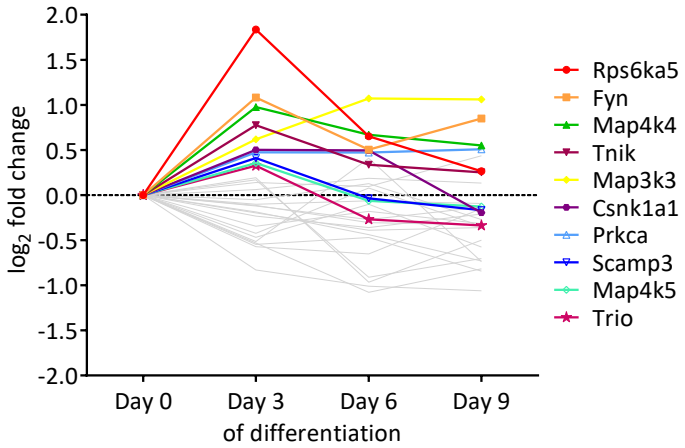

Fig. 4.21.: Changes in log2 expression ratios of kinases during oligodendrocyte precursor cell differentiation. The PSM file, generated by Proteome Discoverer, were filtered for peptides featuring unique quantification results, featuring values > 0 in all reporter ion channels and for proteins detected in ≥ 3 biological replicates. Peptides were summarized to protein level by calculating the median for every channel and each replicate separately. Log2 transformed peptide intensities were normalized to the median per reporter ion channel, combined on protein level by calculating the median and finally replicates were combined by calculating the mean of all protein intensities. Obtained data was filtered for "protein kinases" (UniProt) and for the GO term "protein kinase activity" (AmiGO 2). The line graph depicts the log2 transformed day > 0 / day 0 expression ratios of proteins present in both searches. The top 10 upregulated protein kinases (day 3/0) are differentially labeled.

4.2.2.4. Significantly downregulated proteins (day 0 until day 9)

Investigation of downregulated proteins was performed to detect proteins involved in OPC specific processes as well as factors negatively affecting the OPC differentiation process. For this purpose, continuously downregulated proteins (day 0 until day 9) were examined. The top 40 proteins (according to expression ratios of day 9 to day 0) are depicted including the log2 transformed expression ratios in Table 4.6, while the complete list can be found in the electronic supplement (Supplementary Data S18).
Counting in total 60 proteins, more proteins were significantly downregulated than upregulated. Multiple proteins displayed a steady drop in protein levels, including the proteins RPA1 (cb1-727), LOC100359539 (ribonucleotide reductase M2 polypeptide) and NUDT16l1 (nudix hydrolase 16-like 1). Some proteins, like TOP2A (DNA topoisomerase 2-alpha) [Downes et al., 1994], MAD2L1 (MAD2 mitotic arrest deficient-like 1) [Luo et al., 2000] and KIF11 (kinesin-like protein KIF11) [Rapley et al., 2008] were most likely downregulated upon differentiation of OPCs into oligodendrocytes due to their function as regulator of the cell cycle. Besides, with the proteins RPA1 (replication protein A1) [Lin et al., 1998], RRM1 (ribonucleoside-diphosphate reductase) [Avval & Holmgren, 2009] and MCM4 (DNA helicase Mcm4) [Ishimi, 1997] proteins were strongly downregulated that provide building blocks for deoxyribonucleic acid (DNA) snythesis or that accomplish DNA replication. Furthermore, many proteins belonging to the transcription regulation HMG family, like HMGB3 (high mobility group protein B3), LOC100360316 (high mobility group nucleosomal binding domain 2) or RGD1559962 (similar to high mobility group protein 2) were downregulated. Downregulation of the protein HMGB3 during rat OPC to oligodendrocyte differentiation was previously shown by Dugas and co-workers [Dugas et al., 2006].

Table 4.6.: Top 40 proteins, significantly downregulated in all time points during oligodendrocyte precursor cell differentiation. MS-data of four biological and one technical replicate of oligodendrocyte precursor cell differentiation was searched against the rat UniProtKB/TrEMBL database at 1% false discovery rate using Mascot. The log2 transformed, normalized intensities of proteins detected in ≥ 3 replicates were used to compute the expression ratios of day 3, 6 and 9 to day 0. Proteins, showing a q-value < 0.05 in either Limma or Rank product test were determined as significantly regulated and plotted in the table, arranged according to the log2 expression ratios of day 9/0, starting with the lowest value. Low values are colored in red, high values in blue (color scale at the bottom of the table).

No	Gene	Accession	$\log_2$ day 3/0	$\log_2$ day 6/0	$\log_2$ day 9/0
1	LOC100359539	D4A7M6	-2.3470	-2.7083	-2.9603
2	Pld4	G3V904	-2.6667	-1.7417	-2.1750
3	Top2a	F1M7A0	-1.4856	-1.1586	-2.1374
4	Rpa1	Q7TP21	-1.6706	-1.7434	-2.1345
5	LOC100360316	Q4KLJ0	-1.0755	-1.9954	-2.0785
6	Hmgb3	B0BN99	-1.3481	-2.0794	-1.9902
7	Kif11	F1MAB8	-1.7734	-1.7650	-1.9533
8	Mad2l1	D4ACM2	-1.5649	-1.5611	-1.7617
9	Mcm4	G3V681	-2.0240	-2.0573	-1.7436
10	Rnf2	M5AJY0	-0.7990	-2.0311	-1.5675
11	Rrm1	Q5U2Q5	-1.2348	-1.0516	-1.3589
12	Ugdh	G3V6C4	-1.1432	-0.9818	-1.3471
13	RGD1559962	D3ZN59	-1.2895	-1.3909	-1.3309
14	Elp3	D4ACM1	-0.9284	-0.9123	-1.3278
15	Grhpr	B0BN46	-0.7814	-0.7960	-1.2850
16	Nudt16l1	B0BNG7	-0.6381	-0.9607	-1.2826
17	Nt5c3b	A0A096MK29	-0.7045	-0.8442	-1.2419
18	Tpm1	Q91XN7	-1.1609	-2.1709	-1.2275
19	Dbn1	C6L8E0	-0.6778	-1.1331	-1.2043
20	Dpp6	F1LMR7	-1.6756	-0.7639	-1.2035
21	LOC100360260	Q5RJK5	-0.6445	-1.8452	-1.1945
22	Srsf7	D4A720	-0.8073	-0.8108	-1.1528
23	Rprd1b	B5DEK0	-0.7913	-1.4691	-1.1299
24	Celf2	Z4YNP1	-1.0463	-1.0957	-1.1252
25	Sdha	Q0QF18	-1.0932	-1.5946	-1.1250
26	Sh3bp4	G3V8J0	-0.7868	-0.9101	-1.1086
27	H2afx	D3ZXP3	-0.7434	-0.8212	-1.1042
28	Rbbp4	B5DFB2	-0.5697	-0.9801	-1.0604
29	Snrpb	B0BN51	-0.5918	-0.6561	-1.0535
30	Smc1a	F1LSS1	-0.6987	-1.0988	-1.0435
31	Lsm4	D4A2C6	-0.7005	-1.0842	-1.0298
32	Sardh	F1LRY5	-0.8865	-0.8652	-1.0233
33	Cbfb	Q66HA7	-1.2050	-1.0027	-1.0232
34	Smarcc2	D3ZPF5	-0.5202	-0.6983	-1.0173
35	Hdac2	B1WBY8	-0.5166	-1.0672	-1.0154
36	Prps1l1	M0RBK1	-0.8344	-1.2870	-0.9977
37	Nelfe	Q6MG75	-0.6454	-1.2663	-0.9896
38	Gmpr2	Q5FVP6	-0.6513	-0.7427	-0.9619
39	Ppih	D4A5R0	-0.5883	-0.8252	-0.9560
40	Cpne1	D4A1R8	-0.8466	-0.8953	-0.9498
	Fold change color scale		-0.5000	-1.7500	-3.0000

For GO enrichment analysis all downregulated proteins were searched against all identified proteins within the OPC differentiation data set. Every time point of the experiment was analyzed separately. Accordingly, identified GO terms indicate which biological processes and cellular compartments are enriched in OPCs and which are not or less required in oligodendrocytes. The 25 most enriched GO terms in both ontologies are depicted in Figure 4.22, while the complete list can be found in the electronic supplement (Supplementary Data S19, S20 and S21).

Three days after initiation of OPC differentiation, the GO terms "mitotic cell cycle" and "mitotic sister chromatid segregation" featured lowest -log10 p-values and thus highest enrichment among all GO terms (Figure 4.22 (a)). Moreover, an enrichment of the GO terms "DNA replication", "DNA metabolic process" and "GMP biosynthetic process" was observed. Conclusively, mainly proteins involved in cell cycle processes and proliferation were downregulated upon differentiation of OPCs to oligodendrocytes. Since OPC differentiation was initiated by the complete exchange of proliferation medium to differentiation medium, the enrichment of downregulated proteins related to cell cycle, DNA- and RNA metabolism was expected at day 3.
Between the two GO enrichment analyses performed with either downregulated proteins at day 6 (Figure 4.22 (b)) or at day 9 (Figure 4.22 (c)) of the differentiation process no significant differences regarding main enriched GO terms were detectable. However, the comparison between GO terms enriched at later stages and GO terms enriched at earlier stages indicated a switch in the main biological processes. Although GO terms related to cell cycle and DNA metabolism were overrepresented in the GO term analyses of proteins downregulated at day 6 and day 9, higher -log10 p-values were observed at day 3. In return, GO terms related to RNA metabolism were mainly enriched at later stages of the differentiation process as well as the GO term "gene expression". It can thus be concluded that cell proliferation processes were immediately downregulated in OPCs after differentiation initiation, while RNA processing and gene expression represented the main downregulated biological processes thereafter.
GO term analyses of enriched cellular components based on downregulated proteins showed no significant differences between the three analyses (day 3, 6, 9). Main enriched GO terms within all analyses are assigned to the nucleus, like "nuclear chromosome" or "spliceosomal complex".

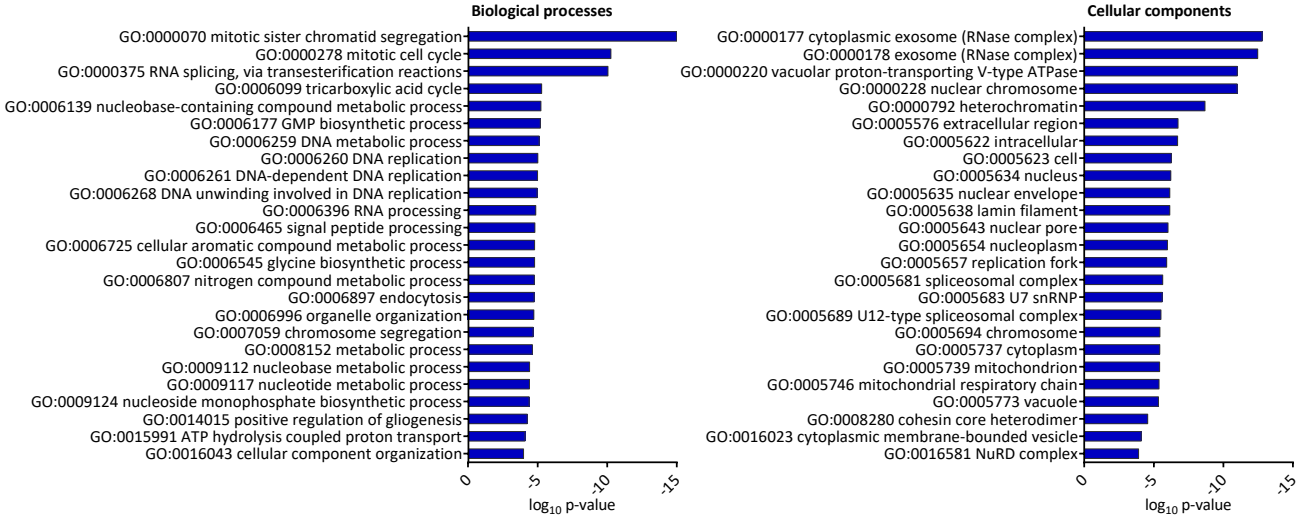

(a) Day 3 - Enriched biological processes and cellular components

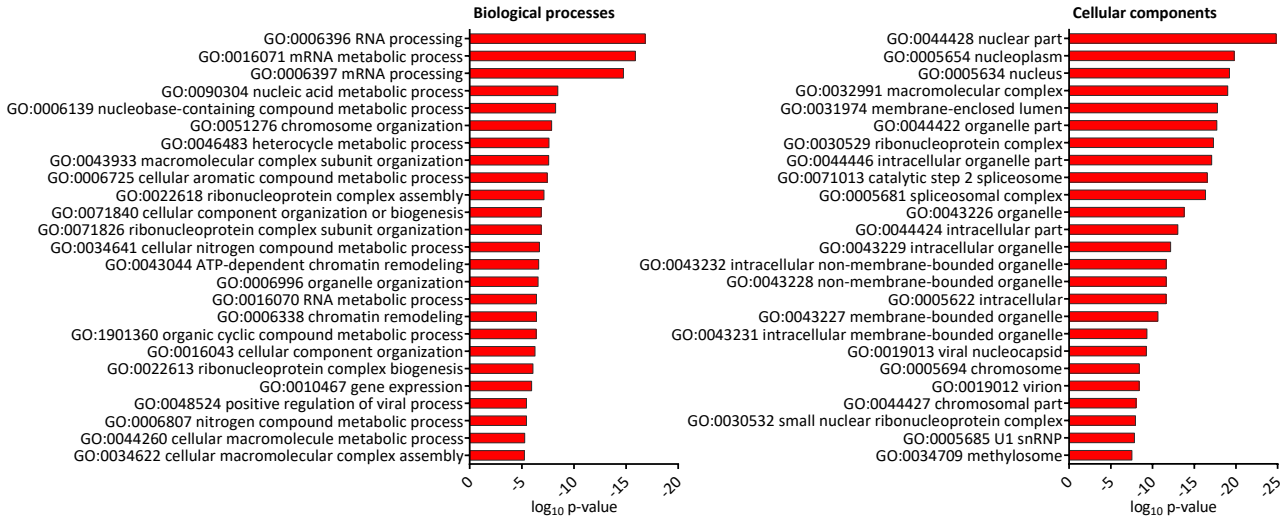

(b) Day 6 - Enriched biological processes and cellular components

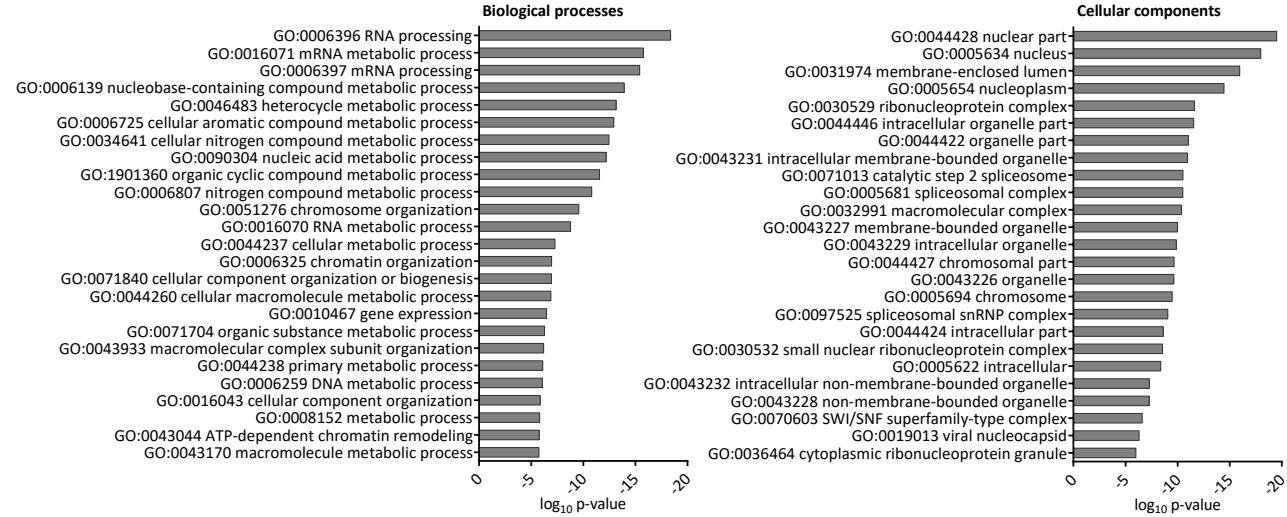

(c) Day 9 - Enriched biological processes and cellular components

Fig. 4.22.: Enriched GO terms of downregulated proteins at (a) day 3, (b) day 6 and (c) day 9 of oligodendrocyte precursor cell differentiation. GO enrichment analyses of significantly downregulated proteins during OPC differentiation were performed against all proteins from the species rattus norvegicus, provided by the gene ontology annotation database (gene association.goa uniprot.142.gz, released on 27.04.2015) using BiNGO. For matching of regulated proteins to GO terms the Go-basic.obo (Gene Ontology consortium, 04/2015) [Ashburner et al., 2000] was applied. As statistical test the hypergeometric test was used and as multiple test correction the Benjamini & Hochberg False Discovery Rate (FDR) was computed from the p-values. The significance level was set to 0.05. Proteins were then applied to REViGO, which summarized the input by removing redundant GO terms. A similarity of 0.7 was set as default. For every time point either the 25 most abundant or all enriched biological processes and cellular components are plotted together with their computed log10 p-values in the graphs. The lower the log10 p-values, the higher the enrichment of the GO term in the data set. GO = gene ontology.

4.3. Investigation of transcriptional activator protein Pur-alpha

The transcriptional activator protein Pur-alpha (PURA) has been identified as one of only few highly upregulated transcription factors during neurospheres differentiation (Figure 4.11). In addition, Pur-alpha expression increased during the development of oligodendrocyte precursor cells (OPCs) to mature oligodendrocytes, revealed by the OPC differentiation experiment (Figure 4.19). Pur-alpha is an ubiquitous protein which can be characterized by the binding to multiple nucleic acids in order to regulate gene expression [Gallia et al., 2000b]. There are several other functions postulated for Pur-alpha, including the initiation of DNA replication, regulation of cell differentiation and cell proliferation processes.

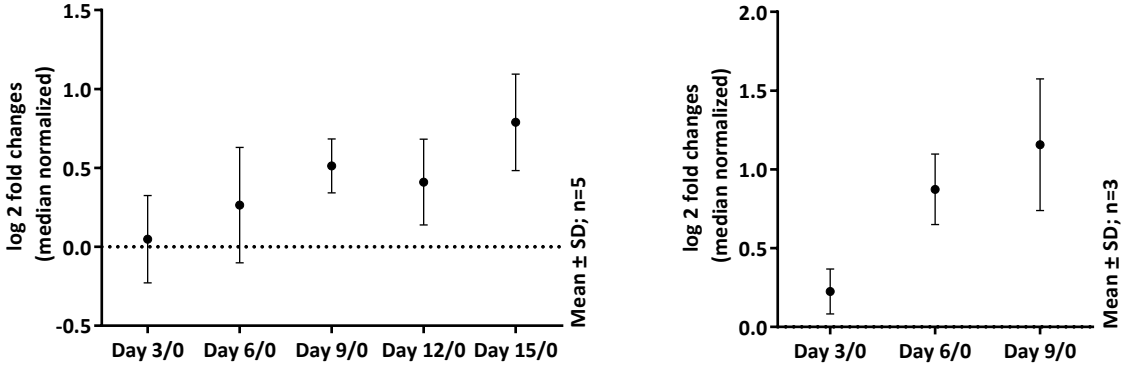

(a) Neurospheres differentiation

(b) OPC differentiation

Fig. 4.23.: Changes in Pur-alpha expression during (a) neurospheres differentiation and (b) oligodendrocyte precursor cell (OPC) differentiation. Using the evidence file (MaxQuant) for the neurosphere experiment (5 biological and 2 concatenated technical replicates) and the PSM file (Mascot) for the OPC experiment (3 biological and 1 concatenated replicate), obtained data was filtered for Pur-alpha peptides featuring unique quantification results and values > 0 in all reporter ion channels. Peptides were summarized to protein level by calculating the median for every channel and each replicate separately. Log2 transformed peptide intensities were normalized to the median per reporter ion channel and combined on protein level by calculating the median. Both graphs depict the mean log2 expression ratios over time, while the error bars represented the calculated standard deviations.

The alteration of Pur-alpha protein levels during neurospheres respectively OPC differentiation is depicted in Figure 4.23 as log2 fold changes (time point $>$ day 0 to day 0) over time. The analyses are based on five biological and two technical (concatenated) neurosphere differentiation replicates and three biological and one technical (concatenated) OPC differentiation replicate. One OPC differentiation replicate was not considered since intensity values of only one peptide were obtained. During neurospheres differentiation the values increased until day 9, while reaching the highest mean log2 fold change value of 0.79 at day 15. A declined log2 fold change value was observed at day 12, which might be the result of quantification errors. In addition, the high standard deviations indicated a distinct variance between the five biological and two technical replicates, especially for time point day 15. Figure 4.23 (b), depicting the log2 Pur-alpha expression ratios during the differentiation from OPCs to oligodendrocytes, indicated a constant increase over time. At day 9, the Pur-alpha mean log2 fold change value amounted 1.16, which equals a more than two times elevated expression of the protein compared to day 0.

4.3.1. GST-Pur-alpha fusion protein generation for antiserum production

Besides a commercial antibody against Pur-alpha, the production of a second antibody was favored to confirm results from western blot (WB) analyses. Although Pur-alpha has a molecular weight of 35 kDa, the purchased polyclonal antibody against Pur-alpha (ab79936, raised against residue 1 - 100 of the human Pur-alpha protein) recognizes particularly polypeptides at 43 and 49 kDa, according to the western blot analyses conducted (Figure 4.27). Moreover, for Pur-alpha immunoprecipitation (IP) and subsequent WB analysis the application of an additional antibody of a different species is reasonable, since the immunoglobulin G (IgG) heavy chain migrates in the 50-55 kDa region, impeding subsequent WB evaluation. Using antibodies from different species, the antibody used for WB will not detect the antibody used for IP, but the antigen of interest. In addition, usually larger amounts of antibody are necessary to perform co-immunoprecipitation analysis, so that the production of an antiserum was favored, also for financial reasons. Accordingly, the production of the Pur-alpha full-length protein, fused to a glutathione S-transferase (GST) protein, was performed in larger quantity.

Cloning of the GST-Pur-alpha construct The Pur-alpha gene was amplified by PCR using the purchased Pur-alpha gene containing plasmid pENTR223.1 as template. Former amplification reactions performed using the Phusion High-Fidelity DNA polymerase or REDTaq DNA polymerase according to the manufacturers instructions and without the addition of any additives resulted in PCR products with deletions in the guanine-cytosine (GC)-rich region. Consequently, multiple approaches were performed using different DNA polymerases, different buffers and PCR annealing temperatures and additives. The agarose gel (Figure 4.24 (a)) depicts the PCR products of the different approaches. Using Taq DNA polymerase, $(NH_4)_2SO_4$ or KCl buffer and two different PCR annealing temperatures (62 ℃ and 67 ℃) no PCR product was generated.

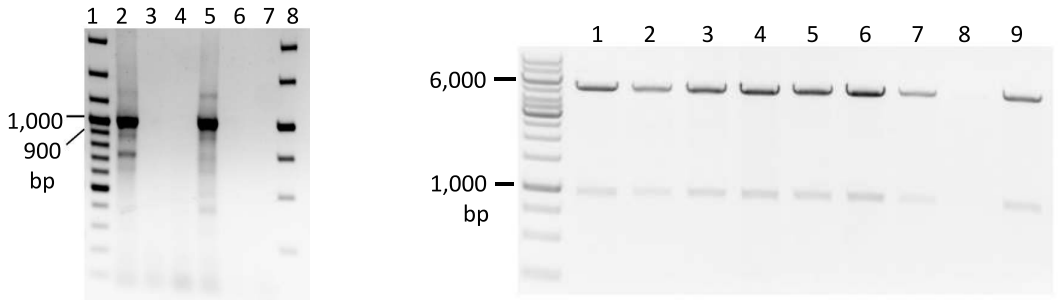

(a) Pur-alpha PCR

(b) Restriction digest after minipreparation

Fig. 4.24.: Pur-alpha polymerase chain reaction and restriction digest of final pGEX-5X-1-GST-Pur-alpha construct. The Pura gene was amplified from the plasmid pENTR223.1 by PCR using different DNA polymerases and PCR annealing temperatures (a). Lane 1 and 8 depict the DNA ladder, lane 2 and 5 depict the PCR product amplified using Phusion polymerase and a Tm of 62 ℃ or 67 ℃. The PCR product amplified using Taq polymerase, $(NH_4)_2SO_4$ buffer and a Tm of 62 ℃ or 67 ℃, were loaded into well 3 and 6, and using KCl buffer and a Tm of 62 ℃ or 67 ℃, were loaded into well 4 and 7. The purified PCR product was then ligated into the pGEX-5X-1-GST vector and transformed into E.coli cells. The agarose gel (b) depicts the digestion products using EcoRI and XhoI (expected sizes: 4,957 bp and 969 bp) of some clones after minipreparation. Tm = annealing temperature.

In contrary, using the Phusion High-Fidelity DNA polymerase in combination with 3% DMSO

in the reaction mixture, PCR products with a size of 966 bp were obtained using annealing temperatures of 62 ℃ or 67 ℃. Subsequently performed sequencing analysis of the PCR product confirmed the amplification of the complete Pur-alpha gene (966 bp).
Thereafter, the amplified Pur-alpha gene was cloned into the pGEX-5X-1-GST expression vector using the restriction enzymes BamHI and XhoI. The Pur-alpha gene was introduced after the GST sequence. The pGEX-5X-1-GST vector was used since it contains a lac operon to induce protein expression in bacteria and because it provides a GST tag, which can be used for protein purification from cell lysates. Competent E.coli cells were transformed with the construct and plated on ampicillin-containing LB-agarose plates to select clones, which have uptaken the construct, the next day. After performing minipreparations of multiple clones, restriction digests were performed and evaluated to detect clones that have incorporated the pGEX-5X-1-GST-Pur-alpha construct (the plasmid map can be found in the Appendix F.1). According to the restriction digest, shown in Figure 4.24 (b), except of clone 8, every clone has incorporated the plasmid, indicated by the right size of fragments observed after cutting with EcoRI and XhoI.

Expression and purification of GST-Pur-alpha fusion protein Expression of the GST-Pur-alpha fusion protein in E.coli was induced by the addition of isopropyl β-D-1-thiogalactopyranoside (IPTG). The Coomassie-stained protein gel (Figure 4.25 (a)) confirmed the successful expression of the fusion protein, indicated by the stronger intensity of the 70 kDa polypeptide in the samples incubated with IPTG (lane 3, 4) compared to samples where expression was not induced using IPTG (lane 1, 2). The GST protein has a molecular weight of 26 kDa, while Pur-alpha usually has a molecular weight of 35 kDa. However, former WB analysis performed using the commercial antibody against Pur-alpha (ab79936) also revealed a polypeptide at 42 kDa. The 42 kDa polypeptide was later on confirmed to be Pur-alpha specific (Figure 4.27). The 70 kDa polypeptide was thus considered as the GST-Pur-alpha fusion protein. After bacterial cell lysis, the fusion protein was purified using Pierce™ Glutathione Agarose. Elution of the GST-Pur-alpha fusion protein was performed with the recommended elution buffer containing reduced glutathione. Fractions containing the fusion protein were determined by SDS-PAGE and subsequent staining with Coomassie and were finally combined.

In order to receive an antibody specific for Pur-alpha, which feature less non-specific binding, high purity of the antigen is required. Since besides the 70 kDa poplypeptide additional polypeptides were detected in the WB analysis (Appendix: Figure A.3 (a)), although lower amounts, a stabilization test was performed to check for degradation products (Figure A.3 (b)). Elution fractions were incubated for 24 hours at 40 ℃ while the original elution fractions served as controls. Subsequent WB analysis revealed that the additional polypeptides observed did not represent degradation products of the fusion protein and most likely represented impurities.
For the immunization of animals with the fusion protein, an antigen concentration of 1 mg/ml in buffered saline solution was recommended. Accordingly, the fusion protein eluates were combined and dialyzed against 10 mM NH_4HCO_3, pH 7.9 for 24 hours. Thereafter, the dialysate was frozen in liquid nitrogen and concentrated using a vacuum centrifuge. The WB performed against recombinant GST showed no difference in size and antibody recognition of the fusion protein before and after dialysis or after evaporation (Figure 4.25 (b)). In total, 2.1 mg purified protein was obtained (concentration was colorimetrically determined using BSA as standard calibration solution) and passed to an external antibody service for antiserum production.

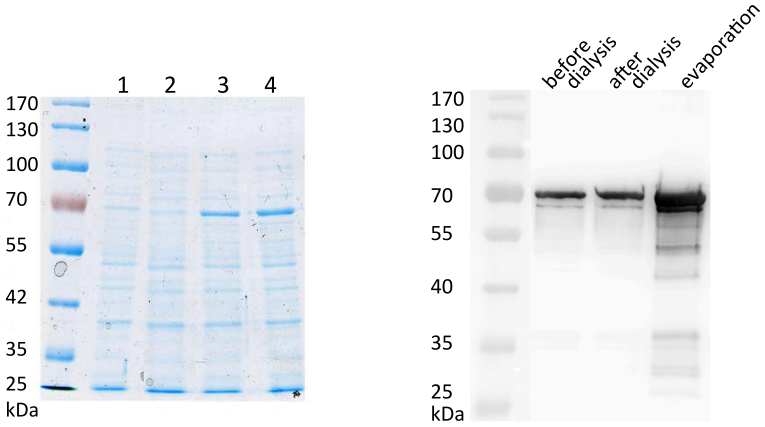

(a) GST-Pur-alpha expression (b) Anti-GST western blot

Fig. 4.25.: Expression and purification of GST-Pur-alpha fusion protein. Protein expression was induced by adding isopropyl β-D-1-thiogalactopyranoside to E.coli cells containing the pGEX-5X-1-GST-Pur-alpha construct and incubation for 4 hours. The Coomassie-stained gel (a) depicts aliquots of not induced (lane 1 and 2) and induced (lane 3 and 4) samples after SDS-PAGE. Western blot of GST-Pur-alpha protein (b). Using Pierce™ Glutathione Agarose the fusion protein was purified and positive elution fractions were combined (sample: before dialysis). The eluate was transferred into a dialysis tubing and dialyzed against 10 mM NH_4HCO_3 pH 7.9 for 24 hours. After dialysis, one sample was taken (after dialysis), while the remaining dialysate was frozen in liquid nitrogen and evaporated at RT using a vacuum centrifuge (after evaporation). The western blot was performed using a GST-antibody (mouse; 1:200; over night; 4 °C) and an α-mouse-HRP antibody (goat; 1:5,000; 1 h; RT). RT = room temperature.

Purification of the guinea pig antiserum The received guinea pig antiserum was first tested for its antigen specifity using a cell lysate derived from fetal neural stem (fNS) cells [Conti et al., 2005] and from an OPC cell line, shortly termed Oli-neu [Jung et al., 1995], together with the received preimmune serum. According to the WB (Figure 4.26 (a)), after an exposition time of 15 minutes, some polypeptides were slightly visible at around 55, 60 and 100 kDa in the sample incubated with preimmune serum. In contrary, using the Pur-alpha antiserum, after an exposition time of 85 seconds, polypeptides were visible at around 42, 48, 50 and 70 kDa. Especially the 48 kDa polypeptide was distinct in fNS cells. Thereafter, the guinea pig antiserum was purified using Affi-Gel 15 (Bio-Rad), a N-hydroxysuccinimide ester which is crosslinked to an agarose gel bead support and binds primary amino groups. For this purpose, the recombinant GST-Pur-alpha fusion protein was incubated together with Affi-Gel 15 to obtain an affinity column to retain antibodies recognizing epitopes of the GST-Pur-alpha protein, while unspecific antibodies were removed. The Coomassie stained gel (Figure 4.26 (b)) indicates that the fusion protein almost completely reacted with the reactive groups of the Affi-Gel 15. Accordingly, the column could be used for antiserum purification, which was subsequently performed. Using an acidic elution buffer (100 mM glycin (pH 2,4) and 150 mM NaCl), the antiserum was eluted from the column in several fractions and neutralized with HEPES buffer (pH = 8).

According to the Coomassie stained gel (Figure 4.26 (c)) the elution of the antiserum was successful, indicated by the IgG heavy chain (55 kDa) and the IgG light chain (25 kDa) in

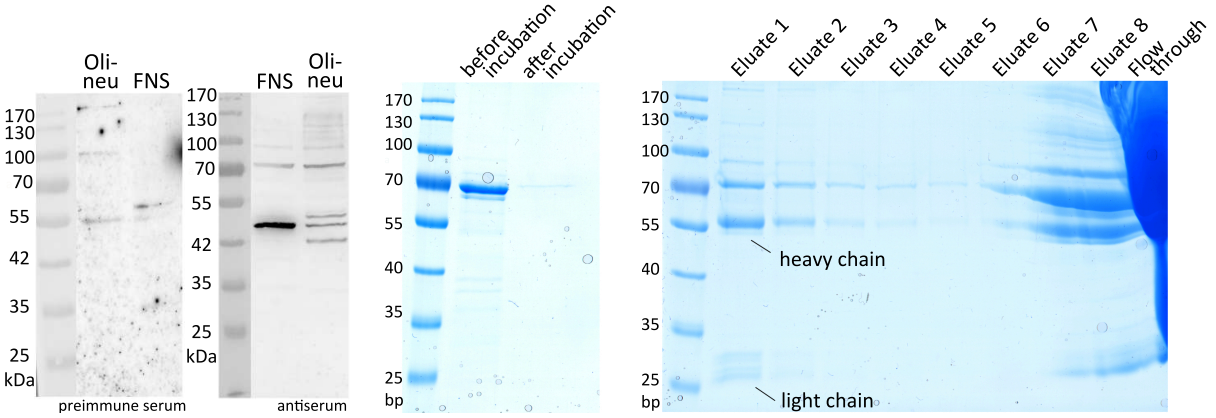

(a) Pur-alpha WB (b) Affi-Gel incubation (c) Affi-Gel elution fractions

Fig. 4.26.: Pura-alpha antiserum purification using Affi-Gel 15. Western blot analysis (a) of fNS and Oli-neu cell lysates using guinea pig preimmune serum and guinea pig antiserum (1:5,000; over night; 4 ℃) and the α-guinea pig-HRP antibody (1:5,000; 1 h; room temperature). Affi-Gel 15 was used for antiserum purification. Affi-Gel 15 was equilibrated and incubated with the purified GST-Pur-alpha fusion protein for 4 hours. SDS-PAGE of incubated sample (after incubation) and original protein (before incubation) including Coomassie staining was performed to confirm protein binding (b). The column was thereafter incubated with ethanolamine HCl for 1 hour, washed several times and incubated with the heat-inactivated antiserum (56 ℃, 30 min) two times for 5 minutes, using the flow-through for second incubation. After washing the column, antiserum was eluted ten times using 100 mM glycin pH 2,4 and 150 mM NaCl into microtubes containing HEPES buffer pH 8. The Coomassie staining (c) shows the first eight eluates and the flow-through. All purification steps were performed at 4 ℃.

fraction 1 - 5. However, an additional polypeptide was detected at around 70 kDa, corresponding with the size of the GST-Pur-alpha fusion protein. For that reason, another SDS-PAGE of the washing fractions (prior to incubation of Affi-Gel 15 and antiserum) was performed to determine whether unbound GST-Pur-alpha protein was still present in the reaction mixture. According to the Coomassie stained gel (Figure A.4) no free fusion protein was present. Thus, the origin of the 70 kDa polypeptide remains so far unknown.

4.3.2. Verification of Pur-alpha expression by Western Blot analyses

Protein level changes during the differentiation process of neurospheres to oligospheres was subsequently tested by quantitative WB analysis. Since multiple polypeptides were detected using the commercial antibody and the self-made guinea pig antiserum, the specificity of both antibodies for Pur-alpha was examined first. For this purpose, HeLa cells were transfected with an expression construct encoding for Pur-alpha, while untransfected HeLa cells served as control. The blots were first incubated with a primary antibody against Pur-alpha and the appropriate HRP-antibody and after evaluation by enhanced chemiluminescent detection, with an antibody against α-Tubulin, serving as a control for loading, was equally detected.

The predicted molecular weight of the murine Pur-alpha protein is 35 kDa. According to Figure 4.27, the commercial antibody against Pur-alpha detected three prominent polypeptides at 92 kDa, 50 kDa and 43 kDa and some additional ones that were only faintly stained. The only

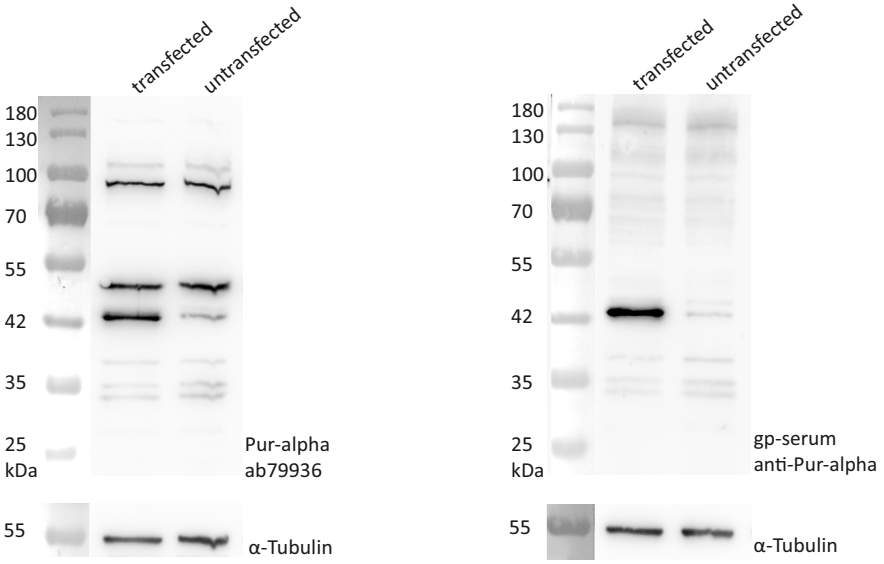

(a) ab79936 against Pur-alpha (b) Pur-alpha antiserum

Fig. 4.27.: Western blot of Pur-alpha transfected sample versus control sample. HeLa cells were transfected with a Pur-alpha construct using Turbofect, while the control population remained untransfected. 24 hours later, cells were harvested, lyzed and SDS-PAGE was performed. Proteins were semi-dry blotted onto nitrocellulose membranes and blocked using 5% filtered skim milk in TBS-T. Incubation with primary antibody was performed overnight at 4 °C with (a) the commercial antibody ab79936 (rabbit; 1:700), with (b) the self-made antiserum against Pur-alpha (guinea pig; 1:200) and the secondary antibodies (α-rabbit-HRP; 1:5,000; α-guinea pig-HRP; 1:5,000) for 90 min at RT. Images were taken using the FUSION-Solo chemiluminescence detection system. Thereafter, incubation with the loading control α-Tubulin (T5168; 1:5,000; 2 h; RT) was performed. RT = room temperature

polypeptide which was expressed with different intensities in transfected and untransfected cells represented the 43 kDa protein. Quantification and normalization to α-Tubulin confirmed that for the two larger polypeptides same expression levels were obtained for transfected and untransfected samples. The finding was further validated by using the self-made guinea pig serum against Pur-alpha, which detected a distinct polypeptide at 43 kDa in the sample transfected with the expression vector encoding Pur-alpha. A probable explanation for the migration of the protein at higher molecular weights might be the phosphorylation status of amino acids. Actually, multiple phosphorylation sites have been detected within Pur-alpha [Trinidad et al., 2012].

Western blots of neurosphere differentiation samples were further conducted to monitor the expression progression of the protein. According to Figure 4.28, after 9 days of differentiation, Pur-alpha protein levels were almost twice as high as in undifferentiated cells and after 15 days, even more than twice as high as in undifferentiated cells. Significant changes in protein expression were observed from day six until the end of the differentiation experiment. In parallel, fetal neural stem (fNS) cells and Oli-neu cells were examined for the expression of Pur-alpha. Apparently, Pur-alpha levels differed between fNS and Oli-neu cells, indicated by a more than four times higher Pur-alpha expression in Oli-neu cells compared to fNS cells, based on quantification results of WB triplicates.

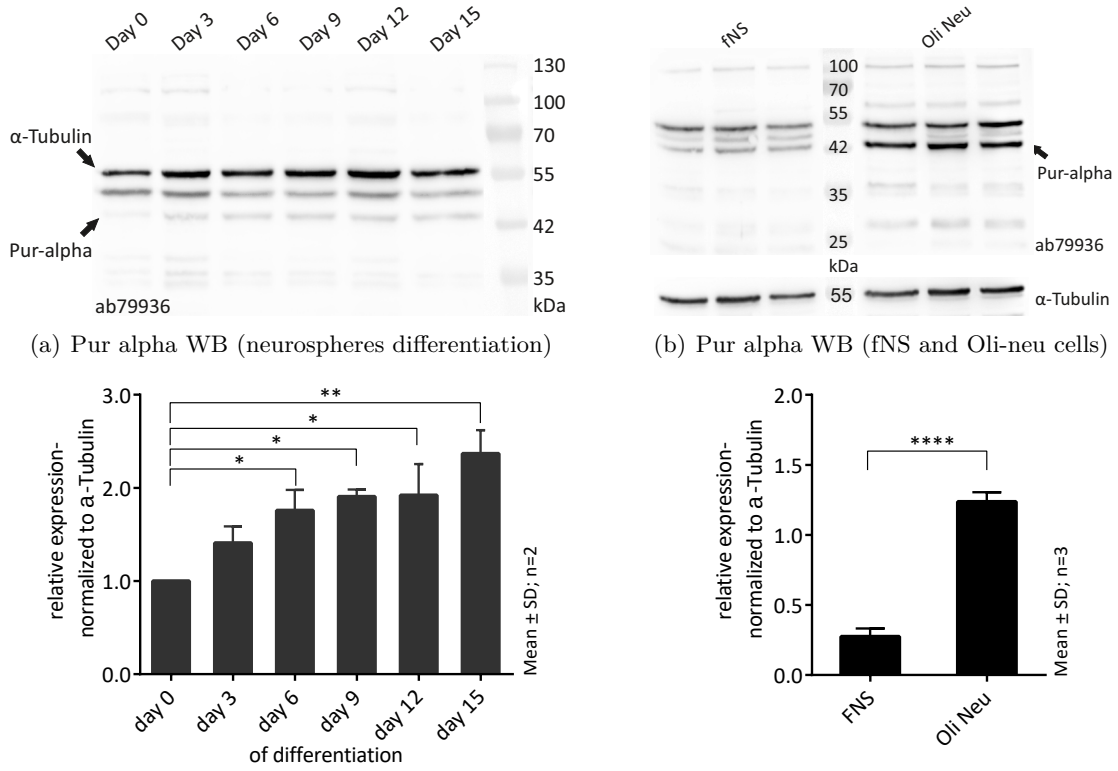

(a) Pur alpha WB (neurospheres differentiation)

(b) Pur alpha WB (fNS and Oli-neu cells)

(c) Quantitation (neurosphere differentiation)

(d) Quantitation (fNS, Oli-neu cells)

Fig. 4.28.: Western blot against Pur-alpha and α-Tubulin (a) of neurosphere differentiation samples and (b) of fNS and Oli-Neu cells. Murine neurospheres were differentiated to oligospheres. Primary cells, fNS cells and Oli-Neu cells were harvested, lyzed and SDS-PAGE was performed. Proteins were semi-dry blotted onto nitrocellulose membranes and blocked using 5% filtered skim milk in TBS-T. Concomitant incubation overnight at 4 ℃ with antibodies against Pur-alpha (rabbit; 1:700) and α-Tubulin (mouse; 1:5,000) and for 90 min at room temperature with α-rabbit-HRP (1:5,000) or α-mouse-HRP (1:5,000) was performed. Images were taken using the FUSION-Solo chemiluminescence detection system. Mean expression ratios of day > 0 / day 0 of two respectively three replicates after normalization to α-Tubulin are depicted for (c) neurosphere differentiation and for (d) fNS and Oli-neu cells. As statistical test the one-way ANOVA test including multiple comparisons test (Dunnett's method) was applied for the neurosphere and the unpaired t-test for the fNS and Oli-neu experiment. Following significance levels were applied: * = $p \leq 0.05$; ** = $p \leq 0.01$; **** = $p \leq 0.0001$.

4.3.3. Comparison of Pur-alpha RNA expression levels between NPCs and OPCs

Considering the results from both analyses, MS and WB, an increase of Pur-alpha expression during the differentiation to oligospheres could be shown. Protein biosynthesis underlies multiple regulatory mechanisms, ranging from gene transcription control via RNA processing and mRNA degradation control to regulation of protein translation [Cooper & Hausman, 2000]. Thus, multiple reasons for increasing Pur-alpha protein levels are conceivable, including an enhanced *Pura* transcription. In order to determine whether Pur-alpha gene expression differs between undifferentiated and differentiated cells, quantitative polymerase chain reaction (PCR) [Nolan et al., 2006] was applied. For this purpose, quadruples of neurosphere differentiation

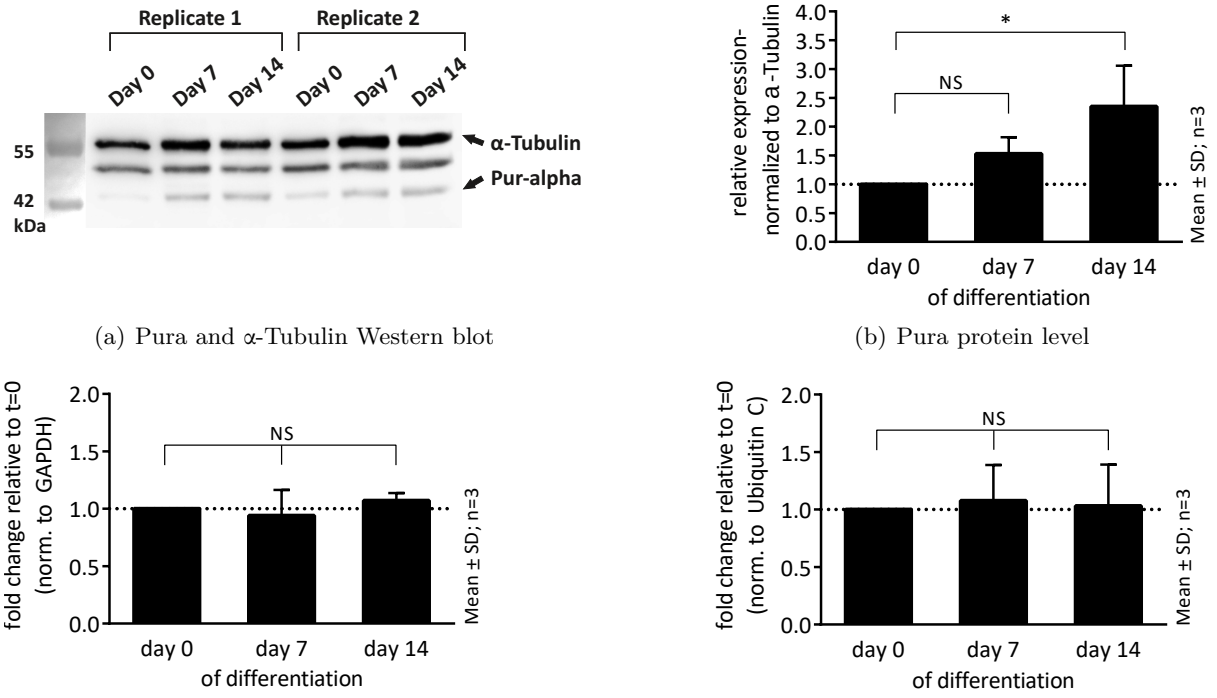

(a) Pura and α-Tubulin Western blot

(b) Pura protein level

(c) Pura RNA level- normalized to GAPDH

(d) Pura RNA level- normalized to Ubiquitin C

Fig. 4.29.: Pur-alpha WB (a, b) and qPCR analyses of neurosphere differentiation experiments, normalized to (c) GAPDH and (d) Ubiquitin C. Neurosphere differentiation samples (day 0, 7, 14) were lyzed. A western blot against Pur-alpha and α-Tubulin (a) is exemplary shown for two replicates. The Pur-alpha mean expression relative to α-Tubulin (WB) of three replicates is shown in (b). Following RNA isolation and concentration, RNA purity was determined, before synthesizing cDNA from up to 5 µg RNA by RT-PCR. cDNA was used as template (or water as control) for qPCR and cycle threshold (Ct) values were determined using a Real Time-PCR System and the SYBR Green I dye. Data were processed by manually adjusting the baseline (range of cycles for determination of background signal) and threshold levels, separately for every detector (Pura, GAPDH, Ubiquitin C). The $\triangle\triangle$Ct method was applied using the mean of three Ct values measured per sample and using sample day 0 as calibrator and GAPDH (c) and Ubiquitin C (d) as normalizer. The bars depict the normalized mean Pur-alpha RNA expression ratios at day 7 and 14, relative to day 0 of three replicates. As statistical test the one way ANOVA test including Dunett's (WB) or Tukey's (qPCR) multiple comparison method was applied, using the following significance levels: NS = ≥ 0.05; * = $p \leq 0.05$.

experiments were conducted and Pur-alpha protein and RNA levels were measured at three different time points (day 0, 7 and 14). In regard to the qPCR approach, RNA isolation using Trizol® and cDNA synthesis by reverse transcriptase (RT)-PCR were performed prior to the amplification of Pur-alpha cDNA by qPCR. Detection of amplified product was achieved by measuring the fluorescent signal emitted by the SYBR Green I dye upon binding to deoxyribonucleic acid molecules.
Quantitation of DNA amount per sample was achieved by determining the cycle threshold (Ct) value, which indicates the point where background fluorescence is exceeded, and subsequent comparison of Ct values between samples of different time points. Since quantitative analyses are sensitive to small changes during sample preparation and measurement, normalization of

Pur-alpha Ct values to two constantly expressed housekeeping genes was additionally considered, namely glyceraldehyde 3-phosphate dehydrogenase (GAPDH) and polyubiquitin-C (Ubc). Both have shown more constant RNA levels compared to beta-actin. Finally, fold changes of Pur-alpha at day 7 and 14 were ascertained relatively to day 0 (calibrator) by applying the $\triangle\triangle$Ct method. The outcome is depicted in Figure 4.29.

Similar to former WB analyses performed, Pur-alpha protein expression increased during the neurosphere differentiation experiment performed in parallel to qPCR analysis (Figure 4.29 (a) and (b)). While the expression was not significantly upregulated at day 7, the protein level at day 14 differed significantly from the one at day 0. In parallel, qPCR analyses were conducted in three replicates, which revealed no significant difference in Pur-alpha RNA levels between samples of different development stages. Normalization of Ct values to the housekeeping gene GAPDH showed a slight increase in expression ratios relative to day 0 (Figure 4.29 (c)) after 14 days of differentiation, whereas normalization to Ubc revealed almost no changes in expression ratios (Figure 4.29 (d)). Calculated standard deviations indicated an existing variability within the three replicates. Particular investigation of every replicate indicated that the variability in Pur-alpha RNA levels between the three time points resulted from both, alterations of housekeeping gene Ct values and Pur-alpha Ct values. For example, variability in one replicate derived from altering Ubc Ct values, indicated by almost consistent Pur-alpha Ct values across all time points and slightly decreasing Ubc Ct values over time, resulting in lower relative Pur-alpha RNA expression levels. It should be noted that in total four replicates were quantitatively assessed. However, only two replicates included both housekeeping genes for normalization, while for the other replicates only one housekeeping gene was utilized. This circumstance is due to the belated decision to additionally include Ubc as housekeeping gene. Summarizing the normalized results of all replicates, Pur-alpha transcription remained almost stable during neurospheres differentiation. The formation of only one PCR product with the right size for all three amplification reactions was confirmed afterwards by separating the generated small DNA fragments by agarose gel electrophoresis. By contrast, no DNA fragment was detected in control samples containing only water.

4.3.4. Degradation of Pur-alpha

The observation of not significantly altered Pur-alpha RNA expression levels across the whole differentiation time suggested another reason for the elevated Pur-alpha protein levels in oligospheres. A probable explanation therefore might be the degradation of the Pur-alpha protein in neurospheres, whereas it is stabilized in oligospheres. Pur-alpha levels use to alter during the cell-cycle, peaking at mitosis and dropping to a minimum at the onset of late G_1 respectively early S phase [Itoh et al., 1998]. So far, it is not known whether the decline during S stage depends on targeted protein degradation or nuclear export. Despite only few information about the turnover of the Pur-alpha protein is available until now, a degradation of the protein by the anaphase promoting complex/cyclosome (APC/C), which is active during late mitosis and G_1 phase, is conceivable. The APC/C is an ubiquitin E3 ligase which assembles polyubiquitin chains to target proteins, denoting them for degradation via the proteasome [Peters, 2006]. Ubiquitination of proteins requires three different ubiquitin ligases and additional co-activators, responsible for the recruitment of substrates containing specific recognition sites, such as the destruction box (D box), KEN box or GxENbox, to the APC/C [Pfleger & Kirschner, 2000] [Castro et al., 2005].

We analyzed the Pur-alpha protein sequence for these recognition motifs and revealed that the D box and the KEN box were present within the molecule (Figure 4.30). Actually, Pur-alpha possesses multiple D box and one KEN box motif. In addition, the protein possesses the potential PEST sequence PAELPEGTSLTVDNKRF which usually acts as a signaling peptide for degradation via a proteosome-mediated pathway [Rechsteiner & Rogers, 1996].

Fig. 4.30.: Pur-alpha amino acid sequence including ubiquitination motifs and identified sites. The protein Pur-alpha contains one full D box (yellow box), three partial D box (blue boxes) and a KEN box motif (green box). The D box is composed of the consensus sequence RxxLxxxN, where R = arginine, L = leucine, N = asparagine and x = any amino acid, whereas the KEN-box consisted of the consensus sequence KENxxxN, where K represented a lysine residue and E a glutamate residue. Five ubiquitination sites have been identified within Pur-alpha by Wagner and co-workers [Wagner et al., 2012a], labeled with red color, while the ubiquitination site specifically detected in brain tissue is circled.

Besides this, Wagner and co-workers performed large-scale proteomic analyses of ubiquitination in murine tissue, whereby they detected five ubiquitinated sites in Pur-alpha [Wagner et al., 2012b]. Interestingly, the Pur-alpha ubiquitination site localized in the D box, was specifically detected only in lucerna and brain tissue. Moreover, another MS experiment was conducted by a member of our group, analyzing the expression of Pur-alpha in HeLa cells after release from cell cycle arrest with thymidine. The obtained results showed an expression pattern of Pur-alpha during mitotic cell cycle, similar to the ones of known APC/C targets.

Pur-alpha was first detected because of its ability to bind to the purine-rich single strand of the PUR element located upstream of the c-myc gene, which in turn regulates the expression of many target genes involved in regulation of cellular proliferation, differentiation and apoptosis [Bergemann & Johnson, 1992]. Thus, we constructed a hypothesis, shown in Figure 4.31, regarding the degradation of Pur-alpha by the APC/C in neurospheres and oligospheres. Consequently, Pur-alpha protein levels decrease, while c-myc expression increases, thereby triggering the proliferation of multipotent progenitor cells. On the other hand, a stabilization of Pur-alpha regarding the degradation by the APC/C leads to elevated Pur-alpha protein levels. Since the transcription of the c-myc gene would be repressed by Pur-alpha, cells would start to differentiate. It should be noted that a transcriptional regulation of c-myc by Pur-alpha has not been evidenced yet and that c-myc is only a representative for a proliferation regulating factor. A regulation of c-myc expression by Pur-alpha is also conceivable via the inhibition of the transcription factor activator protein E2F-1 [Stanelle et al., 2002]. Nevertheless, this hypothesis implies an important role for Pur-alpha, being part of the initiation and regulation machinery that is responsible for the differentiation from neurospheres to oligospheres.

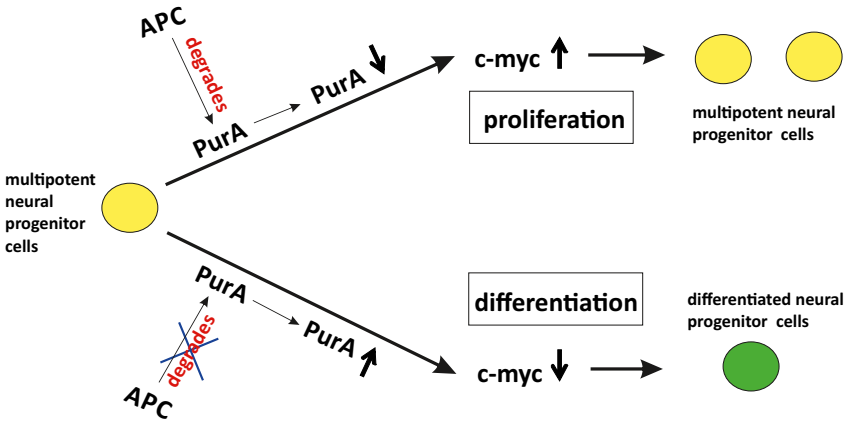

Fig. 4.31.: Hypothesized function of Pur-alpha in promoting proliferation and differentiation of neurospheres. If the APC/C complex degrades Pur-alpha, the cellular protein level would decrease and c-myc gene expression would be activated. As a consequence of increased protein levels of the transcription factor c-myc, multipotent neural precursor cells undergo the cell cycle and proliferate. On the other hand, if Pur-alpha degradation is inhibited, cellular protein concentration would rise, whereas c-myc expression would be suppressed, inducing differentiation to neural progenitor cells.

In a first attempt, cell cycle synchronized HeLa cells were released from the cell cycle block by medium exchange and samples were harvested after distinct time points, followed by quantification of Pur-alpha expression by western blot. HeLa cells were either synchronized with the DNA synthesis-inhibitor thymidine (double thymidine block) and subsequently released after G_1/S phase block, or with thymidine and nocodazole, followed by the release of cells after mitosis block. Although Pur-alpha has been shown to exhibit highest expression levels during mitosis and lowest expression levels during G_1 phase, changes in protein expression between different cell cycle stages were not evident in our WB analyses conducted. Additionally, the expression level of the first control protein α-Tubulin seemed to be likewise effected by the treatment, whereas the molecular weight of the second control beta actin equaled the one of Pur-alpha, making an additional stripping step essential. Thus, three additional experimental approaches were chosen to confirm or reject the degradation hypothesis. The first one included the degradation of *in vitro* synthesized Pur-alpha protein with an active G_1 lysate under appropriate conditions, whereas the second one included the detection of ubiquitinated proteins after Pur-alpha immunoprecipitation in MG132 (proteasome inhibitor) treated samples. Finally, interaction partner analyses were considered to detect both, proteins belonging to the APC/C machinery and proteins interacting with Pur-alpha.

4.3.4.1. Degradation assay

The *in vivo* degradation of proteins by the APC/C is a defined and well regulated mechanism, which requires the cooperation of several factors to form a functional complex able to ubiquitinate proteins for subsequent degradation by the proteasome. This includes an ubiquitin-activating enzyme (E1), an ubiquitin-conjugating enzyme (E2), a co-activator protein, ubiquitin and the APC/C (E3) itself [Peters, 2006]. For *in vitro* degradation assays the APC/C can either be isolated in its inactive form derived by interphase extracts from *Xenopus laevis* eggs

and subsequent activation by the co-activator Cdc20 or Cdh1 [Stewart & Fang, 2005b] or a G_1-synchronized cell lysate containing the active APC/C can be used [Stewart & Fang, 2005a]. In our experiments we used synchronized human and murine G_1 lysates as source for the active APC/C. Detection of the degradation progress of Pur-alpha was achieved by introducing radioactive labeled amino acids (^{35}S) into newly synthesized proteins using the Wheat germ coupled transcription and translation system [Endo & Sawasaki, 2006]. After exposing samples to a bioimaging plate, radioactive signals were quantitatively assessed and the ratio of intensities between starting and end point of the degradation reaction was determined. Since the degradation efficiency depended on many factors, a positive control was degraded in parallel. For this purpose, the well-characterized APC/C substrate Securin (PTTG1) [Peters, 2006] was used to correlate the APC/C degradation efficiency for Pur-alpha to the one for Securin. Besides the positive control, a reaction mixture containing the proteasome inhibiting reagent MG132 was included as negative control to confirm proteasome dependent degradation.

Since our hypothesis implies the degradation of Pur-alpha by the ubiquitin-proteasome pathway in undifferentiated proliferating cells, a degradation complex derived from fNS cells most likely provided the proper conditions. In a first attempt however, G_1- synchronized cell lysates were prepared from HeLa S3 cells. The system provided some advantages, like the well established protocol for cell cycle synchronization or the simple cultivation in suspension cultures in large amounts, whereby the detachment of cells during mitosis in an adherent cell population can be avoided. Additionally, HeLa S3 cells exhibited a doubling time of around 24 hours, enabling a well defined incubation time with the cell cycle arresting reagents thymidine and nocodazole.

Flow cytometric analysis of cell cycle synchronized HeLa S3 cells Although the degradation process mediated by the APC/C required many factors to finally degrade targeted proteins, the success of the reaction is particularly depending on an active and functional APC/C. Since the APC/C is only active during late mitosis and G_1 phase, cells situated at this cell cycle stages were synchronized and harvested. Thus, DNA synthesis in HeLa S3 cells were first blocked using thymidine, arresting cells during S stage of the cell cycle. Thereafter, medium was exchanged, enabling cells to enter G_2 phase to undergo the cell cycle in a synchronous manner before addition of the microtubule interfering reagent nocodazole prevented cells from entering anaphase. Synchronized cells were afterwards released and harvested in G_1 stage. To confirm successful cell cycle synchronization, flow cytometric analyses of samples at different stages of the experiment were performed. Prior to the analyses, samples were incubated with the DNA-binding fluorescent dye propidium iodide (PI), thereby allowing the quantification of DNA content in each cell. At least 10,000 cells were measured to quantitatively assess the percentage of cells present at G_1 phase, S phase and G_2 phase / mitosis and to survey the efficiency of cell cycle synchronization. One exemplary experiment, depicting the results of flow cytometric analyses of HeLa S3 cells, is shown in Figure A.5 (Appendix).
The histogram PI-A versus count (Figure A.5 (c)) which depicts the cell cycle distribution of cells synchronized in G_2 phase / mitosis, indicated that 59.3% of nocodazole treated cells possessed a double chromosome set, while 6.7% possessed a single chromosome set. Accordingly, cell cycle synchronization in G_2 phase / mitosis using nocodazole was successful for 59.3% of total cells. The remaining cells belonged either to the group of dead cells and cell debris, exhibiting low PI-W and PI-A values or cell aggregates, exhibiting high PI-W and PI-A values. Secondly, according to Figure A.5 (d), the release of cells after mitosis block into G_1 phase was successful

for 56.5% of total cells. However, four hours after the nocodazole block, 7.4% of total cells still possessed a double chromosome set, indicating their presence in mitosis. In addition, almost no cells were observed residing in S phase (PI-A of 90 - 130 x 1,000).

***In vitro* degradation of Pur-alpha using HeLa S3 derived G_1 lysate** Besides confirming cell cycle synchronization, a successful *in vitro* synthesis of ^{35}S-labeled Pur-alpha and ^{35}S-labeled Securin had to be verified. Thus, target proteins were first synthesized using the cell-free transcription and translation systems TnT® Coupled Reticulocyte Lysate System and TNT® Coupled Wheat Germ Extract System. Thereafter, proteins were separated by SDS-PAGE and Pur-alpha western blots were performed. As negative control a luciferase protein and the reticulocyte mastermix respectively the *in vitro* synthesized Securin protein and the wheat germ mastermix were used, while a cell lysate derived from oligospheres served as positive control for Pur-alpha. According to Figure 4.32, using both systems, Pur-alpha *in vitro* synthesis was successful.

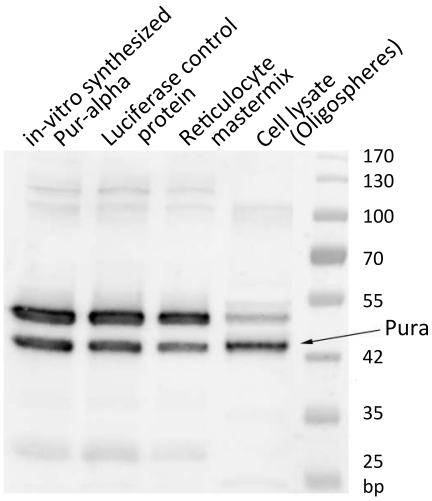

(a) Pura WB (Reticulocyte Lysate System)

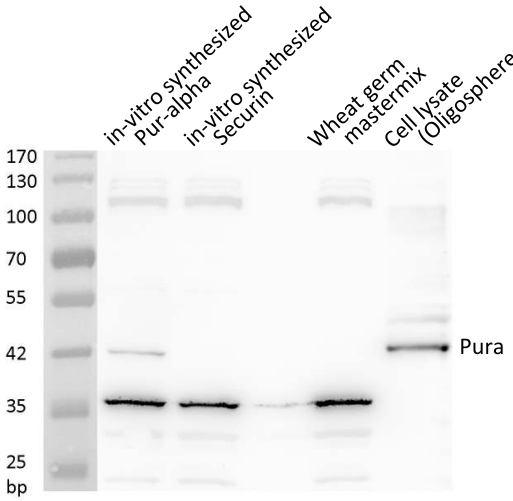

(b) Pura WB (Wheat Germ Extract System)

Fig. 4.32.: Pur-alpha western blot of samples derived from two *in vitro* transcription and translation systems. Murine Pur-alpha and human Securin were *in vitro* synthesized using (a) the TnT® Coupled Reticulocyte Lysate System (Pur-alpha) and the Reticulocyte Lysate System (Securin) and (b) the TnT® Coupled Wheat Germ Extract System. The linearized and purified pBluescript-SK-Pura plasmid and the Securin-His8-tag RNA (Reticulocyte System) or the PCS2-Securin-His8-Sp6 plasmid (Wheat Germ System) served as templates. *In vitro* synthesis was performed at 30 ℃ for 90 - 120 min. Proteins were separated by SDS-PAGE together with a luciferase control protein and the reticulocyte mastermix, respectively, the *in vitro* synthesized Securin and wheat germ mastermix. An oligosphere cell lysate was used as control. The western blot was incubated with the Pur-alpha antibody ab79936 (rabbit; 1:700) at 4 ℃ overnight and with the secondary antibody α-rabbit-HRP (1:5,000; 90 min; room temperature). Images were taken using the FUSION-Solo chemiluminescence detection system.

In both blots, the Pur-alpha protein was detected at 43 kDa in the oligosphere cell lysate and the *in vitro* synthesized Pur-alpha sample. However, a polypeptide was detected at the same size in the luciferase protein and the reticulocyte lysate mastermix, assuming that endogenous Pur-alpha is present in the reticulocyte lysate (Figure 4.32 (a)). Mass spectrometry analysis of the gel bands, cut out in the 43 kDa region, confirmed the presence of Pur-alpha in the

reticulocyte lysate mastermix. In contrary, no Pur-alpha was detected within the wheat germ mastermix (Figure 4.32 (b)), while an additional polypeptide at around 36 kDa was recognized by the Pur-alpha antibody. Thus, the TnT® Coupled Wheat Germ Extract System was used for the *in vitro* synthesis of both proteins.

During the *in vitro* transcription and translation reaction, radioactively labeled ^{35}S-methionine was incorporated into newly synthesized proteins to relatively assess the amount of Pur-alpha and Securin at the beginning and the end of the *in vitro* degradation experiment. In a first step, successful *in vitro* synthesis of both proteins needed to be confirmed. In addition, the amount of protein to be used for degradation assay needed to be titrated first, since the radioactivity of the synthesized proteins depend, for example, on the number of methionine residues within the protein. The appropriate amount for the degradation assay equals the lowest amount of ^{35}S-labeled protein that still gives signals, well distinguishable from background signals. For this purpose, different amounts of ^{35}S-labeled target protein were separated by SDS-PAGE, before drying the gel by applying heat and vacuum. The blot was attached to a bioimaging plate and both placed into an imaging plate cassette for 24 hours. Thereafter, radioactive signal intensities were analyzed using a bioimaging analyzer. An exemplary blot for *in vitro* synthesized Pur-alpha is shown in Figure 4.33 (a) and for Securin in Figure 4.33 (b).

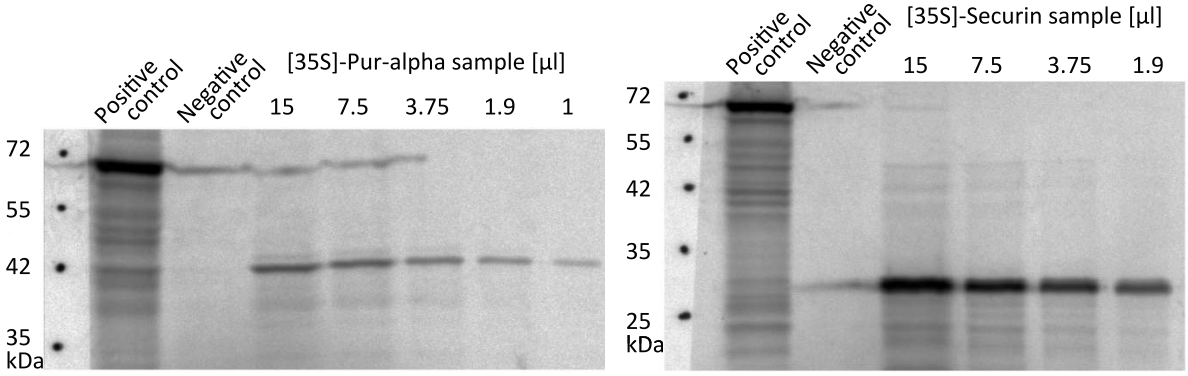

(a) *in vitro* synthesized ^{35}S-Pur-alpha

(b) *in vitro* synthesized ^{35}S-Securin

Fig. 4.33.: Radiation blot of (a) *in vitro* synthesized ^{35}S-Pur-alpha and (b) *in vitro* synthesized ^{35}S-Securin. The linearized and purified pBluescript-SK-Pura plasmid respectively the PCS2-Securin-His8-Sp6 plasmid served as templates for *in vitro* synthesis using the TnT® Coupled Wheat Germ Extract System and the EXPRESS ^{35}S-protein labeling mix. The T7 RNA polymerase was used for Pur-alpha and the SP6 polymerase for Securin synthesis. ^{35}S-Pur-alpha and ^{35}S-Securin were *in vitro* synthesized at 30 ℃ for 90 min (Pur-alpha) or 120 min (Securin). Different amounts of synthesized protein were separated by SDS-PAGE, before exposing the dried gel for 24 hours to a bioimaging plate in the dark and evaluating radioactive signals the next day. A radioactive luciferase protein (Promega) served as positive control, while the negative control consisted of the reaction mixture lacking DNA.

The *in vitro* synthesized Securin was detected at approximately 30 kDa, while for Pur-alpha a signal was obtained at around 43 kDa. The size of endogenous human Securin usually amounts to 22 kDa, while it can vary for *in vitro* synthesized proteins, depending on the location of the RNA polymerase promoter and terminator region on the plasmid. In addition, the Securin protein contains a polyhistidine-tag consisting of eight histidine molecules. Comparison of band

intensities of same amounts of radioactive labeled protein (Figure 4.33 (a) and (b)) revealed a stronger band for ^{35}S-Securin compared to ^{35}S-Pur-alpha. Securin contains more methionine residues, which can be radioactively labeled, than Pur-alpha so that stronger radioactive signals were observed for Securin. For subsequent degradation assay performed, 1 µl of the ^{35}S-Pur-alpha sample was used per sample (per time point). Since 1.9 µl of ^{35}S-Securin sample still displayed a strong radiation, only 0.75 µl was used per sample.

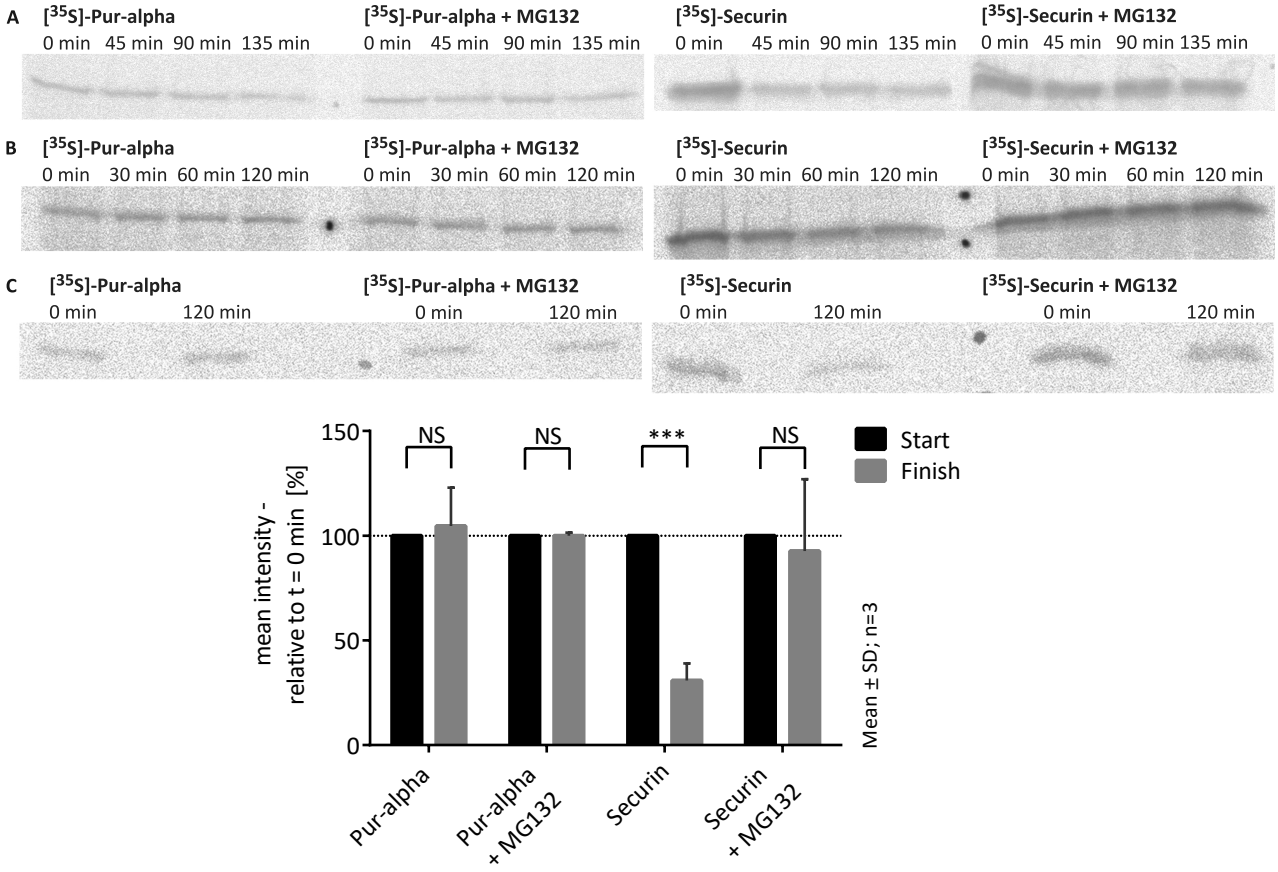

Fig. 4.34.: Degradation assays of *in vitro* synthesized ^{35}S-labeled Pur-alpha and ^{35}S-labeled Securin in HeLa S3 G_1 cell lysates. ^{35}S-Pur-alpha and ^{35}S-Securin were *in vitro* synthesized using the TnT® Coupled Wheat Germ Extract System, followed by the titration of the appropriate protein amount. Labeled proteins were degraded in the presence of HeLa S3 G_1 lysate, ubiquitin-conjugating enzymes, regeneration mix and MG132 (in parts) for 120 min respectively 135 min. SDS-PAGE was performed, before exposing the dried gel to a bioimaging plate in the dark and measuring radioactive signals after 24 hours. The blots depict the result of three degradation experiments (A, B, C) of radioactive-labeled Pur-alpha and Securin using G_1 lysates from two cell cycle synchronization experiments. Signals were densitometrically evaluated, the background signals substracted and normalized to the initial value at the beginning of the reaction using the AIDA Image analyzer software. Mean intensities of the start and the end point of three experiments including standard deviations are plotted in the histogram. As statistical test the unpaired t test was applied (NS = $p \geq 0.05$; *** = $p \leq 0.001$).

Following these preliminary tests, degradation of Pur-alpha and Securin by the APC/C was investigated. For this purpose, the target substrates were mixed together with the HeLa G_1 lysate and appropriate factors, necessary for the formation of the functional APC/C degradation

complex. Four different approaches were set up, including the degradation of Securin and Pur-alpha as well as the degradation inhibition of both proteins by adding the proteasome inhibitor MG132 to confirm the degradation by the APC/C-proteasome pathway. Incubation of the reaction mixture was usually performed for 120 minutes (one experiment for 135 minutes), while samples were harvested at least at the beginning and the end of the experiment. It should be noted that if enough G_1 lysate was available, the reaction was stopped not only at two time points, but at additional time points to better follow the degradation kinetics of Securin and Pur-alpha. Degradation experiments were performed in triplicates with two different HeLa S3 G_1 lysates. The radiation blots obtained are shown in Figure 4.34.

No difference in radioactive signals between the starting and the end point of the degradation reaction was observed for Pur-alpha within three degradation experiments conducted. In the first approach the final mean intensity value amounted 87,04%, whereas for the other experiments the terminal value equaled the initial values or were rather higher, so that the mean intensity accounted 104,65%. This was probably caused by sample evaporation, leading to more concentrated reaction mixtures towards the end of the degradation experiment. Evaluation inaccuracy due to high background noise is also conceivable. Regarding the degradation of Pur-alpha in presence of the proteasome inhibitor MG132 no differences in intensities were observed. In contrary, successful degradation of Securin after incubation with the APC/C could be observed in all experiments lacking the proteasome inhibitor MG132. By analyzing the two experiments conducted with four time points, a strong decline in signal intensity was detectable within the first 30 minutes. Afterwards, the decrease in signal intensity slowed down so that mean intensities at the end of the degradation reaction amounted 30,87% of the initial value (100%). Both reactions containing MG132 showed no difference in initial and final mean intensity (92,71%) values, indicating an inhibition of substrate degradation by the proteasome. It can therefore be concluded that in contrary to Pur-alpha, Securin was degraded by the APC/C and that the proper conditions for degradation of proteins by the APC/C were accordingly given.

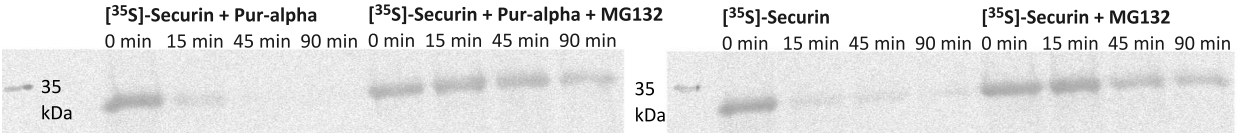

Fig. 4.35.: Radioactive degradation assay of *in vitro* synthesized ^{35}S-labeled Securin in presence of Pur-alpha using HeLa S3 G_1 cell lysate. Using the Reticulocyte Lysate System and the EXPRESS ^{35}S-protein labeling mix ^{35}S-Securin was synthesized. Pur-alpha was synthesized using the TnT® Coupled Rabbit Reticulocyte Lysate System and the amino acid mixture provided by the kit. Degradation of Securin was performed by incubating labeled protein, HeLa S3 G_1 cell lysate, ubiquitin-conjugating enzymes and regeneration mix for 90 min. In parallel, degradation of Securin was performed in presence of equal amounts of *in vitro* synthesized Pur-alpha. The blots depict the degradation of Securin, with or without the presence of MG132 and with or without the presence of Pur-alpha. Radioactive signals were evaluated after 24 hours of exposition to a bioimaging plate in the dark.

Subsequently, the degradation of *in vitro* synthesized ^{35}S-labeled Securin was performed alone and in presence of *in vitro* synthesized Pur-alpha (Figure 4.35) to check for altered APC/C activity in the presence of Pur-alpha. For this purpose, the TnT® Reticulocyte Lysate System was used, which was previously shown to already contain Pur-alpha. Additional not radioactive labeled *in vitro* synthesized Pur-alpha was added in a ratio relative to ^{35}S-labeled Securin of 1:1.

Moreover, approaches were included containing MG132. According to Figure 4.35, Securin was quickly degraded by the APC/C, while in presence of MG132 the degradation of Securin was diminished. Same results regarding the degradation of Securin were obtained in the presence of Pur-alpha. Accordingly, the activity of the APC/C system was not impaired by Pur-alpha.

Flow cytometric analysis of cell cycle synchronized fNS cells Although Pur-alpha proteins possess a strongly conserved structure throughout different organisms and human Pur-alpha likewise possesses the APC/C recognition sites, it it conceivable that the *in vitro* synthesized murine Pur-alpha is only degraded by a system containing murine degradation factors, like murine Cdc20 or Cdh1 specific for Pur-alpha. Additionally, the proteomic approach revealing the ubiquitination sites within Pur-alpha was performed using murine tissue. Thus, in another attempt APC/C and cofactors derived from fetal neural stem (fNS) cells were used to degrade *in vitro* synthesized Pur-alpha and Securin.
Accordingly, G_1 lysate from fNS cells were prepared to perform subsequent degradation of Pur-alpha and Securin. In former experiments performed it became apparent that fNS cells, cultivated in suspension culture, form aggregates and tend to differentiate into progenitor cells. Consequently, fNS cells were cultivated in adherent cell cultures, which unfortunately limited the yield of final G_1 protein extract. Another consequence of low fNS cell numbers was that the flow cytometric analysis was limited to one measurement, the G_1 release, in order to increase the amount of G_1 lysate for the degradation experiment. It should be noted that prior to this measurement, the cell cycle synchronization protocol was established with fNS cells of other passage numbers. The flow cytometric analysis of cell cycle synchronized fNS cells are shown in Figure A.6 in the Appendix.

According to the FSC-A versus SSC-A plot (Figure A.6, Image 1), the fNS cell population represented a quite inhomogeneous population. The forward scatter indicates the size of the cell, while the side scatter indicates the composition or complexity of the cell [Tzur et al., 2011]. Usually dead cells or cell debris feature small forward and side scatters ($< 70 \cdot 10^3$). Cells featuring these characteristics were not considered for further analysis. Moreover, the PI-W versus PI-A plot (Figure A.6, Image 2) revealed that many cells either possessed a single or double chromosome set and that only less doublets (two cohesive cells), but a lot of cell debris was detected. Thus, population P3 was chosen as the population of interest, possessing either a single or a double chromosome set. This included 52,5% of total cells. Cells of the population P3 were further divided into three groups (Population P4, P5 and P6), due to the observed PI-A values. The higher the PI-A value the larger the DNA amount per cell. 24,3% of the cell population was located in G_1 (Population P4), while 23,8% of total cells were still located in G_2 / mitosis (Population P5). In total, 4,2% of all cells were situated in S phase (Population P6).

Comparison of flow cytometer results, obtained by fNS and HeLa S3 cells, revealed that fNS cells reacted more sensitive to the harsh treatment with the cell cycle interfering reagents thymidine and nocodazole. While four hours after the release from the mitosis block 7,4% of total Hela S3 cells were still located in mitosis (Figure A.5), this was the case for 23,8% of total fNS cells (Figure A.6). Nevertheless, 24,3% of total fNS cells were localized in G_1 phase. Besides this, the APC/C is not only active during G_1 phase, but also during the two last stages of mitosis, anaphase and telophase. Accordingly, enough active APC/C should be available to perform degradation of its target proteins.

***In vitro* degradation of Pur-alpha using fetal neural stem (fNS) cell derived G_1 lysate** According to the degradation assays performed with HeLa S3 cell lysates (Figure 4.34), this time fNS cell lysates synchronized in G_1 phase were used to assess the degradation of Pur-alpha and Securin by the APC/C-proteasome pathway. Results are shown in Figure 4.36. In total, two G_1 lysates from fNS cells were produced. Unfortunately, caused by a broken gel during the drying process in the second replicate, only one degradation experiment was suitable for evaluation of APC/C mediated Pur-alpha and Securin degradation.

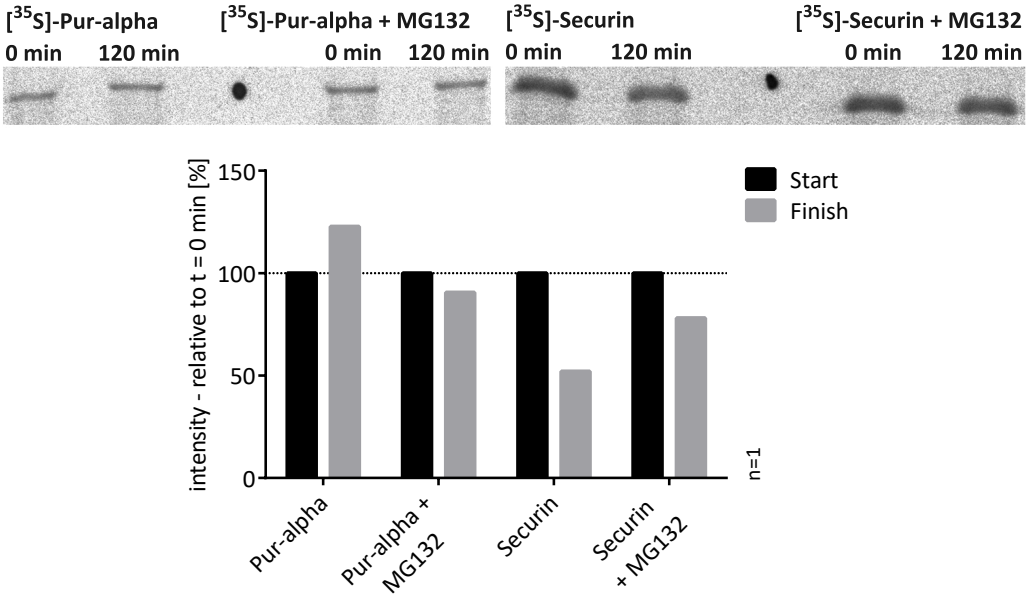

Fig. 4.36.: Radioactive degradation assays of *in vitro* synthesized ^{35}S-Pur-alpha and ^{35}S-Securin using fetal neural stem (fNS) G_1 cell lysate. ^{35}S-Pur-alpha and ^{35}S-Securin were *in vitro* synthesized using the TnT® Coupled Wheat Germ Extract System, followed by the titration of appropriate protein amounts. Degradation of both proteins, with or without the addition of MG132, was performed by incubating labeled protein, fNS derived G_1 lysate, ubiquitin-conjugating enzymes and regeneration mix for 120 min. SDS-PAGE was performed, before exposing the dried gel to a bioimaging plate in the dark and measuring radioactive signals after 24 hours. The blot depicts radioactively labeled Pur-alpha and Securin at the beginning and the end of one degradation experiment. Signals were densitometrically evaluated, subtracted from the background signal and normalized to the initial value (0 min; 100%) using the AIDA Image analyzer software and results were plotted in the histogram.

Likewise to the degradation assay performed with APC/C derived from HeLa S3 cells, no degradation of Pur-alpha was detectable using fNS derived G_1 lysate. Evaluation of Pur-alpha protein amounts using the AIDA software revealed that at the end of the degradation experiment the amount of Pur-alpha had increased to 122% (Figure 4.36 (b)). Probable explanations therefor are sample evaporation during the degradation experiment, leading to more concentrated reaction mixtures towards the end of the experiment or evaluation inaccuracy due to high background noise. Pur-alpha level decreased to 90,52% of the initial protein level in the reaction containing the proteasome inhibitor MG132. The degradation of the APC/C substrate Securin was less distinct compared to former experiments using HeLa S3 G_1 lysate. Nonetheless, degradation was still evident, since at the end of the degradation reaction only 52,04% of the original protein amount (100%) remained. Securin level decreased to 78,06% of the initial protein level

in the reaction containing MG132. Certainly, no final conclusion could be made from one single experiment, but still the experiment indicated that under these conditions Pur-alpha is not degradable by the APC/C.

4.3.4.2. Alteration in Pur-alpha ubiquitination after proteasome inhibition

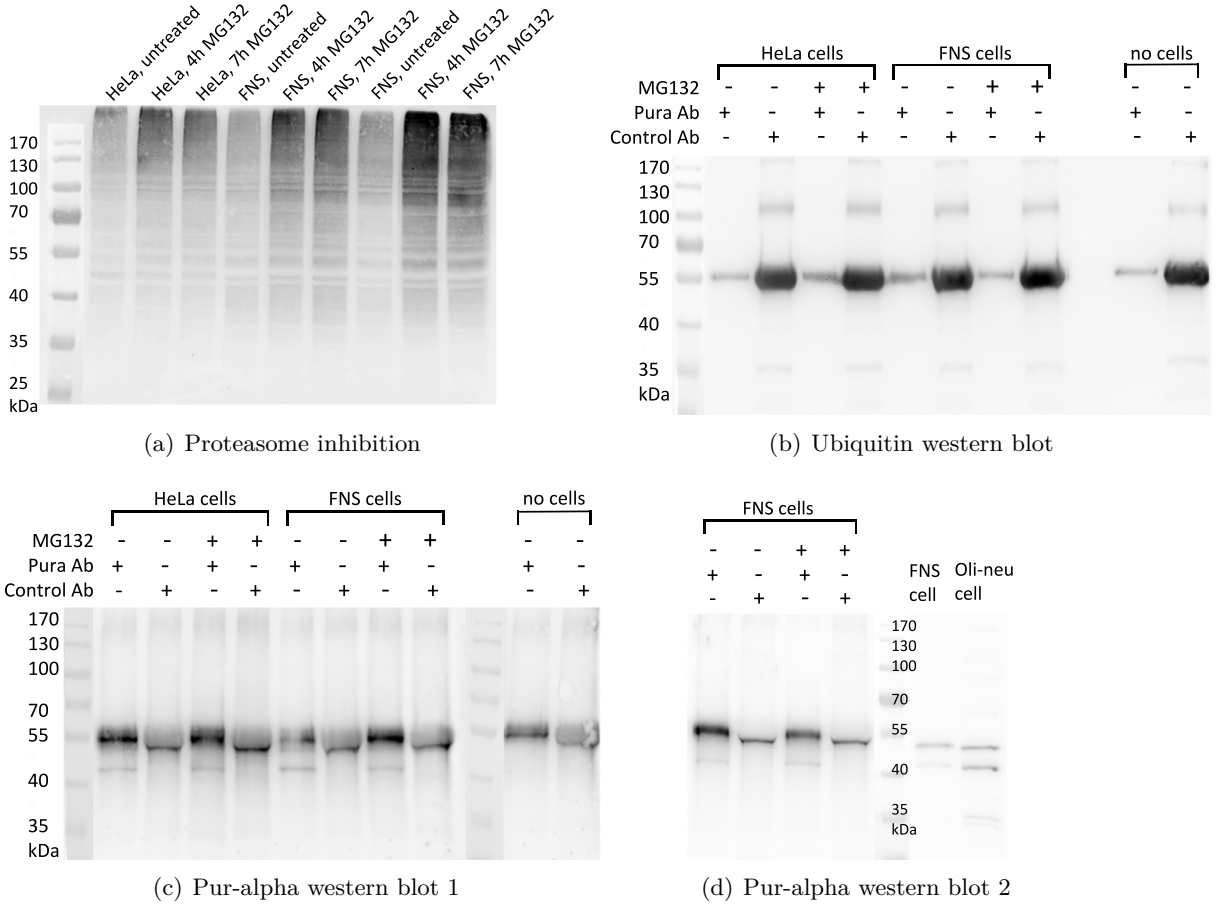

(a) Proteasome inhibition

(b) Ubiquitin western blot

(c) Pur-alpha western blot 1

(d) Pur-alpha western blot 2

Fig. 4.37.: Ubiquitin and Pur-alpha western blots of Pur-alpha immunoprecipitated samples following proteasome inhibition. Western blot (a) of HeLa and fNS cell lysates, untreated and treated with 25 µM MG132 for 4 or 7 h using an ubiquitin (mouse, 1:1,000, 4 ℃, over night) and an α-mouse-HRP antibody (1:5,000; 90 min; RT). HeLa and fNS cell lysates, untreated and treated for 4 h with 25 µM MG132 were immunoprecipitated using the Pur-alpha guinea pig antiserum (Pura Ab) and preimmune serum (control Ab), followed by Sepharose Protein A incubation. Western blot of samples boiled in 4x Lämmli buffer was performed using (b) the ubiquitin and α-mouse-HRP antibody or (c) and (d) the Pur-alpha (ab79936, rabbit; 1:700; 4 ℃, over night) and α-rabbit-HRP antibody (1:5,000; 1 h; RT). Pur-alpha WB using fNS and Oli-neu cells as control. RT = room temperature; + = used; - = not used.

Using an ubiquitin antibody, which detects ubiquitinated proteins, differences in the ubiquitination pattern of Pur-alpha in samples untreated and treated with the proteasome inhibitor MG132 were examined. First, inhibition of the proteasome was tested by inhibiting HeLa and fNS cells for 4 and 7 hours with MG132. The ubiquitin western blot (Figure 4.37 (a)) displays a stronger staining for samples treated with MG132 compared to untreated samples,

so that more proteins were ubiquitinated after the treatment. This implies, that the inhibition of the proteasome was successful. Thereafter, HeLa and fNS cell lysates of samples untreated and treated for 4 hours with MG132 were immunoprecipitated using the Pur-alpha guinea pig antiserum or as control the preimmune serum. A western blot using the ubiquitin antibody was performed to determine ubiquitinated Pur-alpha, while a second western blot was conducted using the commercial Pur-alpha antibody to confirm successful immunoprecipitation of the Pur-alpha protein. The experiment was conducted in a way, that both cell lines were incubated with MG132, while controls were not incubated with MG132, and immunoprecipitated using Pur-alpha antibody and control antibody. In addition, controls containing only guinea pig antiserum and preimmune serum were plotted to determine background signals of the antibodies.

According to (Figure 4.37 (b)) no difference in ubiquitination can be observed between samples incubated with Pur-alpha antiserum and treated with MG132 versus untreated samples. All visible bands seem to derive from the antibodies (according to the antibody controls). The strong bands observed at 55 kDa might be a result of unspecific binding of the purchased Pur-alpha antibody to the IgG heavy chain, although the secondary antibody was raised against mice. Pur-alpha immunoprecipitation was successful, according to Figure 4.37 (c) and (d). FNS and Oli-neu cell lysates served as control and polypeptides with a molecular size of around 43 kDa and 50 kDa were detected. Likewise, only in samples immunoprecipitated with the Pur-alpha antiserum a polypeptide at 43 kDa was detected.

4.3.5. Identification of Pur-alpha interaction partners

So far, only few proteins have been identified to interact with Pur-alpha. However, as a transcription factor, Pur-alpha regulates the expression of multiple proteins and besides this it plays a role in several biological processes. Using two different approaches, the BioID (proximity-dependent biotin identification) assay (Subsection 4.3.5.2) and the co-immunoprecipitation assay (Subsection 4.3.5.3), the identification of probable Pur-alpha interaction partners was attempted.

4.3.5.1. Cloning, verification of expression and functionality of BirA*-Pura

First of all, the BirA* (myc-BioID) and BirA*-Pura constructs were cloned and the expression and the functionality of both was verified. BirA*- and Pura-sequences with compatible restriction sites were amplified by PCR and subcloned into a vector containing a RSV-promoter by triple ligation. The Pura-sequence was thereby introduced downstream of the BirA*-sequence. The control vector in contrary only contained the BirA*-part. The amplification of Pur-alpha and the BirA* sequence by PCR was confirmed by agarose gel (Appendix: Figure A.7 (a)), showing one PCR product at 966 bp for Pur-alpha and at 993 bp for BirA*. Restriction digest of the BirA*-Pura construct (Figure A.7 (b)) and the BirA* construct (Figure A.7 (c)) as well as sequencing analyses confirmed the successful transformation of some clones.

First, HEK293T cells were transiently transfected with the BirA*-Pura (G0656pFIV3.2RSVmcs-Pura-mycBioID) construct (plasmid card can be found in the Appendix F.1) and the BirA*-mock (G0656pFIV3.2RSVmcs) construct. After incubation for 24 hours in transfection medium, fresh medium including biotin was added and cells were harvested 24 hours later to confirm successful transfection by Streptavidin and Pur-alpha western blot. The strepativdin-HRP

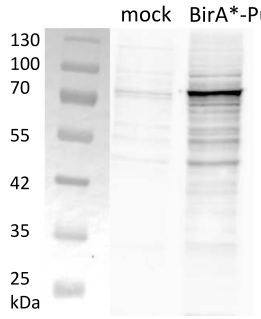

(a) Streptavidin-HRP western blot

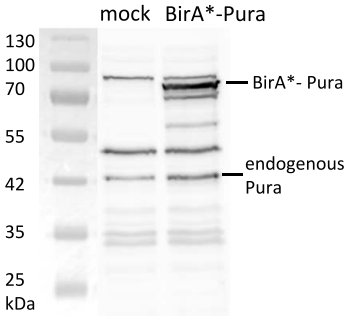

(b) Pur-alpha western blot

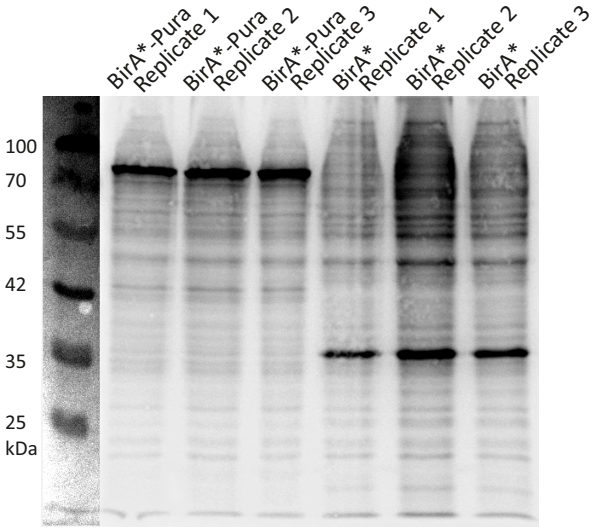

(c) Streptavidin-HRP-Western blot

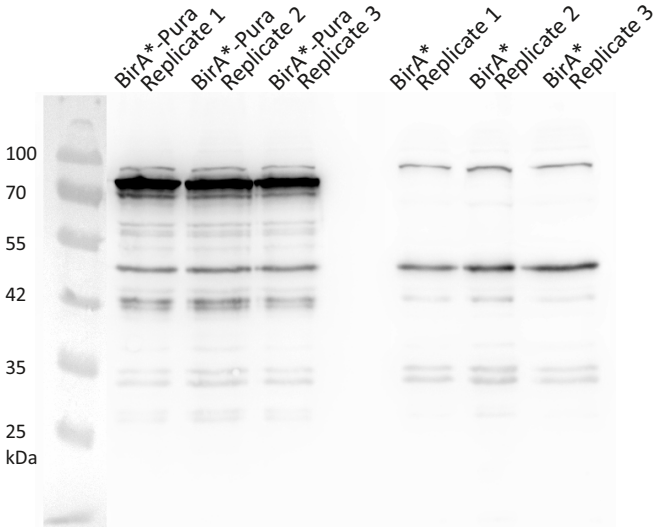

(d) Western blot against Pur alpha

Fig. 4.38.: Streptavidin and Pur-alpha western blot of Mock, BirA* and BirA*-Pura transfected HEK293T cells. HEK293T cells were transfected with either mock or BirA*-Pura constructs (a, b) using TurboFect, while three replicates of HEK293T cells, grown in either SILAC light or heavy medium, were transfected with either BirA*-Pura- or BirA*-construct (c, d) for 24 hours. Cells were washed and incubated with fresh medium and 10% FCS or SILAC medium and 10% SILAC-FCS and biotin (final concentration 50 µM) for 24 hours. Cells were harvested, lyzed and proteins were separated by SDS-PAGE and semi-dry blotted. Blots were blocked with 2.5% BSA, 0.4% Triton X-100 in PBS (Streptavidin WB) or 5% filtered skim milk in TBS-T (Pura WB) and incubated with either Streptavidin-HRP ab (1:10,000; 1 h; RT) or Pur-alpha ab79936 (1:700; 4 ℃; over night) and ∝-rabbit-HRP ab (1:5,000; 1 h; RT). Blot (a) depicts the results of HEK293T cell transfection with mock and BirA*-Pura using the streptavidin ab and (b) the Pur-alpha ab. Blot (c) depicts the SILAC-HEK293T cell transfection with BirA* and BirA*-Pura using the streptavidin ab and (d) the Pur-alpha ab. ab = antibody; SILAC = Stable Isotope Labeling by Amino Acids in Cell Culture; FCS = fetal calf serum; RT = room temperature.

antibody detects biotinylated proteins. The Streptavidin-HRP WB for BirA*-Pura detected a polypeptide at around 75 kDa (determined using the Fusion software), which might correspond to the size of the BirA*-Pura protein (78 kDa), besides many slightly detected polypeptides (Figure 4.38 (a)). In contrary, no distinct proteins were detected in the western blot of the

mock transfected sample. Successful transfection and expression of the BirA*-Pura protein was evidenced by WB using the anti-Pur-alpha antibody. A polypeptide at 78 kDa was detected which corresponds to the size of the BirA*-Pura fusionprotein (determined using the Fusion software) (Figure 4.38 (b)). Endogenous Pur-alpha was observed in both samples at around 42 kDa.

Thereafter, HEK293T cells were transiently transfected with either the BirA*-Pura construct or the BirA*-control construct (G0656pFIV3.2RSVmcs-mycBioID) in triplicates to assess expression and functionality of both constructs. The Streptavidin-HRP WB (Figure 4.38 (c)) confirmed the transfection of cells with both constructs, as well as the expression and functionality of BirA*-Pura and BirA*. In the samples transfected with the BirA*-Pura vector a polypeptide was detected at around 76 kDa, which nearly correlates with the expected size of the BirA*-Pura protein. On the other hand, in the samples transfected with the control vector a polypeptide was detected at around 36 kDA, corresponding to the size of the myc-BioID protein. Proteins containing the active biotin ligase usually exhibit the strongest biotinylation in comparison to other proteins. Multiple polypeptides with same sizes were detected in the BirA*-Pura sample and the BirA* sample, emerging two possible assumptions. One possible explanation could be that both proteins were localized in the same cell compartment and therefore same proteins were biotinylated. Since expression of the BirA* protein (myc-BioID) usually occurs in the cytoplasm and nucleoplasm, this could also be conceivable for the BirA*-Pura protein. Investigations performed by other research groups revealed a mainly cytoplasmic localization of Pur-alpha, while during distinct cell cycle stages Pur-alpha is translocated into the nucleus [Barr & Johnson, 2001]. Another explanation would simply be the detection of biotinylated endogenous proteins. Although biotinylation in all three BirA*-Pura samples seemed to be consistent, replicate two of the BirA* experiment exhibited a more effective biotinylation of proteins compared to the other replicates, but still detected proteins of same sizes, according to the band pattern observed. The anti-Pura-HRP-WB (Figure 4.38 (d)) further confirmed the expression of fused Pur-alpha in the BirA*-Pura samples (77 kDa), but not in the BirA*-samples. Endogenous Pur-alpha was detected in both experiments at 42 kDa, although higher amounts were detected in the BirA*-Pura samples. Since same protein amounts were applied for all samples it can be assumed that a cleavage of the fusion protein into the Pur-alpha protein and the myc-BioID protein caused the higher Pur-alpha amounts in the BirA*-Pura samples.

4.3.5.2. Detection of Pur-alpha-interacting proteins using the BioID approach

Identification of Pur-alpha interaction partners was achieved by applying the BioID assay in combination with the SILAC method. The BirA*-Pura construct consisted of a permanently active biotin-ligase mutant from E.coli (BirA*), fused to the bait protein, Pur-alpha, while the control construct only consisted of the BirA* sequence. The expressed biotin-ligase specifically biotinylates proteins, located in the vicinity of the bait protein, allowing for screening of interaction partners after selective enrichment with NeutrAvidin agarose. Using the SILAC (Stable Isotope Labeling by Amino Acids in Cell Culture) [Roux et al., 2012] approach, sample and control sample were metabolically labeled with light or heavy isotope labeled amino acids. This allows for the combined measurement of differentially labeled sample and control sample by LC-MS/MS and for subsequent relative quantification of proteins.
Accordinlgy, HEK293-T cells, labeled with light isotope labeled amino acids (SILAC light), were transfected with the BirA* construct, while HEK293-T cells, labeled with heavy isotope

labeled amino acids (SILAC heavy), were transfected with the BirA*-Pura construct. Thereafter, biotin was added to enable biotinylation of proteins and samples were harvested and lyzed after 24 hours. To selectively purify biotinylated proteins among all other proteins, samples were incubated with NeutrAvidin Agarose beads, followed by tryptic on-bead digestion to overcome the strong binding of proteins to NeutrAvidin, which would prevent complete sample elution. Digested peptides were extracted the next day, followed by sample combination of samples labeled with light and heavy isotope labeled aminoacids and subsequent sample fractionation using self-made strong anion exchange (SAX) tip-columns [Wiśniewski et al., 2009], before applying samples to LC-MS/MS. The acquired data were analyzed using MaxQuant for identification and quantification of proteins. To minimize the detection of false positives only proteins were considered which exhibited valid values in at least two replicates. Using Perseus [Tyanova et al., 2016], intensities were log2 transformed and SILAC heavy to SILAC light ratios (log2 fold change) were calculated and statistically evaluated by applying a one-sample-t-test against 0. Finally, the threshold for revealing significant and relevant interaction partners was set to a log2 fold change > 0.585 (fold change > 1.5) and a p-value < 0.05.

Altogether, 1,293 proteins were identified and quantified with valid values in at least two replicates by the SILAC-BioID assay using the workflow shown in Figure 4.39 (a). After application of statistical tests, 87 proteins remained, which exhibited at the same time a sufficient degree of enrichment and a good level of confidence. Thus, proteins showing both features were considered as possible and promising Pur-alpha interaction partners and thirty proteins featuring highest log2 fold change ratios were depicted in Table 4.7 with their respective log2 fold change values and -log10 p-values. The complete table can be found in the Appendix (Table A.1).
The volcano plot was further used to visualize proteins by their log2 fold change values and -log10 p-values. Obviously, proteins were equally contributed by BioID-Pura and control sample, indicated by the approximation of most proteins to a log2 fold change of 0. Proteins, simultaneously exhibiting high values of enrichment and high confidence values are labeled in blue. The blue dot at the right side of the plot belongs to Pur-alpha, the bait protein. Expectantly, the high degree of enrichment was not surprising, since transfection of cells with the BirA*-Pura construct resulted in an overexpression of the Pur-alpha protein.

Due to Pur-alphas function as a RNA- and DNA-binding protein and its involvement in DNA replication and gene expression regulation, it was not surprising to identify proteins which are mainly involved in these processes (Table 4.7). For instance, this was applicable to proteins exhibiting high log2 fold change values and low p-values, including EBNA1BP2 (probable rRNA-processing protein EBP2), PABPC1 (polyadenylate-binding protein 1) or LSM14A (protein LSM14 homolog). Consistent with the already investigated regulatory function of Pur-alpha in viral processes [Gallia et al., 2000a], many proteins involved in this process were identified using the Bio-ID assay (red labeled proteins). A strong and confident interaction of Pur-alpha could also be shown for the proteins DDX3 (ATP-dependent RNA helicase DDX3), STAU1 (double-stranded RNA-binding protein staufen homolog 1) and ZC3HAV1 (zinc finger CCCH-type antiviral protein 1).
It should be noted that with MAD2L1 (mitotic spindle assembly checkpoint protein MAD2A) only one protein involved in APC/C^{Cdc20} mediated degradation of mitotic proteins (GO term) was identified within the group of probable Pur-alpha interaction partners. With the protein ANAP16 (anaphase-promoting complex subunit 16) a component of the APC/C complex and

with PSMA5 (proteasome subunit alpha type-5) a component of the proteasome complex was detected, albeit the proteins failed the one-sample-t-test and were thus not significantly enriched.

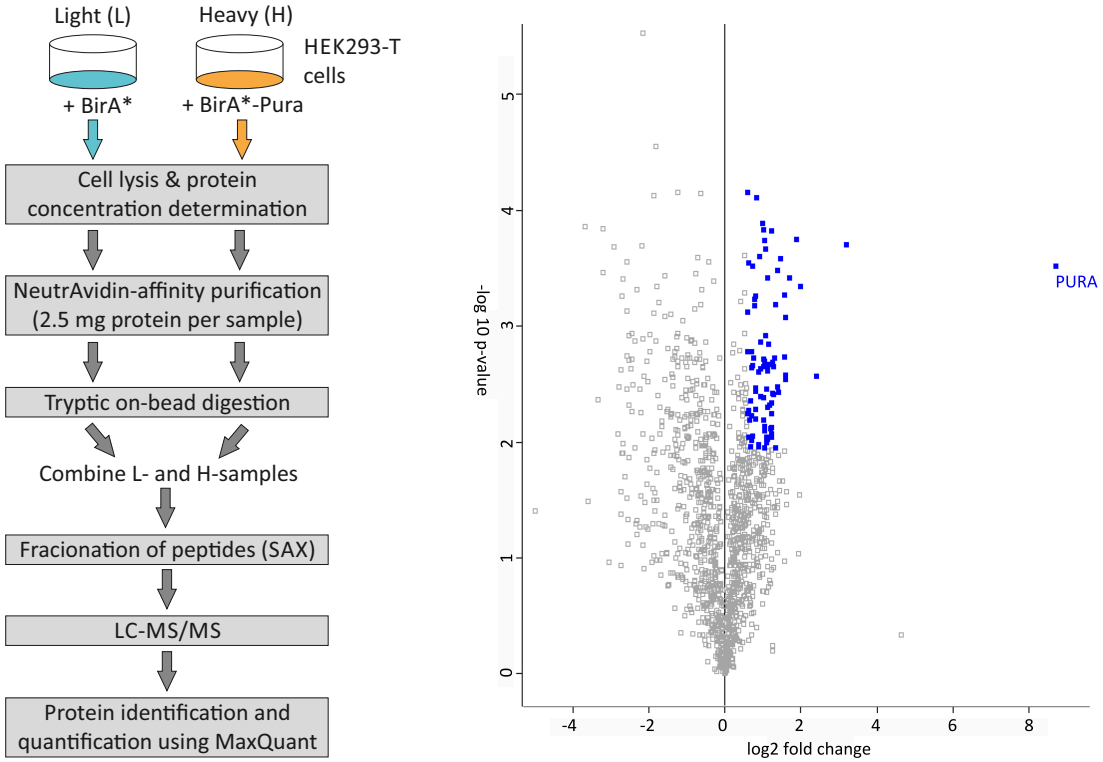

(a) BioID workflow

(b) Volcano plot of identified proteins

Fig. 4.39.: Identification of Pur-alpha interaction partners using the SILAC-BioID-Pura assay. The workflow (a) was applied to three replicates: HEK293T cells, cultivated in SILAC heavy (H) medium, were transfected with the BirA*-Pura plasmid and HEK293T cells, cultivated in SILAC light (L) medium, were transfected with the BirA*-construct using TurboFect for 24 h. Fresh medium including biotin (final concentration 50 µM) was added for 24 h prior to cell harvest and lysis. NeutrAvidin affinity purification was performed with 2.5 mg of protein per replicate, followed by tryptic on-bead digestion and extraction of biotinylated proteins. Always one SILAC light and heavy sample was combined, desalted via solid phase extraction and peptides were separated by strong anion exchange chromatography. Samples were analyzed by LC-MS/MS and data evaluated using MaxQuant. Using Perseus, intensities were log2 transformed, normalized to the median of each replicate and statistically analyzed by applying a one-sample t-test against 0, assuming normally distributed data (tested by visualizing H / L ratios). In the volcano plot (b) all proteins featuring valid values in at least two replicates are depicted according to their mean log2 fold change values (x-axis) and -log10 p-values (y-axis). Blue labeled proteins exhibit a log2 fold change ≥ 0.585 and a false discovery rate adjusted p-value of ≤ 0.05 (-log10 p-value ≥ 1.901).

To further characterize the potential interaction partner regarding their biological processes, molecular functions and cellular localization, GO enrichment analyses using the GOrilla tool were conducted (Figure A.8 (Appendix)). The target list, consisting of the 87 significantly enriched proteins, was searched against the background list, containing all identified proteins among three experiments (identified by MaxQuant).
All enriched GO terms within the category of biological processes were related to either mRNA stabilization or regulation of viral genome replication and regulation of posttranscriptional re-

Table 4.7.: Significantly enriched protein groups in BirA*-Pura samples. The evidence files (MaxQuant) of three BioID experiments were processed using Perseus. Proteins were filtered for potential contaminants, positive reverse sequences and for proteins, which featured valid values in less than two replicates. SILAC heavy to light ratios were calculated, log2 transformed and normalized to the median of every replicate. The one-sample t-test against 0 in combination with the Benjamini Hochberg correction was applied. Proteins featuring a false discovery rate adjusted p-value ≤ 0.05 and a log2 fold change ≥ 0.585 were considered as interaction partner and arranged according to the log2 fold changes, starting with the highest value. Proteins involved in viral genome replication regulation are labeled in red (determined using GOrilla). Always one protein of a protein group is mentioned in the list.

No	Gene	log2 fold change	-log10 p-value	No	Gene	log2 fold change	-log10 p-value
1	PURA	8.6992	3.5170	16	SACM1L	1.3405	3.1865
2	EBNA1BP2	3.2086	3.7015	17	FUBP3	1.3239	1.9497
3	YBX1	2.4169	2.5700	18	SLC25A3	1.3079	2.7238
4	PABPC1	1.9877	3.3395	19	MTHFD1L	1.2737	2.4145
5	LSM14A	1.8750	3.7466	20	YTHDC2	1.2720	2.6497
6	DDX17	1.6964	3.4189	21	FXR2	1.2631	2.6908
7	PABPC4	1.6072	2.5776	22	PAIP2	1.2483	2.4163
8	IGF2BP1	1.6019	3.0758	23	HNRNPR	1.2415	3.8242
9	PCBP2	1.5982	2.5423	24	TIMM50	1.2409	2.0455
10	CSDE1	1.5748	3.2648	25	TM9SF3	1.2390	2.3339
11	NDUFA10	1.5616	2.7322	26	NUFIP2	1.2369	2.0671
12	ZC3HAV1	1.4807	3.5823	27	STAU1	1.2348	2.2456
13	YIPF1	1.4157	2.4318	28	PHB	1.2294	2.1218
14	MRPS18B	1.4023	3.4778	29	GNAI1	1.2105	2.1141
15	TRAP1	1.3770	2.4765	30	STT3A	1.1695	2.3154

spectively translational processes (Figure A.8). Enriched GO terms in the ontology of molecular functions are assigned to the three parent terms ”binding”, ”translation regulator activity” and ”catalytic activity”. However, most enriched GO terms are associated with the term ” RNA binding”, a molecular function carried out by 55 out of 87 proteins identified. The overrepresentation of the GO terms ”eukaryotic initiation factor 4E binding”, ”poly(A) binding” and ”RNA helicase activity” further underlined the function of the detected proteins in the translation process. Enriched GO terms in the ontology of cellular components revealed two main localizations, namely ribonucleoprotein granules and mitochondrial membranes. Interestingly, many Pur-alpha interaction partners were localized in cytoplasmic stress granules.

4.3.5.3. Co-immunoprecipitation (co-IP) using Pur-alpha antibody

In the second approach mass spectrometry based quantitative proteomics was applied to identify proteins co-immunoprecipitating together with Pur-alpha in two cell lines. For this purpose, fNS cells and Oli-neu cells were cultivated in triplicates, harvested and directly lyzed under non-denaturing conditions to retain physiological protein-protein interactions. Cell lysates were first incubated with the anti-Pur-alpha guinea pig serum overnight, followed by incubation with Protein A Agarose to capture interacting proteins and bait protein complexes. Since nonspecific binding of proteins to Agarose molecules is most likely, control samples were conducted in parallel, consisting of cell lysate, guinea pig preimmune serum and Protein A Agarose. Because of limited preimmune serum less amounts of preimmune serum was used compared to Pur-

alpha antiserum. A western blot against Pur-alpha was performed to confirm the successful immunoprecipitation (IP) of Pur-alpha and to determine positive IP fractions, before analyzing IP and control samples by quantitative mass spectrometry.

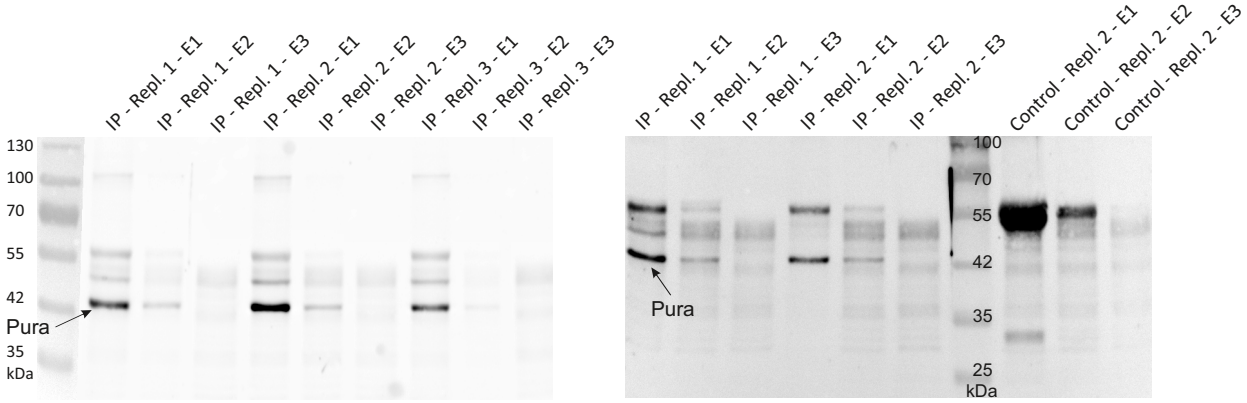

(a) Pur-alpha WB of Pur-alpha-IP samples (Oli-neu cells) (b) Pur-alpha WB of Pur-alpha-IP samples (fNS cells)

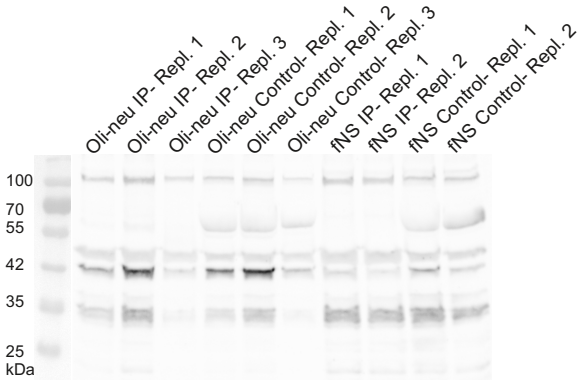

(c) Pur-alpha WB of flow-throughs

Fig. 4.40.: Pur-alpha western blots of Oli-neu cell and fNS cell samples, immunoprecipitated using Pur-alpha antiserum. Oli-neu cells (3 replicates) and fNS cells (2 replicates) were harvested by cell lysis. Next, 3 mg cell lysate was mixed with either 500 µl Pur-alpha antiserum or 100 µl preimmune serum (control), incubated overnight in an overhead-shaker at 4 ℃, followed by incubation with pre-cleared 140 µl Protein A Agarose for 3 h at 4 ℃. Samples were transferred onto micro-spin columns and flow-throughs collected. Samples were washed several times, incubated at 95 ℃ for 5 min and eluted 3x (E1, E2, E3) with 4X Lämmli buffer. 5 µl of every fraction and 20 µl of the flow-throughs were used for WB analyses. Samples were blocked with 5% filtered skim milk in TBS-T and incubated with Pur-alpha ab79936 (1:700, rabbit, 4 ℃, over night) and α-rabbit-HRP (1:5,000, 1 h, room temperature). Figure (a) depicts the WB of the IP eluates of three Oli-neu replicates, while (b) depicts the WB of the IP eluates of two fNS replicates and the control eluates of one replicate. WB (c) indicates the flow-throughs of all replicates, Oli-neu and fNS cells. WB = western blot; IP = immunoprecipitation; Repl. 1/2/3 = Replicate 1/2/3; E1/E2/E3 = eluate 1/2/3.

The Pur-alpha western blot, shown in Figure 4.40 (a) and (b), confirmed the successful IP of Pur-alpha (43 kDa) in Oli-neu cell and fNS cell samples. The protein was almost completely eluted within the first elution step, while less protein was detected in fraction two and none in fraction

three. In contrary, the exemplary control sample (Figure 4.40 (b)) detected only two proteins at $\sim$ 55 kDa respectively 30 kDa, which most likely represented the light and heavy immunoglobulin chain. It should be noted that although a commercial Pur-alpha antibody in combination with a secondary antibody against rabbit was used for WB, the polyclonal secondary antibody seemed to detect fragments of the self-made guinea pig antibody used for the IP. However, according to the Pur-alpha WB (Figure 4.40 (c)) performed with the flow-throughs, taken prior to the washing and elution steps, a polypeptide was detected at around 42 kDa in the Oli-neu replicate 2. This leads to the assumption that a part of the Pur-alpha protein did not bind to the Protein A Agarose and was thus not considered for subsequent mass spectrometry analysis conducted (Subsection 4.3.5.4). According to Figure 4.40 (a), larger amounts of Pur-alpha were present in replicate 2 compared to the other two replicates, so that most probably the binding capacity of Protein A Agarose was exceeded or the amount of Pur-alpha antiserum was insufficient. It should be noted that protein amounts in eluates and flow-throughs cannot be compared with each other, since different sample volumes were applied. Usually, one would expect Pur-alpha in the flow-through of the control samples. Since in the elution fraction no Pur-alpha was however detected, most probably Pur-alpha was removed during the six washing steps. For further analyses only IP elution fraction 1 and 2 were considered.

4.3.5.4. Identification of Pur-alpha interaction partners using an affinity capture-mass spectrometry approach

The identification of Pur-alpha associated proteins was performed in triplicates using fetal neural stem (fNS) cells and Oli-neu cells. FNS cells and neurospheres as well as Oli-neu cells and oligospheres share similar cellular features. fNS cells possess the ability to perform symmetrical self-renewing and to differentiate into neuronal and glial cells. Moreover, fNS cells do not feature the cell heterogeneity of neurospheres, which composition of stem and progenitor cells is variable, depending, for example, on culture conditions. The Oli-neu cell line displays the properties of oligodendrocyte precursor cells (OPCs). In contrary to oligospheres, which develop from neurospheres and exhibit a higher cellular complexity, Oli-neu cells represent a more defined cell population. Finally, the cultivation and maintenance of cell lines is easier than the one of primary cells so that fNS and Oli-neu cells were used instead.

Accordingly, probable interaction partners of Pur-alpha were determined in a clearly defined culture of neural stem cells and in a clearly defined culture of OPCs. The affinity capture-mass spectrometry approach consisted of the pull-down of Pur-alpha and its interacting proteins with a Pur-alpha antibody and subsequent identification and quantification of those proteins by mass spectrometry. The workflow applied is shown in Figure 4.41. Co-immunoprecipitation (co-IP) was performed using the guinea pig antiserum against Pur-alpha (target-IP) or the guinea pig preimmune serum (control-IP). Protein A Agarose, which specifically binds to immunoglobulines, was used to purify Pur-alpha and its interacting proteins. Multiple washing steps were performed to eliminate proteins loosely bound to the bait complex. After sample elution, samples were applied to SDS-PAGE to separate proteins from agarose, which in turn was retained in the stacking gel and from smaller molecules, which migrate faster through the SDS-polyacrylamide matrix. SDS-PAGE was stopped as proteins started to separate in the separation gel.
Quantification was achieved by labeling three replicates of target-IP samples and control-IP samples with TMTsixplex™ and computing log2 ratios of target-IP to control-IP sample inten-

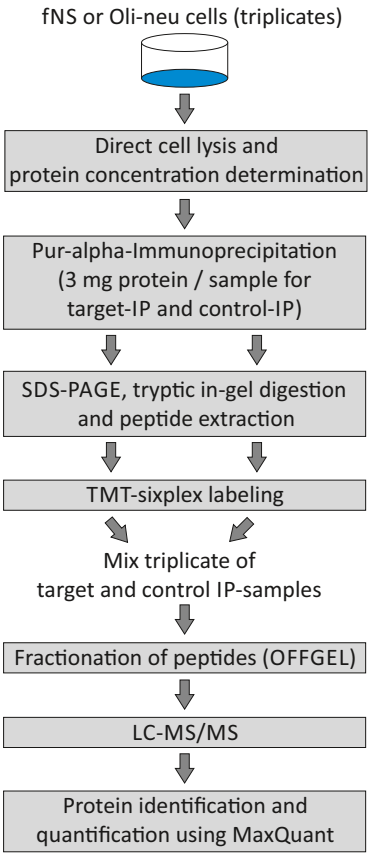

(a) Affinity capture-MS workflow

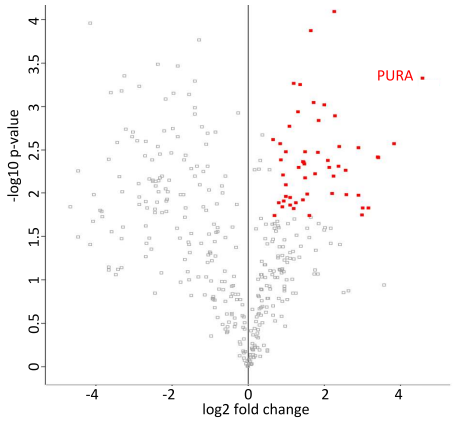

(b) fNS cells - Pur-alpha co-IP assay

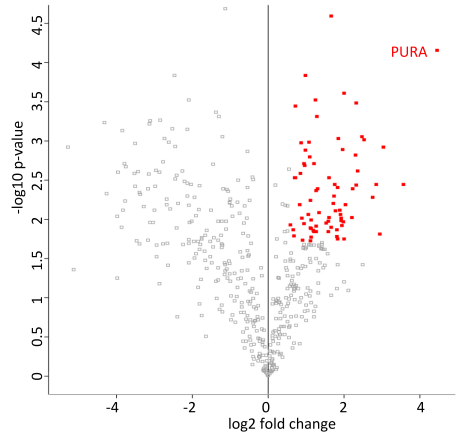

(c) Oli-neu cells - Pur-alpha co-IP assay

Fig. 4.41.: Identification of Pur-alpha interaction partners in fNS and Oli-neu cells by affinity capture mass spectrometry. Three replicates of fNS and Oli-neu cell lysates were incubated with Pur-alpha antiserum (target-IP) or preimmune serum (control-IP) and then with pre-cleared Protein A Agarose. Samples were washed and eluted three times with 4X Lämmli buffer. SDS-PAGE of the first two eluates was stopped after proteins ran for a short distance in the separation gel. Appropriate gel regions were cut out, digested with trypsin and peptides extracted. Three target and control samples were labeled using TMTsixplex™ reagents, combined to one sample and fractionated. Data were acquired using the LTQ Orbitrap Velos and data analysis was done using MaxQuant and Perseus. Positive reversed hits and potential contaminants were removed. Intensities of proteins featuring valid values in at least two replicates were log2 transformed, normalized to the median per replicate and target-IP to control-IP ratios were evaluated using the one-sample t-test against 0. Every dot in the volcano plot of fNS (b) and Oli-neu (c) cells depicts a protein with its log2 fold change (x-axis) and -log10 p-value (y-axis). Proteins featuring a -log10 p-value ≥ 1.901 and a log2 fold change ≥ 0.585 are labeled in red.

sities. This ratio was further termed as log2 fold change and was statistically evaluated using a one-sample t-test against 0. Moreover, only proteins displaying valid values in at least two replicates were included in the statistical analysis. Proteins identified using the fNS cell affinity capture-MS approach are depicted in the volcano plot together with their log2 fold changes and -log10 p-values (Figure 4.41 (b)), while proteins which were identified in Oli-neu cells are shown

in the volcano plot in Figure (4.41 (c)). Proteins, which feature a false discovery rate adjusted p-value ≤ 0.05 (-log10 p-value ≥ 1.901) and a fold change ≥ 1.5 (log2 fold change ≥ 0.585) were considered as probable interaction partner of Pur-alpha.

4.3.5.5. Identification of Pur-alpha interaction partners in fNS cells

Altogether, 390 proteins were identified with valid values in at least two fNS cell replicates. After statistical analysis, the definition of an adequate confidence level (FDR adjusted p-value < 0.05) and a sufficient degree of enrichment (log2 fold change ≥ 0.585), 53 significantly enriched proteins remained. These proteins are signed as red colored dots in the scatter plot, shown in Figure 4.41 (b). Usually, most of the non-interacting proteins should cluster around a log2 fold change of 0, applicable to many proteins in this experiment. Nevertheless, some proteins existed which possessed large negative log2 fold change values, indicating a strong binding of these proteins to the Protein A Agarose matrix. Though the bait protein Pur-alpha showed the highest fold change and at the same time a high level of confidence, there were some other proteins displaying a better confidence level alongside with a good enrichment score, including DDB1 (DNA damage-binding protein 1) or MYEF2 (myelin expression factor 2). A listing of the top 30 significantly enriched proteins can be found in Table 4.8, while the complete list can be found in the Appendix (Table A.2).

Table 4.8.: Significantly enriched protein groups in fetal neural stem (fNS) cells, identified using an affinity capture-mass spectrometry approach. The evidence files (MaxQuant) of three replicates were processed using Perseus. Potential contaminants, positive reverse sequences and proteins, which featured valid values in less than two replicates were removed. Target IP (Pur-alpha antiserum) to control IP (preimmune serum) ratios were calculated, log2 transformed and normalized to the median per replicate. The one-sample t-test against 0 in combination with the Benjamini Hochberg correction was applied. Proteins featuring a false discovery rate adjusted p-value ≤ 0.05 and a log2 fold change ≥ 0.585 were considered as interaction partner and arranged according to the log2 fold changes, starting with the highest value. Proteins involved in viral genome replication regulation are labeled in red (determined using GOrilla). Always one protein of a protein group is mentioned in the list.

No	Gene	log2 fold change	-log10 p-value	No	Gene	log2 fold change	-log10 p-value
1	Pura	4.5644	3.3275	16	Ncbp1	2.2317	2.1936
2	Ybx1	3.8184	2.5719	17	Hnrnpa0	2.2107	1.9957
3	Ikbkg	3.4192	2.4118	18	Syncrip	2.1246	2.2947
4	Chuk	3.4002	2.4189	19	Purb	2.0958	2.3794
5	Ikbkb	3.1568	1.8311	20	Larp4	1.9912	3.0212
6	Ncl	3.0083	1.8287	21	Rbmx	1.8563	2.8392
7	Hnrnpab	2.9791	1.7459	22	Sec13	1.8328	2.4719
8	Hnrnpdl	2.8973	2.5253	23	Igf2bp3	1.7522	2.2202
9	Upf1	2.8892	1.9760	24	Fmr1	1.7200	3.0476
10	Elavl1	2.5820	1.9843	25	Myef2	1.6405	3.8744
11	Ilf2	2.5506	2.2601	26	Tardbp	1.6098	1.7426
12	Ssb	2.3810	2.5369	27	Rps4x	1.5572	1.9912
13	Larp1	2.3790	2.3066	28	Rps3a	1.4983	2.4753
14	Prkar2a	2.2838	2.8890	29	Hnrnpu	1.4924	2.1740
15	Ddb1	2.2492	4.0952	30	Elavl2	1.4706	2.3336

The top ranked proteins regarding the enrichment value were mainly related to the NF-κB signaling pathway, like IKBKG (NF-κB essential modulator), CHUK (inhibitor of nuclear factor kappa B kinase subunit alpha) and IKBKB (inhibitor of nuclear factor kappa B kinase subunit beta). Besides these proteins, the protein YBX1, already detected in the BioID experiment, was highly enriched. Moreover, many proteins belonging to the family of heterogeneous nuclear ribonucleoproteins (hnRNPs) represented probable Pur-alpha interaction partners. For example, the single-stranded and double-stranded DNA and RNA-binding proteins HNRNPAB (heterogeneous nuclear ribonucleoprotein A/B) and HNRNPD (heterogeneous nuclear ribonucleoprotein D0), to name but a few of the highest enriched ones. Additionally, many proteins belonging to the ribosomal subunits S40 and S60 were enriched, including RPL11 and RPS3a as well as DEAD box (Ddx) proteins, which regulate gene expression levels [Linder & Jankowsky, 2011].
Some significant proteins identified in this experiment have already been detected in previous researches. This applies to YBX1 [Kelm et al., 1999], which was also detected in the BioID assay, FMR1 (synaptic functional regulator FMR1) [Ohashi et al., 2002], PURB (transcriptional activator protein Pur-beta) [Kelm et al., 1999] and MYEF2 (myelin expression factor 2) [Muralidharan et al., 1997].
No significant connection to proteins of the ubiquitin-proteasome pathway were identified in this approach. Nevertheless, few subunits of the proteasome complex, like PSMA2, PSMA6 (proteasome subunit alpha type-2 and type-6) and PSMC1 (26S proteasome regulatory subunit 4) were identified within the not-significantly enriched group of proteins.

GO enrichment analyses were performed to characterize the potential Pur-alpha interaction partners regarding their function and localization in fNS cells. The histograms depicting enriched GO terms can be found in the Appendix (Figure A.9). Most enriched GO terms within the category of biological processes are associated with viral regulatory processes, like the highest enriched GO term "regulation of viral genome replication" or "regulation of viral life cycle". Moreover, GO terms related to RNA metabolism, including "RNA splicing" and "mRNA processing" represented a second major group of enriched GO terms. In addition, many probable Pur-alpha interaction partner were involved in the regulation of gene expression. In the ontology "molecular function" all enriched GO terms identified can be summarized by the parent GO term "binding". Especially the GO term "nucleic acid binding" was strongly enriched. Although the GO term "DNA binding" was enriched, most proteins identified preferentially bind to RNA molecules and indicated by the enriched GO terms "poly(A) RNA binding" and "mRNA 3'UTR binding" also to posttranscriptional modified RNA molecules. Interestingly, results are mainly consistent with GO term enrichment analyses performed with proteins identified using the BioID approach (Figure A.8).
In the ontology cellular component, only the GO term "ribnonuclear complexes" was enriched in both analyses. Moreover, many probable interaction partners were localized in nucleus associated regions, including "spliceosomal complexes" and "iκB kinase complexes". The prominent localization of Pur-alpha and its interaction partner in the nucleus is not surprising, since fNS cells are highly proliferative and exhibit an enhanced transcription and translation machinery.

4.3.5.6. Identification of Pur-alpha interaction partners in Oli-neu cells

The Pur-alpha affinity capture-MS approach using samples derived from Oli-neu cells resulted in the identification of 475 proteins, featuring valid values in at least two replicates. Thereof, 75

proteins are probable Pur-alpha interaction partners, exhibiting a target-IP to control-IP log2 fold change ≥ 0.585 and a Benjamini-Hochberg FDR adjusted p-value ≤ 0.05. These proteins are labeled with red color in the scatter plot (Figure 4.41 (c)). The distribution of proteins resembled the one of the fNS approach, with Pur-alpha showing the highest log2 fold change at a high confidence level. Based on the log2 fold changes, the top 30 significantly enriched proteins are depicted in Table 4.9. The complete list can be found in the Appendix (Table A.3).

Besides Pur-alpha, 75 other proteins featured high enrichment rates and simultaneously good levels of confidence. About the second most enriched protein however, the uncharacterized protein C2orf71 homolog, less is known so far. The few existing information suggested an involvement in retinal development due to its detection in the developing eye of E14 old mice [Collin et al., 2010]. Moreover, similarly to the fNS co-IP experiment (Table 4.8), mainly proteins belonging to the family of heterogeneous nuclear ribonucleoproteins (hnRNPs) were enriched. Actually, four proteins within the 14 most enriched proteins and in total seven out of 75 proteins belonged to the family of hnRNPs. Moreover, altogether eight proteins involved in the regulation of viral genome replication were identified, signed with red color in Table 4.9.

Table 4.9.: Significantly enriched protein groups in Oli-neu cells, identified using an affinity capture-mass spectrometry approach. The evidence files (MaxQuant) of three replicates were processed using Perseus. Potential contaminants, positive reverse sequences and proteins, featuring valid values in less than two replicates, were removed. Target IP (Pur-alpha antiserum) to control IP (preimmune serum) ratios were log2 transformed and normalized to the median per replicate. The one-sample t-test against 0 including the Benjamini Hochberg correction was applied. Proteins featuring a false discovery rate adjusted p-value ≤ 0.05 and a log2 fold change ≥ 0.585 were arranged according to the log2 fold changes, starting with the highest value. Proteins involved in viral genome replication regulation are labeled in red (determined using GOrilla). Always one protein of a protein group is listed in the table.

No	Gene	log2 fold change	-log10 p-value	No	Gene	log2 fold change	-log10 p-value
1	Pura	4.4607	4.1553	16	Twf1	2.0102	1.7467
2	C2orf71	3.5721	2.4447	17	Ilf2	2.0022	3.6080
3	Hnrnpab	3.0401	2.9186	18	Acta1	1.9790	1.9710
4	Ncl	2.9395	1.8117	19	Elavl1	1.9710	2.8894
5	Hnrnpa1	2.8629	2.4418	20	Capzb	1.9563	1.9241
6	Fmr1	2.7624	2.2847	21	Syncrip	1.9293	2.0121
7	Ilf3	2.5376	3.0186	22	Capza1	1.9215	1.9829
8	Hnrnpa0	2.4815	3.0567	23	Myef2	1.9096	2.0613
9	Ces1f	2.3618	2.6191	24	Chuk	1.8855	2.1196
10	Upf1	2.3330	2.4355	25	Pabpc1	1.8571	3.0306
11	Fxr1	2.3194	3.4838	26	Hnrnpu	1.8439	1.7470
12	Mov10	2.2995	2.8239	27	Hnrnpa2b1	1.8300	2.4039
13	Ncbp1	2.2265	2.3895	28	Coro1c	1.8133	1.7773
14	Hnrnpd	2.2085	2.0209	29	Lgals8	1.8110	1.8685
15	Purb	2.0420	2.1845	30	Rps9	1.7878	2.1098

GO enrichment analysis of significant Pur-alpha interaction partners, identified in Oli-neu cells, revealed that GO terms associated with regulation of viral processes and mRNA stability were overrepresented. The histograms depicting enriched GO terms can be found in the Appendix

(Figure A.10). Many significantly detected proteins possessed regulatory functions on gene expression, indicated by the enriched GO terms "positive regulation of gene expression" and "negative regulation of gene expression". Besides, identified proteins regulate gene expression on posttranscriptional level, indicated by the GO terms "regulation of posttranscriptional gene silencing" or "regulation of translation". In the category of molecular functions only a few terms were enriched, however they largely equaled the enriched GO terms of previous interaction partner analyses conducted. Regarding terms enriched in the ontology cellular component, ribonucleoprotein complexes displayed the highest enrichment p-value (Figure A.9). In addition, some proteins were localized in polysomes, which are complexes consisting of mRNA molecules and ribosomes [Yazaki et al., 2000]. The translation of proteins takes place in polysomes.

4.3.5.7. Comparison of interaction partner screening methods

Three interaction partner screenings using three different cell types and two different identification methods including statistical evaluation of target to control ratios resulted in the detection of altogether 170 potential Pur-alpha interaction partners. Comparison of GO enrichment analyses conducted of all approaches revealed many overlaps regarding biological processes and cellular components. Nevertheless, though statistical tests were performed, the detection of false positive interaction partner should be considered. In the case of the BioID assay, they could result from unspecific biotinylation, whereas in the case of immunoprecipitation, they could result from unspecific binding to the Pur-alpha antibody. Accordingly, each possible candidate usually needed to be verified using additional assays, such as colocalization experiments or western blot analyses. Since this was not feasible (due to time limit), already performed interaction partner analyses (Interaction Partner* in Table 4.10) were examined to enhance the probability of detecting true interaction partners of Pur-alpha. Moreover, proteins which were identified not only in one but several screening experiments were more likely true interaction partners. Thus, the proteins of three replicates were compared to each other and results were plotted in a Venn diagram (Figure 4.42). Every big circle represents one experiment including the number of significantly identified proteins. Proteins are distributed in different compartments, depending on their occurrence in only one, two or every experiment. The overlapping areas thereby represent the number of proteins shared between every experiment.

According to the Venn diagram (Figure 4.42), more identified Pur-alpha interaction partners were shared between both co-immunoprecipitation (co-IP) assays than between one of the co-IP assays and the Bio-ID assay. However, many proteins were only detected in a single experiment, while the number increased from 19 single detected proteins in the fNS co-IP approach, via 40 proteins in the Oli-neu co-IP approach to 72 proteins in the HEK293T BioID approach. Nevertheless, five proteins were shared between all three experiments. Furthermore, both co-IP methods shared 25 proteins and additionally six similar proteins were identified using the Oli-neu co-IP assay and the HEK293T BioID assay and five proteins using the fNS co-IP assay and the HEK293T BioID assay.

The probability of finding true interaction partners increases with the number of identifications. Accordingly, proteins identified in all three interaction partner analysis were most probably interacting with Pur-alpha, as well as proteins, which were identified using the BioID method and one co-IP method. Thus, only proteins detected in at least two experiments were further

considered and depicted in Table 4.10. These proteins were listed according to their experimental detection and were checked for already verified interaction with Pur-alpha by Kanai and co-workers [Kanai et al., 2004] [Johnson et al., 2006]. Using a KIF5-pulldown-assay, they were able to pull down a RNase-sensitive granule, containing several proteins besides Pur-alpha. These granules are mainly responsible for the transport of RNA. All tagged proteins within the last column derived from this experiment.

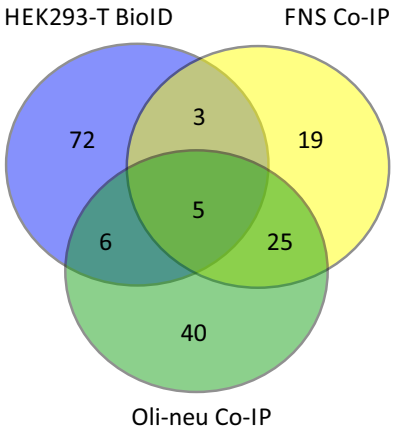

Fig. 4.42.: Venn diagram, containing all significantly enriched proteins of three interaction partner experiments. As identifier the human (BioID) and murine (co-IP) leading razor proteins were used. Protein accessions were converted to gene names using the Retrieve/ID mapping tool provided by UniProtKB [Apweiler et al., 2004]. Using the Venn diagram tool, provided by UGent Bioinformatics & Evolutionary Genomics, all proteins, significantly identified using the HEK293T BioID, the fNS co-IP and the Oli-neu co-IP approach were analyzed. co-IP = co-immunoprecipitation

As already mentioned, five proteins were detected in all three experiments. This included the bait protein Pur-alpha, as well as DDX3X (ATP-dependent RNA helicase DDX3X) and SYNCRIP (heterogenous nuclear ribonucleoprotein Q). A connection between these three proteins in RNA granules was already evidenced [Kanai et al., 2004]. Moreover, the proteins PABPC1 (polyadenylate-binding protein 1) and LARP1 (La-related protein 1) were detected in all three interaction partner studies. The proteins depicted in Table 4.10 can most likely be classified by their biological function as RNA binding proteins. 35 of 41 proteins mentioned in the list were associated with RNA binding, especially with mRNA binding and single and double stranded RNA binding. Additional biological functions included the binding of DNA and ATP-dependent helicase activity. Using BioID and co-IP approaches, prominently Pur-alpha interaction partners were detected which are localized in ribonucleoprotein complexes, together with RNA molecules. These complexes are further assembled in ribonucleoprotein granules, macromolecular complexes responsible for localization, stability and translation of their RNA cargo. With the two serine kinases, CHUK and IKBKB, two proteins related to the NF-κB signaling pathway were detected in both co-IP experiments.
All considered proteins were identified as significant interaction partners of Pur-alpha, successfully passing statistical analyses. Nevertheless, it occurred that some proteins were detected with valid values in the target but not in the control replicates. Indeed, the appropriate control samples featured missing values, thereby preventing the calculation of a target-IP to control-IP ratio. For some proteins it also happened that an intensity was measured in a single control

Table 4.10.: Proteins, significantly enriched in at least two screening experiments. All proteins identified in three interaction partner experiments were analyzed for proteins present in at least two experiments. Positive findings are depicted in this table with their leading razor protein names and gene names. Applicable experiments were marked with a " × " in the following columns, where B_{HEK} represented the BioID experiment using HEK293T cells, while IP_{fNS} and IP_{ON} represented the fNS and Oli-Neu co-IP experiments. In the last column, called Interaction partner*, all proteins are labeled, which were already identified as potential interaction partner of Pur-alpha by [Kanai et al., 2004].

Gene name	Protein name	B_{HEK}	IP_{FNS}	IP_{Oli}	Interaction partner*
Ddx3x / D1Pas1	ATP-dependent RNA helicase DDX3X	x	x	x	x
Larp1	La-related protein 1	x	x	x	
Pabpc1	Polyadenylate-binding protein 1	x	x	x	
Pura	Purine rich element binding protein A	x	x	x	x
Syncrip	Heterogeneous nuclear ribonucleoprotein Q	x	x	x	x
Cltc	Clathrin	x	x		
Stau1	Double-stranded RNA-binding protein Staufen homolog 1	x	x		x
Ybx1	Y box protein 1	x	x		
Actg1	Actin, cytoplasmic 2	x		x	
Csde1	Cold shock domain-containing protein E1	x		x	
Dhx30	Putative ATP-dependent RNA helicase DHX30	x		x	
Fxr1	Fragile X mental retardation syndrome-related protein 1	x		x	x
Fxr2	Fragile X mental retardation syndrome-related protein 2	x		x	x
Slc25a1	Tricarboxylate transport protein, mitochondrial	x		x	
Chuk	Conserved helix-loop-helix ubiquitous kinase		x	x	
Ddb1	Damage specific DNA binding protein 1		x	x	
Ddx17	Probable ATP-dependent RNA helicase DDX17		x	x	
Ddx5	Probable ATP-dependent RNA helicase DDX5		x	x	x
Elavl1	ELAV-like protein 1		x	x	
Elavl2	ELAV-like protein 2		x	x	
Fip1l1	Pre-mRNA 3-end-processing factor FIP1		x	x	
Fmr1	Synaptic functional regulator FMR1		x	x	x
Hnrnpa0	Heterogeneous nuclear ribonucleoprotein A0		x	x	x
Hnrnpab	Heterogeneous nuclear ribonucleoprotein A/B		x	x	x
Hnrnpdl	Heterogeneous nuclear ribonucleoprotein D-like		x	x	
Hnrnpu	Heterogeneous nuclear ribonucleoprotein U		x	x	x
Ikbkb	Inhibitor of nuclear factor kappa-B kinase subunit beta		x	x	
Ilf2	Interleukin enhancer-binding factor 2		x	x	
Ilf3	Interleukin enhancer-binding factor 3		x	x	
Larp4	La-related protein 4		x	x	
Myef2	Myelin expression factor 2		x	x	
Ncbp1	Nuclear cap binding protein subunit 1		x	x	
Ncl	Nucleolin		x	x	x
Purb	Purine rich element binding protein B		x	x	x
Rpl17	Ribosomal protein L17		x	x	
Rpl23a	Ribosomal protein L23A		x	x	
Rps4x	40S ribosomal protein S4, X isoform		x	x	
Tardbp	TAR DNA-binding protein 43		x	x	
Upf1	UPF1 regulator of nonsense transcripts homolog		x	x	

sample. Since proteins with less than two calculated target-IP to control-IP ratios were removed, they were likewise not considered as potential interaction partners. However, they might though be a potential interaction partner of Pur-alpha. For that reason, the protein list was searched for proteins, featuring valid intensity values in at least two target replicates and no measured

intensities in the appropriate control samples. In addition, if though a protein featured intensity values in the control sample, only proteins with a log2 target to control ratio of ≥ 0.585 were considered. These 21 proteins are depicted in Table A.11 in the Appendix.

Four proteins, labeled with red color in Table A.11, were already identified as significantly enriched within other interaction partner analyses. Applicable to FXR2, which was formerly identified in the BioID and the Oli-neu co-IP assay, MOV10 (protein putative helicase MOV-10) (Table 4.9), DDX6 (probable ATP-dependent RNA helicase DDX6) (Table A.1) and the NF-$\varkappa$B modulator IKBKG (Table 4.8).

4.3.5.8. Oli-neu specific interaction partner of Pur-alpha

Representing one of the highest upregulated transcription factors during neurosphere differentiation, Pur-alpha seems to play an important role during the differentiation process. However, the mechanism how differentiation was supported could only be shown theoretically by activating or repressing proteins like c-myc or E2F-1. Thus, the comparison between Pur-alpha interacting proteins enriched in Oli-neu cells and in fNS cells should provide a first hint to identify proteins interacting with Pur-alpha and thereby having an impact on the development of neural progenitor cells to oligodendrocyte precursor cells.

Table 4.11.: Probable Pur-alpha interaction partners, that are significantly enriched in Oli-neu cells and underrepresented in fNS cells. The table depicts those proteins which were only identified in the Oli-neu co-IP approach or which displayed a log2 fold change ratio of Oli-neu cells to fNS cells > 1. In this table, proteins were sorted by their log2 fold change values, starting with the highest one. Proteins labeled in red are related to actin.

No	Gene name	Protein name	No	Gene name	Protein name
1	N/A	Uncharacterized protein C2orf71 homolog	20	Actr3	Actin-related protein 3
2	Ces1f	Carboxylesterase 1F	21	Atp1a2	Sodium/potassium-transporting ATPase subunit alpha-2
3	Ilf3	Interleukin enhancer-binding factor 3	22	C3	Complement C3
4	Fxr1	Fragile X mental retardation syndrome-related protein 1	23	Htra1	Htra Serine Peptidase 1
6	Twf1	Twinfilin-1	24	Flii	Protein flightless-1 homolog
7	Actg1	Actin, cytoplasmic 2	25	Puf60	Poly(U)-binding-splicing factor PUF60
8	Capzb	F-actin-capping protein subunit beta	26	Oas1b	Inactive 2'-5'-oligoadenylate synthase 1B
9	Capza2	F-actin-capping protein subunit alpha-2	27	Pgam5	Phosphoglycerate Mutase Family Member 5
10	Hnrnpa2b1	Heterogeneous Nuclear Ribonucleoprotein A2/B1	28	Rbmx	RNA-binding motif protein, X chromosome
11	Coro1c	Coronin-1C	29	Xrcc6	X-ray repair cross-complementing protein 6
12	Lgals8	Galectin-8	30	Dhx30	Putative ATP-dependent RNA helicase DHX30
13	Itih1	Inter-alpha-trypsin inhibitor heavy chain H1	31	Gpr157	Probable G-protein coupled receptor 157
14	Eif4g3	Eukaryotic Translation Initiation Factor 4 Gamma 3	32	Cdc73	Parafibromin
15	Arpc2	Actin-related protein 2/3 complex subunit 2	33	Rps7	40S Ribosomal Protein S7
16	Pcmtd2	Protein-L-isoaspartate O-methyltransferase domain-containing protein 2	34	Slc25a1	Tricarboxylate transport protein, mitochondrial
17	Arpc4	Actin-related protein 2/3 complex subunit 4	35	Lclat1	Lysocardiolipin Acyltransferase 1
18	Hnrnpa3	Heterogeneous Nuclear Ribonucleoprotein A3	36	Ago2	Protein argonaute-2
19	Arpc1b	Actin-related protein 2/3 complex subunit 1B			

Altogether, 36 proteins interacting with Pur-alpha were identified in Oli-neu cells, which were

not or less enriched in fNS cells (Table 4.11). The threshold for considering proteins as primarily detected in Oli-neu cells was set to a log2 fold change ratio of Oli-neu cells to fNS cells > 1. A lacking detection of the listed proteins in fNS cells by the co-IP assay does not automatically exclude their interaction with Pur-alpha. Since sample preparation and MS data acquisition introduce variability into the data set one could not reliably say that the listed proteins are no interaction partners of Pur-alpha in fNS cells. Nevertheless, conducting every approach in three replicates minimizes the occurrence of missing potential interaction partners.

Many proteins related to actin were enriched within the Oli-neu co-IP data set, labeled with red color in Table 4.11. These proteins were mainly involved in biological processes related to cytoskeleton organization, particularly in regulation of actin filament polymerization and in Arp2/3 complex-mediated actin nucleation. Besides, Pur-alpha interacts with several other hnRNP proteins in Oli-neu cells by regulating processes on transcription and translation level, including ILF3, AGO2, FMR1, FXR1 and FXR2. Furthermore, EIF4G3 (eukaryotic translation initiation factor 4 gamma 3) was overrepresented in Oli-neu cells compared to fNS cells and besides EIF4G3 several other members of the eukaryotic translation initiation factor family have been shown to interact with Pur-alpha [Kanai et al., 2004]. Another possible interaction partner of Pur-alpha represented HTRA1 (serine protease HTRA1), which usually is involved in different regulatory processes causing the cleavage of peptide bonds [Clausen et al., 2002]. Interestingly, HTRA1 represented one of the highest upregulated proteases within the neurosphere data set, indicating a probable cooperation of Pur-alpha and HTRA1 proteins in promoting the differentiation from NSCs to OPCs. Another protein worth mentioning is CDC73 (parafibromin), which might act as a negative regulator of cell proliferation and progression through the cell cycle [Zhang et al., 2006a]. The three proteins CES1F (carboxylesterase 1F), SLC25A1 (mitochondrial tricarboxylate transport protein) and LCLAT 1 (lysocardiolipin acyltransferase 1) are related to lipid metabolism, especially to fatty acids. However, an implementation of Pur-alpha in fatty acid metabolism was not shown yet.

5. Discussion

Differentiation of multipotent progenitor cells (NPCs) to oligodendrocyte precursor cells (OPCs)

Neurosphere assay and quantification strategy

The Neurosphere assay [Chen et al., 2007] was chosen as most suitable cell culture model system in combination with a quantitative large scale mass spectrometry approach to determine protein level changes during the development from multipotent NPCs to OPCs. The neurosphere assay takes advantage of the short cell cultivation period, enabling a total sample recovery within three weeks by simultaneously ensuring the generation of large numbers of cells, required for performing meaningful quantitative proteomics. In addition, compared to the protocol established by Pedraza and co-workers [Pedraza et al., 2008] for OPC production, the neurosphere assay reflects a progressive change in protein expression based on a gradual exchange from proliferation to differentiation medium. This means that growth factors necessary for NPC proliferation diminish, while factors inducing cell fate determination and differentiation to OPCs increase, resulting in an onward increase in numbers of cells undergoing differentiation.

The usual analysis setup includes experiments with two time points which only allows for comparison of proteins regulated between the two states and finally resulted in a large list of up- and downregulated proteins, impeding the determination of proteins regulated due to the mechanism investigated or due to other reasons. Broughton and co-workers, for example, compared expression levels between pre-oligodendrocytes and mature oligodendrocytes by microarray analysis, thereby identifying more than 300 upregulated proteins in mature oligodendrocytes compared to pre-oligodendrocytes [Broughton et al., 2007]. In contrary, experiments consisting of multiple states allow for the generation of protein kinetics, covering several developmental stages between the starting and the end point of the differentiation process and allowing for the determination of early and late upregulated proteins. Especially in the case of development studies, the identification of effector proteins, which are upregulated at the beginning, is required to understand the biological mechanisms underlying the differentiation process and to identify target proteins for induction of differentiation. Using the TMT 6-plex isobaric labeling technique in combination with the neurosphere assay, changes in protein expression were quantitatively monitored by labeling six different time points. Certainly, *in vivo* large scale mass spectrometric experiments designed to analyze several differentiation stages of developing OPCs would be the gold standard, though it is technically highly challenging.

Nonetheless, one needs to consider that neurospheres represent a complex system of single cells with heterogeneous character [Jensen & Parmar, 2006]. They might differ in the amount of neural stem cells, progenitor cells, postmitotic neurons and glial cells. Thus, to keep the amount of differentiated cells to a minimum, for each experiment a sufficient number of cells was isolated from murine cortices rather than passaging neurospheres to increase cell population. Influenced by varying culture conditions, like cell density or growth factor concentrations, neurospheres

might exhibit varying proliferation rates and differentiation capacities, so that cell culture conditions were kept as constant as possible. While reaching the appropriate size, neurospheres were immediately differentiated to oligospheres and medium exchange was carried out according to the established protocol every second day to ensure consistent differentiation conditions.

Microscopic monitoring of neurospheres differentiation

For the reasons mentioned above, the differentiation process from neurospheres to oligospheres was monitored by immunocytochemistry (ICC) staining. Quantitative ICC analyses of single cells revealed that 90% of total cells expressed the stem cell and progenitor cell marker nestin, 7% the OPC specific marker NG2 and 1% the astrocyte specific marker GFAP prior to differentiation initiation, indicating the presence of only few differentiated cells. However, one needs to consider that neurons are highly vulnerable cells which might not survive the dissociation process and were thus not detected. Accordingly, there might also be some neurons present in neurospheres. The final number of NG2-positive cells increased to 58% nine days after differentiation initiation. Moreover, differentiation of neurospheres derived from cortical cells of NG2-EYFP-knockin mice revealed a visible expression of the NG2 protein two days after differentiation initiation, which continuously increased for at least the following two weeks. However, also the ratio of astrocytes ascended to 11% at time point day 9. In addition, some OPCs were already differentiated into oligodendrocytes, indicated by the significant upregulation of some oligodendrocyte specific proteins after nine days of differentiation, including MBP and UGT8A [Honke et al., 2002].

Drawing comparisons to ICC analyses performed by other researchers is quite difficult, since most differentiation experiments conducted are based on rat neurospheres [Broughton et al., 2007] [Zhang et al., 1999]. More than 90% of rat cells differentiated into oligospheres, indicated by the expression of a common OPC marker. Only Chen and co-workers mentioned that they achieved an almost pure (98%) murine OPC culture using the neurosphere assay [Chen et al., 2007]. It was previously shown that NPCs divide in response to the mitogens EGF and bFGF by retaining their multipotency to differentiate into neurons and glia [Tropepe et al., 1999]. However, they also showed that with lowering mitogen concentrations the ability of neurospheres to differentiate into oligodendrocytes was diminished, whereas astrocytes development was not affected. Besides this, commitment of neurospheres to differentiate into oligospheres depends on the mitogens PDGF-AA and bFGF [Hu et al., 2012a]. Conclusively, a probable explanation for the generation of astrocytes might be the withdrawal of mitogens necessary for differentiation into OPCs. Most likely, this mitogen lack occurs to cells located within the center of a neurosphere cluster. Cultivation of cells in suspension culture as cell aggregates thus displays the disadvantage of not guaranteeing the access of every cell to necessary factors for commitment to the oligodendroglial lineage or even to essential nutrition for cell survival. Secondly, Pedraza and co-workers have ascertained that the time point of cell isolation has an impact on the commitment of cells [Pedraza et al., 2008]. They observed a higher number of astrocytes in cultures derived from E15.5 embryos than from E14.5 embryos. Accordingly, the isolation of cortical cells from neonatal mice might be another cause for the presence of lower OPC numbers. In summary, it can be stated that using the assay, mostly multipotent NPCs differentiated into mainly NG2-expressing OPCs and a few astrocytes, while another part was most probably still at NPC stage. One should keep in mind that differences in protein expression detected between

different development stages are most probably linked to OPCs and not to astrocytes.
In addition, the circumstance of cells undergoing apoptosis after dissociation of spheres at later stages of differentiation, needs to be considered. A possible explanation therefore is provided by Horiuchi and co-workers [Horiuchi et al., 2010]. They showed that in comparison to rat OPCs, mouse OPCs that were cultivated in B104 conditioned medium displayed lower levels of phosphorylated ERK1/2 and CREB, pathways known to be involved in cell survival. Besides, intrinsic pathway-mediated apoptosis occurs more often in murine OPCs, which indeed can be overcome by inhibiting the activation using the adenylyl cyclase activator forskolin. According to our experience, less cells recovered from the dissociation process after a differentiation time of nine days. It can thus be postulated that forskolin addition is not sufficient for overcoming apoptosis induction in cells passing over a certain, not exactly determinable point in the development process. Possibly, the harsh dissociation procedure might be a second factor underlying.

Analyses of time dependent alterations in protein levels

Data analysis strategies Conduction of five biological replicates of *in vitro* NPC to OPC differentiation samples and subsequent application of TMT sixplex based quantitative proteomics, resulted in the identification of 6,150 proteins using MaxQuant. In terms of quality, more than half of total identified proteins were detected in all replicates and additional 25% in at least three replicates. Quantitative analyses of regulated proteins were performed with 4,276 proteins (72% of total proteins), featuring valid intensity values in at least three replicates. Due to the large amount of identified proteins, different analysis strategies were considered. First, hierarchical clustering of proteins into seven clusters of similarly regulated proteins was performed to simplify the data set and to get a first impression of the expression pattern of identified proteins. Using this approach, 179 proteins were identified which most likely are involved in the differentiation process, indicated by continuously increasing expression.

In addition, the application of statistical tests was conducted to enhance the confidence of the conclusions drawn. This was especially recommended since mass spectrometric measurements of five replicates introduced additional variance into the data set, indicated by a medium Pearson's correlation coefficient, based on normalized intensity values of all replicates [Evans, 1996]. This was among others due to the occurrence of missing values, leading to slightly identical biological data sets [Schwämmle et al., 2013]. For statistical evaluation of log2 transformed expression ratios the moderated t test (limma) method and the versus null distribution method (rank pro-duct) were applied. Limma and rank product were tested on mass spectrometry data in terms of limited replicates and missing values. Both approaches were chosen since they were proven to outperform the standard t-test method in experiments consisting of at least three replicates and 1,000 differentially regulated proteins [Schwämmle et al., 2013]. Using this approach, proteins differentially regulated during the differentiation process were determined at a high confidence level. Altogether, 932 significantly up- and 1,184 downregulated proteins were identified. With prolonged differentiation time the number of significantly regulated proteins continuously increased.
Although we expected to identify proteins responsible for cell fate commitment or differentiation initiation, which are expectably upregulated during early stages of the differentiation experiment, no significantly upregulated proteins could be detected three days after differentiation initiation. According to the ICC staining conducted and the information obtained from

NG2-EYFP-knockin mice-derived spheres, cells did not differentiate simultaneously but rather differentiated consecutively, which complicated the identification of proteins responsible for differentiation initiation. Thus, with in total 83 proteins, significantly upregulated from day six until the end of the experiment, only candidate proteins responsible for initiation and accomplishment of differentiation could be identified. The 403 proteins, permanently upregulated after either nine or twelve days of differentiation, represent potential candidates involved in OPC specific processes, whereas downregulated proteins are mainly involved in NPC specific processes.

Therefore, a third approach was considered, where distinct protein classes, known to be involved in initial processes of cellular differentiation were investigated. This included proteins responsible for extrinsic and intrinsic signaling as well as gene expression regulating proteins. In the case of data processing, log2 peptide intensities were normalized on the median of all intensities per time point and replicate, since the median is robust against outliers compared to the mean. In addition, peptides showing missing values at any time point were discarded since a large number of missing values was observed in some replicates. This was a necessary step to allow for median-normalization of peptides. After normalization, peptides were combined on protein level by calculating the median of all peptide intensities assigned to the same protein. The protein intensities determined per replicate were then combined to the mean protein intensity of all replicates. This time, the mean was chosen to also include outliers. Conclusively, the protein intensities obtained for the protein classes of receptors, kinases and transcription regulating factors are not statistically evaluated.

Enriched biological processes Gene ontology enrichment (GO) analysis revealed that proteins constantly upregulated during the differentiation process (day 6 - 15) are especially involved in cell adhesion processes. Most likely, the main function of cellular adhesion molecules (CAMs) in neurospheres and oligospheres represents the organization of the microenvironment by providing the interaction between single cells within the sphere. However, the interaction between CAMs expressed on multiple cells already occurrs in neurospheres, suggesting another function of upregulated CAMs within developing oligospheres. Actually, CAMs are assumed to ensure signal transduction of distinct pathways to regulate cell survival, proliferation, differentiation and migration of the cell [Bian, 2013]. This is also consistent with our finding that proteins responsible for cell adhesion, like the cell adhesion molecules 2 and 3 (CADM2; CADM3), were already upregulated during early stages of the differentiation experiment. Moreover, another probable function can be assumed, based on the fact that proteins which support cell adhesion were also prominently involved in cell migratory processes, including the endothelin receptor-B (EDNRB) [Gadea et al., 2009], the uracil nucleotide/cysteinyl leukotriene receptor (GPR17) [Coppi et al., 2013] and the neural cell adhesion molecule NCAM1. Especially PSA-NCAM, the post-translational modified NCAM1 protein, was evidenced to strongly influence OPC migration [Czepiel et al., 2014]. Although, the mentioned proteins might possess further functions, it is still interesting that many proteins involved in cell migration are upregulated during *in vitro* differentiation of NPCs to OPCs. Especially, since oligospheres were cultivated in absence of axons or extracellular matrix molecules. The elevated protein levels of CAMs are probably explainable by the theory that their expression is governed within the oligodendroglial development process [Temple & Raff, 1986]. It was at least shown, that oligodendrocytes are able to produce a myelin like membrane in the absence of axons [Szuchet et al., 1986].

GO enrichment analysis further revealed that mainly processes affecting oxidation-reduction processes and the lipid metabolism, especially the fatty acid metabolism, were enriched during later stages (day 9 - 15) of the development process. Although few proteins assigned to mature oligodendrocytes were significantly upregulated after nine days of differentiation, mainly NG2-expressing cells were present at this differentiation stage. It can thus be assumed that the lipid metabolism is already augmented in the progenitor cells of lipid and myelin synthesizing oligodendrocytes [Baumann & Pham-Dinh, 2001]. The overrepresentation of oxidation-reduction processes further indicated that the differentiating cells required additional energy. Since NPCs undergo distinct changes during the differentiation process, an augmentation of the energy metabolism is conceivable. However, GO enrichment analyses further revealed an enrichment of lipid catabolic processes and especially fatty acid catabolic processes towards the end of the differentiation experiment. Accordingly, energy is among others provided by the oxidation of fatty acids. This is however contradictory with the fact that oligodendrocytes produce large amounts of lipids to ensure proper myelination of axons. Eventually, fatty acids were used for energy production in oligospheres since they were not yet required for the synthesis of myelin lipids, including cerebrosides and sulfatides [Menkes et al., 1966] [Morell et al., 1999].

Probable candidates involved in NPC to OPC differentiation

Successful differentiation of NPCs was confirmed by the detection of several downregulated proteins known to be involved in mitotic cell cycle, chromosome organization and nuclear chromosome segregation processes. It could be further shown that cells undergoing differentiation shifted from a highly proliferative status, indicated by an enrichment of RNA and DNA metabolic processes, to a relatively quiescent status. Visual morphological changes and the detection of OPC specific marker proteins further confirmed the development of OPCs.

Receptors and protein kinases *In vitro* differentiation was induced by changing from EGF- and bFGF-containing medium to B104-conditioned differentiation medium. Thereby, mainly the growth factors PDGF-AA and bFGF induce proliferation of OPCs by binding to their appropriate receptors [Hu et al., 2012b]. Additionally, it was shown that PDGF-AA possesses the ability to positively affect multipotent NSCs to differentiate into cells of the oligodendroglial cell lineage via the activation of diverse cell signaling pathways, including ERK, PI3K and p38 MAPK [Hu et al., 2012a]. In our experiment, the response to PDGF-AA is reflected by continuously increasing expression levels of platelet derived growth factor receptor alpha (PDGFRA) and increasing expression levels of the growth factor receptor-bound protein 2 (GRB2). A supportive function of GRB2 for PDGFRA can be assumed, since GRB2 usually serves as an adapter protein between cell surface receptor tyrosine kinases and the Ras signaling pathway, thereby providing the connection between extracellular and intracellular signaling [Lowenstein et al., 1992]. Moreover, accumulating evidence suggests a collaboration of integrin and growth factor dependent signaling, thereby regulating survival, proliferation and development in cells of the oligodendroglial lineage [Benninger et al., 2006] [Baron et al., 2005]. More precisely, it was shown that integrins interfere with the receptor tyrosine kinases PDGFR, EGFR and FGFR. In our case, several integrins were upregulated, including ITGA7, ITGA5, ITGAV and ITGB8.

The expression of several other cell surface receptors was highly augmented during early stages (day 6) of the differentiation process. Interestingly, this applies to the protein sphingosine 1-

phosphate receptor 1 (S1PR1), which acts as a mediator of ERK and p38 MAPK signaling pathways, similar to PDGFRA [Cui et al., 2014]. This strengthens the assumption of the involvement of both pathways in the oligodendroglial development process. Additionally, belonging to the early upregulated proteins, the protein kinase C theta type (PRKCQ) might be involved in early NPC differentiation processes by activating the transcription factor NF-κB [Lin et al., 2000]. The presumption is based on the findings of Zhang and co-workers, who showed that NF-κB signaling initiates the differentiation of nestin positive NSPCs [Zhang et al., 2012b]. Moreover, NF-κB activation can be induced by several mediators, to which the mitogen PDGF-AA and the downstream RAS and PI3K signaling cascades belong [Romashkova & Makarov, 1999], which further strengthens the probability of PI3K mediated cell fate commitment.

Transcription factors and epigenetic modulators Cell fate decision and subsequent cellular differentiation processes are often determined by transcription factors, most likely located downstream of earlier mentioned signaling cascades. Transcription factors might trigger transcription of differentiation supporting genes or repress transcription of differentiation inhibiting genes. Previous investigations identified several transcription factors responsible for oligodendroglial cell fate determination, like the transcription factors OLIG1, OLIG2, NKX2-1 and NKX2-1 [Wen et al., 2009]. However, mentioned proteins were either not detected or not upregulated in the neurosphere experiment. The missing upregulation of mentioned factors is due to the fact that their activity is hedgehog signaling pathway dependent [Ortega et al., 2013]. Oligodendrogenesis can be induced by several factors *in vitro*, albeit the percentage of oligodendroglial cells might vary. The addition of PDGF was shown to increase the formation of OPCs, whereas SHH predominantly favors the formation of mature oligodendrocytes. [Gibney & McDermott, 2007].

A potential transcription factor inducing OPC differentiation represents the protein signal transducer and activator of transcription 3 (STAT3), which was particularly upregulated during the first six days of the experiment, by amplifying the cellular response of fibroblast growth factor mediated differentiation [Hart et al., 2001]. At least, it was shown that genetic ablation of STAT3 prevents OPC differentiation and that it enhances NG2 cell proliferation after spinal cord injuries [Steelman et al., 2016] [Hackett et al., 2016]. However, STAT3 is not only expressed in oligodendroglias but is also required for astrogliogenesis [Fukuda et al., 2007], so that increased STAT3 levels might not only promote differentiation to OPCs but also to astrocytes.
In addition, the upregulation of the two proteins prohibitin (PHB) and transcriptional activator protein Pur-alpha (PURA), which have been shown to interfere with the cell proliferation promoter transcription factor E2F1, identifies both as interesting key proteins of cell fate determination [Wang et al., 1999] [Darbinian et al., 2001c]. Proliferation of NSCs was shown to be diminished upon inhibition of E2F1 by distinct miRNAs *in vivo*, leading in neurogenic areas to the differentiation of NSCs into neurons [Palm et al., 2013]. In addition, E2F1 was shown to regulate the transcription of cell cycle genes and epigenetic modulators during the transition of OPCs from proliferation to differentiation [Magri et al., 2014]. Conclusively, it might be probable that PHB and PURA regulate the expression of distinct cell cycle genes via inhibition of E2F1 activity, thereby promoting NPC to OPC differentiation.

Moreover, the highly upregulated histone modifier NAD-dependent protein deacetylase sirtuin-2 (SIRT2) might promote differentiation to OPCs. SIRT2 modifies lysine residues on histones and transcription factors and thus alters as an epigenetic regulator gene expression on tran-

scriptional level [Rodriguez et al., 2013]. So far, SIRT2 is implicated in the regulation of the cell cycle exit and enhancement of OPC to oligodendrocyte differentiation [Dryden et al., 2003] [Ji et al., 2011]. Less is known about its function during NPC to OPC differentiation, although the already initially elevated protein levels suggest a role for SIRT2 in differentiation initiation. One probable explanation was given by Dryden and co-workers, who showed that SIRT2 overexpression can prevent cells from reentering the cell cycle. On the other hand, an epigenetic mechanism is conceivable, whereby SIRT2 regulates the expression of differentiation influencing genes by chromatin modification or interaction with appropriate transcription factors.

On the other hand, downregulation of transcription regulating factors responsible for NSC maintenance and expansion was observed, indicating that cells exposed to differentiation medium start to differentiate into progenitor cells instead of sustaining stem cell like characteristics. A probable candidate regulating self-renewing processes is the highly downregulated REST corepressor 2 (RCOR2) protein, a subunit of the C-terminal cofactor (CoREST) of the REST complex. The repressor element-1 silencing transcription factor (REST) in turn recruits transcriptional and epigenetic regulatory cofactors, like CoREST, to target promoters, thereby regulating the gene expression of proteins involved in pluripotency networks [Abrajano et al., 2010] [Qureshi et al., 2010]. Moreover, the functional complex of REST and RCOR2 targets the silencing of neuronal genes in NSCs and non-neuronal cells [Abrajano et al., 2009]. RCOR2 exhibited positive log2 fold change values three days after differentiation initiation, while the value dropped noticeably thereafter. This expression pattern is explainable by the fact that REST and CoREST target genes, like *Neurog2*, *Id2* or *Id4* [Abrajano et al., 2010], which are involved in the regulation of neural cell fate decision. It can thus be assumed that during neurospheres differentiation, REST and its cofactors are responsible for transcriptional repression of neuronal genes and for oligodendroglial cell fate determination. However, once initial cell fate decision is accomplished, RCOR2 is downregulated. Furthermore, it is to mention that a protein that usually promotes the differentiation of NPCs to neurons was stronlgy downregulated during the differentiation process, namely the transcriptional repressor protein zinc finger E-box-binding homeobox 1 (ZEB1) [Ravanpay et al., 2010].
Conclusively, NSC to OPC differentiation requires the upregulation of oligodendrogliogenesis promoting factors and the downregulation of proteins repressing oligodendroglial characteristical gene expression and of proteins enhancing the differentiation into other cell types.

Differentiation of rat oligodendrocyte precursor cells (OPCs) to oligodendrocytes

The differentiation process of oligodendrocyte precursor cells (OPCs) to oligodendrocytes represents an important process regulated by a large number of proteins. Although many factors have already been identified being involved in oligodendrogenesis, the potential of large scale proteomic analyses to uncover new factors or networks that regulate oligodendrolgial differentiation has not been exploited so far. Most experiments investigating the differentiation process were performed on gene level using microarray assays [Dugas et al., 2006] [Broughton et al., 2007] [Kippert et al., 2008]. Former proteomic approaches conducted prominently focused on mapping the oligodendrocyte proteome [Colello et al., 2002] [Dumont et al., 2007a] [Sharma et al., 2015]. Only Tyler and co-workers so far analyzed the differentiation process from OPCs to oligodendrocytes in order to identify target proteins of the mammalian target of rapamycin pathway (mTOR), which plays an important role during OPC differentiation [Tyler et al., 2011].

Around 8% of glial cells reside as adult OPCs (NG2 cells) in the white matter of rats [Dawson et al., 2003]. In the event of oligodendrocyte cell death or demyelination, OPCs in the vicinity of the affected region are thought to be a major source for new oligodendrocytes and thus for remyelination of affected axons [Watanabe et al., 2002] [Franklin & Ffrench-Constant, 2008]. For this purpose, quiescent OPCs have to be activated to migrate, proliferate and differentiate into myelinating oligodendrocytes. Multiple mediators, known to be commonly involved in OPC development, were shown to be early upregulated in OPCs upon demyelination [Franklin & Ffrench-Constant, 2008] [Patel & Klein, 2011]. Accordingly, investigations of the OPC differentiation process on protein level is critical for a better understanding of the processes taking place during OPC maturation and to reveal proteins involved in these processes. Although additional factors play a role during remyelination, such as mediators activated by inflammatory cues, conclusions can be drawn for potential factors promoting remyelination from investigating the OPC development process.

Experimentally, cortices of newborn rats were used because during this development stage cells of the oligodendroglial lineage predominantly existed as OPCs or pre-oligodendrocytes. Proliferating OPCs were cultivated in mixed glial cell cultures, subsequently isolated by taking advantage of different adhesion properties and lately cultivated in adherent cultures. In response to specific differentiation triggering mitogens, like triiodothyronine (T3) and ciliary neurotrophic factor (CNTF) [Baas et al., 1997] [Talbott et al., 2007], OPCs differentiated into oligodendrocytes. Peptides were isbarically labeled using TMT reagents to quantitatively detect changes in protein levels. For this purpose, the serine protease trypsin was used which specifically cleaves C-terminal to lysine and arginine residues [Olsen et al., 2004].
Cell culture plates needed to be coated prior to seeding of OPCs. In contrary to poly-L-lysine (PLL), the D-conformation of the reagent, poly-D-lysine (PDL), is resistant to cleavage by trypsin [Tsuyuki et al., 1956]. Since TMT reagents react with lysine residues and peptide N-termini, PDL was chosen as coating reagent of cell culture plates. In addition, cells were harvested by trypsinization instead of cell scraping to avoid contamination from coating reagents in subsequent processing steps, albeit it might occur that membrane or cell surface proteins suffer from this procedure. As an alternative quantification method to iTRAQ labeling pertains the stable isotope labeling by amino acids in cell culture (SILAC) or stable isotope dimethyl labeling [Ong et al., 2002]. The labeling of proteins already on cell level is the main advantage of the SILAC approach. As a result, almost 100% labeling efficiency can be achieved while minimizing the import of variance during sample preparation. However, under primary cell culture conditions SILAC performance can hardly be achieved. Labeling with dimethyl reagents is less expensive, however its utilization is also inappropriate, since the system is more suitable for the comparison of only three samples. In conclusion, the TMT labeling system is the most suitable one to compare peptides derived from a complex protein mixture and four different samples.

Monitoring of OPC differentiation by microscopy OPC isolation from mixed glial cell cultures by shaking cells off requires the confirmation of OPC population purity. Immunofluorescence staining revealed that three days after differentiation initiation almost all cells isolated were positive for the OPC surface protein NG2 and the oligodendrocyte marker MBP. In addition, only few astrocytes and neurons and no microglia were identified after OPC isolation. Immunocytochemistry analyses conducted at several time points further confirmed the successful development of NG2-expressing cells to MBP-expressing cells. However, a few cells were not

detectable with either the NG2 or the MBP antibody, rising the hypothesis that unstained cells might derive from a few other cell types present at the beginning of differentiation. Accordingly, regarding the changes in protein levels detected by relative quantification, most probably they occur in oligodendroglial cells and not in other cell types. Nonetheless, it should be considered that a minority of cells are no oligodendroglial cells.

Analyses of time dependent alterations in protein levels

Using the data analysis software Proteome Discoverer including the Mascot search engine, in total 3,876 unique proteins from four biological and one technical replicate were identified. The reproducibility of identified proteins between the replicates is satisfying, since more than 49% of totally identified proteins were detected in all four replicates, while 67% of total proteins were detected in at least three replicates. However, replicate four was less correlating with the other replicates, indicated by the calculated Pearson correlation coefficients of normalized intensities. The low correlation between measured intensities and replicates occurred noticeably at time point day 6. The reason therefore can be determined by manual analyses of the PSM file obtained of replicate four. Compared to the other time points, many peptides featured missing values in the time point day 6 sample. Accordingly, the amount of PSMs useable for quantification dropped extremely. Since similar peptides labeled with distinguishable isobaric tags for different time points were combined to one single sample, the drop in quantifiable PSMs is not explainable by inaccurate measurement during MS data acquisition. Most probably, the drop in numbers is caused by an inappropriate sample preparation.

From totally detected 3,876 unique proteins only 2,162 proteins, which were detected in at least three replicates, were considered for further investigations. As statistical tests, the moderated t test (limma) method and the versus null distribution method (rank product) were applied to the log2 transformed expression ratios. Both methods were chosen for the reason that they provide high-confidence results in experiments displaying missing intensity values [Schwämmle et al., 2013]. After application of statistical tests, 402 significantly upregulated and 485 significantly downregulated proteins remained. In contrary to the neurosphere differentiation experiment, significantly regulated proteins were already detected three days after differentiation initiation. This is most probably due to the complete medium exchange to differentiation medium at the beginning of the experiment. In addition, cells were cultivated as single cells in monolayers and thus an almost coinciding differentiation of cells can be expected.

Verification of OPCs differentiating into oligodendrocytes Comparison of total identified proteins within our OPC differentiation data set with the proteomic large scale analysis carried out by Sharma and co-workers revealed a distinct overlap in identifications. They analyzed *in vitro* cultured and isolated neuronal and glial cells and identified 13,200 protein groups [Sharma et al., 2015]. Altogether, 86% of total proteins identified in our OPC differentiation data set were likewise detected in *in vitro* cultured or isolated oligodendrocytes by Sharma and co-workers. As identifier the gene names were applied. The proportion of overlapping proteins might even be higher, since some proteins in our data set are assigned to the Rat Genome Database (RGD) nomenclature, while Sharma and co-workers used the mouse UniProt database. Nevertheless, the large proportion of overlapping proteins provides a good indication for successful OPC to oligodendrocyte differentiation.

In addition, several proteins specific for oligodendrocytes were continuously upregulated during the differentiation process, including the proteins myelin proteolipid protein (PLP1), 2',3'-cyclic-nucleotide 3'-phosphodiesterase (CNP), ectonucleotide pyrophosphatase/phosphodiesterase family member 6 (ENPP6) and claudin-11 (CLDN11). Furthermore, the myelin-oligodendrocyte glycoprotein (MOG) was strongly upregulated after six days of differentiation. According to former analyses conducted, MOG expression occurs during late stages of oligodendrocyte maturation [Solly et al., 1996]. The expression pattern of MOG thus suggests that mature oligodendrocytes were developed after a differentiation period of six days so that proteins upregulated after this time point can most probably be assigned to mature oligodendrocytes. In addition, the expression of MOG is associated with the deposition of myelin sheaths *in vivo*. Thus, its expression *in vitro* indicates that *Mog* transcription is intrinsic to the oligodendroglial maturation process and does not depend on axonal or neuronal signals [Solly et al., 1996].

Furthermore, for some constantly upregulated proteins a connection to oligodendrocytes is assumed. The protein guanidinoacetate N-methyltransferase GAMT was more than two times upregulated in all differentiation time points compared to OPCs, indicating its importance in the differentiation process and in mature oligodendrocytes. It was shown to promote oligodendrocyte survival and to exert protective functions on regenerated oligodendrocytes after demyelination induction [Chamberlain et al., 2017]. Thus, GAMT might exert protective functions on oligodendroglial cells, which are especially vulnerable to various damage pathways at pre-oligodendrocyte stage [Back et al., 2002] [McDonald et al., 1998]. Moreover, since creatine represents a main compound in the energy metabolism of cells [Schmidt et al., 2004], GAMT upregulation might be the result of altered energy requirements in differentiating cells.
The integral membrane proteins tetraspanin CD9 and CD81 were likewise continuously upregulated. Compared to undifferentiated cells, CD81 exhibited increased expression levels three days after differentiation initiation, while highest expression ratios were observed after six days, indicating its involvement in the differentiation process but more prominent in mature oligodendrocytes. This correlates with the assumption that CD81 is involved in oligodendrocyte maturation and its detection in myelin sheaths [Sullivan & Geisert, 1998]. Since tetraspanin proteins, such as CD9 and CD81, are abundant in exosomes, both proteins might also be involved in the transport of myelin proteins to myelin sheaths [Krämer-Albers et al., 2007]. Moreover, CD9 and CD81 are assumed to be involved in the formation of the tetraspanin web in OPCs or premyelinating oligodendrocytes, responsible for the accomplishment of multiple processes, such as signal transduction, cell adhesion and migration [Terada et al., 2002]. However, both proteins are not essential for OPC maturation and myelination [Levy & Shoham, 2005].

Analyses performed on downregulated proteins further confirmed the success of OPC differentiation. Regarding the distribution of downregulated proteins, most proteins were significantly regulated six days after differentiation initiation. Assuming that downregulated proteins are mainly involved in OPC associated processes or that OPC differentiation requires the downregulation of these proteins, the overrepresentation of significantly downregulated proteins, especially at day 6 of the differentiation process, suggests that most cells were committed to differentiation at least six days after differentiation initiation. This is consistent with the expression pattern observed for MOG. Moreover, gene ontology (GO) enrichment analyses performed of downregulated proteins further revealed a prominent enrichment of proteins related to the mitotic

cell cycle and chromosome organization. This is consistent with the fact that prior to OPC differentiation, cells exit the cell cycle [Raff et al., 2001]. Remarkably, several proteins related to RNA processing and RNA splicing, mainly belonging to the families of dead box proteins, splicing factors or heterogeneous nuclear ribonucleoproteins were immediately and continuously downregulated. This is further consistent with the assumption that RNA splicing is linked to cell cycle progression [Ben-Yehuda et al., 2000] [Russell et al., 2000].

Biological processes involved in OPC maturation GO enrichment analyses were performed for all three time points separately and all upregulated proteins were searched against total identified proteins. For this purpose, Gene Ontology Annotation (GOA) databases were used, annotating proteins listed in UniProt to GO term identifiers [Barrell et al., 2008]. As a result, based on proteins assigned to same GO term identifiers, distinct biological processes and cellular components were found to be significantly overrepresented among others. During the initial period of OPC differentiation small GTPases were enriched. Several protein families involved in small GTPase mediated signal transduction were upregulated, like members of the Rho family (RHOA, RHOG), the Rab family (RAB10, RAB3B), the Dock family (DOCK4, DOCK6) and the Ras family (RRAS2). Besides cell signaling, cell migration and vesicular membrane trafficking, mainly the assembling and organization of the actin cytoskeleton is regulated by small GTPases [Wennerberg et al., 2005]. This is consistent with the upregulation of many proteins involved in the organization of the cytoskeleton. These proteins were especially upregulated at the beginning of the differentiation experiment, including RHOA, ARHGAP35, TNIK and CTTN, while also some proteins, including RHOG, FYN, SEPT5 and DPYSL4 were continuously upregulated. The cytoskeleton undertakes different functions within a cell reaching from mechanical support, via accomplishing transport processes, cell shape performance to intercellular communication [Geiger et al., 2009]. Since OPCs undergo considerable changes regarding their molecular cytoarchitecture during their differentiation, it is not surprising that proteins responsible for actin cytoskeleton and microtubules organization were upregulated. The upregulation of the proteins tyrosine-protein kinase Fyn and Rho GTPase-activating protein 35 (ARHGAP35) strengthen previous investigations regarding their importance in the OPC differentiation process. The kinase FYN was previously shown to be essential for morphological differentiation of OPCs [Osterhout et al., 1999] by activating the effector protein ARHGAP35 [Wolf et al., 2001]. Moreover, the process of axon myelination also requires alterations of the cytoskeleton [Wilson & Brophy, 1989]. Cytoskeleton organization is, for example, supported by the myelin proteolipid (PLP1), the protein 2',3'-cyclic-nucleotide 3'-phosphodiesterase (CNP) or MOG, who has been shown to regulate the stability of microtubules [Bauer et al., 2009] [Lee et al., 2005]. Conclusively, the upregulation of many proteins involved in cytoskeleton remodeling indicates its complexity and necessity for the differentiation and myelination process.

Moreover, GO enrichment analyses revealed that during the complete differentiation process, carbohydrate catabolic processes, including pyruvate metabolic processes or glycolytic processes, were overrepresented. GO terms related to carbohydrate catabolic processes were enriched in all analyses performed (day 3 - 9), which indicates that differentiating cells and mature oligodendrocytes exhibit an increased energy production to, for example, accomplish morphological and transcriptional changes during the differentiation process or to produce myelin lipids. In addition, glycolytic processes provide acetyl-CoA molecules, which are essential for the synthesis of fatty acids, triglycerides and cholesterol [Siegel et al., 1999].

The production of lipids was mainly enriched at day 3 of the differentiation process, including proteins providing cytosolic acetyl-CoA, derived from acetate and citrate molecules of the citric acid cycle, such as the acetyl-coenzyme A synthetase, cytoplasmic (ACSS2) and the ATP-citrate synthase (ACLY). In addition, biosynthetic processes generating isoprenoid molecules were enriched, precursor molecules usually used for cholesterin synthesis [Stryer et al., 2002]. This is consistent with the detection of proteins involved in cholesterol biosynthesis, including lanosterol synthase (LSS), farnesyl diphosphate synthase (FDPS) and transmembrane 7 superfamily member 2 (TM7SF2). The upregulation of proteins generating cholesterol is essential to ensure the compaction of myelin sheaths, which contain higher cholesterol levels than other biological membranes, or to organize lipid molecules within the myelin membrane [Morell et al., 1999] [Saher et al., 2009] [Chrast et al., 2011]. Proteins responsible for sphingolipid synthesis were upregulated during the first three days of the differentiation process, such as the ceramide synthase 1 (CERS1) or the serine incorporator 5 (SERINC5). Moreover, after six days of differentiation, proteins assigned to lipid metabolic processes were enriched, whereof some are involved in sphingolipid synthesis, such as the ceramide synthase 2 (CERS2) and the 3-ketodihydrosphingosine reductase (KDSR). Myelin contains proportionally higher amounts of long-chain fatty acids compared to other biological membranes, which might be synthesized by the at day 6 upregulated very-long-chain (3R)-3-hydroxyacyl-CoA dehydratase 3 (HACD3) [Ikeda et al., 2008].
Conclusively, the synthesis of lipids, especially cholesterol, already occurred during early stages of OPC differentiation, while proteins catalyzing the synthesis of sphingolipids were prominently enriched after six days of differentiation. The enrichment of upregulated proteins involved in lipid metabolism underlines the function of oligodendrocytes as lipid synthesizing cells.

Early upregulated proteins A particularly interesting protein for oligodendroglial development represents the peptidyl arginine deiminase, type II (PADI2). The protein was significantly upregulated three days after OPC differentiation initiation and in addition, it was significantly and strongly upregulated nine days after neurosphere differentiation initiation. PADI2 is involved in posttranscriptional modification of arginine residues in proteins, especially histones, by citrullination [Zhang et al., 2012a]. Albeit PADI2 was so far not linked to NPC to OPC differentiation, it can still be assumed that PADI2 regulates gene expression in NPCs through epigenetic modulation. Because of its strong upregulation towards the end of the experiment, also a function of PADI2 in OPCs is reasonable. The upregulation of PADI2 during OPC differentiation might be, among others, due to its function as posttranscriptional modifier of the myelin basic protein (MBP) [Akiyama et al., 1999]. Although pathological elevated PADI2 protein levels are thought to contribute to the demyelination process in multiple sclerosis patients [Musse et al., 2008], citrullination of MBP by PADI2 seems to be necessary for prenatal CNS plasticity because the proportion of citrullinated MBP diminishes rapidly in postnatal life [György et al., 2006].

The ribosomal protein S6 kinase alpha-5 (RPS6KA5) was especially upregulated three days after differentiation initiation, which might be associated with its function as activator of the transcription factor STAT3. RPS6KA5 was shown to phosphorylate a serine residue that is essential for STAT3 activation [Zhang et al., 2001]. STAT3 in turn is involved in remyelination and *in vitro* oligodendrocyte maturation [Steelman et al., 2016] as well as in OPC survival [Dell'Albani et al., 1998]. However, STAT3 was not detected in our data set. So far, CNTF and PDGF-AA are known to activate STAT3 via phosphorylation of a tyrosine residue. Accordingly, RPS6KA5 might represent an additional activator of STAT3 and thus of OPC maturation.

Further potential candidates involved in initial oligodendrocyte differentiation steps by activating subsequent signaling cascades belong to the group of cell adhesion molecules, including the cell adhesion molecule CADM4 and the nectin cell adhesion molecule 1 (NECTIN1). Both transmembrane proteins showed strongly elevated expression levels immediately after exposition to differentiation stimulating conditions, while protein levels decreased thereafter. So far, CADM4 seems to be essential for axonal myelination in the peripheral nervous system, but not for axonal myelination in the central nervous system [Golan et al., 2013] [Zhu et al., 2013]. Nonetheless, based on the expression of different nectin-like protein family members in oligodendrocytes and axons, cell adhesion molecules are suggested to be involved in early glia - axon communication, leading to the initiation of the myelination program [White & Krämer-Albers, 2013]. Accordingly, CADM4 upregulation during the initial differentiation phase might occur in order to interact with axons. Albeit the hypothesis regarding the influence of cell adhesion molecules on myelination is not consistent with the observation of decreasing protein expression levels during later stages of the differentiation experiment, the decrease indeed might be a result of missing interaction with axons due to the *in vitro* cultivation of an unique oligodendroglia population.

Moreover, the protein inositol 1,4,5-trisphosphate receptor type 2 (ITPR2) was upregulated during the OPC differentiation process until day 6, while expression levels dropped afterwards. The expression kinetic observed suggests an involvement of ITRP2 in differentiation initiation and differentiation accomplishment. So far, our results regarding ITPR2 expression are consistent with the findings of Marques and co-workers, who detected higher ITPR2 RNA levels in differentiation-committed OPCs and in newly-formed oligodendrocytes, compared to myelinating oligodendrocytes [Marques et al., 2016]. According to Marques and co-workers, cells expressing ITPR2 are the progeny of OPCs. So far, little is known about ITPR2, but that is involved in rapid myelination during complex motor learning. Its upregulation in developing oligodendrocytes might thus promote the myelination process.

Investigation of transcriptional activator protein Pur-alpha

Pur-alpha expression pattern during neural precursor cell to oligodendrocyte differentiation

The transcriptional activator protein Pur-alpha (PURA) belongs to the top upregulated transcription factors during the differentiation from neurospheres to oligospheres and from oligodendrocyte precursor cells to oligodendrocytes. Quantitative analyses of Pur-alpha expression using mass spectrometry revealed its continuous upregulation during the differentiation from neurospheres to oligospheres. Compared to undifferentiated cells, two times higher protein levels were detected after 15 days of neurospheres differentiation. The Pur-alpha protein has a molecular weight of 35 kDa. Western blots conducted using a purchased antibody against Pur-alpha always detected polypeptides at 43 and 49 kDa while the 35 kDa polypeptide was only slightly visible. Thus, the full length Pur-alpha sequence was cloned into a GST-expression vector and the protein expressed in E.coli cells. An antiserum against the purified GST-Pur-alpha fusion protein was thereafter produced. Transfection of HeLa cells with an expression vector encoding Pur-alpha and subsequent western blots performed using the commercial antibody and the antiserum confirmed that only the 43 kDa protein is Pur-alpha-specific. Most probably, the migration of Pur-alpha at higher molecular weights is caused by amino acid phosphorylations [Trinidad et al., 2012]. Accordingly, the 43 kDa protein was considered for quantification and

anti-Pur-alpha western blots further confirmed increasing protein levels during neurospheres to oligospheres differentiation. Compared to undifferentiated cells, more than two times higher protein levels were detected after 15 days of neurospheres differentiation. Moreover, anti-Pur-alpha western blot analyses using lysates derived from fetal neural stem (fNS) cells and Oli-neu cells displayed a four times higher expression in Oli-neu cells compared to fNS cells. Since fNS cells represent a homogeneous population that possesses stem cell properties, while Oli-neu cells represent a homogeneous population of oligodendrocyte precursor cells, the enhanced gene expression during neurospheres differentiation is most likely associated with oligodendroglial cells. It further suggests an even larger difference in Pur-alpha protein levels between neurospheres and oligospheres than detected, if a homogeneous population would have actually existed.

Pur-alpha expression further increased more than two fold upon differentiation of OPCs into mature oligodendrocytes, revealed by quantitative mass spectrometry. The main function of mature oligodendrocytes is the synthesis of myelin sheaths, including the expression of major myelin proteins, such as the myelin basic protein (MBP). Pur-alpha itself binds to the MBP promoter and activates the transcription of the *Mbp* gene [Haas et al., 1995]. Simultaneously, Pur-alpha prevents the binding of the MBP repressor protein MYEF2 to the promoter region. The interaction between Pur-alpha and MYEF2 was further evidenced by two affinity capture-mass spectrometry approaches performed in this thesis.

Changes in intracellular protein concentrations can have various reasons, like enhanced or repressed transcription activity, altered post-transcriptional modifications, miRNA-depending inhibition of translation or enhanced or reduced protein degradation [Cooper & Hausman, 2000] [Catalanotto et al., 2016]. The most common way how cells alter protein levels represents the regulation of transcription via transcription factors and histone modifiers. Comparison of Pur-alpha RNA levels by quantitative real-time PCR in triplicates revealed no difference between samples of undifferentiated cells and cells differentiated for 7 respectively 14 days, regarding an altered transcription activity. After normalization to two housekeeping genes, no significant changes in RNA level were detected, assuming another reason for elevated protein levels. Literature research and investigations concerning the Pur-alpha amino acid sequence conducted, most likely suggested a degradation of the Pur-alpha protein by the ubiquitin ligase enzyme anaphase-promoting complex/cyclosome (APC/C) and the proteasome pathway. Radioactive degradation assays conducted in triplicates using G1-synchronized HeLa cell lysates however did not provide any evidence of Pur-alpha being degraded by the APC/C. In contrary, the already identified APC/C substrate Securin (PTTG1) showed significant degradation by the APC/C, whereas the addition of the proteasome inhibitor MG132 diminished the degradation of Securin. Moreover, a single degradation experiment conducted using G1-synchronized fNS cell lysate did as well not confirm the degradation of Pur-alpha by the APC/C. Since APC/C activity might be influenced by Pur-alpha, a radioactive degradation assay was performed of Securin in presence of Pur-alpha using a HeLa G1-cell lysate. However, no altered degradation of Securin and thus no altered APC/C activity was observed. Besides, using the Pur-alpha antiserum, Pur-alpha was successfully immunoprecipitated after performing proteasome inhibition in HeLa and fNS cells using MG132. Subsequent performed western blots detecting ubiquitinylated Pur-alpha proteins showed no differences between control samples and proteasome inhibited samples.
Based on these findings, interaction partner analyses were performed using different approaches and cell types. Taking advantage of Pur-alpha co-immunoprecipitation approaches, few subunits

of the proteasome complex were identified, however no single protein of the APC/C was significantly detected. On the other hand, using the Pur-alpha Bio-ID approach, several proteins belonging to the proteasome complex were identified as well as proteins responsible for APC/C mediated degradation of proteins and even a component of the APC/C was significantly detected. Nevertheless, one should keep in mind that due to unspecific biotinylation, proteins are mistakenly detected as interaction partners. Consequently, more specific interaction partner analyses, like immunoprecipitation assays combined with western blot analyses are required.
Accordingly, we could not confirm the hypothesis of Pur-alpha being a substrate of the APC/C on experimental level yet. Thus, we could also not provide evidence for our hypothesis that degradation of Pur-alpha is inhibited in cells committed to the oligodendroglial lineage, thereby promoting differentiation from neurospheres to oligospheres via downregulation of c-myc.

Pur-alpha interaction partner analyses

Two different approaches and three different cell lines were used to identify proteins interacting with Pur-alpha. The cell lines fNS and Oli-neu were used for interaction partner analyses to determine proteins specifically interacting with Pur-alpha in OPCs which might thus be involved in the differentiation process from NPCs to OPCs. Each experiment was performed in biological triplicates including controls to increase the probability of identifying true interaction partners while minimizing the finding of false positives. Using the BioID assay, labeling of interacting proteins is achieved in livings cells and thus reflects the interaction of Pur-alpha in its natural environment. On the other hand, using the co-immunoprecipitation (co-IP) assay, proteins are detected in endogenous protein lysates due to their interacting nature with Pur-alpha or with a bridging molecule that interacts with Pur-alpha. However, unspecific biotinylation of proteins in the vicinity of the enzyme using the BioID assay increases the risk of detecting false positive interaction partners. Moreover, the impossibility of distinguishing between proteins that interact directly or indirectly, via another protein, with Pur-alpha in co-IP systems usually requires the confirmation using additional approaches. Since only screening experiments were performed, only proteins which were detected in more than one interaction partner analysis were considered to increase the probability of detecting true Pur-alpha interaction partner. Moreover, in the co-IP approaches proteins needed to be detected in the target and the control sample to be able to determine target to control ratios. If no ratio can be generated, the protein is not considered as interaction partner, even if the protein is highly enriched in the target co-IP assay. This was, for example, the case for four proteins that were identified as significantly enriched within one or even both other interaction partner analyses.
Altogether, 87 proteins were identified by the SILAC-BioID approach, whereas 53 respectively 76 candidates were identified by the fNS respectively Oli-neu affinity-capture MS approach. Most of these proteins were detected in only one experiment, while 34 proteins were significantly enriched in two and five proteins in all approaches. Gene ontology (GO) enrichment analyses conducted of all approaches identified similar overrepresented biological processes, suggesting that the BioID and the co-IP assay gave reasonable results. In addition, our findings are largely consistent with former findings of research groups regarding the biological function and cellular localization of Pur-alpha and its interaction partners, assuming that the identified proteins are most likely true interaction partners. According to former findings, Pur-alpha is involved in the regulation of several human viruses in the CNS and in the regulation of transcription and probably translation [Gallia et al., 2000b]. Moreover, it is responsible for the transportation of RNA

and was detected in granules together with proteins involved in protein synthesis, regulation of translation and additional RNA transporting proteins [Kanai et al., 2004]. According to our GO enrichment analyses, identified proteins are mainly involved in processes regulating viral genome replication and gene expression. Most of the Pur-alpha interaction partners we detected are RNA-binding proteins, responsible for the transport and localization of RNA molecules and similar to Pur-alpha, they play a role in the regulation of transcription, post-transcription and translation processes. During transcription initiation, Pur-alpha often forms multimeric complexes with different proteins, consisting, among others, of the transcriptional activator protein Pur-beta (PURB) [Kelm et al., 1999], nuclease-sensitive element-binding protein 1 (YB1) [Safak et al., 1999] and myelin expression factor 2 (MYEF2) [Muralidharan et al., 1997]. The identification of these proteins using BioID and co-IP assays further strengthened the interaction of mentioned proteins with Pur-alpha and the function of Pur-alpha in the transcription process.

Moreover, the proteins inhibitor of nuclear factor kappa-B kinase subunit beta and alpha (IKBKB; CHUK) and NF-kappa-B essential modulator (IKBKG) were significantly identified as Pur-alpha interaction partners using both co-IP experiments. Interestingly, these three proteins together form the IκB kinase complex, which affects the release of NF-κB by phosphorylating the NF-κB inhibitor. As a consequence, NF-κB can translocate into the nucleus, where it regulates the transcription of different genes. Since not a single, but all three subunits are immunoprecipitated together with Pur-alpha, a direct interaction of the IκB kinase complex and Pur-alpha can be assumed. Although, no connection of Pur-alpha to IκB kinases or the NF-κB pathway has been shown yet, it is though possible. Proteins regulated by NF-κB are connected to diverse processes, including proliferation, cell survival, apoptosis or inflammation [Oeckinghaus & Ghosh, 2009]. Pur-alpha, for instance, interacts with cyclin A/Cdk2 to promote cell cycle progress [Liu et al., 2005] and controls cell survival by regulating the *fas* promoter (tumor necrosis factor receptor superfamily member 6) together with YBX1 [Lasham et al., 2000]. Another connection between Pur-alpha and NF-κB exists via the regulation of viral replication of the JC virus (JCV) and the human immunodeficiency virus (HIV) in neural cells by both factors [O'Neill & Kaltschmidt, 1997] [Safak et al., 1999].

According to GO enrichment analyses, many Pur-alpha interaction partners are assigned to ribonucleoprotein (RNP) complexes, due to their function as RNA-binding proteins. RNP complexes consists of RNA-binding proteins and RNAs and represents a carrier for RNA to reach their destination [Glisovic et al., 2008]. RNA-binding proteins are responsible for the stability, function, transport and cellular localization of RNAs and especially for post-transcriptional modifications of RNAs. Actually, Ohashi and co-workers as well as Kanai and co-workers provide evidence for the involvement of Pur-alpha and multiple other detected interaction partners in the transport of specific mRNAs to dendrites [Ohashi et al., 2002] [Kanai et al., 2004]. Both groups further showed that the interaction between Pur-alpha and its target proteins is RNAse sensitive, indicating an indirect connection between Pur-alpha and those proteins, based on RNA molecules. In order to determine indirect or direct interactions between Pur-alpha and the identified proteins, co-IP assays plus the addition of RNAse is required. The necessity of this testing becomes more evident by the occurrence that mainly RNA binding proteins were detected with both methods. For instance, the four proteins ATP-dependent RNA helicase DDX3X (DDX3X), heterogeneous nuclear ribonucleoprotein Q (SYNCRIP), la-related protein 1 (LARP1) and polyadenylate-binding protein 1 (PABPC1) were significantly detected in every

experiment. DDX3X and SYNCRIP were already detected in RNA-transporting granules by Kanai and co-workers [Kanai et al., 2004], together with Pur-alpha and several other proteins identified by BioID or co-IP. LARP1 and PABPC1 in contrary, were shown to interact with each other [Suzuki et al., 2016], while PABPC1 was detected together with several other Pur-alpha interacting proteins in argonaute-containing RNA–protein complexes [Höck et al., 2007]. The argonaute protein family is mainly involved in RNA silencing processes. Besides, LARP1 usually binds RNA molecules and regulates translation, similar to Pur-alpha and thus might also directly interact with Pur-alpha. Nonetheless, proteins detected in all interaction partner analyses can be assigned to Pur-alpha through interaction with RNAs. Moreover, results further suggest that Pur-alpha is a component of ribonucleoprotein complexes and that it is involved in post-transcriptional modification of RNAs.

Furthermore, the nine proteins detected by either BioID assay and one co-immunoprecipitation assay represent promising interaction partners. Indeed, a relation of fragile X mental retardation syndrome-related protein 1 and 2 (FXR1; FXR2), double-stranded RNA-binding protein staufen homolog 1 (STAU1) and YBX1 to Pur-alpha was already shown. The first three mentioned proteins were detected in RNA transporting granules [Kanai et al., 2004]. Additionally, while the synaptic functional regulator FMR1, another protein homologous to FXR1 and FXR2, was significantly identified in both co-IP approaches, it was not identified in the HEK293T BioID assay. That is because the protein is prominently expressed in neurons and oligodendroglia [Wang et al., 2004]. With clathrin heavy chain 1 (CLTC), a protein was significantly detected by BioID and fNS co-IP assay, which is required for the function of the mitotic spindle by contributing to the kinetochore fibre stability [Royle et al., 2005], for the generation of vesicles for protein transfer [Huang et al., 2004] and which is most probably able to bind RNA molecules. At least, CLTC and Pur-alpha were detected in a mass spectrometry approach aiming the identification of the mRNA-bound proteome [Baltz et al., 2012] and thus might be connected via RNA in RNP complexes. In total, Baltz and co-workers identified 800 RNA-binding proteins, including cold shock domain-containing protein E1 (CSDE1), another Pur-alpha interaction partner identified using BioID and Oli-neu co-IP assay. Several more potential Pur-alpha interaction partners were detected within these complexes, like the mRNA stabilizing proteins ELAV-like protein 1 and 2 (ELAV1; ELAV2) or the interleukin enhancer-binding factors ILF2 and ILF3.

Pur-alpha function during neural precursor cell to oligodendrocyte differentiation

So far, multiple functions are postulated for Pur-alpha, including DNA replication initiation or transcriptional regulation by activating and repressing transcription of target genes. Originally, Pur-alpha was characterized by its ability to bind to the PUR element, a DNA sequence located upstream of the *c-myc* gene [Bergemann & Johnson, 1992]. MYC itself affects several cellular processes including cell proliferation, differentiation and apoptosis [Evan & Littlewood, 1993] [Evan et al., 1994]. Although MYC functions might vary between different cell types, considerable evidence suggests that MYC promotes cell proliferation while inhibiting cell differentiation. This is consistent with the observations that MYC inactivation uncovered pluripotent differentiation [Shachaf et al., 2004] and that cell cycle arrest leads to the downregulation of MYC expression upon differentiation of pancreatic endocrine cells [Demeterco et al., 2002]. Moreover, MYC plays a role in controlling the switching mechanism between proliferation and differentiation in these cells. Accordingly, upon regulating *c-myc* gene expression, Pur-alpha might

affect NPC to OPC differentiation. In addition, Pur-alpha positively regulates platelet-derived growth factor A (PDGFA) expression upon binding to its promoter region [Zhang et al., 2005]. The growth factor PDGFA in turn was shown to be a major factor of NPC to OPC differentiation *in vitro* by activating distinct signaling pathways involved in cell proliferation and differentiation [Hu et al., 2012a]. This leads to the assumption that Pur-alpha might promote the differentiation to OPCs as a transcriptional activator of *Pdgfa* gene expression. Besides, Pur-alpha was shown to directly bind to the transcription factor E2F1, which in turn plays an essential role in regulating the transition from proliferation to quiescence. Moreover, its nuclear protein levels was shown to decline upon differentiation to oligodendrocytes and thus its impact on transcriptional regulation likewise declines [Magri et al., 2014]. Accordingly, the interaction of Pur-alpha and E2F1 might have a negative impact on NPC proliferation by inhibiting its function as enhancer of cell cycle progression [Darbinian et al., 2004]. Conclusively, since Pur-alpha seems to regulate the transcription of various proteins or to inhibit the activity of transcription factors involved in proliferation and differentiation processes, increasing Pur-alpha levels during neurosphere differentiation are most likely to promote differentiation to oligospheres.

Additional Pur-alpha interaction partners driving the differentiation process At a first glance, many Pur-alpha interaction partners identified in Oli-neu cells were similarly detected in fNS cells and additionally enriched biological processes were mainly equal between both groups. This is most probably due to the prominent detection of RNA-binding proteins. Nevertheless, some interesting proteins were significantly identified using the Oli-neu co-IP assay, that were not or less enriched (Oli-neu / fNS log2 fold change ratio greater 1) in the fNS co-IP assay.
This applied, for example, to the G-protein coupled receptor 157 (GPR157). Little is known about the protein, except that it promotes the differentiation of radial glial progenitor cells to neurons. Two probable explanations regarding the interaction between both proteins is conceivable. Since the functions of neurons and oligodendroglia are closely linked to each other, Pur-alpha might promote differentiation of neurons upon interacting with GPR157 [Takeo et al., 2016]. However, since the interaction between Pur-alpha and GPR157 was detected in oligodendroglial cells, another relation between both proteins is more likely. Since Pur-alpha also negatively affects proteins, it might promote the differentiation of radial glial progenitor cells to oligodendroglial cells instead of neuronal cells by interfering with GPR157.
In addition, the serine protease HTRA1 was identified in the interaction partner analyis conducted using Oli-neu cells and most intrestingly, the protein levels of Pur-alpha and HTRA1 increased significantly during the neurosphere to oligosphere differentiation experiment. Several functions for the protease have been postulated yet. The most likely explanation for increasing HTRA1 protein levels during neurosphere differentiation is that HTRA1 inhibits the bone morphogenetic protein (BMP) pathway. HTRA1 binds to several proteins of the transforming growth factor (TGF)-β family, including BMP4, an inducer of BMP signaling, which inhibits oligodendrogenesis, while favoring astrogliogenesis [Oka et al., 2004] [Samanta & Kessler, 2004]. It can thus be assumed, that HTRA1 is an important mediator of oligodendroglial cell fate determination. Although HTRA1 and Pur-alpha seem to drive the differentiation process in differential ways by affecting varying pathways, the detected interaction between both proteins in Oli-neu cells suggests an additional mechanism how Pur-alpha and HTRA1 affect NPC to OPC differentiation. Nonetheless, first, the direct interaction of both proteins need to be confirmed before additional experiments regarding their functions in OPCs should be performed.

Multiple Pur-alpha interaction partners identified in Oli-neu cells, including protein argonaute-2 (AGO2), synaptic functional regulator FMR1 (FMRP) and its homologous proteins fragile X mental retardation syndrome-related protein 1 and 2 (FXR1; FXR2) are associated with the microRNA (miRNA) pathway. MicroRNAs, together with AGO2, form the RNA-induced silencing complex (RISC), which targets and cleaves mRNA [Goff et al., 2009]. FMRP in contrary interacts with microRNAs and Dicer, a miRNA-processing enzyme, which produces functional miRNAs from precursor miRNAs [Jin et al., 2004]. MicroRNAs in turn are small non-coding RNAs that regulates gene expression at the post-transcriptional level and are implicated, among others, in the regulation of neural stem cell fate and in oligodendrocyte differentiation [Lopez-Ramirez & Nicoli, 2014] [Galloway & Moore, 2016]. The interaction of Pur-alpha with mentioned proteins thus suggets a function of Pur-alpha in the miRNA pathway and probably in the regulation of cell fate determination. However, Pur-alpha was formerly identified together with FMRP in mRNP complexes [Jin et al., 2007], while an interaction between FMRP and AGO2 was likewise evidenced [Kenny et al., 2014]. Conclusively, the detected interaction of Pur-alpha and AGO2 in Oli-neu cells using the co-IP assay might also result from an indirect interaction via FRMP. Therefore the enrichment of miRNA associated proteins in the Oli-neu cell assay might be the result of indirect interaction. Conclusively, the association of Pur-alpha to the microRNA pathway remains hypothetic and needs to be confirmed by further studies.

Summary and outlook

In summary, using quantitative mass spectometry approaches, a proteomic database of neural precursor cell to oligodendrocyte precursor cell differentiation and of oligodendrocyte precursor cell to oligodendrocyte differentiation could be generated. In the course of this, multiple promising effector proteins of differentiation were identified, whose impact on the differentiation process have to be verified by additional experiments. Regarding the OPC differentiation experiment, the measurement of additional time points at the beginning of the differentiation process should be considered, since most likely the main processes of OPC differentiation took place during the first three days and differentiation seemed to be accomplished after six days of differentiation. As a result, one might be able to draw more distinct conclusions regarding the regulation and the functions of interesting proteins, based on a more detailed expression pattern.

In this thesis, increasing Pur-alpha protein levels were observed during neural progenitor cell to oligodendrocyte precursor cell differentiation, while RNA levels stayed constant during the differentiation process. Pur-alpha degradation by the anaphase-promoting complex/cyclosome in HeLa or fNS cells could not be proven using ubiquitination and degradation assays. Nonetheless, although no experimental confirmation could be given yet, a complete exclusion would not be reasonable before trying other approaches. Many research groups, for example, commonly use an alternative protocol by isolating APC/C from *Xenopus laevis* eggs instead of using a G1-synchronized cell lysate, containing less concentrated APC/C.
Regarding the identification of Pur-alpha interaction partners, quantitative affinity capture-MS assays and BioID assays coupled to mass spectrometry are well suitable approaches to perform interaction partner screenings. Nonetheless, follow-up experiments are necessary to either confirm the interaction between bait protein and its interaction partners as well as to determine a direct or indirect interaction.

Bibliography

[Abrajano et al., 2010] Abrajano, J. J., Qureshi, I. A., Gokhan, S., Molero, A. E., Zheng, D., Bergman, A., & Mehler, M. F. (2010). Corepressor for element-1–silencing transcription factor preferentially mediates gene networks underlying neural stem cell fate decisions. *Proceedings of the National Academy of Sciences*, 107(38), 16685–16690.

[Abrajano et al., 2009] Abrajano, J. J., Qureshi, I. A., Gokhan, S., Zheng, D., Bergman, A., & Mehler, M. F. (2009). Differential deployment of rest and corest promotes glial subtype specification and oligodendrocyte lineage maturation. *PloS one*, 4(11), e7665.

[Aebersold & Mann, 2016] Aebersold, R. & Mann, M. (2016). Mass-spectrometric exploration of proteome structure and function. *Nature*, 537(7620), 347–355.

[Akiyama et al., 1999] Akiyama, K., Sakurai, Y., Asou, H., & Senshu, T. (1999). Localization of peptidylarginine deiminase type ii in a stage-specific immature oligodendrocyte from rat cerebral hemisphere. *Neuroscience letters*, 274(1), 53–55.

[Alizadeh et al., 2015] Alizadeh, A., Dyck, S. M., & Karimi-Abdolrezaee, S. (2015). Myelin damage and repair in pathologic cns: challenges and prospects. *Frontiers in molecular neuroscience*, 8, 35.

[Almazan et al., 1985] Almazan, G., Honegger, P., & Matthieu, J.-M. (1985). Triiodothyronine stimulation of oligodendroglial differentiation and myelination. *Developmental neuroscience*, 7(1), 45–54.

[Altevogt et al., 2002] Altevogt, B. M., Kleopa, K. A., Postma, F. R., Scherer, S. S., & Paul, D. L. (2002). Connexin29 is uniquely distributed within myelinating glial cells of the central and peripheral nervous systems. *Journal of Neuroscience*, 22(15), 6458–6470.

[Anthony et al., 2004] Anthony, T. E., Klein, C., Fishell, G., & Heintz, N. (2004). Radial glia serve as neuronal progenitors in all regions of the central nervous system. *Neuron*, 41(6), 881–890.

[Apweiler et al., 2004] Apweiler, R., Bairoch, A., Wu, C. H., Barker, W. C., Boeckmann, B., Ferro, S., Gasteiger, E., Huang, H., Lopez, R., Magrane, M., et al. (2004). Uniprot: the universal protein knowledgebase. *Nucleic acids research*, 32(suppl_1), D115–D119.

[Araque & Navarrete, 2010] Araque, A. & Navarrete, M. (2010). Glial cells in neuronal network function. *Philosophical Transactions of the Royal Society of London B: Biological Sciences*, 365(1551), 2375–2381.

[Ariyannur et al., 2010] Ariyannur, P. S., Moffett, J. R., Madhavarao, C. N., Arun, P., Vishnu, N., Jacobowitz, D. M., Hallows, W. C., Denu, J. M., & Namboodiri, A. (2010). Nuclear-cytoplasmic localization of acetyl coenzyme a synthetase-1 in the rat brain. *Journal of Comparative Neurology*, 518(15), 2952–2977.

[Ashburner et al., 2000] Ashburner, M., Ball, C. A., Blake, J. A., Botstein, D., Butler, H., Cherry, J. M., Davis, A. P., Dolinski, K., Dwight, S. S., Eppig, J. T., et al. (2000). Gene ontology: tool for the unification of biology. *Nature genetics*, 25(1), 25–29.

[Aston et al., 2005] Aston, C., Jiang, L., & Sokolov, B. (2005). Transcriptional profiling reveals evidence for signaling and oligodendroglial abnormalities in the temporal cortex from patients with major depressive disorder. *Molecular psychiatry*, 10(3), 309–322.

[Avval & Holmgren, 2009] Avval, F. Z. & Holmgren, A. (2009). Molecular mechanisms of thioredoxin and glutaredoxin as hydrogen donors for mammalian s phase ribonucleotide reductase. *Journal of Biological Chemistry*, 284(13), 8233–8240.

[Azevedo et al., 2009] Azevedo, F. A., Carvalho, L. R., Grinberg, L. T., Farfel, J. M., Ferretti, R. E., Leite, R. E., Lent, R., Herculano-Houzel, S., et al. (2009). Equal numbers of neuronal and nonneuronal cells make the human brain an isometrically scaled-up primate brain. *Journal of Comparative Neurology*, 513(5), 532–541.

[Baas et al., 1997] Baas, D., Bourbeau, D., Sarlieve, L. L., Ittel, M.-E., Dussault, J. H., & Puymirat, J. (1997). Oligodendrocyte maturation and progenitor cell proliferation are independently regulated by thyroid hormone. *Glia*, 19(4), 324–332.

[Back et al., 2002] Back, S. A., Han, B. H., Luo, N. L., Chricton, C. A., Xanthoudakis, S., Tam, J., Arvin, K. L., & Holtzman, D. M. (2002). Selective vulnerability of late oligodendrocyte progenitors to hypoxia–ischemia. *Journal of Neuroscience*, 22(2), 455–463.

[Baltz et al., 2012] Baltz, A. G., Munschauer, M., Schwanhäusser, B., Vasile, A., Murakawa, Y., Schueler, M., Youngs, N., Penfold-Brown, D., Drew, K., Milek, M., Wyler, E., Bonneau, R., Selbach, M., Dieterich, C., & Landthaler, M. (2012). The mRNA-Bound Proteome and Its Global Occupancy Profile on Protein-Coding Transcripts. *Molecular Cell*, 46(5), 674–690.

[Bannister & Kouzarides, 2011] Bannister, A. J. & Kouzarides, T. (2011). Regulation of chromatin by histone modifications. *Cell research*, 21(3), 381–395.

[Bantscheff et al., 2007] Bantscheff, M., Schirle, M., Sweetman, G., Rick, J., & Kuster, B. (2007). Quantitative mass spectrometry in proteomics: a critical review. *Analytical and bioanalytical chemistry*, 389(4), 1017–1031.

[Baron et al., 2005] Baron, W., Colognato, H., & Ffrench-Constant, C. (2005). Integrin-growth factor interactions as regulators of oligodendroglial development and function. *Glia*, 49(4), 467–479.

[Barr & Johnson, 2001] Barr, S. M. & Johnson, E. M. (2001). Ras-induced colony formation and anchorage-independent growth inhibited by elevated expression of purα in nih3t3 cells. *Journal of cellular biochemistry*, 81(4), 621–638.

[Barrell et al., 2008] Barrell, D., Dimmer, E., Huntley, R. P., Binns, D., O'donovan, C., & Apweiler, R. (2008). The goa database in 2009—an integrated gene ontology annotation resource. *Nucleic acids research*, 37(suppl_1), D396–D403.

[Barry & McDermott, 2005] Barry, D. & McDermott, K. (2005). Differentiation of radial glia from radial precursor cells and transformation into astrocytes in the developing rat spinal cord. *Glia*, 50(3), 187–197.

[Bauer et al., 2009] Bauer, N. G., Richter-Landsberg, C., & Ffrench-Constant, C. (2009). Role of the oligodendroglial cytoskeleton in differentiation and myelination. *Glia*, 57(16), 1691–1705.

[Baumann & Pham-Dinh, 2001] Baumann, N. & Pham-Dinh, D. (2001). Biology of oligodendrocyte and myelin in the mammalian central nervous system. *Physiological reviews*, 81(2), 871–927.

[Ben-Yehuda et al., 2000] Ben-Yehuda, S., Dix, I., Russell, C. S., McGarvey, M., Beggs, J. D., & Kupiec, M. (2000). Genetic and physical interactions between factors involved in both cell cycle progression and pre-mrna splicing in saccharomyces cerevisiae. *Genetics*, 156(4), 1503–1517.

[Benninger et al., 2006] Benninger, Y., Colognato, H., Thurnherr, T., Franklin, R. J., Leone, D. P., Atanasoski, S., Nave, K.-A., Suter, U., Relvas, J. B., et al. (2006). β1-integrin signaling mediates premyelinating oligodendrocyte survival but is not required for cns myelination and remyelination. *Journal of Neuroscience*, 26(29), 7665–7673.

[Bergemann & Johnson, 1992] Bergemann, A. D. & Johnson, E. M. (1992). The hela pur factor binds single-stranded dna at a specific element conserved in gene flanking regions and origins of dna replication. *Molecular and cellular biology*, 12(3), 1257–1265.

[Bernstein et al., 2012] Bernstein, H.-G., Smalla, K.-H., Dürrschmidt, D., Keilhoff, G., Dobrowolny, H., Steiner, J., Schmitt, A., Kreutz, M. R., & Bogerts, B. (2012). Increased density of prohibitin-immunoreactive oligodendrocytes in the dorsolateral prefrontal white matter of subjects with schizophrenia suggests extraneuronal roles for the protein in the disease. *Neuromolecular medicine*, 14(4), 270–280.

[Bez et al., 2003] Bez, A., Corsini, E., Curti, D., Biggiogera, M., Colombo, A., Nicosia, R. F., Pagano, S. F., & Parati, E. A. (2003). Neurosphere and neurosphere-forming cells: morphological and ultrastructural characterization. *Brain research*, 993(1), 18–29.

[Bian, 2013] Bian, S. (2013). Cell adhesion molecules in neural stem cell and stem cell-based therapy for neural disorders. In *Neural Stem Cells-New Perspectives*. InTech.

[Bjartmar & Trapp, 2001] Bjartmar, C. & Trapp, B. D. (2001). Axonal and neuronal degeneration in multiple sclerosis: mechanisms and functional consequences. *Current opinion in neurology*, 14(3), 271–278.

[Blank & Prinz, 2014] Blank, T. & Prinz, M. (2014). Nf-κb signaling regulates myelination in the cns. *Frontiers in molecular neuroscience*, 7, 47.

[Boersema et al., 2009] Boersema, P. J., Raijmakers, R., Lemeer, S., Mohammed, S., & Heck, A. J. R. (2009). Multiplex peptide stable isotope dimethyl labeling for quantitative proteomics. *Nature protocols*, 4(4), 484–94.

[Bouwmeester et al., 2004] Bouwmeester, T., Bauch, A., Ruffner, H., Angrand, P.-O., Bergamini, G., Croughton, K., Cruciat, C., Eberhard, D., Gagneur, J., Ghidelli, S., et al. (2004). A physical and functional map of the human tnf-[alpha]/nf-[kappa] b signal transduction pathway. *Nature cell biology*, 6(2), 97.

[Broughton et al., 2007] Broughton, S. K., Chen, H., Riddle, A., Kuhn, S. E., Nagalla, S., Roberts, C. T., & Back, S. A. (2007). Large-scale generation of highly enriched neural stem-cell-derived oligodendroglial cultures: maturation-dependent differences in insulin-like growth factor-mediated signal transduction. *Journal of neurochemistry*, 100(3), 628–638.

[Bylund et al., 2003] Bylund, M., Andersson, E., Novitch, B. G., & Muhr, J. (2003). Vertebrate neurogenesis is counteracted by sox1-3 activity. *Nature neuroscience*, 6(11), 1162.

[Cahoy et al., 2008] Cahoy, J. D., Emery, B., Kaushal, A., Foo, L. C., Zamanian, J. L., Christopherson, K. S., Xing, Y., Lubischer, J. L., Krieg, P. A., Krupenko, S. A., et al. (2008). A transcriptome database for astrocytes, neurons, and oligodendrocytes: a new resource for understanding brain development and function. *Journal of Neuroscience*, 28(1), 264–278.

[Canoll et al., 1996] Canoll, P. D., Musacchio, J., Hardy, R., Reynolds, R., Marchionni, M. A., & Salzer, J. L. (1996). Ggf/neuregulin is a neuronal signal that promotes the proliferation and survival and inhibits the differentiation of oligodendrocyte progenitors. *Neuron*, 17(2), 229–243.

[Carbon et al., 2008] Carbon, S., Ireland, A., Mungall, C. J., Shu, S., Marshall, B., & Lewis, S. (2008). Amigo: online access to ontology and annotation data. *Bioinformatics*, 25(2), 288–289.

[Castro et al., 2005] Castro, A., Bernis, C., Vigneron, S., Labbe, J.-C., & Lorca, T. (2005). The anaphase-promoting complex: a key factor in the regulation of cell cycle. *Oncogene*, 24(3), 314–325.

[Catalanotto et al., 2016] Catalanotto, C., Cogoni, C., & Zardo, G. (2016). Microrna in control of gene expression: an overview of nuclear functions. *International journal of molecular sciences*, 17(10), 1712.

[Catherman et al., 2014] Catherman, A. D., Skinner, O. S., & Kelleher, N. L. (2014). Top down proteomics: facts and perspectives. *Biochemical and biophysical research communications*, 445(4), 683–693.

[Chaerkady et al., 2011] Chaerkady, R., Letzen, B., Renuse, S., Sahasrabuddhe, N. a., Kumar, P., All, A. H., Thakor, N. V., Delanghe, B., Gearhart, J. D., Pandey, A., & Kerr, C. L. (2011). Quantitative temporal proteomic analysis of human embryonic stem cell differentiation into oligodendrocyte progenitor cells. *Proteomics*, 11(20), 4007–20.

[Chahrour et al., 2015] Chahrour, O., Cobice, D., & Malone, J. (2015). Stable isotope labelling methods in mass spectrometry-based quantitative proteomics. *Journal of pharmaceutical and biomedical analysis*, 113, 2–20.

[Chamberlain et al., 2017] Chamberlain, K. A., Chapey, K. S., Nanescu, S. E., & Huang, J. K. (2017). Creatine enhances mitochondrial-mediated oligodendrocyte survival after demyelinating injury. *Journal of Neuroscience*, 37(6), 1479–1492.

[Chandran et al., 2003] Chandran, S., Kato, H., Gerreli, D., Compston, A., Svendsen, C. N., & Allen, N. D. (2003). Fgf-dependent generation of oligodendrocytes by a hedgehog-independent pathway. *Development*, 130(26), 6599–6609.

[Cheli et al., 2015] Cheli, V., González, D. S., Spreuer, V., & Paez, P. (2015). Voltage-gated ca++ entry promotes oligodendrocyte progenitor cell maturation and myelination in vitro. *Experimental neurology*, 265, 69–83.

[Chen et al., 2007] Chen, Y., Balasubramaniyan, V., Peng, J., Hurlock, E. C., Tallquist, M., Li, J., & Lu, Q. R. (2007). Isolation and culture of rat and mouse oligodendrocyte precursor cells. *Nature protocols*, 2(5), 1044–1051.

[Choe et al., 2014] Choe, Y., Huynh, T., & Pleasure, S. J. (2014). Migration of oligodendrocyte progenitor cells is controlled by transforming growth factor β family proteins during corticogenesis. *Journal of Neuroscience*, 34(45), 14973–14983.

[Chojnacki & Weiss, 2008] Chojnacki, A. & Weiss, S. (2008). Production of neurons, astrocytes and oligodendrocytes from mammalian cns stem cells. *Nature protocols*, 3(6), 935–940.

[Chrast et al., 2011] Chrast, R., Saher, G., Nave, K.-A., & Verheijen, M. H. (2011). Lipid metabolism in myelinating glial cells: lessons from human inherited disorders and mouse models. *Journal of lipid research*, 52(3), 419–434.

[Clausen et al., 2002] Clausen, T., Southan, C., & Ehrmann, M. (2002). The htra family of proteases: implications for protein composition and cell fate. *Molecular cell*, 10(3), 443–455.

[Colangelo et al., 2013] Colangelo, C. M., Chung, L., Bruce, C., & Cheung, K.-H. (2013). Review of software tools for design and analysis of large scale mrm proteomic datasets. *Methods*, 61(3), 287–298.

[Colello et al., 2002] Colello, R. J., Fuss, B., Fox, M. A., & Alberti, J. (2002). A proteomic approach to rapidly elucidate oligodendrocyte-associated proteins expressed in the myelinating rat optic nerve. *Electrophoresis*, 23(1), 144–151.

[Collin et al., 2010] Collin, R. W., Safieh, C., Littink, K. W., Shalev, S. A., Garzozi, H. J., Rizel, L., Abbasi, A. H., Cremers, F. P., den Hollander, A. I., Klevering, B. J., et al. (2010). Mutations in c2orf71 cause autosomal-recessive retinitis pigmentosa. *The American Journal of Human Genetics*, 86(5), 783–788.

[Conti et al., 2005] Conti, L., Pollard, S. M., Gorba, T., Reitano, E., Toselli, M., Biella, G., Sun, Y., Sanzone, S., Ying, Q.-L., Cattaneo, E., & Smith, A. (2005). Niche-independent symmetrical self-renewal of a mammalian tissue stem cell. *PLoS biology*, 3(9), e283.

[Cooper & Hausman, 2000] Cooper, G. M. & Hausman, R. E. (2000). *The cell: a molecular approach*. Sinauer Associates, Inc., Publishers, 2 edition.

[Coppi et al., 2013] Coppi, E., Maraula, G., Fumagalli, M., Failli, P., Cellai, L., Bonfanti, E., Mazzoni, L., Coppini, R., Abbracchio, M. P., Pedata, F., & Pugliese, A. M. (2013). UDP-glucose enhances outward K+ currents necessary for cell differentiation and stimulates cell migration by activating the GPR17 receptor in oligodendrocyte precursors. *Glia*, 61(7), 1155–1171.

[Copray et al., 2009] Copray, S., Huynh, J. L., Sher, F., Casaccia-Bonnefil, P., & Boddeke, E. (2009). Epigenetic mechanisms facilitating oligodendrocyte development, maturation, and aging. *Glia*, 57(15), 1579–1587.

[Cottrell & London, 1999] Cottrell, J. S. & London, U. (1999). Probability-based protein identification by searching sequence databases using mass spectrometry data. *electrophoresis*, 20(18), 3551–3567.

[Cox & Mann, 2008] Cox, J. & Mann, M. (2008). Maxquant enables high peptide identification rates, individualized ppb-range mass accuracies and proteome-wide protein quantification. *Nature biotechnology*, 26(12), 1367–1372.

[Cox et al., 2011] Cox, J., Neuhauser, N., Michalski, A., Scheltema, R. A., Olsen, J. V., & Mann, M. (2011). Andromeda: a peptide search engine integrated into the maxquant environment. *Journal of proteome research*, 10(4), 1794–1805.

[Cui et al., 2014] Cui, Q. L., Fang, J., Kennedy, T. E., Almazan, G., & Antel, J. P. (2014). Role of p38MAPK in S1P receptor-mediated differentiation of human oligodendrocyte progenitors. *Glia*, 62(8), 1361–1375.

[Czepiel et al., 2014] Czepiel, M., Leicher, L., Becker, K., Boddeke, E., & Copray, S. (2014). Overexpression of polysialylated neural cell adhesion molecule improves the migration capacity of induced pluripotent stem cell-derived oligodendrocyte precursors. *Stem cells translational medicine*, 3(9), 1100–1109.

[Darbinian et al., 2001a] Darbinian, N., Gallia, G. L., & Khalili, K. (2001a). Helix-destabilizing properties of the human single-stranded dna-and rna-binding protein purα. *Journal of cellular biochemistry*, 80(4), 589–595.

[Darbinian et al., 2001b] Darbinian, N., Gallia, G. L., King, J., Del Valle, L., Johnson, E. M., & Khalili, K. (2001b). Growth inhibition of glioblastoma cells by human purα. *Journal of cellular physiology*, 189(3), 334–340.

[Darbinian et al., 2001c] Darbinian, N., Sawaya, B. E., Khalili, K., Jaffe, N., Wortman, B., Giordano, A., & Amini, S. (2001c). Functional interaction between cyclin t1/cdk9 and purα determines the level of tnfα promoter activation by tat in glial cells. *Journal of neuroimmunology*, 121(1), 3–11.

[Darbinian et al., 2004] Darbinian, N., White, M. K., Gallia, G. L., Amini, S., Rappaport, J., & Khalili, K. (2004). Interaction between the purα and e2f-1 transcription factors. *Anticancer research*, 24(5A), 2585–2594.

[Davey et al., 2011] Davey, J. W., Hohenlohe, P. A., Etter, P. D., Boone, J. Q., Catchen, J. M., & Blaxter, M. L. (2011). Genome-wide genetic marker discovery and genotyping using next-generation sequencing. *Nature reviews. Genetics*, 12(7), 499.

[Dawson et al., 2003] Dawson, M. R., Polito, A., Levine, J. M., & Reynolds, R. (2003). Ng2-expressing glial progenitor cells: an abundant and widespread population of cycling cells in the adult rat cns. *Molecular and Cellular Neuroscience*, 24(2), 476–488.

[De Castro & Bribián, 2005] De Castro, F. & Bribián, A. (2005). The molecular orchestra of the migration of oligodendrocyte precursors during development. *Brain Research Reviews*, 49(2), 227–241.

[De Rossi et al., 2016] De Rossi, P., Buggia-Prévot, V., Clayton, B. L., Vasquez, J. B., van Sanford, C., Andrew, R. J., Lesnick, R., Botté, A., Deyts, C., Salem, S., et al. (2016). Predominant expression of alzheimer's disease-associated bin1 in mature oligodendrocytes and localization to white matter tracts. *Molecular neurodegeneration*, 11(1), 59.

[Decker et al., 2000] Decker, L., Avellana-Adalid, V., Nait-Oumesmar, B., Durbec, P., & Baron-Van Evercooren, A. (2000). Oligodendrocyte precursor migration and differentiation: combined effects of psa residues, growth factors, and substrates. *Molecular and Cellular Neuroscience*, 16(4), 422–439.

[Dell'Albani et al., 1998] Dell'Albani, P., Kahn, M., Cole, R., Condorelli, D., Giuffrida-Stella, A., & De Vellis, J. (1998). Oligodendroglial survival factors, pdgf-aa and cntf, activate similar jak/stat signaling pathways. *Journal of neuroscience research*, 54(2), 191–205.

[Demeterco et al., 2002] Demeterco, C., Itkin-Ansari, P., Tyrberg, B., Ford, L. P., Jarvis, R. A., & Levine, F. (2002). c-myc controls proliferation versus differentiation in human pancreatic endocrine cells. *The Journal of Clinical Endocrinology & Metabolism*, 87(7), 3475–3485.

[Deneen et al., 2006] Deneen, B., Ho, R., Lukaszewicz, A., Hochstim, C. J., Gronostajski, R. M., & Anderson, D. J. (2006). The transcription factor nfia controls the onset of gliogenesis in the developing spinal cord. *Neuron*, 52(6), 953–968.

[Di Salvio et al., 2015] Di Salvio, M., Piccinni, V., Gerbino, V., Mantoni, F., Camerini, S., Lenzi, J., Rosa, A., Chellini, L., Loreni, F., Carrì, M. T., Bozzoni, I., Cozzolino, M., & Cestra, G. (2015). Pur-alpha functionally interacts with FUS carrying ALS-associated mutations. *Cell death & disease*, 6, e1943.

[Dimou et al., 2008] Dimou, L., Simon, C., Kirchhoff, F., Takebayashi, H., & Götz, M. (2008). Progeny of olig2-expressing progenitors in the gray and white matter of the adult mouse cerebral cortex. *Journal of Neuroscience*, 28(41), 10434–10442.

[Dincman et al., 2012] Dincman, T. A., Beare, J. E., Ohri, S. S., & Whittemore, S. R. (2012). Isolation of cortical mouse oligodendrocyte precursor cells. *Journal of neuroscience methods*, 209(1), 219–226.

[Dion et al., 2015] Dion, V., Boerboom, A., Pieltain, A., Chariot, A., & Franzen, R. (2015). Role of elongator in central nervous system remyelination. In *Front. Neurosci. Conference*

Abstract: 11th National Congress of the Belgian Society for Neuroscience. doi: 10.3389/conf. fnins, volume 26.

[Dowell et al., 2008] Dowell, J. A., Frost, D. C., Zhang, J., & Li, L. (2008). Comparison of two-dimensional fractionation techniques for shotgun proteomics. *Analytical chemistry*, 80(17), 6715–6723.

[Downes et al., 1994] Downes, C. S., Clarke, D. J., Mullinger, A. M., Giménez-Abián, J. F., Creighton, A. M., & Johnson, R. T. (1994). A topoisomerase ii-dependent g2 cycle checkpoint in mammalian cells. *Nature*, 372(6505), 467–470.

[Doyle et al., 2012] Doyle, A., McGarry, M. P., Lee, N. A., & Lee, J. J. (2012). The construction of transgenic and gene knockout/knockin mouse models of human disease. *Transgenic research*, 21(2), 327–349.

[Dryden et al., 2003] Dryden, S. C., Nahhas, F. A., Nowak, J. E., Goustin, A.-S., & Tainsky, M. A. (2003). Role for human sirt2 nad-dependent deacetylase activity in control of mitotic exit in the cell cycle. *Molecular and cellular biology*, 23(9), 3173–3185.

[Dubois-Dalcq et al., 1986] Dubois-Dalcq, M., Behar, T., Hudson, L., & Lazzarini, R. (1986). Emergence of three myelin proteins in oligodendrocytes cultured without neurons. *The Journal of cell biology*, 102(2), 384–392.

[Duchala et al., 1995] Duchala, C. S., Asotra, K., & Macklin, W. B. (1995). Expression of cell surface markers and myelin proteins in cultured oligodendrocytes from neonatal brain of rat and mouse: A comparative study (part 1 of 2). *Developmental neuroscience*, 17(2), 70–75.

[Dugas et al., 2006] Dugas, J. C., Tai, Y. C., Speed, T. P., Ngai, J., & Barres, B. A. (2006). Functional genomic analysis of oligodendrocyte differentiation. *Journal of Neuroscience*, 26(43), 10967–10983.

[Dumont et al., 2007a] Dumont, D., Noben, J.-P., Moreels, M., Vanderlocht, J., Hellings, N., Vandenabeele, F., Lambrichts, I., Stinissen, P., & Robben, J. (2007a). Characterization of mature rat oligodendrocytes: a proteomic approach. *Journal of neurochemistry*, 102(2), 562–576.

[Dumont et al., 2007b] Dumont, D., Noben, J.-P., Moreels, M., Vanderlocht, J., Hellings, N., Vandenabeele, F., Lambrichts, I., Stinissen, P., & Robben, J. (2007b). Characterization of mature rat oligodendrocytes: a proteomic approach. *Journal of neurochemistry*, 102(2), 562–76.

[Eden et al., 2009] Eden, E., Navon, R., Steinfeld, I., Lipson, D., & Yakhini, Z. (2009). Gorilla: a tool for discovery and visualization of enriched go terms in ranked gene lists. *BMC bioinformatics*, 10(1), 48.

[El Waly et al., 2014] El Waly, B., Macchi, M., Cayre, M., & Durbec, P. (2014). Oligodendrogenesis in the normal and pathological central nervous system. *Frontiers in neuroscience*, 8, 145.

[Ellenbroek & Youn, 2016] Ellenbroek, B. & Youn, J. (2016). Rodent models in neuroscience research: is it a rat race? *Disease models & mechanisms*, 9(10), 1079–1087.

[Ellinger-Ziegelbauer et al., 1997] Ellinger-Ziegelbauer, H., Brown, K., Kelly, K., & Siebenlist, U. (1997). Direct activation of the stress-activated protein kinase (sapk) and extracellular signal-regulated protein kinase (erk) pathways by an inducible mitogen-activated protein kinase/erk kinase kinase 3 (mekk) derivative. *Journal of Biological Chemistry*, 272(5), 2668–2674.

[Emery, 2010] Emery, B. (2010). Regulation of oligodendrocyte differentiation and myelination. *Science*, 330(6005), 779–782.

[Endo & Sawasaki, 2006] Endo, Y. & Sawasaki, T. (2006). Cell-free expression systems for eukaryotic protein production. *Current opinion in biotechnology*, 17(4), 373–380.

[Eto et al., 2008] Eto, M., Sumi, H., Fujimura, H., Yoshikawa, H., & Sakoda, S. (2008). Pioglitazone promotes peripheral nerve remyelination after crush injury through cd36 upregulation. *Journal of the Peripheral Nervous System*, 13(3), 242–248.

[Etxeberria et al., 2010] Etxeberria, A., Mangin, J.-M., Aguirre, A., & Gallo, V. (2010). Adult-born svz progenitors receive transient synapses during remyelination in corpus callosum. *Nature neuroscience*, 13(3), 287–289.

[Evan et al., 1994] Evan, G., Harrington, E., Fanidi, A., Land, H., Amati, B., & Bennett, M. (1994). Integrated control of cell proliferation and cell death by the c-myc oncogene. *Philosophical Transactions of the Royal Society of London B: Biological Sciences*, 345(1313), 269–275.

[Evan & Littlewood, 1993] Evan, G. I. & Littlewood, T. D. (1993). The role of c-myc in cell growth. *Current opinion in genetics & development*, 3(1), 44–49.

[Evans, 1996] Evans, J. D. (1996). *Straightforward statistics for the behavioral sciences*. Brooks/Cole.

[Fanarraga et al., 1995] Fanarraga, M. L., Sommer, I., & Griffiths, I. R. (1995). O-2a progenitors of the mouse optic nerve exhibit a developmental pattern of antigen expression different from the rat. *Glia*, 15(2), 95–104.

[Febbraio et al., 1999] Febbraio, M., Abumrad, N. A., Hajjar, D. P., Sharma, K., Cheng, W., Pearce, S. F. A., & Silverstein, R. L. (1999). A null mutation in murine cd36 reveals an important role in fatty acid and lipoprotein metabolism. *Journal of Biological Chemistry*, 274(27), 19055–19062.

[Feist & Hummon, 2015] Feist, P. & Hummon, A. B. (2015). Proteomic challenges: sample preparation techniques for microgram-quantity protein analysis from biological samples. *International journal of molecular sciences*, 16(2), 3537–3563.

[Franco et al., 2008] Franco, P., Silvestroff, L., Soto, E., & Pasquini, J. (2008). Thyroid hormones promote differentiation of oligodendrocyte progenitor cells and improve remyelination after cuprizone-induced demyelination. *Experimental neurology*, 212(2), 458–467.

[Franklin & Ffrench-Constant, 2008] Franklin, R. J. & Ffrench-Constant, C. (2008). Remyelination in the cns: from biology to therapy. *Nature reviews. Neuroscience*, 9(11), 839.

[Free et al., 2009] Free, R. B., Hazelwood, L. A., & Sibley, D. R. (2009). Identifying novel protein-protein interactions using co-immunoprecipitation and mass spectroscopy. *Current Protocols in Neuroscience*, (pp. 5–28).

[Frost et al., 2009] Frost, E. E., Zhou, Z., Krasnesky, K., & Armstrong, R. C. (2009). Initiation of oligodendrocyte progenitor cell migration by a pdgf-a activated extracellular regulated kinase (erk) signaling pathway. *Neurochemical research*, 34(1), 169–181.

[Fuchs & Chen, 2013] Fuchs, E. & Chen, T. (2013). A matter of life and death: self-renewal in stem cells. *EMBO reports*, 14(1), 39–48.

[Fukuda et al., 2007] Fukuda, S., Abematsu, M., Mori, H., Yanagisawa, M., Kagawa, T., Nakashima, K., Yoshimura, A., & Taga, T. (2007). Potentiation of astrogliogenesis by stat3-mediated activation of bone morphogenetic protein-smad signaling in neural stem cells. *Molecular and cellular biology*, 27(13), 4931–4937.

[Fukushi et al., 2004] Fukushi, J.-i., Makagiansar, I. T., & Stallcup, W. B. (2004). Ng2 proteoglycan promotes endothelial cell motility and angiogenesis via engagement of galectin-3 and $\alpha 3\beta 1$ integrin. *Molecular biology of the cell*, 15(8), 3580–3590.

[Gadea et al., 2009] Gadea, A., Aguirre, A., Haydar, T. F., & Gallo, V. (2009). Endothelin-1 regulates oligodendrocyte development. *Journal of Neuroscience*, 29(32), 10047–10062.

[Gallia et al., 2000a] Gallia, G. L., Johnson, E. M., & Khalili, K. (2000a). Puralpha: a multifunctional single-stranded DNA- and RNA-binding protein. *Nucleic acids research*, 28(17), 3197–205.

[Gallia et al., 2000b] Gallia, G. L., Johnson, E. M., & Khalili, K. (2000b). Survey and summary purα: a multifunctional single-stranded dna-and rna-binding protein. *Nucleic acids research*, 28(17), 3197–3205.

[Galloway & Moore, 2016] Galloway, D. A. & Moore, C. S. (2016). mirnas as emerging regulators of oligodendrocyte development and differentiation. *Frontiers in cell and developmental biology*, 4.

[Gavin et al., 2002] Gavin, A.-C., Bösche, M., Krause, R., Grandi, P., Marzioch, M., Bauer, A., Schultz, J., Rick, J. M., Michon, A.-M., Cruciat, C.-M., et al. (2002). Functional organization of the yeast proteome by systematic analysis of protein complexes. *Nature*, 415(6868), 141–147.

[Geiger et al., 2009] Geiger, B., Spatz, J. P., & Bershadsky, A. D. (2009). Environmental sensing through focal adhesions. *Nature reviews Molecular cell biology*, 10(1), 21–33.

[Geiger et al., 2011] Geiger, T., Wisniewski, J. R., Cox, J., Zanivan, S., Kruger, M., Ishihama, Y., & Mann, M. (2011). Use of stable isotope labeling by amino acids in cell culture as a spike-in standard in quantitative proteomics. *Nature protocols*, 6(2), 147.

[Gibbs et al., 2004] Gibbs, R. A., Weinstock, G. M., Metzker, M. L., Muzny, D. M., Sodergren, E. J., Scherer, S., Scott, G., Steffen, D., Worley, K. C., Burch, P. E., et al. (2004). Genome sequence of the brown norway rat yields insights into mammalian evolution. *Nature*, 428(6982), 493–521.

[Gibney & McDermott, 2007] Gibney, S. M. & McDermott, K. W. (2007). Differentiation of oligodendrocytes in neurospheres derived from embryonic rat brain using growth and differentiation factors. *Journal of neuroscience research*, 85(9), 1912–1920.

[Gieselmann et al., 2003] Gieselmann, V., Franken, S., Klein, D., Mansson, J., Sandhoff, R., Rauch, R. L., Hartmann, D., Saravanan, V., Deyn, P., D'Hooge, R., et al. (2003). Metachromatic leukodystrophy: consequences of sulphatide accumulation. *Acta Paediatrica*, 92(s443), 74–79.

[Gil-Perotín et al., 2013] Gil-Perotín, S., Duran-Moreno, M., Cebrián-Silla, A., Ramírez, M., García-Belda, P., & García-Verdugo, J. M. (2013). Adult neural stem cells from the subventricular zone: A review of the neurosphere assay. *Anatomical Record*, 296(9), 1435–1452.

[Giorgianni et al., 2003] Giorgianni, F., Desiderio, D. M., & Beranova-Giorgianni, S. (2003). Proteome analysis using isoelectric focusing in immobilized ph gradient gels followed by mass spectrometry. *Electrophoresis*, 24(1-2), 253–259.

[Glisovic et al., 2008] Glisovic, T., Bachorik, J. L., Yong, J., & Dreyfuss, G. (2008). Rna-binding proteins and post-transcriptional gene regulation. *FEBS letters*, 582(14), 1977–1986.

[Goff et al., 2009] Goff, L. A., Davila, J., Swerdel, M. R., Moore, J. C., Cohen, R. I., Wu, H., Sun, Y. E., & Hart, R. P. (2009). Ago2 immunoprecipitation identifies predicted microrna in human embryonic stem cells and neural precursors. *PloS one*, 4(9), e7192.

[Golan et al., 2013] Golan, N., Kartvelishvily, E., Spiegel, I., Salomon, D., Sabanay, H., Rechav, K., Vainshtein, A., Frechter, S., Maik-Rachline, G., Eshed-Eisenbach, Y., et al. (2013). Genetic deletion of cadm4 results in myelin abnormalities resembling charcot-marie-tooth neuropathy. *Journal of Neuroscience*, 33(27), 10950–10961.

[Gow et al., 1999] Gow, A., Southwood, C. M., Li, J. S., Pariali, M., Riordan, G. P., Brodie, S. E., Danias, J., Bronstein, J. M., Kachar, B., & Lazzarini, R. A. (1999). Cns myelin and sertoli cell tight junction strands are absent in osp/claudin-11 null mice. *Cell*, 99(6), 649–659.

[Gregorich & Ge, 2014] Gregorich, Z. R. & Ge, Y. (2014). Top-down proteomics in health and disease: Challenges and opportunities. *Proteomics*, 14(10), 1195–1210.

[Greiner-Tollersrud et al., 2013] Greiner-Tollersrud, L., Berg, T., Stensland, H. M., Evjen, G., & Greiner-Tollersrud, O. K. (2013). Bovine brain myelin glycerophosphocholine choline phosphodiesterase is an alkaline lysosphingomyelinase of the enpp-family, regulated by lysosomal sorting. *Neurochemical research*, 38(2), 300–310.

[Guerrera & Kleiner, 2005] Guerrera, I. C. & Kleiner, O. (2005). Application of mass spectrometry in proteomics. *Bioscience Reports*, 25(1-2), 71–93.

[György et al., 2006] György, B., Tóth, E., Tarcsa, E., Falus, A., & Buzás, E. I. (2006). Citrullination: a posttranslational modification in health and disease. *The international journal of biochemistry & cell biology*, 38(10), 1662–1677.

[Haas et al., 1995] Haas, S., Thatikunta, P., Steplewski, A., Johnson, E. M., Khalili, K., & Amini, S. (1995). A 39-kD DNA-binding protein from mouse brain stimulates transcription of myelin basic protein gene in oligodendrocytic cells. *Journal of Cell Biology*, 130(5), 1171–1179.

[Hackett et al., 2016] Hackett, A. R., Lee, D.-H., Dawood, A., Rodriguez, M., Funk, L., Tsoulfas, P., & Lee, J. K. (2016). Stat3 and socs3 regulate ng2 cell proliferation and differentiation after contusive spinal cord injury. *Neurobiology of disease*, 89, 10–22.

[Hart et al., 2001] Hart, K. C., Robertson, S. C., & Donoghue, D. J. (2001). Identification of tyrosine residues in constitutively activated fibroblast growth factor receptor 3 involved in mitogenesis, stat activation, and phosphatidylinositol 3-kinase activation. *Molecular biology of the cell*, 12(4), 931–942.

[Hauser & Oksenberg, 2006] Hauser, S. L. & Oksenberg, J. R. (2006). The neurobiology of multiple sclerosis: genes, inflammation, and neurodegeneration. *Neuron*, 52(1), 61–76.

[Hiraiwa et al., 1997] Hiraiwa, M., Taylor, E. M., Campana, W. M., Darin, S. J., & O'Brien, J. S. (1997). Cell death prevention, mitogen-activated protein kinase stimulation, and increased sulfatide concentrations in schwann cells and oligodendrocytes by prosaposin and prosaptides. *Proceedings of the National Academy of Sciences*, 94(9), 4778–4781.

[Ho et al., 2002] Ho, Y., Gruhler, A., Heilbut, A., Bader, G. D., Moore, L., Adams, S.-L., Millar, A., Taylor, P., Bennett, K., Boutilier, K., et al. (2002). Systematic identification of protein complexes in saccharomyces cerevisiae by mass spectrometry. *Nature*, 415(6868), 180–183.

[Höck et al., 2007] Höck, J., Weinmann, L., Ender, C., Rüdel, S., Kremmer, E., Raabe, M., Urlaub, H., & Meister, G. (2007). Proteomic and functional analysis of argonaute-containing mrna–protein complexes in human cells. *EMBO reports*, 8(11), 1052–1060.

[Hockfield & McKay, 1985] Hockfield, S. & McKay, R. (1985). Identification of major cell classes in the developing mammalian nervous system. *Journal of Neuroscience*, 5(12), 3310–3328.

[Hong et al., 2011] Hong, F., Wittner, B., Breitling, R., Smith, C., Battke, F., et al. (2011). Rankprod: Rank product method for identifying differentially expressed genes with application in meta-analysis. *R package version*, 2(0).

[Honke et al., 2002] Honke, K., Hirahara, Y., Dupree, J., Suzuki, K., Popko, B., Fukushima, K., Fukushima, J., Nagasawa, T., Yoshida, N., Wada, Y., et al. (2002). Paranodal junction formation and spermatogenesis require sulfoglycolipids. *Proceedings of the National Academy of Sciences*, 99(7), 4227–4232.

[Horiuchi et al., 2010] Horiuchi, M., Lindsten, T., Pleasure, D., & Itoh, T. (2010). Differing in vitro survival dependency of mouse and rat NG2+ oligodendroglial progenitor cells. *Journal of neuroscience research*, 88(5), 957–70.

[Hu et al., 2004] Hu, J.-G., Fu, S.-L., Zhang, K.-H., Li, Y., Yin, L., Lu, P.-H., & Xu, X.-M. (2004). Differential gene expression in neural stem cells and oligodendrocyte precursor cells: a cdna microarray analysis. *Journal of neuroscience research*, 78(5), 637–646.

[Hu et al., 2012a] Hu, J.-G., Wang, Y.-X., Wang, H.-J., Bao, M.-S., Wang, Z.-H., Ge, X., Wang, F.-C., Zhou, J.-S., & Lü, H.-Z. (2012a). Pdgf-aa mediates b104cm-induced oligodendrocyte precursor cell differentiation of embryonic neural stem cells through erk, pi3k, and p38 signaling. *Journal of Molecular Neuroscience*, 46(3), 644–653.

[Hu et al., 2012b] Hu, J. G., Wu, X. J., Feng, Y. F., Xi, G. M., Wang, Z. H., Zhou, J. S., & Lü, H. Z. (2012b). PDGF-AA and bFGF mediate B104CM-induced proliferation of oligodendrocyte precursor cells. *International Journal of Molecular Medicine*, 30(5), 1113–1118.

[Huang et al., 2008] Huang, D. W., Sherman, B. T., & Lempicki, R. A. (2008). Bioinformatics enrichment tools: paths toward the comprehensive functional analysis of large gene lists. *Nucleic acids research*, 37(1), 1–13.

[Huang et al., 2004] Huang, F., Khvorova, A., Marshall, W., & Sorkin, A. (2004). Analysis of clathrin-mediated endocytosis of epidermal growth factor receptor by rna interference. *Journal of Biological Chemistry*, 279(16), 16657–16661.

[Huang et al., 2013] Huang, H., Zhao, X.-F., Zheng, K., & Qiu, M. (2013). Regulation of the timing of oligodendrocyte differentiation: mechanisms and perspectives. *Neuroscience bulletin*, 29(2), 155.

[Hunt et al., 2014] Hunt, D., Leventer, R. J., Simons, C., Taft, R., Swoboda, K. J., Gawne-Cain, M., Magee, A. C., Turnpenny, P. D., Baralle, D., et al. (2014). Whole exome sequencing in family trios reveals de novo mutations in pura as a cause of severe neurodevelopmental delay and learning disability. *Journal of medical genetics*, (pp. jmedgenet–2014).

[Hutchinson et al., 2012] Hutchinson, E. C., Denham, E. M., Thomas, B., Trudgian, D. C., Hester, S. S., Ridlova, G., York, A., Turrell, L., & Fodor, E. (2012). Mapping the phosphoproteome of influenza a and b viruses by mass spectrometry. *PLoS Pathog*, 8(11), e1002993.

[Ikeda et al., 2008] Ikeda, M., Kanao, Y., Yamanaka, M., Sakuraba, H., Mizutani, Y., Igarashi, Y., & Kihara, A. (2008). Characterization of four mammalian 3-hydroxyacyl-coa dehydratases involved in very long-chain fatty acid synthesis. *FEBS letters*, 582(16), 2435–2440.

[Ishimi, 1997] Ishimi, Y. (1997). A dna helicase activity is associated with an mcm4,-6, and-7 protein complex. *Journal of Biological Chemistry*, 272(39), 24508–24513.

[Ito et al., 2001] Ito, T., Chiba, T., Ozawa, R., Yoshida, M., Hattori, M., & Sakaki, Y. (2001). A comprehensive two-hybrid analysis to explore the yeast protein interactome. *Proceedings of the National Academy of Sciences*, 98(8), 4569–4574.

[Itoh et al., 1998] Itoh, H., Wortman, M. J., Kanovsky, M., Uson, R. R., Gordon, R. E., Alfano, N., & Johnson, E. M. (1998). Alterations in pur (alpha) levels and intracellular localization in the cv-1 cell cycle. *Cell growth & differentiation: the molecular biology journal of the American Association for Cancer Research*, 9(8), 651–665.

[Jackson et al., 2004] Jackson, M., Krassowska, A., Gilbert, N., Chevassut, T., Forrester, L., Ansell, J., & Ramsahoye, B. (2004). Severe global dna hypomethylation blocks differentiation and induces histone hyperacetylation in embryonic stem cells. *Molecular and cellular biology*, 24(20), 8862–8871.

[Jensen & Parmar, 2006] Jensen, J. B. & Parmar, M. (2006). Strengths and limitations of the neurosphere culture system. *Molecular neurobiology*, 34(3), 153–161.

[Ji et al., 2011] Ji, S., Doucette, J. R., & Nazarali, A. J. (2011). Sirt2 is a novel in vivo downstream target of nkx2. 2 and enhances oligodendroglial cell differentiation. *Journal of molecular cell biology*, (pp. mjr009).

[Jin et al., 2007] Jin, P., Duan, R., Qurashi, A., Qin, Y., Tian, D., Rosser, T. C., Liu, H., Feng, Y., & Warren, S. T. (2007). Pur α binds to rcgg repeats and modulates repeat-mediated neurodegeneration in a drosophila model of fragile x tremor/ataxia syndrome. *Neuron*, 55(4), 556–564.

[Jin et al., 2004] Jin, P., Zarnescu, D. C., Ceman, S., Nakamoto, M., Mowrey, J., Jongens, T. A., Nelson, D. L., Moses, K., & Warren, S. T. (2004). Biochemical and genetic interaction between the fragile x mental retardation protein and the microrna pathway. *Nature neuroscience*, 7(2), 113–117.

[Johnson et al., 1995] Johnson, E. M., Chen, P.-L., Krachmarov, C. P., Barr, S. M., Kanovsky, M., Ma, Z.-W., & Lee, W.-H. (1995). Association of human purα with the retinoblastoma protein, rb, regulates binding to the single-stranded dna purα recognition element. *Journal of Biological Chemistry*, 270(41), 24352–24360.

[Johnson et al., 2013] Johnson, E. M., Daniel, D. C., & Gordon, J. (2013). The pur protein family: genetic and structural features in development and disease. *Journal of cellular physiology*, 228(5), 930–937.

[Johnson et al., 2006] Johnson, E. M., Kinoshita, Y., Weinreb, D. B., Wortman, M. J., Simon, R., Khalili, K., Winckler, B., & Gordon, J. (2006). Role of purα in targeting mrna to sites of translation in hippocampal neuronal dendrites. *Journal of neuroscience research*, 83(6), 929–943.

[Johnson, 1967] Johnson, S. C. (1967). Hierarchical clustering schemes. *Psychometrika*, 32(3), 241–254.

[Jung et al., 2007] Jung, C.-G., Kim, H., Miron, V., Cook, S., Kennedy, T., Foster, C., Antel, J., & Soliven, B. (2007). Functional consequences of s1p receptor modulation in rat oligodendroglial lineage cells. *Glia*, 55(16), 1656–1667.

[Jung et al., 1995] Jung, M., Krämer, E., Grzenkowski, M., Tang, K., Blakemore, W., Aguzzi, A., Khazaie, K., Chlichlia, K., Blankenfeld, G. v., Kettenmann, H., et al. (1995). Lines of murine oligodendroglial precursor cells immortalized by an activated neu tyrosine kinase show distinct degrees of interaction with axons in vitro and in vivo. *European Journal of Neuroscience*, 7(6), 1245–1265.

[Kanai et al., 2004] Kanai, Y., Dohmae, N., & Hirokawa, N. (2004). Kinesin transports RNA: Isolation and characterization of an RNA-transporting granule. *Neuron*, 43(4), 513–525.

[Kang et al., 2010] Kang, S. H., Fukaya, M., Yang, J. K., Rothstein, J. D., & Bergles, D. E. (2010). Ng2+ cns glial progenitors remain committed to the oligodendrocyte lineage in postnatal life and following neurodegeneration. *Neuron*, 68(4), 668–681.

[Karlsson et al., 1997] Karlsson, M., Contreras, J. A., Hellman, U., Tornqvist, H., & Holm, C. (1997). cdna cloning, tissue distribution, and identification of the catalytic triad of monoglyceride lipase evolutionary relationship to esterases, lysophospholipases, and haloperoxidases. *Journal of Biological Chemistry*, 272(43), 27218–27223.

[Karram et al., 2008] Karram, K., Goebbels, S., Schwab, M., Jennissen, K., Seifert, G., Steinhäuser, C., Nave, K.-A., & Trotter, J. (2008). NG2-expressing cells in the nervous system revealed by the NG2-EYFP-knockin mouse. *Genesis (New York, N.Y. : 2000)*, 46(12), 743–757.

[Kazanis et al., 2008] Kazanis, I., Lathia, J., Moss, L., et al. (2008). The neural stem cell microenvironment.

[Keirstead & Blakemore, 1997] Keirstead, H. S. & Blakemore, W. F. (1997). Identification of post-mitotic oligodendrocytes incapable of remyelination within the demyelinated adult spinal cord. *Journal of Neuropathology & Experimental Neurology*, 56(11), 1191–1201.

[Kelm et al., 1999] Kelm, R. J., Cogan, J. G., Elder, P. K., Strauch, A. R., & Getz, M. J. (1999). Molecular interactions between single-stranded dna-binding proteins associated with an essential mcat element in the mouse smooth muscle α-actin promoter. *Journal of Biological Chemistry*, 274(20), 14238–14245.

[Kelm et al., 1997] Kelm, R. J., Elder, P. K., Strauch, A. R., & Getz, M. J. (1997). Sequence of cdnas encoding components of vascular actin single-stranded dna-binding factor 2 establish identity to purα and purβ. *Journal of Biological Chemistry*, 272(42), 26727–26733.

[Kenny et al., 2014] Kenny, P. J., Zhou, H., Kim, M., Skariah, G., Khetani, R. S., Drnevich, J., Arcila, M. L., Kosik, K. S., & Ceman, S. (2014). Mov10 and fmrp regulate ago2 association with microrna recognition elements. *Cell reports*, 9(5), 1729–1741.

[Kerr et al., 2010] Kerr, C. L., Letzen, B. S., Hill, C. M., Agrawal, G., Thakor, N. V., Sterneckert, J. L., Gearhart, J. D., & All, A. H. (2010). Efficient differentiation of human embryonic stem cells into oligodendrocyte progenitors for application in a rat contusion model of spinal cord injury. *International Journal of Neuroscience*, 120(4), 305–313.

[Keshishian et al., 2007] Keshishian, H., Addona, T., Burgess, M., Kuhn, E., & Carr, S. A. (2007). Quantitative, multiplexed assays for low abundance proteins in plasma by targeted mass spectrometry and stable isotope dilution. *Molecular & Cellular Proteomics*, 6(12), 2212–2229.

[Kessaris et al., 2006] Kessaris, N., Fogarty, M., Iannarelli, P., Grist, M., Wegner, M., & Richardson, W. D. (2006). Competing waves of oligodendrocytes in the forebrain and postnatal elimination of an embryonic lineage. *Nature neuroscience*, 9(2), 173–179.

[Kettenbach et al., 2011] Kettenbach, A. N., Rush, J., & Gerber, S. A. (2011). Absolute quantification of protein and post-translational modification abundance with stable isotope–labeled synthetic peptides. *Nature protocols*, 6(2), 175.

[Khalili et al., 2003] Khalili, K., Del Valle, L., Muralidharan, V., Gault, W. J., Darbinian, N., Otte, J., Meier, E., Johnson, E. M., Daniel, D. C., Kinoshita, Y., et al. (2003). Purα is essential for postnatal brain development and developmentally coupled cellular proliferation as revealed by genetic inactivation in the mouse. *Molecular and cellular biology*, 23(19), 6857–6875.

[Kim et al., 2014] Kim, M.-S., Pinto, S. M., Getnet, D., Nirujogi, R. S., Manda, S. S., Chaerkady, R., Madugundu, A. K., Kelkar, D. S., Isserlin, R., Jain, S., et al. (2014). A draft map of the human proteome. *Nature*, 509(7502), 575.

[Kim et al., 2006] Kim, W. S., Guillemin, G. J., Glaros, E. N., Lim, C. K., & Garner, B. (2006). Quantitation of atp-binding cassette subfamily-a transporter gene expression in primary human brain cells. *Neuroreport*, 17(9), 891–896.

[Kippert et al., 2008] Kippert, A., Fitzner, D., Trajkovic, K., Opitz, L., & Simons, M. (2008). Identification of tmem10/opalin as a novel marker for oligodendrocytes using gene expression profiling. *BMC neuroscience*, 9(1), 40.

[Kohlschütter & Eichler, 2011] Kohlschütter, A. & Eichler, F. (2011). Childhood leukodystrophies: a clinical perspective. *Expert review of neurotherapeutics*, 11(10), 1485–1496.

[Krämer-Albers et al., 2007] Krämer-Albers, E.-M., Bretz, N., Tenzer, S., Winterstein, C., Möbius, W., Berger, H., Nave, K.-A., Schild, H., & Trotter, J. (2007). Oligodendrocytes secrete exosomes containing major myelin and stress-protective proteins: Trophic support for axons? *Proteomics-clinical applications*, 1(11), 1446–1461.

[Kriegstein & Alvarez-Buylla, 2009] Kriegstein, A. & Alvarez-Buylla, A. (2009). The glial nature of embryonic and adult neural stem cells. *Annual review of neuroscience*, 32, 149–184.

[Kristensen et al., 2012] Kristensen, A. R., Gsponer, J., & Foster, L. J. (2012). A high-throughput approach for measuring temporal changes in the interactome. *Nature methods*, 9(9), 907–909.

[Lange et al., 2008] Lange, V., Picotti, P., Domon, B., & Aebersold, R. (2008). Selected reaction monitoring for quantitative proteomics: a tutorial. *Molecular systems biology*, 4(1), 222.

[Lappe-Siefke et al., 2003] Lappe-Siefke, C., Goebbels, S., Gravel, M., Nicksch, E., Lee, J., Braun, P. E., Griffiths, I. R., & Nave, K.-A. (2003). Disruption of cnp1 uncouples oligodendroglial functions in axonal support and myelination. *Nature genetics*, 33(3), 366–374.

[Larsson et al., 2008] Larsson, J., Forsberg, M., Bränvall, K., Zhang, X.-Q., Enarsson, M., Hedborg, F., & Forsberg-Nilsson, K. (2008). Nuclear receptor binding protein 2 is induced during neural progenitor differentiation and affects cell survival. *Molecular and Cellular Neuroscience*, 39(1), 32–39.

[Lasham et al., 2000] Lasham, A., Lindridge, E., Rudert, F., Onrust, R., & Watson, J. (2000). Regulation of the human fas promoter by yb-1, purα and ap-1 transcription factors. *Gene*, 252(1), 1–13.

[LeClerc et al., 1991] LeClerc, S., Palaniswami, R., Xie, B., & Govindan, M. (1991). Molecular cloning and characterization of a factor that binds the human glucocorticoid receptor gene and represses its expression. *Journal of Biological Chemistry*, 266(26), 17333–17340.

[Lee et al., 2003] Lee, C.-L., Hsiao, H.-H., Lin, C.-W., Wu, S.-P., Huang, S.-Y., Wu, C.-Y., Wang, A. H.-J., & Khoo, K.-H. (2003). Strategic shotgun proteomics approach for efficient construction of an expression map of targeted protein families in hepatoma cell lines. *Proteomics*, 3(12), 2472–2486.

[Lee et al., 2005] Lee, J., Gravel, M., Zhang, R., Thibault, P., & Braun, P. E. (2005). Process outgrowth in oligodendrocytes is mediated by cnp, a novel microtubule assembly myelin protein. *The Journal of cell biology*, 170(4), 661–673.

[Levine et al., 2001] Levine, J. M., Reynolds, R., & Fawcett, J. W. (2001). The oligodendrocyte precursor cell in health and disease. *Trends in neurosciences*, 24(1), 39–47.

[Levy & Shoham, 2005] Levy, S. & Shoham, T. (2005). Protein-protein interactions in the tetraspanin web. *Physiology*, 20(4), 218–224.

[Li & Clevers, 2010] Li, L. & Clevers, H. (2010). Coexistence of quiescent and active adult stem cells in mammals. *Science*, 327(5965), 542–545.

[Li et al., 2007] Li, W., Zhang, B., Tang, J., Cao, Q., Wu, Y., Wu, C., Guo, J., Ling, E.-A., & Liang, F. (2007). Sirtuin 2, a mammalian homolog of yeast silent information regulator-2 longevity regulator, is an oligodendroglial protein that decelerates cell differentiation through deacetylating α-tubulin. *Journal of Neuroscience*, 27(10), 2606–2616.

[Liang et al., 2004] Liang, X., Draghi, N. A., & Resh, M. D. (2004). Signaling from integrins to fyn to rho family gtpases regulates morphologic differentiation of oligodendrocytes. *Journal of Neuroscience*, 24(32), 7140–7149.

[Lin et al., 2000] Lin, X., O'Mahony, A., Mu, Y., Geleziunas, R., & Greene, W. C. (2000). Protein kinase c-θ participates in nf-κb activation induced by cd3-cd28 costimulation through selective activation of iκb kinase β. *Molecular and cellular biology*, 20(8), 2933–2940.

[Lin et al., 1998] Lin, Y.-L., Shivji, M. K., Chen, C., Kolodner, R., Wood, R. D., & Dutta, A. (1998). The evolutionarily conserved zinc finger motif in the largest subunit of human replication protein a is required for dna replication and mismatch repair but not for nucleotide excision repair. *Journal of Biological Chemistry*, 273(3), 1453–1461.

[Linder & Jankowsky, 2011] Linder, P. & Jankowsky, E. (2011). From unwinding to clamping—the dead box rna helicase family. *Nature reviews Molecular cell biology*, 12(8), 505–516.

[Liu et al., 2005] Liu, H., Barr, S. M., Chu, C., Kohtz, D. S., Kinoshita, Y., & Johnson, E. M. (2005). Functional interaction of purα with the cdk2 moiety of cyclin a/cdk2. *Biochemical and biophysical research communications*, 328(4), 851–857.

[Liu & Casaccia, 2010] Liu, J. & Casaccia, P. (2010). Epigenetic regulation of oligodendrocyte identity. *Trends in neurosciences*, 33(4), 193–201.

[Loh et al., 2007] Loh, Y.-H., Zhang, W., Chen, X., George, J., & Ng, H.-H. (2007). Jmjd1a and jmjd2c histone h3 lys 9 demethylases regulate self-renewal in embryonic stem cells. *Genes & development*, 21(20), 2545–2557.

[Lopez-Ramirez & Nicoli, 2014] Lopez-Ramirez, M. A. & Nicoli, S. (2014). Role of mirnas and epigenetics in neural stem cell fate determination. *Epigenetics*, 9(1), 90–100.

[Lowenstein et al., 1992] Lowenstein, E., Daly, R., Batzer, A., Li, W., Margolis, B., Lammers, R., Ullrich, A., Skolnik, E., Bar-Sagi, D., & Schlessinger, J. (1992). The sh2 and sh3 domain-containing protein grb2 links receptor tyrosine kinases to ras signaling. *Cell*, 70(3), 431–442.

[Ludwin, 1979] Ludwin, S. (1979). The perineuronal satellite oligodendrocyte. *Acta neuropathologica*, 47(1), 49–53.

[Luo et al., 2000] Luo, X., Fang, G., Coldiron, M., Lin, Y., Yu, H., Kirschner, M. W., & Wagner, G. (2000). Structure of the mad2 spindle assembly checkpoint protein and its interaction with cdc20. *Nature Structural & Molecular Biology*, 7(3), 224–229.

[Mabie et al., 1999] Mabie, P. C., Mehler, M. F., & Kessler, J. A. (1999). Multiple roles of bone morphogenetic protein signaling in the regulation of cortical cell number and phenotype. *Journal of Neuroscience*, 19(16), 7077–7088.

[Macklin et al., 1986] Macklin, W., Weill, C., & Deininger, P. (1986). Expression of myelin proteolipid and basic protein mrnas in cultured cells. *Journal of neuroscience research*, 16(1), 203–217.

[Maere et al., 2005] Maere, S., Heymans, K., & Kuiper, M. (2005). Bingo: a cytoscape plugin to assess overrepresentation of gene ontology categories in biological networks. *Bioinformatics*, 21(16), 3448–3449.

[Magri et al., 2014] Magri, L., Swiss, V. A., Jablonska, B., Lei, L., Pedre, X., Walsh, M., Zhang, W., Gallo, V., Canoll, P., & Casaccia, P. (2014). E2f1 coregulates cell cycle genes and chromatin components during the transition of oligodendrocyte progenitors from proliferation to differentiation. *Journal of Neuroscience*, 34(4), 1481–1493.

[Maher et al., 2015] Maher, S., Jjunju, F. P., & Taylor, S. (2015). Colloquium: 100 years of mass spectrometry: Perspectives and future trends. *Reviews of Modern Physics*, 87(1), 113.

[Maier et al., 2009] Maier, T., Güell, M., & Serrano, L. (2009). Correlation of mrna and protein in complex biological samples. *FEBS letters*, 583(24), 3966–3973.

[Malatesta et al., 2000] Malatesta, P., Hartfuss, E., & Gotz, M. (2000). Isolation of radial glial cells by fluorescent-activated cell sorting reveals a neuronal lineage. *Development*, 127(24), 5253–5263.

[Mallick & Kuster, 2010] Mallick, P. & Kuster, B. (2010). Proteomics: a pragmatic perspective. *Nature biotechnology*, 28(7), 695–709.

[Marques et al., 2016] Marques, S., Zeisel, A., Codeluppi, S., van Bruggen, D., Falcão, A. M., Xiao, L., Li, H., Häring, M., Hochgerner, H., Romanov, R. A., et al. (2016). Oligodendrocyte heterogeneity in the mouse juvenile and adult central nervous system. *Science*, 352(6291), 1326–1329.

[Mathivanan et al., 2010] Mathivanan, S., Ji, H., & Simpson, R. J. (2010). Exosomes: extracellular organelles important in intercellular communication. *Journal of proteomics*, 73(10), 1907–1920.

[Mayer & Noble, 1994] Mayer, M. & Noble, M. (1994). N-acetyl-l-cysteine is a pluripotent protector against cell death and enhancer of trophic factor-mediated cell survival in vitro. *Proceedings of the National Academy of Sciences*, 91(16), 7496–7500.

[McDonald et al., 1998] McDonald, J. W., Levine, J. M., & Qu, Y. (1998). Multiple classes of the oligodendrocyte lineage are highly vulnerable to excitotoxicity. *Neuroreport*, 9(12), 2757–2762.

[Menkes et al., 1966] Menkes, J. H., Philippart, M., & Concone, M. C. (1966). Concentration and fatty acid composition of cerebrosides and sulfatides in mature and immature human brain. *Journal of lipid research*, 7(4), 479–486.

[Menn et al., 2006] Menn, B., Garcia-Verdugo, J. M., Yaschine, C., Gonzalez-Perez, O., Rowitch, D., & Alvarez-Buylla, A. (2006). Origin of oligodendrocytes in the subventricular zone of the adult brain. *J Neurosci*, 26(30), 7907–7918.

[Messam et al., 2000] Messam, C. A., Hou, J., & Major, E. O. (2000). Coexpression of nestin in neural and glial cells in the developing human cns defined by a human-specific anti-nestin antibody. *Experimental neurology*, 161(2), 585–596.

[Meunier et al., 2007] Meunier, B., Dumas, E., Piec, I., Béchet, D., Hébraud, M., & Hocquette, J.-F. (2007). Assessment of hierarchical clustering methodologies for proteomic data mining. *Journal of proteome research*, 6(1), 358–366.

[Miller, 2002] Miller, R. H. (2002). Regulation of oligodendrocyte development in the vertebrate cns. *Progress in neurobiology*, 67(6), 451–467.

[Milner et al., 1997] Milner, R., Anderson, H. J., Rippon, R. F., McKay, J. S., Franklin, R. J., Marchionni, M. A., Reynolds, R., & Ffrench-Constant, C. (1997). Contrasting effects of mitogenic growth factors on oligodendrocyte precursor cell migration. *Glia*, 19(1), 85–90.

[Milner et al., 1996] Milner, R., Edwards, G., Streuli, C., et al. (1996). A role in migration for the $\alpha v\beta 1$ integrin expressed on oligodendrocyte precursors. *Journal of Neuroscience*, 16(22), 7240–7252.

[Miyamoto et al., 2008] Miyamoto, Y., Yamauchi, J., & Tanoue, A. (2008). Cdk5 phosphorylation of wave2 regulates oligodendrocyte precursor cell migration through nonreceptor tyrosine kinase fyn. *Journal of Neuroscience*, 28(33), 8326–8337.

[Morell et al., 1999] Morell, P., Quarles, R., et al. (1999). Characteristic composition of myelin. *Basic Neurochemistry: Molecular, Cellular and Medical Aspects,*.

[Morshead et al., 1994] Morshead, C. M., Reynolds, B. A., Craig, C. G., McBurney, M. W., Staines, W. A., Morassutti, D., Weiss, S., & van der Kooy, D. (1994). Neural stem cells in the adult mammalian forebrain: a relatively quiescent subpopulation of subependymal cells. *Neuron*, 13(5), 1071–1082.

[Motoyama et al., 2006] Motoyama, A., Venable, J. D., Ruse, C. I., & Yates, J. R. (2006). Automated ultra-high-pressure multidimensional protein identification technology (uhp-mudpit) for improved peptide identification of proteomic samples. *Analytical chemistry*, 78(14), 5109–5118.

[Muralidharan et al., 2001] Muralidharan, V., Sweet, T., Nadraga, Y., Amini, S., & Khalili, K. (2001). Regulation of purα gene transcription: evidence for autoregulation of purα promoter. *Journal of cellular physiology*, 186(3), 406–413.

[Muralidharan et al., 1997] Muralidharan, V., Tretiakova, A., Steplewski, A., Haas, S., Amini, S., Johnson, E., & Khalili, K. (1997). Evidence for inhibition of myef-2 binding to mbp promoter by mef-1/pur. *Journal of cellular biochemistry*, 66(4), 524–531.

[Musse et al., 2008] Musse, A. A., Li, Z., Ackerley, C. A., Bienzle, D., Lei, H., Poma, R., Harauz, G., Moscarello, M. A., & Mastronardi, F. G. (2008). Peptidylarginine deiminase 2 (pad2) overexpression in transgenic mice leads to myelin loss in the central nervous system. *Disease models & mechanisms*, 1(4-5), 229–240.

[Nait-Oumesmar et al., 1999] Nait-Oumesmar, B., Decker, L., Lachapelle, F., Avellana-Adalid, V., Bachelin, C., Evercooren, V., & Baron, A. (1999). Progenitor cells of the adult mouse subventricular zone proliferate, migrate and differentiate into oligodendrocytes after demyelination. *European Journal of Neuroscience*, 11(12), 4357–4366.

[Nelissen et al., 2012] Nelissen, K., Mulder, M., Smets, I., Timmermans, S., Smeets, K., Ameloot, M., & Hendriks, J. J. (2012). Liver x receptors regulate cholesterol homeostasis in oligodendrocytes. *Journal of neuroscience research*, 90(1), 60–71.

[Niehaus et al., 1999] Niehaus, A., Stegmüller, J., Diers-Fenger, M., & Trotter, J. (1999). Cell-surface glycoprotein of oligodendrocyte progenitors involved in migration. *Journal of Neuroscience*, 19(12), 4948–4961.

[Nielsen et al., 2002] Nielsen, J. A., Hudson, L. D., & Armstrong, R. C. (2002). Nuclear organization in differentiating oligodendrocytes. *Journal of cell science*, 115(21), 4071–4079.

[Nikolov et al., 2012] Nikolov, M., Schmidt, C., & Urlaub, H. (2012). Quantitative mass spectrometry-based proteomics: an overview. *Quantitative methods in proteomics*, (pp. 85–100).

[Nishiyama et al., 1996] Nishiyama, A., Lin, X.-H., Giese, N., Heldin, C.-H., & Stallcup, W. (1996). Co-localization of ng2 proteoglycan and pdgf α-receptor on o2a progenitor cells in the developing rat brain. *Journal of neuroscience research*, 43(3), 299–314.

[Noble et al., 1988] Noble, M., Murray, K., Stroobant, P., Waterfield, M. D., & Riddle, P. (1988). Platelet-derived growth factor promotes division and motility and inhibits premature differentiation of the oligodendrocyte/type-2 astrocyte progenitor ceil. *Nature*, 333(6173), 560–562.

[Nolan et al., 2006] Nolan, T., Hands, R. E., & Bustin, S. A. (2006). Quantification of mrna using real-time rt-pcr. *Nature protocols*, 1(3), 1559–1582.

[Nooren & Thornton, 2003] Nooren, I. M. & Thornton, J. M. (2003). Structural characterisation and functional significance of transient protein–protein interactions. *Journal of molecular biology*, 325(5), 991–1018.

[Oeckinghaus & Ghosh, 2009] Oeckinghaus, A. & Ghosh, S. (2009). The nf-κb family of transcription factors and its regulation. *Cold Spring Harbor perspectives in biology*, 1(4), a000034.

[Ohashi et al., 2002] Ohashi, S., Koike, K., Omori, A., Ichinose, S., Ohara, S., Kobayashi, S., Sato, T.-A., & Anzai, K. (2002). Identification of mrna/protein (mrnp) complexes containing purα, mstaufen, fragile x protein, and myosin va and their association with rough endoplasmic reticulum equipped with a kinesin motor. *Journal of Biological Chemistry*, 277(40), 37804–37810.

[Oka et al., 2004] Oka, C., Tsujimoto, R., Kajikawa, M., Koshiba-Takeuchi, K., Ina, J., Yano, M., Tsuchiya, A., Ueta, Y., Soma, A., Kanda, H., et al. (2004). Htra1 serine protease inhibits signaling mediated by tgfβ family proteins. *Development*, 131(5), 1041–1053.

[Old et al., 2005] Old, W. M., Meyer-Arendt, K., Aveline-Wolf, L., Pierce, K. G., Mendoza, A., Sevinsky, J. R., Resing, K. A., & Ahn, N. G. (2005). Comparison of label-free methods for quantifying human proteins by shotgun proteomics. *Molecular & cellular proteomics*, 4(10), 1487–1502.

[Olsen et al., 2004] Olsen, J. V., Ong, S.-E., & Mann, M. (2004). Trypsin cleaves exclusively c-terminal to arginine and lysine residues. *Molecular & Cellular Proteomics*, 3(6), 608–614.

[O'Meara et al., 2011] O'Meara, R. W., Michalski, J.-P., & Kothary, R. (2011). Integrin signaling in oligodendrocytes and its importance in CNS myelination. *Journal of signal transduction*, 2011(354091), 1–11.

[O'Neill & Kaltschmidt, 1997] O'Neill, L. A. & Kaltschmidt, C. (1997). Nf-kb: a crucial transcription factor for glial and neuronal cell function. *Trends in neurosciences*, 20(6), 252–258.

[Ong et al., 2002] Ong, S.-E., Blagoev, B., Kratchmarova, I., Kristensen, D. B., Steen, H., Pandey, A., & Mann, M. (2002). Stable isotope labeling by amino acids in cell culture, silac, as a simple and accurate approach to expression proteomics. *Molecular & cellular proteomics*, 1(5), 376–386.

[Ong & Mann, 2005] Ong, S.-E. & Mann, M. (2005). Mass spectrometry-based proteomics turns quantitative. *Nature chemical biology*, 1(5), 252.

[Ono et al., 1997] Ono, K., Yasui, Y., Rutishauser, U., & Miller, R. H. (1997). Focal ventricular origin and migration of oligodendrocyte precursors into the chick optic nerve. *Neuron*, 19(2), 283–292.

[Opiteck et al., 1997] Opiteck, G. J., Lewis, K. C., Jorgenson, J. W., & Anderegg, R. J. (1997). Comprehensive on-line lc/lc/ms of proteins. *Analytical chemistry*, 69(8), 1518–1524.

[Ortega et al., 2013] Ortega, J. A., Radonjic, N. V., & Zecevic, N. (2013). Sonic hedgehog promotes generation and maintenance of human forebrain olig2 progenitors. *Frontiers in cellular neuroscience*, 7, 254.

[Osterhout et al., 1999] Osterhout, D. J., Wolven, A., Wolf, R. M., Resh, M. D., & Chao, M. V. (1999). Morphological differentiation of oligodendrocytes requires activation of fyn tyrosine kinase. *The Journal of cell biology*, 145(6), 1209–1218.

[Pagano et al., 1992] Pagano, M., Pepperkok, R., Verde, F., Ansorge, W., & Draetta, G. (1992). Cyclin a is required at two points in the human cell cycle. *The EMBO journal*, 11(3), 961.

[Palm et al., 2013] Palm, T., Hemmer, K., Winter, J., Fricke, I. B., Tarbashevich, K., Sadeghi Shakib, F., Rudolph, I.-M., Hillje, A.-L., De Luca, P., Bahnassawy, L., et al. (2013). A systemic transcriptome analysis reveals the regulation of neural stem cell maintenance by an e2f1–mirna feedback loop. *Nucleic acids research*, 41(6), 3699–3712.

[Parent et al., 2006] Parent, J. M., von dem Bussche, N., & Lowenstein, D. H. (2006). Prolonged seizures recruit caudal subventricular zone glial progenitors into the injured hippocampus. *Hippocampus*, 16(3), 321–328.

[Park et al., 2010] Park, D., Xiang, A. P., Mao, F. F., Zhang, L., Di, C.-G., Liu, X.-M., Shao, Y., Ma, B.-F., Lee, J.-H., Ha, K.-S., et al. (2010). Nestin is required for the proper self-renewal of neural stem cells. *Stem cells*, 28(12), 2162–2171.

[Patel & Klein, 2011] Patel, J. R. & Klein, R. S. (2011). Mediators of oligodendrocyte differentiation during remyelination. *FEBS letters*, 585(23), 3730–3737.

[Patrikios et al., 2006] Patrikios, P., Stadelmann, C., Kutzelnigg, A., Rauschka, H., Schmidbauer, M., Laursen, H., Sorensen, P. S., Brück, W., Lucchinetti, C., & Lassmann, H. (2006). Remyelination is extensive in a subset of multiple sclerosis patients. *Brain*, 129(12), 3165–3172.

[Pedraza et al., 2008] Pedraza, C. E., Monk, R., Lei, J., Hao, Q., & Macklin, W. B. (2008). Production, characterization, and efficient transfection of highly pure oligodendrocyte precursor cultures from mouse embryonic neural progenitors. *Glia*, 56(12), 1339–1352.

[Penberthy et al., 2004] Penberthy, W. T., Zhao, C., Zhang, Y., Jessen, J. R., Yang, Z., Bricaud, O., Collazo, A., Meng, A., & Lin, S. (2004). Pur alpha and sp8 as opposing regulators of neural gata2 expression. *Developmental biology*, 275(1), 225–234.

[Perry et al., 1985] Perry, V., Hume, D. A., & Gordon, S. (1985). Immunohistochemical localization of macrophages and microglia in the adult and developing mouse brain. *Neuroscience*, 15(2), 313–326.

[Pesheva et al., 1997] Pesheva, P., Gloor, S., Schachner, M., & Probstmeier, R. (1997). Tenascin-r is an intrinsic autocrine factor for oligodendrocyte differentiation and promotes cell adhesion by a sulfatidemediated mechanism. *Journal of Neuroscience*, 17(12), 4642–4651.

[Peters, 2004] Peters, A. (2004). A fourth type of neuroglial cell in the adult central nervous system. *Journal of neurocytology*, 33(3), 345–357.

[Peters, 2006] Peters, J.-M. (2006). The anaphase promoting complex/cyclosome: a machine designed to destroy. *Nature reviews. Molecular cell biology*, 7(9), 644–56.

[Pfleger & Kirschner, 2000] Pfleger, C. M. & Kirschner, M. W. (2000). The ken box: an apc recognition signal distinct from the d box targeted by cdh1. *Genes & development*, 14(6), 655–665.

[Phizicky & Fields, 1995] Phizicky, E. M. & Fields, S. (1995). Protein-protein interactions: methods for detection and analysis. *Microbiological reviews*, 59(1), 94–123.

[Picciotto & Wickman, 1998] Picciotto, M. R. & Wickman, K. (1998). Using knockout and transgenic mice to study neurophysiology and behavior. *Physiological reviews*, 78(4), 1131–1163.

[Popescu et al., 2007] Popescu, S. C., Popescu, G. V., Bachan, S., Zhang, Z., Seay, M., Gerstein, M., Snyder, M., & Dinesh-Kumar, S. (2007). Differential binding of calmodulin-related proteins to their targets revealed through high-density arabidopsis protein microarrays. *Proceedings of the National Academy of Sciences*, 104(11), 4730–4735.

[Potter & Petryniak, 2016] Potter, G. B. & Petryniak, M. A. (2016). Neuroimmune mechanisms in krabbe's disease. *Journal of Neuroscience Research*, 94(11), 1341–1348.

[Qian et al., 1997] Qian, X., Davis, A. A., Goderie, S. K., & Temple, S. (1997). Fgf2 concentration regulates the generation of neurons and glia from multipotent cortical stem cells. *Neuron*, 18(1), 81–93.

[Qureshi et al., 2010] Qureshi, I. A., Gokhan, S., & Mehler, M. F. (2010). Rest and corest are transcriptional and epigenetic regulators of seminal neural fate decisions. *Cell cycle*, 9(22), 4477–4486.

[Raff et al., 2001] Raff, M., Apperly, J., Kondo, T., Tokumoto, Y., & Tang, D. (2001). Timing cell-cycle exit and differentiation in oligodendrocyte development. In *Novartis Foundation symposium* (pp. 100–112).: Chichester; New York; John Wiley; 1999.

[Raff et al., 1988] Raff, M. C., Lillien, L. E., Richardson, W. D., Burne, J. F., & Noble, M. D. (1988). Platelet-derived growth factor from astrocytes drives the clock that times oligodendrocyte development in culture. *Nature*, 333(6173), 562–565.

[Ramakrishnan et al., 2007] Ramakrishnan, H., Hedayati, K. K., Lüllmann-Rauch, R., Wessig, C., Fewou, S. N., Maier, H., Goebel, H.-H., Gieselmann, V., & Eckhardt, M. (2007). Increasing sulfatide synthesis in myelin-forming cells of arylsulfatase a-deficient mice causes demyelination and neurological symptoms reminiscent of human metachromatic leukodystrophy. *Journal of Neuroscience*, 27(35), 9482–9490.

[Rapley et al., 2008] Rapley, J., Nicolàs, M., Groen, A., Regué, L., Bertran, M. T., Caelles, C., Avruch, J., & Roig, J. (2008). The nima-family kinase nek6 phosphorylates the kinesin eg5 at a novel site necessary for mitotic spindle formation. *Journal of cell science*, 121(23), 3912–3921.

[Rappsilber et al., 2007] Rappsilber, J., Mann, M., & Ishihama, Y. (2007). Protocol for micro-purification, enrichment, pre-fractionation and storage of peptides for proteomics using StageTips. *Nature protocols*, 2(8), 1896–906.

[Rauniyar & Yates III, 2014] Rauniyar, N. & Yates III, J. R. (2014). Isobaric labeling-based relative quantification in shotgun proteomics. *Journal of proteome research*, 13(12), 5293–5309.

[Ravanpay et al., 2010] Ravanpay, A. C., Hansen, S. J., & Olson, J. M. (2010). Transcriptional inhibition of rest by neurod2 during neuronal differentiation. *Molecular and Cellular Neuroscience*, 44(2), 178–189.

[Rechsteiner & Rogers, 1996] Rechsteiner, M. & Rogers, S. W. (1996). Pest sequences and regulation by proteolysis. *Trends in biochemical sciences*, 21(7), 267–271.

[Reynolds & Weiss, 1992] Reynolds, B. & Weiss, S. (1992). Generation of neurons and astrocytes from isolated cells of the adult mammalian central nervous system. *Science*, 255(5052), 1707–1710.

[Reynolds & Weiss, 1996] Reynolds, B. A. & Weiss, S. (1996). Clonal and population analyses demonstrate that an egf-responsive mammalian embryonic cns precursor is a stem cell. *Developmental biology*, 175(1), 1–13.

[Reynolds & Wilkin, 1988] Reynolds, R. & Wilkin, G. P. (1988). Development of macroglial cells in rat cerebellum. ii. an in situ immunohistochemical study of oligodendroglial lineage from precursor to mature myelinating cell. *Development*, 102(2), 409–425.

[Ritchie et al., 2015] Ritchie, M. E., Phipson, B., Wu, D., Hu, Y., Law, C. W., Shi, W., & Smyth, G. K. (2015). limma powers differential expression analyses for rna-sequencing and microarray studies. *Nucleic acids research*, 43(7), e47–e47.

[Rivers et al., 2008] Rivers, L. E., Young, K. M., Rizzi, M., Jamen, F., Psachoulia, K., Wade, A., Kessaris, N., & Richardson, W. D. (2008). Pdgfra/ng2 glia generate myelinating oligodendrocytes and piriform projection neurons in adult mice. *Nature neuroscience*, 11(12).

[Rodriguez et al., 2013] Rodriguez, R., Fernandez, A., & Fraga, M. (2013). Role of sirtuins in stem cell differentiation. *Genes & cancer*, 4(3-4), 105–111.

[Roher et al., 2002] Roher, A. E., Weiss, N., Kokjohn, T. A., Kuo, Y.-M., Kalback, W., Anthony, J., Watson, D., Luehrs, D. C., Sue, L., Walker, D., et al. (2002). Increased aβ peptides and reduced cholesterol and myelin proteins characterize white matter degeneration in alzheimer's disease. *Biochemistry*, 41(37), 11080–11090.

[Romashkova & Makarov, 1999] Romashkova, J. A. & Makarov, S. S. (1999). Nf-κb is a target of akt in anti-apoptotic pdgf signalling. *Nature*, 401(6748), 86–90.

[Roux et al., 2012] Roux, K. J., Kim, D. I., Raida, M., & Burke, B. (2012). A promiscuous biotin ligase fusion protein identifies proximal and interacting proteins in mammalian cells. *The Journal of cell biology*, 196(6), 801–10.

[Rowitch & Kriegstein, 2010] Rowitch, D. H. & Kriegstein, A. R. (2010). Developmental genetics of vertebrate glial-cell specification. *Nature*, 468(7321), 214–222.

[Royle et al., 2005] Royle, S. J., Bright, N. A., & Lagnado, L. (2005). Clathrin is required for the function of the mitotic spindle. *Nature*, 434(7037), 1152–1157.

[Rubenstein & Rakic, 2013] Rubenstein, J. & Rakic, P. (2013). *Patterning and Cell Type Specification in the Developing CNS and PNS: Comprehensive Developmental Neuroscience*, volume 1. Academic Press.

[Russell et al., 2000] Russell, C. S., Ben-Yehuda, S., Dix, I., Kupiec, M., & Beggs, J. D. (2000). Functional analyses of interacting factors involved in both pre-mrna splicing and cell cycle progression in saccharomyces cerevisiae. *Rna*, 6(11), 1565–1572.

[Rytkönen et al., 2006] Rytkönen, A. K., Vaara, M., Nethanel, T., Kaufmann, G., Sormunen, R., Läärä, E., Nasheuer, H.-P., Rahmeh, A., Lee, M. Y., Syväoja, J. E., et al. (2006). Distinctive activities of dna polymerases during human dna replication. *The FEBS journal*, 273(13), 2984–3001.

[Safak et al., 1999] Safak, M., Gallia, G. L., & Khalili, K. (1999). Reciprocal interaction between two cellular proteins, purα and yb-1, modulates transcriptional activity of jcvcy in glial cells. *Molecular and cellular biology*, 19(4), 2712–2723.

[Saher et al., 2009] Saher, G., Quintes, S., Möbius, W., Wehr, M. C., Krämer-Albers, E.-M., Brügger, B., & Nave, K.-A. (2009). Cholesterol regulates the endoplasmic reticulum exit of the major membrane protein p0 required for peripheral myelin compaction. *Journal of Neuroscience*, 29(19), 6094–6104.

[Samanta & Kessler, 2004] Samanta, J. & Kessler, J. A. (2004). Interactions between id and olig proteins mediate the inhibitory effects of bmp4 on oligodendroglial differentiation. *Development*, 131(17), 4131–4142.

[Sarlieve et al., 1983] Sarlieve, L., Fabre, M., Susz, J., & Matthieu, J. (1983). Investigations on myelination in vitro: Iv. "'myelin-like"' or premyelin structures in cultures of dissociated brain cells from 14–15-day-old embryonic mice. *Journal of neuroscience research*, 10(2), 191–210.

[Schmidt et al., 2004] Schmidt, A., Marescau, B., Boehm, E. A., Renema, W. K. J., Peco, R., Das, A., Steinfeld, R., Chan, S., Wallis, J., Davidoff, M., et al. (2004). Severely altered guanidino compound levels, disturbed body weight homeostasis and impaired fertility in a mouse model of guanidinoacetate n-methyltransferase (gamt) deficiency. *Human molecular genetics*, 13(9), 905–921.

[Schubert et al., 1974] Schubert, D., Heinemann, S., Carlisle, W., Tarikas, H., Kimes, B., Patrick, J., Steinbach, J. H., Culp, W., & Brandt, B. (1974). Clonal cell lines from the rat central nervous system. *Nature*, 249(5454), 224–227.

[Schumacher et al., 2012] Schumacher, M., Hussain, R., Gago, N., Oudinet, J.-P., Mattern, C., & Ghoumari, A. M. (2012). Progesterone synthesis in the nervous system: implications for myelination and myelin repair. *Neurosteroids*, (pp. 234).

[Schwämmle et al., 2013] Schwämmle, V., León, I. R., & Jensen, O. N. (2013). Assessment and improvement of statistical tools for comparative proteomics analysis of sparse data sets with few experimental replicates. *Journal of proteome research*, 12(9), 3874–3883.

[Shachaf et al., 2004] Shachaf, C. M., Kopelman, A. M., Arvanitis, C., Karlsson, Å., Beer, S., Mandl, S., Bachmann, M. H., Borowsky, A. D., Ruebner, B., Cardiff, R. D., et al. (2004). Myc inactivation uncovers pluripotent differentiation and tumour dormancy in hepatocellular cancer. *Nature*, 431(7012), 1112–1117.

[Shannon et al., 2003] Shannon, P., Markiel, A., Ozier, O., Baliga, N. S., Wang, J. T., Ramage, D., Amin, N., Schwikowski, B., & Ideker, T. (2003). Cytoscape: a software environment for integrated models of biomolecular interaction networks. *Genome research*, 13(11), 2498–2504.

[Sharma et al., 2015] Sharma, K., Schmitt, S., Bergner, C. G., Tyanova, S., Kannaiyan, N., Manrique-Hoyos, N., Kongi, K., Cantuti, L., Hanisch, U.-K., Philips, M.-A., et al. (2015). Cell type-and brain region-resolved mouse brain proteome. *Nature neuroscience*, 18(12), 1819–1831.

[Shen et al., 2005] Shen, S., Li, J., & Casaccia-Bonnefil, P. (2005). Histone modifications affect timing of oligodendrocyte progenitor differentiation in the developing rat brain. *The Journal of cell biology*, 169(4), 577–589.

[Sidman et al., 1964] Sidman, R. L., Dickie, M. M., & Appel, S. H. (1964). Mutant mice (quaking and jimpy) with deficient myelination in the central nervous system. *Science*, (pp. 309–311).

[Siegel et al., 1999] Siegel, G., Agranoff, B., & Albers, R. (1999). *Basic neurochemistry: molecular, cellular and medical aspects*. Lippincott-Raven, 6th edition.

[Skaper et al., 2009] Skaper, S. D., Evans, N. A., Soden, P. E., Rosin, C., Facci, L., & Richardson, J. C. (2009). Oligodendrocytes are a novel source of amyloid peptide generation. *Neurochemical research*, 34(12), 2243–2250.

[Sofroniew & Vinters, 2010] Sofroniew, M. V. & Vinters, H. V. (2010). Astrocytes: biology and pathology. *Acta neuropathologica*, 119(1), 7–35.

[Solly et al., 1996] Solly, S., Thomas, J.-L., Monge, M., Demerens, C., Lubetzki, C., Gardinier, M., Matthieu, J.-M., & Zalc, B. (1996). Myelin/oligodendrocyte glycoprotein (mog) expression is associated with myelin deposition. *Glia*, 18(1), 39–48.

[Soloaga et al., 2003] Soloaga, A., Thomson, S., Wiggin, G. R., Rampersaud, N., Dyson, M. H., Hazzalin, C. A., Mahadevan, L. C., & Arthur, J. S. C. (2003). Msk2 and msk1 mediate the mitogen-and stress-induced phosphorylation of histone h3 and hmg-14. *The EMBO journal*, 22(11), 2788–2797.

[Sørlie et al., 2001] Sørlie, T., Perou, C. M., Tibshirani, R., Aas, T., Geisler, S., Johnsen, H., Hastie, T., Eisen, M. B., Van De Rijn, M., Jeffrey, S. S., et al. (2001). Gene expression patterns of breast carcinomas distinguish tumor subclasses with clinical implications. *Proceedings of the National Academy of Sciences*, 98(19), 10869–10874.

[Stacey et al., 1999] Stacey, D. W., Hitomi, M., Kanovsky, M., Gan, L., & Johnson, E. M. (1999). Cell cycle arrest and morphological alterations following microinjection of nih3t3 cells with pur. *Oncogene*, 18(29), 4254–4261.

[Stanelle et al., 2002] Stanelle, J., Stiewe, T., Theseling, C. C., Peter, M., & Pützer, B. M. (2002). Gene expression changes in response to e2f1 activation. *Nucleic acids research*, 30(8), 1859–1867.

[Steelman et al., 2016] Steelman, A. J., Zhou, Y., Koito, H., Kim, S., Payne, H. R., Lu, Q. R., & Li, J. (2016). Activation of oligodendroglial stat3 is required for efficient remyelination. *Neurobiology of disease*, 91, 336–346.

[Sternberger et al., 1978] Sternberger, N. H., Itoyama, Y., Kies, M. W., & Webster, H. d. F. (1978). Immunocytochemical method to identify basic protein in myelin-forming oligodendrocytes of newborn rat cns. *Journal of neurocytology*, 7(2), 251–263.

[Stewart & Fang, 2005a] Stewart, S. & Fang, G. (2005a). Anaphase-promoting complex/cyclosome controls the stability of tpx2 during mitotic exit. *Molecular and cellular biology*, 25(23), 10516–10527.

[Stewart & Fang, 2005b] Stewart, S. & Fang, G. (2005b). Destruction box–dependent degradation of aurora b is mediated by the anaphase-promoting complex/cyclosome and cdh1. *Cancer research*, 65(19), 8730–8735.

[Streit, 2002] Streit, W. J. (2002). Microglia as neuroprotective, immunocompetent cells of the cns. *Glia*, 40(2), 133–139.

[Stryer et al., 2002] Stryer, L., Tymoczko, J. L., & Berg, J. M. (2002). *Biochemistry*. W H Freeman, 5th edition.

[Sugiarto et al., 2011] Sugiarto, S., Persson, A. I., Munoz, E. G., Waldhuber, M., Lamagna, C., Andor, N., Hanecker, P., Ayers-Ringler, J., Phillips, J., Siu, J., et al. (2011). Asymmetry-defective oligodendrocyte progenitors are glioma precursors. *Cancer cell*, 20(3), 328–340.

[Sullivan & Geisert, 1998] Sullivan, C. & Geisert, E. (1998). Expression of rat target of the antiproliferative antibody (tapa) in the developing brain. *Journal of Comparative Neurology*, 396(3), 366–380.

[Sullivan, 1988] Sullivan, K. F. (1988). Structure and utilization of tubulin isotypes. *Annual review of cell biology*, 4(1), 687–716.

[Supek et al., 2011] Supek, F., Bošnjak, M., Škunca, N., & Šmuc, T. (2011). Revigo summarizes and visualizes long lists of gene ontology terms. *PloS one*, 6(7), e21800.

[Suzuki et al., 2016] Suzuki, Y., Chin, W.-X., Ichiyama, K., Lee, C. H., Eyo, Z. W., Ebina, H., Takahashi, H., Takahashi, C., Tan, B. H., Hishiki, T., et al. (2016). Characterization of ryden (c19orf66) as an interferon-stimulated cellular inhibitor against dengue virus replication. *PLoS Pathog*, 12(1), e1005357.

[Swiss et al., 2011] Swiss, V. A., Nguyen, T., Dugas, J., Ibrahim, A., Barres, B., Androulakis, I. P., & Casaccia, P. (2011). Identification of a gene regulatory network necessary for the initiation of oligodendrocyte differentiation. *PloS one*, 6(4), e18088.

[Syed et al., 2008] Syed, Y. a., Baer, A. S., Lubec, G., Hoeger, H., Widhalm, G., & Kotter, M. R. (2008). Inhibition of oligodendrocyte precursor cell differentiation by myelin-associated proteins. *Neurosurgical focus*, 24(3-4), E5.

[Sze et al., 2002] Sze, S. K., Ge, Y., Oh, H., & McLafferty, F. W. (2002). Top-down mass spectrometry of a 29-kda protein for characterization of any posttranslational modification to within one residue. *Proceedings of the National Academy of Sciences*, 99(4), 1774–1779.

[Szuchet et al., 1986] Szuchet, S., Polak, P. E., & Yim, S. H. (1986). Mature oligodendrocytes cultured in the absence of neurons recapitulate the ontogenic development of myelin membranes. *Developmental neuroscience*, 8(4), 208–221.

[Szuchet & Yim, 1984] Szuchet, S. & Yim, S. (1984). Characterization of a subset of oligodendrocytes separated on the basis of selective adherence properties. *Journal of neuroscience research*, 11(2), 131–144.

[Takasaki et al., 2010] Takasaki, C., Yamasaki, M., Uchigashima, M., Konno, K., Yanagawa, Y., & Watanabe, M. (2010). Cytochemical and cytological properties of perineuronal oligodendrocytes in the mouse cortex. *European Journal of Neuroscience*, 32(8), 1326–1336.

[Takeo et al., 2016] Takeo, Y., Kurabayashi, N., Nguyen, M. D., & Sanada, K. (2016). The g protein-coupled receptor gpr157 regulates neuronal differentiation of radial glial progenitors through the gq-ip3 pathway. *Scientific reports*, 6.

[Talbott et al., 2007] Talbott, J. F., Cao, Q., Bertram, J., Nkansah, M., Benton, R. L., Lavik, E., & Whittemore, S. R. (2007). Cntf promotes the survival and differentiation of adult spinal cord-derived oligodendrocyte precursor cells in vitro but fails to promote remyelination in vivo. *Experimental neurology*, 204(1), 485–489.

[Tang & Chua, 2008] Tang, B. L. & Chua, C. E. L. (2008). SIRT2, tubulin deacetylation, and oligodendroglia differentiation. *Cell Motility and the Cytoskeleton*, 65(3), 179–182.

[Tekki-Kessaris et al., 2001] Tekki-Kessaris, N., Woodruff, R., Hall, A. C., Gaffield, W., Kimura, S., Stiles, C. D., Rowitch, D. H., & Richardson, W. D. (2001). Hedgehog-dependent oligodendrocyte lineage specification in the telencephalon. *Development*, 128(13), 2545–2554.

[Temple, 2001] Temple, S. (2001). The development of neural stem cells. *Nature*, 414(6859), 112–117.

[Temple & Raff, 1986] Temple, S. & Raff, M. C. (1986). Clonal analysis of oligodendrocyte development in culture: evidence for a developmental clock that counts cell divisions. *Cell*, 44(5), 773–779.

[Terada et al., 2002] Terada, N., Baracskay, K., Kinter, M., Melrose, S., Brophy, P. J., Boucheix, C., Bjartmar, C., Kidd, G., & Trapp, B. D. (2002). The tetraspanin protein, cd9, is expressed by progenitor cells committed to oligodendrogenesis and is linked to β1 integrin, cd81, and tspan-2. *Glia*, 40(3), 350–359.

[Thompson et al., 2003] Thompson, A., Schäfer, J., Kuhn, K., Kienle, S., Schwarz, J., Schmidt, G., Neumann, T., & Hamon, C. (2003). Tandem mass tags: a novel quantification strategy for comparative analysis of complex protein mixtures by ms/ms. *Analytical chemistry*, 75(8), 1895–1904.

[Thorburne & Juurlink, 1996] Thorburne, S. K. & Juurlink, B. H. (1996). Low glutathione and high iron govern the susceptibility of oligodendroglial precursors to oxidative stress. *Journal of neurochemistry*, 67(3), 1014–1022.

[Tiwari-Woodruff et al., 2001] Tiwari-Woodruff, S. K., Buznikov, A. G., Vu, T. Q., Micevych, P. E., Chen, K., Kornblum, H. I., & Bronstein, J. M. (2001). Osp/claudin-11 forms a complex with a novel member of the tetraspanin super family and β1 integrin and regulates proliferation and migration of oligodendrocytes. *The Journal of cell biology*, 153(2), 295–306.

[Toby et al., 2016] Toby, T. K., Fornelli, L., & Kelleher, N. L. (2016). Progress in top-down proteomics and the analysis of proteoforms. *Annual Review of Analytical Chemistry*, 9, 499–519.

[Tokumoto et al., 1999] Tokumoto, Y. M., Durand, B., & Raff, M. C. (1999). An analysis of the early events when oligodendrocyte precursor cells are triggered to differentiate by thyroid hormone, retinoic acid, or pdgf withdrawal. *Developmental biology*, 213(2), 327–339.

[Traiffort et al., 2016] Traiffort, E., Zakaria, M., Laouarem, Y., & Ferent, J. (2016). Hedgehog: A key signaling in the development of the oligodendrocyte lineage. *Journal of Developmental Biology*, 4(3), 28.

[Tran et al., 2011] Tran, J. C., Zamdborg, L., Ahlf, D. R., Lee, J. E., Catherman, A. D., Durbin, K. R., Tipton, J. D., Vellaichamy, A., Kellie, J. F., Li, M., et al. (2011). Mapping intact protein isoforms in discovery mode using top down proteomics. *Nature*, 480(7376), 254.

[Trapp et al., 1999] Trapp, B. D., Ransohoff, R., & Rudick, R. (1999). Axonal pathology in multiple sclerosis: relationship to neurologic disability. *Current opinion in neurology*, 12(3), 295–302.

[Tretiakova et al., 1999] Tretiakova, A., Steplewski, A., Johnson, E. M., Khalili, K., & Amini, S. (1999). Regulation of myelin basic protein gene transcription by sp1 and purα: evidence for association of sp1 and purα in brain. *Journal of cellular physiology*, 181(1), 160–168.

[Trinidad et al., 2012] Trinidad, J. C., Barkan, D. T., Gulledge, B. F., Thalhammer, A., Sali, A., Schoepfer, R., & Burlingame, A. L. (2012). Global identification and characterization of both o-glcnacylation and phosphorylation at the murine synapse. *Molecular & Cellular Proteomics*, 11(8), 215–229.

[Trinkle-Mulcahy et al., 2008] Trinkle-Mulcahy, L., Boulon, S., Lam, Y. W., Urcia, R., Boisvert, F.-M., Vandermoere, F., Morrice, N. A., Swift, S., Rothbauer, U., Leonhardt, H., et al. (2008). Identifying specific protein interaction partners using quantitative mass spectrometry and bead proteomes. *The Journal of cell biology*, 183(2), 223–239.

[Tropepe et al., 1999] Tropepe, V., Sibilia, M., Ciruna, B. G., Rossant, J., Wagner, E. F., & van der Kooy, D. (1999). Distinct neural stem cells proliferate in response to EGF and FGF in the developing mouse telencephalon. *Developmental biology*, 208(1), 166–88.

[Tsuyuki et al., 1956] Tsuyuki, E., Tsuyuki, H., & Stahmann, M. A. (1956). The synthesis and enzymatic hydrolysis of poly-d-lysine. *Journal of Biological Chemistry*, 222(1), 479–485.

[Tyanova et al., 2016] Tyanova, S., Temu, T., Sinitcyn, P., Carlson, A., Hein, M. Y., Geiger, T., Mann, M., & Cox, J. (2016). The perseus computational platform for comprehensive analysis of (prote) omics data. *Nature methods*.

[Tyler et al., 2011] Tyler, W. a., Jain, M. R., Cifelli, S. E., Li, Q., Ku, L., Feng, Y., Li, H., & Wood, T. L. (2011). Proteomic identification of novel targets regulated by the mammalian target of rapamycin pathway during oligodendrocyte differentiation. *Glia*, 59(11), 1754–69.

[Tzur et al., 2011] Tzur, A., Moore, J. K., Jorgensen, P., Shapiro, H. M., & Kirschner, M. W. (2011). Optimizing optical flow cytometry for cell volume-based sorting and analysis. *PloS one*, 6(1), e16053.

[Uhlén et al., 2015] Uhlén, M., Fagerberg, L., Hallström, B. M., Lindskog, C., Oksvold, P., Mardinoglu, A., Sivertsson, Å., Kampf, C., Sjöstedt, E., Asplund, A., et al. (2015). Tissue-based map of the human proteome. *Science*, 347(6220), 1260419.

[Valdar & Thornton, 2001] Valdar, W. S. & Thornton, J. M. (2001). Protein–protein interfaces: analysis of amino acid conservation in homodimers. *Proteins: Structure, Function, and Bioinformatics*, 42(1), 108–124.

[Vogel & Marcotte, 2012] Vogel, C. & Marcotte, E. M. (2012). Insights into the regulation of protein abundance from proteomic and transcriptomic analyses. *Nature Reviews Genetics*, 13(4), 227–232.

[Wagner et al., 2012a] Wagner, S. A., Beli, P., Weinert, B. T., Schölz, C., Kelstrup, C. D., Young, C., Nielsen, M. L., Olsen, J. V., Brakebusch, C., & Choudhary, C. (2012a). Proteomic analyses reveal divergent ubiquitylation site patterns in murine tissues. *Molecular & Cellular Proteomics*, 11(12), 1578–1585.

[Wagner et al., 2012b] Wagner, S. a., Beli, P., Weinert, B. T., Schölz, C., Kelstrup, C. D., Young, C., Nielsen, M. L., Olsen, J. V., Brakebusch, C., & Choudhary, C. (2012b). Proteomic analyses reveal divergent ubiquitylation site patterns in murine tissues. *Molecular & cellular proteomics : MCP*, 11(12), 1578–85.

[Wang et al., 2006] Wang, G., Wu, W. W., Zeng, W., Chou, C.-L., & Shen, R.-F. (2006). Label-free protein quantification using lc-coupled ion trap or ft mass spectrometry: Reproducibility, linearity, and application with complex proteomes. *Journal of proteome research*, 5(5), 1214–1223.

[Wang et al., 2004] Wang, H., Ku, L., Osterhout, D. J., Li, W., Ahmadian, A., Liang, Z., & Feng, Y. (2004). Developmentally-programmed fmrp expression in oligodendrocytes: a potential role of fmrp in regulating translation in oligodendroglia progenitors. *Human molecular genetics*, 13(1), 79–89.

[Wang et al., 1999] Wang, S., Nath, N., Adlam, M., & Chellappan, S. (1999). Prohibitin, a potential tumor suppressor, interacts with rb and regulates e2f function. *Oncogene*, 18(23), 3501–3510.

[Ward Jr, 1963] Ward Jr, J. H. (1963). Hierarchical grouping to optimize an objective function. *Journal of the American statistical association*, 58(301), 236–244.

[Warrington et al., 1993] Warrington, A., Barbarese, E., & Pfeiffer, S. (1993). Differential myelinogenic capacity of specific developmental stages of the oligodendrocyte lineage upon transplantation into hypomyelinating hosts. *Journal of neuroscience research*, 34(1), 1–13.

[Watanabe et al., 2002] Watanabe, M., Toyama, Y., & Nishiyama, A. (2002). Differentiation of proliferated ng2-positive glial progenitor cells in a remyelinating lesion. *Journal of neuroscience research*, 69(6), 826–836.

[Watkins et al., 2007] Watkins, P. A., Maiguel, D., Jia, Z., & Pevsner, J. (2007). Evidence for 26 distinct acyl-coenzyme a synthetase genes in the human genome. *Journal of lipid research*, 48(12), 2736–2750.

[Weber et al., 2016] Weber, J., Bao, H., Hartlmüller, C., Wang, Z., Windhager, A., Janowski, R., Madl, T., Jin, P., & Niessing, D. (2016). Structural basis of nucleic-acid recognition and double-strand unwinding by the essential neuronal protein pur-alpha. *eLife*, 5, e11297.

[Wehr, 2006] Wehr, T. (2006). Top-down versus bottom-up approaches in proteomics. *Lc Gc North America*, 24(9).

[Wen et al., 2009] Wen, S., Li, H., & Liu, J. (2009). Dynamic signaling for neural stem cell fate determination. *Cell adhesion & migration*, 3(1), 107–117.

[Wennerberg et al., 2005] Wennerberg, K., Rossman, K. L., & Der, C. J. (2005). The ras superfamily at a glance. *J cell Sci*, 118(5), 843–846.

[Werner et al., 2007] Werner, H. B., Kuhlmann, K., Shen, S., Uecker, M., Schardt, A., Dimova, K., Orfaniotou, F., Dhaunchak, A., Brinkmann, B. G., Möbius, W., Guarente, L., Casaccia-Bonnefil, P., Jahn, O., & Nave, K.-A. (2007). Proteolipid protein is required for transport of sirtuin 2 into CNS myelin. *The Journal of neuroscience : the official journal of the Society for Neuroscience*, 27(29), 7717–30.

[White & Krämer-Albers, 2013] White, R. & Krämer-Albers, E.-M. (2013). Axon-glia interaction and membrane traffic in myelin formation. *Frontiers in cellular neuroscience*, 7.

[Wiese et al., 2007] Wiese, S., Reidegeld, K. A., Meyer, H. E., & Warscheid, B. (2007). Protein labeling by itraq: a new tool for quantitative mass spectrometry in proteome research. *Proteomics*, 7(3), 340–350.

[Wilson & Brophy, 1989] Wilson, R. & Brophy, P. (1989). Role for the oligodendrocyte cytoskeleton in myelination. *Journal of neuroscience research*, 22(4), 439–448.

[Wiśniewski et al., 2009] Wiśniewski, J. R., Zougman, A., & Mann, M. (2009). Combination of fasp and stagetip-based fractionation allows in-depth analysis of the hippocampal membrane proteome. *Journal of proteome research*, 8(12), 5674–5678.

[Wiśniewski et al., 2009] Wiśniewski, J. R., Zougman, A., Nagaraj, N., & Mann, M. (2009). Universal sample preparation method for proteome analysis. *Nature methods*, 6(5), 359–362.

[Wolf et al., 2001] Wolf, R. M., Wilkes, J. J., Chao, M. V., & Resh, M. D. (2001). Tyrosine phosphorylation of p190 rhogap by fyn regulates oligodendrocyte differentiation. *Developmental Neurobiology*, 49(1), 62–78.

[Xing et al., 2016] Xing, S., Wallmeroth, N., Berendzen, K. W., & Grefen, C. (2016). Techniques for the analysis of protein-protein interactions in vivo. *Plant physiology*, 171(2), 727–758.

[Yates et al., 2009] Yates, J. R., Ruse, C. I., & Nakorchevsky, A. (2009). Proteomics by mass spectrometry: approaches, advances, and applications. *Annual review of biomedical engineering*, 11, 49–79.

[Yazaki et al., 2000] Yazaki, K., Yoshida, T., Wakiyama, M., & Miura, K.-i. (2000). Polysomes of eukaryotic cells observed by electron microscopy. *Microscopy*, 49(5), 663–668.

[Yoshizawa-Sugata & Masai, 2007] Yoshizawa-Sugata, N. & Masai, H. (2007). Human tim/timeless-interacting protein, tipin, is required for efficient progression of s phase and dna replication checkpoint. *Journal of Biological Chemistry*, 282(4), 2729–2740.

[Young et al., 2013] Young, K. M., Psachoulia, K., Tripathi, R. B., Dunn, S.-J., Cossell, L., Attwell, D., Tohyama, K., & Richardson, W. D. (2013). Oligodendrocyte dynamics in the healthy adult cns: evidence for myelin remodeling. *Neuron*, 77(5), 873–885.

[Zawadzka et al., 2010] Zawadzka, M., Rivers, L. E., Fancy, S. P., Zhao, C., Tripathi, R., Jamen, F., Young, K., Goncharevich, A., Pohl, H., Rizzi, M., et al. (2010). Cns-resident glial progenitor/stem cells produce schwann cells as well as oligodendrocytes during repair of cns demyelination. *Cell stem cell*, 6(6), 578–590.

[Zhang et al., 2006a] Zhang, C., Kong, D., Tan, M.-H., Pappas, D. L., Wang, P.-F., Chen, J., Farber, L., Zhang, N., Koo, H.-M., Weinreich, M., et al. (2006a). Parafibromin inhibits cancer cell growth and causes g1 phase arrest. *Biochemical and biophysical research communications*, 350(1), 17–24.

[Zhang & Ge, 2011] Zhang, H. & Ge, Y. (2011). Comprehensive analysis of protein modifications by top-down mass spectrometry. *Circulation: Cardiovascular Genetics*, 4(6), 711–711.

[Zhang et al., 2005] Zhang, Q., Pedigo, N., Shenoy, S., Khalili, K., & Kaetzel, D. M. (2005). Purα activates pdgf-a gene transcription via interactions with a g-rich, single-stranded region of the promoter. *Gene*, 348, 25–32.

[Zhang et al., 1999] Zhang, S. C., Ge, B., & Duncan, I. D. (1999). Adult brain retains the potential to generate oligodendroglial progenitors with extensive myelination capacity. *Proceedings of the National Academy of Sciences of the United States of America*, 96(7), 4089–94.

[Zhang et al., 1998] Zhang, S.-C., Lundberg, C., Lipsitz, D., O'connor, L. T., & Duncan, I. D. (1998). Generation of oligodendroglial progenitors from neural stem cells. *Journal of neurocytology*, 27(7), 475–489.

[Zhang et al., 2012a] Zhang, X., Bolt, M., Guertin, M. J., Chen, W., Zhang, S., Cherrington, B. D., Slade, D. J., Dreyton, C. J., Subramanian, V., Bicker, K. L., et al. (2012a). Peptidylarginine deiminase 2-catalyzed histone h3 arginine 26 citrullination facilitates estrogen receptor α target gene activation. *Proceedings of the National Academy of Sciences*, 109(33), 13331–13336.

[Zhang et al., 2013] Zhang, Y., Fonslow, B. R., Shan, B., Baek, M.-C., & Yates III, J. R. (2013). Protein analysis by shotgun/bottom-up proteomics. *Chemical reviews*, 113(4), 2343–2394.

[Zhang et al., 2001] Zhang, Y., Liu, G., & Dong, Z. (2001). Msk1 and jnks mediate phosphorylation of stat3 in uva-irradiated mouse epidermal jb6 cells. *Journal of Biological Chemistry*, 276(45), 42534–42542.

[Zhang et al., 2012b] Zhang, Y., Liu, J., Yao, S., Li, F., Xin, L., Lai, M., Bracchi-Ricard, V., Xu, H., Yen, W., Meng, W., et al. (2012b). Nuclear factor kappa b signaling initiates early differentiation of neural stem cells. *Stem Cells*, 30(3), 510–524.

[Zhang et al., 2006b] Zhang, Y. W., Denham, J., & Thies, R. S. (2006b). Oligodendrocyte progenitor cells derived from human embryonic stem cells express neurotrophic factors. *Stem cells and development*, 15(6), 943–952.

[Zhao et al., 2010] Zhao, X., He, X., Han, X., Yu, Y., Ye, F., Chen, Y., Hoang, T., Xu, X., Mi, Q.-S., Xin, M., et al. (2010). Microrna-mediated control of oligodendrocyte differentiation. *Neuron*, 65(5), 612–626.

[Zhu et al., 2009] Zhu, W., Smith, J. W., & Huang, C.-M. (2009). Mass spectrometry-based label-free quantitative proteomics. *BioMed Research International*, 2010.

[Zhu et al., 2011] Zhu, X., Hill, R. A., Dietrich, D., Komitova, M., Suzuki, R., & Nishiyama, A. (2011). Age-dependent fate and lineage restriction of single ng2 cells. *Development*, 138(4), 745–753.

[Zhu et al., 2013] Zhu, Y., Li, H., Li, K., Zhao, X., An, T., Hu, X., Park, J., Huang, H., Bin, Y., Qiang, B., et al. (2013). Necl-4/syncam-4 is expressed in myelinating oligodendrocytes but not required for axonal myelination. *PloS one*, 8(5), e64264.

A. Appendix

A.1. Differentiation of neural progenitor cells (NPCs) to oligodendrocyte precursor cells (OPCs)

Gene ontology term enrichment analysis of proteins significantly upregulated from day 9 - 15 and from day 12 - 15 of neurosphere differentiation

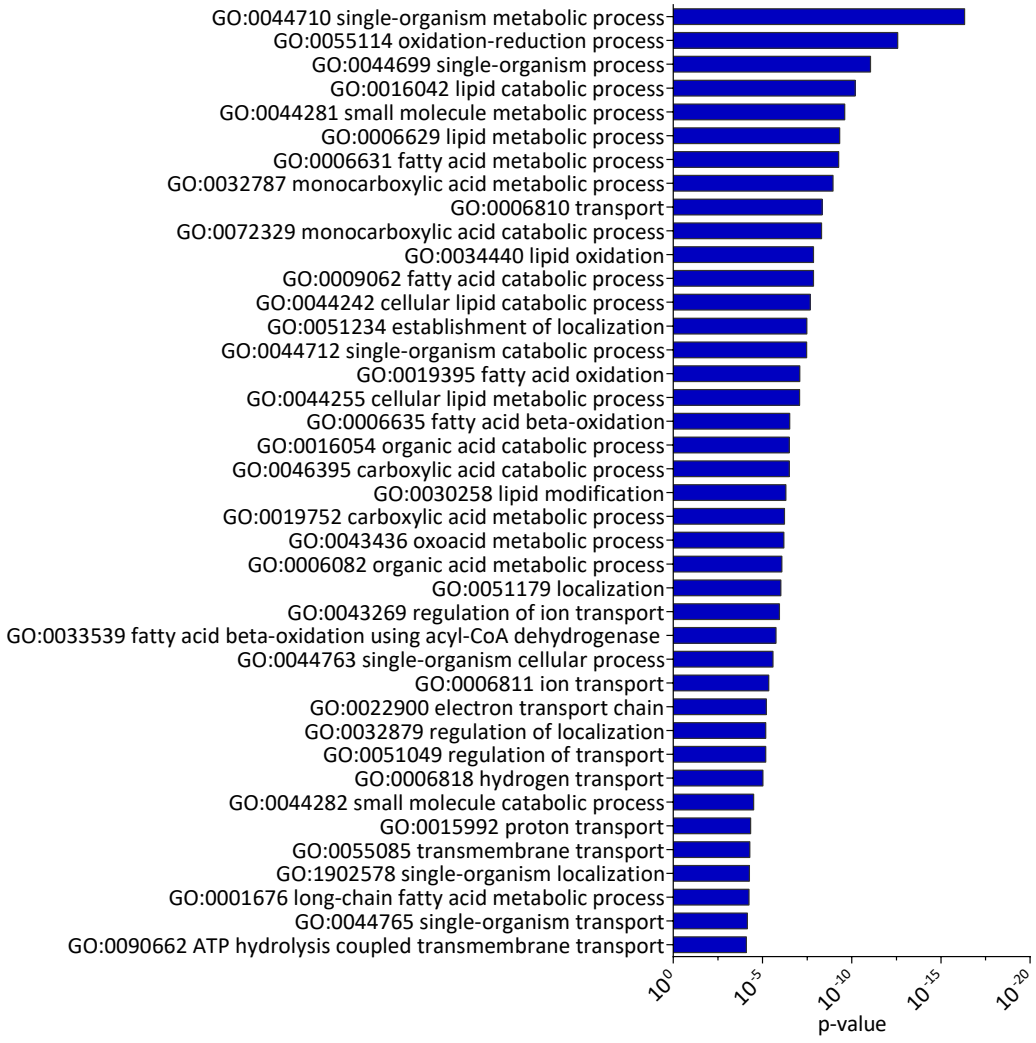

(a) Upregulated proteins - Biological process

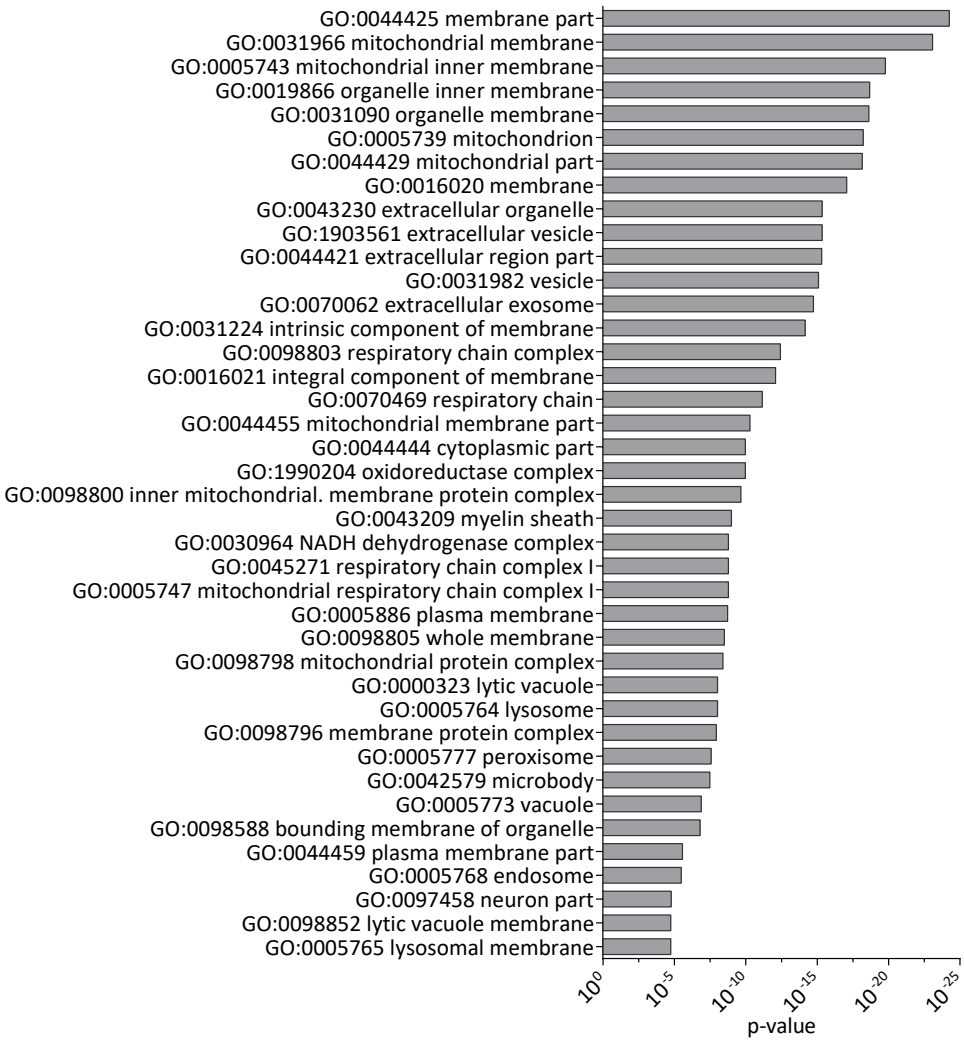

(b) Upregulated proteins - Cellular component

Fig. A.1.: GO term enrichment analysis of proteins significantly upregulated from day 9 - 15 and day 12 - 15 of the neurosphere differentiation experiment. Functional GO enrichment analysis focusing on the ontologies (a) biological process and (b) cellular component was carried out using the GOrilla [Eden et al., 2009] application. Therefore, 403 (341 proteins associated with GO terms) significantly upregulated proteins from day 9 until day 15 and from day 12 until day 15 were searched for enriched GO terms (target proteins) against all proteins, identified in five biological and two technical replicates using MaxQuant (background proteins). The leading razor protein thereby functioned as identifier. After removing not identified genes, duplicates and proteins without any GO term association the remaining 5,254 proteins were utilized for functional gene analysis. Identification of enriched GO terms was achieved using the standard Hyper Geometric testing by calculating an enrichment p-value (x-axis) for each GO term. The diagram depicts the top 40 overrepresented GO terms together with the appertaining p-values in decreasing order, represented as bar-charts. Again, no multiple hypothesis correction on the number of tested GO terms was performed. GO = gene ontology

Gene ontology term enrichment analysis of proteins significantly downregulated during neurosphere differentiation

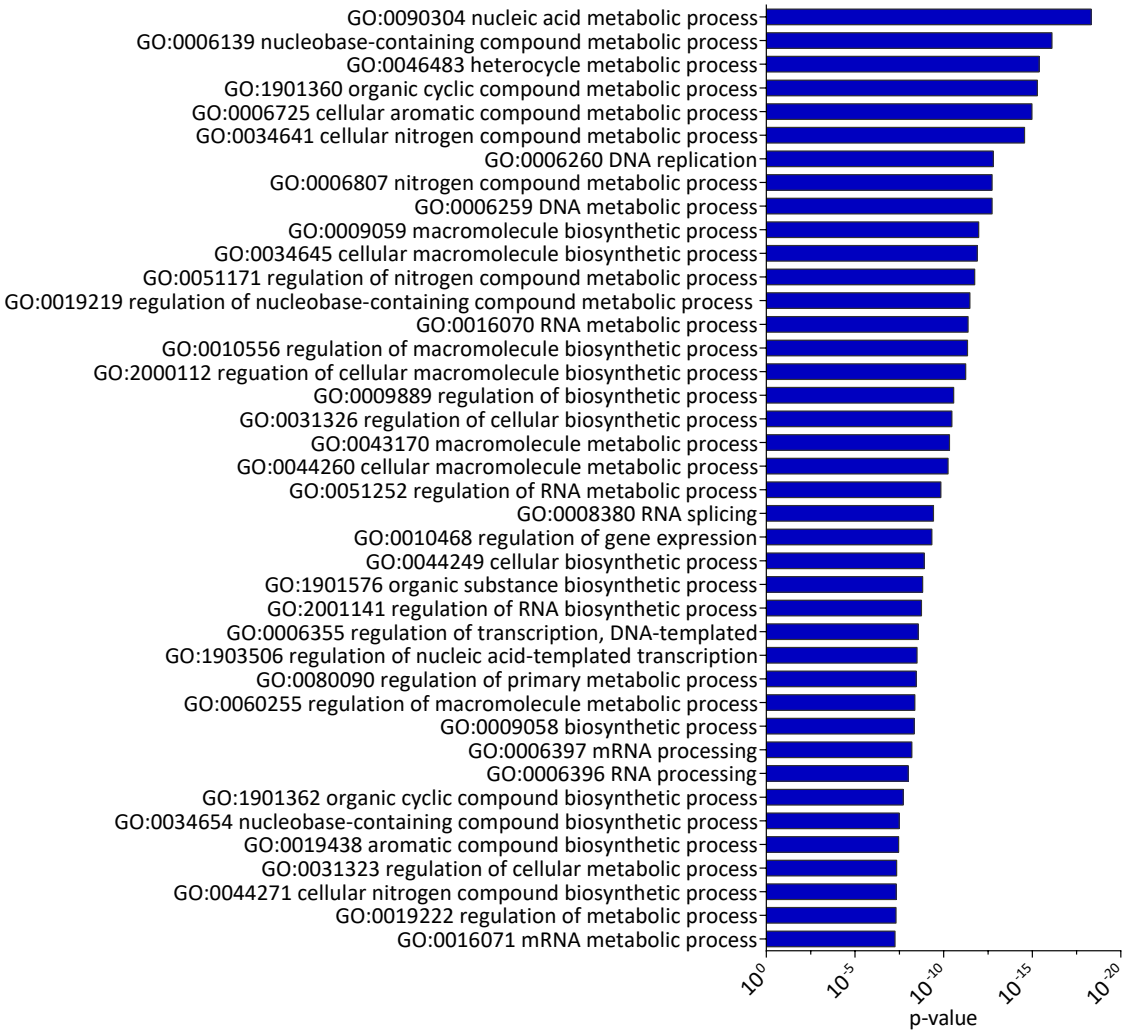

(a) Downregulated proteins - Biological process

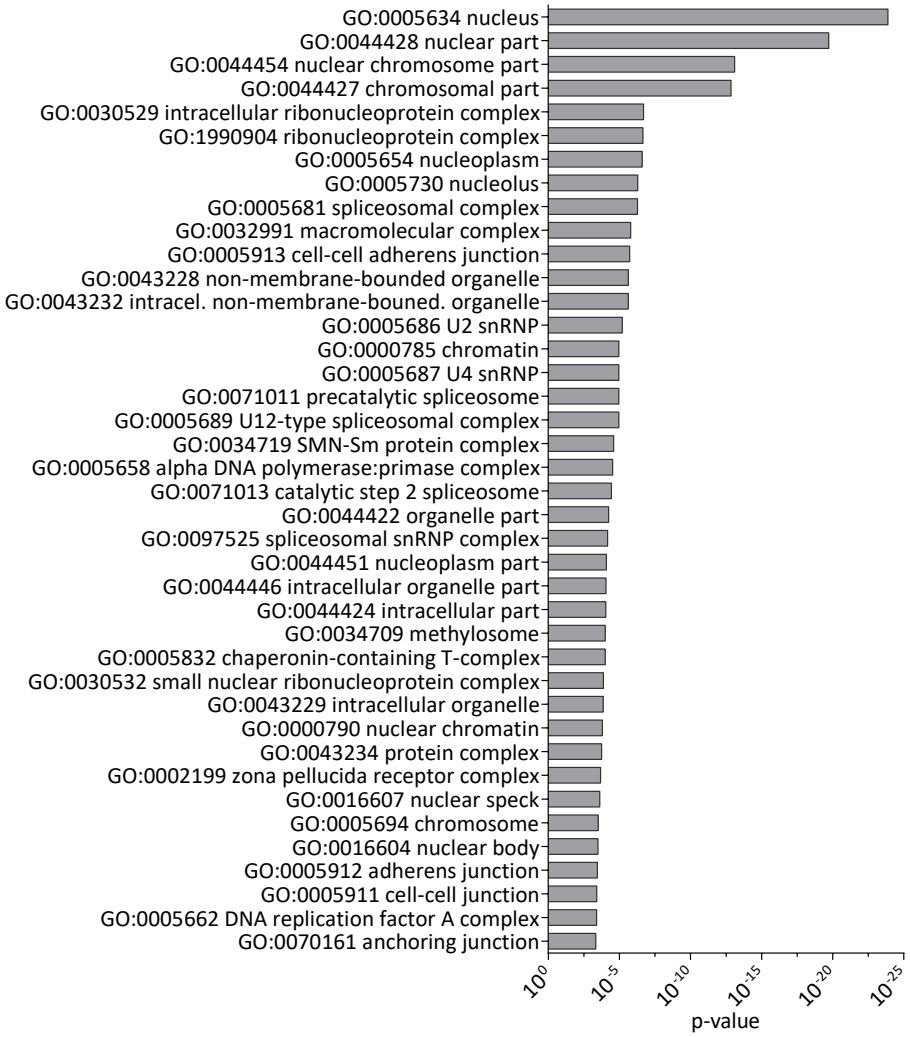

(b) Downregulated proteins - Cellular component

Fig. A.2.: GO term enrichment analysis of proteins significantly downregulated from day 6 until day 15, day 9 until day 15 and day 12 until day 15 of neurosphere differentiation. Functional GO enrichment analysis of (a) biological processes and (b) cellular components was carried out with the GOrilla tool [Eden et al., 2009]. Therefore, the 483 (386 proteins associated with GO terms) significantly downregulated proteins were searched for enriched GO terms (target proteins) against all proteins, identified in five biological and two technical replicates using MaxQuant (background proteins). After removing not identified genes, duplicates and genes without any GO term association the remaining 5,254 proteins were utilized for GO term analysis. Identification of augmented GO terms was achieved using the standard Hyper Geometric testing by calculating an enrichment p-value for each GO term. The diagram depicts the top 40 enriched (a) biological processes and (b) cellular components featuring enrichment p-values < 0.001 together with the appertaining p-values (x-axis) in decreasing order, represented as bar-charts. It should be noted that the depicted p-values did not include the multiple hypothesis correction on the number of tested GO terms. GO = gene ontology

A.2. Investigation of transcriptional activator protein Pur-alpha

Expression and purification of GST-Pur-alpha fusion protein

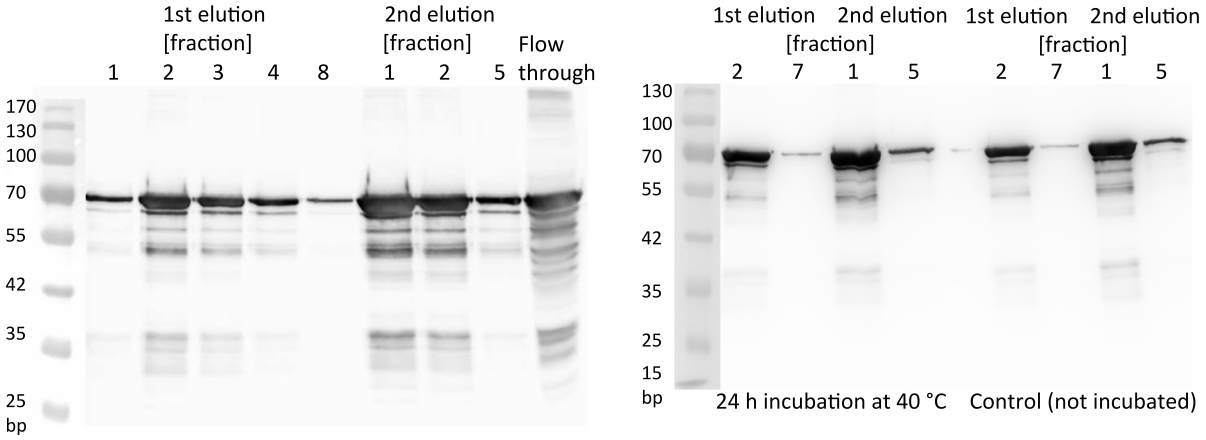

(a) Anti-GST western blot of elution fractions

(b) Anti-GST western blot after stability test

Fig. A.3.: GST-Pur-alpha fusion protein elution and protein stability check. GST-Pur-alpha fusion protein was purified using Pierce™ Glutathione Agarose. Elution was performed with 50 mM Tris, 150 mM NaCl and 10 mM reduced glutathione pH 8.0 (1st elution). Beads were thereafter incubated in elution buffer overnight to perform a 2nd elution the next day. (a) Western blot of elution fractions was performed using the GST-antibody (mouse, 1:200, 4 ℃, over night) and the α-mouse-HRP (goat, 1:5,000, 1h, room temperature). The flow-through sample was taken after incubation of Glutathione Agarose and fusion protein. Two fractions of each elution batch were incubated at 40 ℃ for 24 hours. (b) Anti-GST Western blot of incubated samples and control samples (original elution fraction).

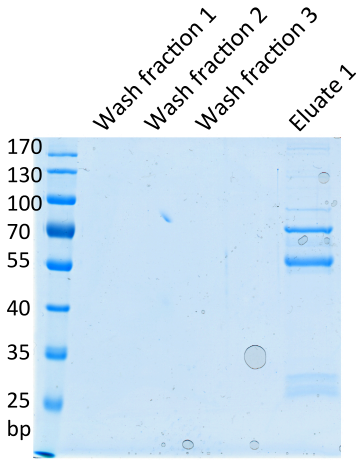

Fig. A.4.: Antiserum purification using Affi-Gel 15 - Washing steps prior to antiserum incubation. The Coomassie staining depicts the three wash fractions before the guinea pig antiserum was applied to the Affi-Gel 15 column as well as eluate 1 of the antiserum elution.

Flow cytometric analyses of cell cycle synchronized in HeLa S3 and fNS cells

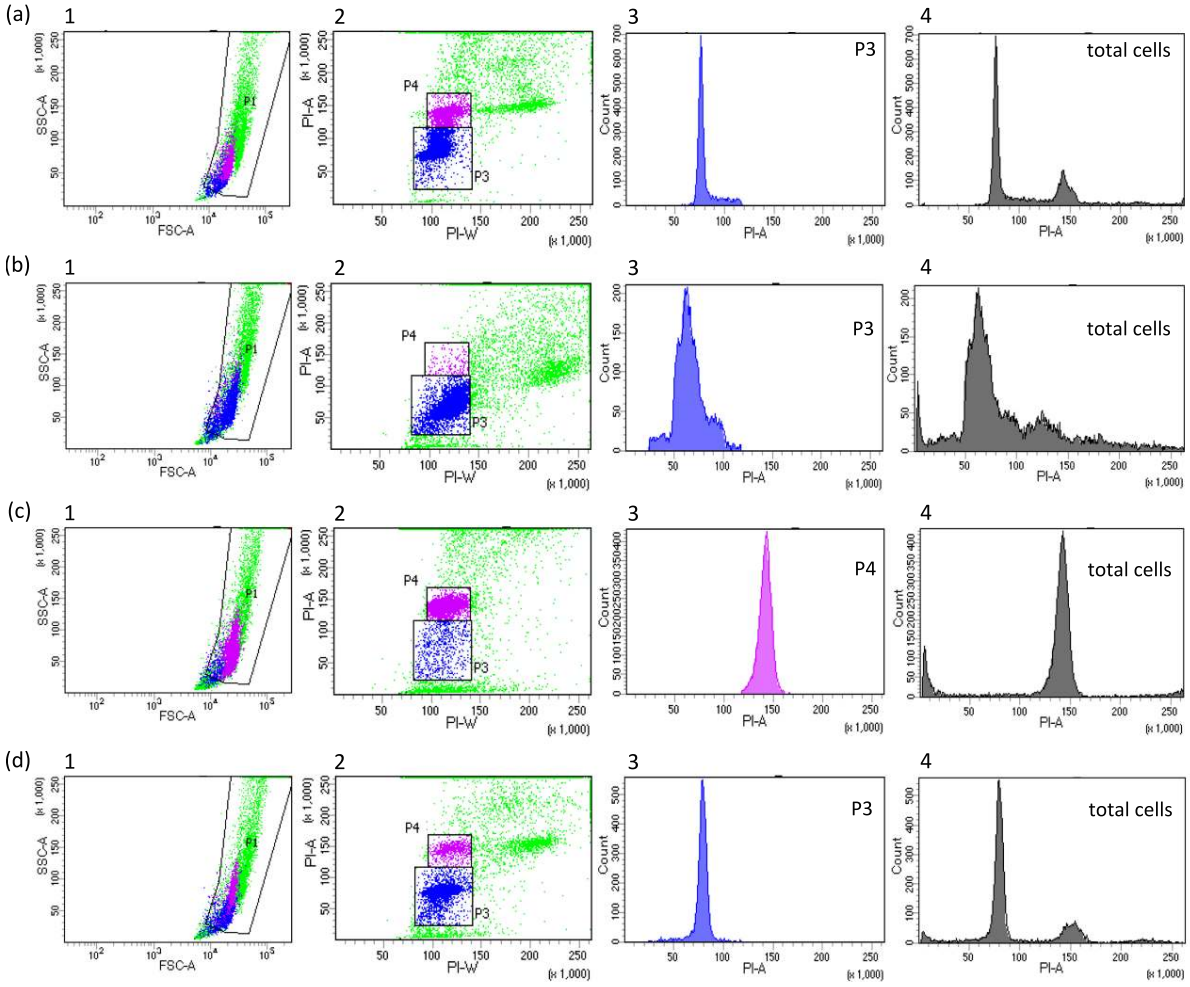

(a) HeLa S3 - Cell cycle synchronization

	Sample	Total (%)	P3 (%)	P4 (%)
(a)	Unsynchronized	100	49.1	16
(b)	Thymidine arrest	100	56	1.6
(c)	Nocodazole arrest	100	6.7	59.3
(d)	Release (4 hours)	100	56.5	7.4

(b) Amount of cells in population P3 and P4

Fig. A.5.: Flow cytometric analysis of cell cycle synchronized HeLa S3 cells Unsynchronized HeLa S3 cells (a), were arrested for 24 hours in S phase using thymidine (b), followed by a medium exchange and release for 3 hours, before arresting cells for 11 hours in mitosis using nocodazole (c) and releasing cells again for 4 hours (d). Cells were harvested at mentioned time points by trypsinization, fixed and stored at -20 ℃. Prior to measurement, samples were treated with 50 µg/ml PI and 10 µ/ml RNase in 1X PBS. Samples were measured using a BD FACSCanto™ II flow cytometer (488nm excitation laser, red detector, 695/40 emission filter). Forward (FSC-A) and side scatter (SSC-A) (Image1) and propidium iodide parameters were manually adjusted and 10,000 cells measured thereafter. The plot PI width (PI-W) versus PI area (PI-A) (Image 2) enables to distinguish cells with a single chromosome set (Population 3, manually determined) from cells with a double chromosome set (Population 4), which displays same PI-W but larger PI-A values, as well as from cell aggregates (high PI-A and PI-W value) and cell debris (low PI-A value). The histogram PI-A (propidium iodide) versus count (total cells) indicates how many cells possess one (50 - 100 x 1,000) or two (150 x 1,000) chromosome sets (Image 3, 4). Image 3 depicts all cells in either population P3 or P4, while image 4 depicts all cells measured. The table (e) depicts the amount of cells per sample present in population P3 and P4. PI = propidium iodide.

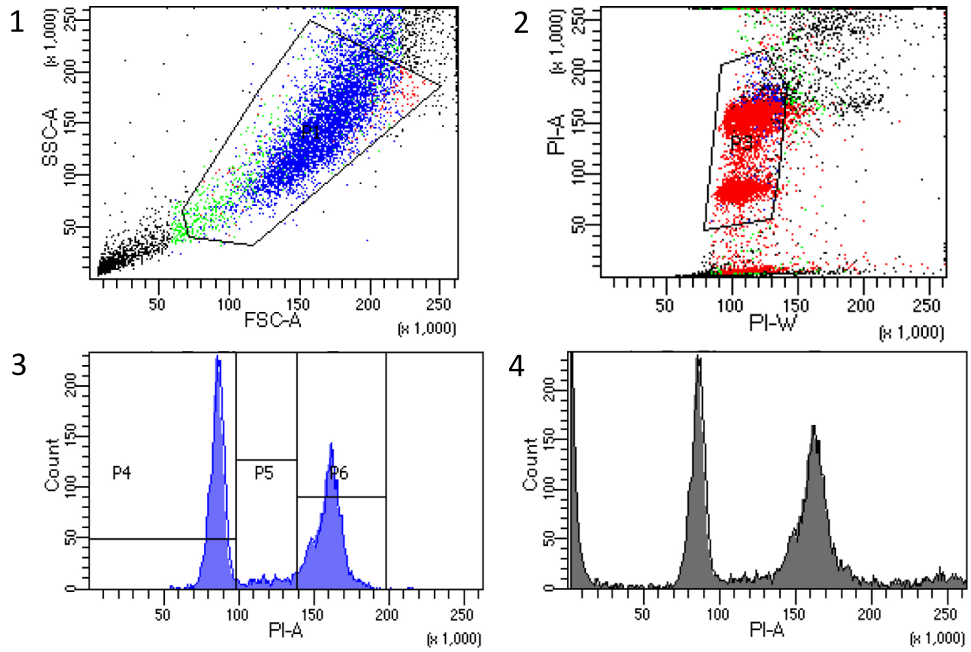

(a) synchronized FNS cells - Four hours after release from mitotic arrest

Population	Total (%)	% total
Population P3	100	52.5
Population P4	100	24.3
Population P5	100	4.2
Population P6	100	23.8

(b) Amount of cells per population

Fig. A.6.: Flow cytometric analysis of cell cycle synchronized fetal neural stem (fNS) cells Unsynchronized fNS cells, cultivated in adherent cultures, were arrested for 22 hours in S phase using thymidine, followed by a medium exchange and release for 3 hours, before arresting cells for 16 hours in mitosis using nocodazole and releasing cells again for 4 hours by exchanging to fresh medium. Cells were harvested by trypsinization, fixed, stored at -20 ℃ and treated with 50 µg/ml PI and 10 µ/ml RNase in 1X PBS prior to measurement. Samples were measured using a BD FACSCanto™ II flow cytometer (488nm excitation laser, red detector, 695/40 emission filter). Forward (FSC-A) and side scatter (SSC-A) (Image1) and propidium iodide parameters were manually adjusted and 10,000 cells measured thereafter. The plot PI width (PI-W) versus PI area (PI-A) (Image 2) enables to distinguish cells with a single chromosome set from cells and a double chromosome set (Population P3) from cell aggregates (high PI-A and PI-W value) and cell debris (low PI-A value). The histogram PI-A (propidium iodide) versus count (total cells) indicates how many cells possess one (Population P4) or two (Population P6) chromosome sets (Image 3, 4). Image 3 depicts all cells gated in population P3, while image 4 depicts all cells measured. Population P3 was further divided into the populations P4, P5 and P6.

Cloning, verification of expression and functionality of BirA*-Pura

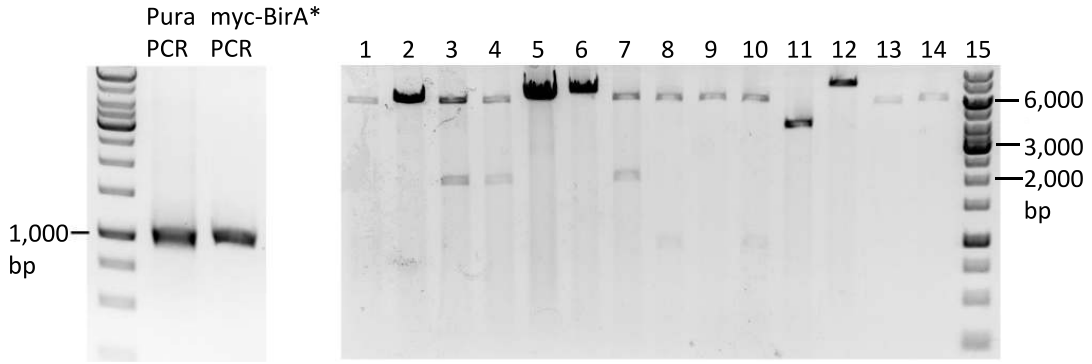

(a) Polymerase chain reaction

(b) BirA*-Pura - Restriction digest after minipreperation

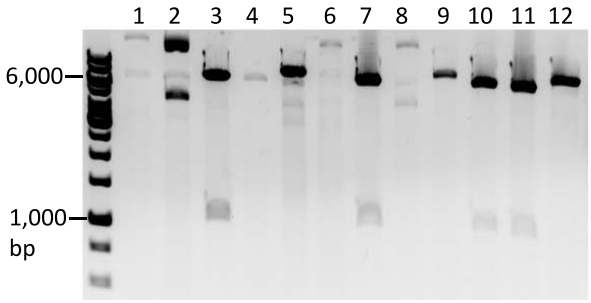

(c) BirA* - Restriction digest after minipreperation

Fig. A.7.: Cloning of BirA*-Pura and BirA*. The Pur-alpha and the myc-BioID (BirA*) gene were amplified by PCR using pBluescript SK-PurA and pcDNA3.1-mycBioID as templates. PCR products were subcloned into the G0656pFIV3.2RSVmcs vector to yield the BirA*-Pura construct, while only the myc gene was subcloned into the vector to yield the BirA* construct. The agarose gel (a) depicts both PCR products. After ligation and transformation, E.coli cells were cultivated and selected by adding ampicillin to the LB agarose plates and clones picked for minipreperation. The agarose gel (b) depicts the restriction digest using NsiI and SpeI of picked clones of BirA*-Pura, while (c) depicts the restriction digest using NsiI and SalI of picked clones of BirA*. The expected product sizes of restriction digestion using NsiI and SpeI are 6,231 bp and 1,975 bp and using NsiI and SalI 6,223 bp and 1,000 bp.

Interaction partner analysis - SILAC-BioID-Pur-alpha

Table A.1.: Significantly enriched protein groups in BirA*-Pura samples. The evidence files (MaxQuant) of three replicates were processed using Perseus. Proteins were filtered for potential contaminants, positive reverse sequences and for proteins, which featured valid values in less than two replicates. SILAC heavy / light ratios were calculated, log2 transformed and normalized to the median of every replicate. The one-sample t-test against 0 in combination with the Benjamini Hochberg correction was applied. Proteins featuring a false discovery rate adjusted p-value ≤ 0.05 and a log2 fold change ≥ 0.585 were considered as interaction partner and arranged in the table according to the log2 fold changes, starting with the highest value. Proteins involved in viral genome replication regulation are labeled in red (determined using GOrilla). Always one protein of a protein group is mentioned in the list.

No	Gene	log2 fold change	-log10 p-value	No	Gene	log2 fold change	-log10 p-value
1	PURA	8.6992	3.5170	45	TOMM40	1.0502	1.9534
2	EBNA1BP2	3.2086	3.7015	46	DDX6	1.0465	3.7389
3	YBX1	2.4169	2.5700	47	VDAC2	1.0421	2.1319
4	PABPC1	1.9877	3.3395	48	HSD17B4	1.0398	2.1311
5	LSM14A	1.8750	3.7466	49	CIRH1A	1.0280	2.1931
6	DDX17	1.6964	3.4189	50	SERPINH1	1.0215	3.8347
7	PABPC4	1.6072	2.5776	51	RPN1	1.0149	2.7177
8	IGF2BP1	1.6019	3.0758	52	DHX30	1.0112	2.6525
9	PCBP2	1.5982	2.5423	53	KIF1A	1.0107	2.3818
10	CSDE1	1.5748	3.2648	54	STRAP	1.0066	3.8842
11	NDUFA10	1.5616	2.7322	55	DHX57	0.9526	2.8653
12	ZC3HAV1	1.4807	3.5823	56	DDX54	0.9426	2.6287
13	YIPF1	1.4157	2.4318	57	FAF2	0.9346	2.3932
14	MRPS18B	1.4023	3.4778	58	FXR1	0.9148	3.6015
15	TRAP1	1.3770	2.4765	59	PTPRK	0.9007	2.6032
16	SACM1L	1.3405	3.1865	60	NOC4L	0.8930	1.9559
17	FUBP3	1.3239	1.9497	61	MRTO4	0.8831	1.9756
18	SLC25A3	1.3079	2.7238	62	NUP85	0.8282	4.1123
19	MTHFD1L	1.2737	2.4145	63	LARP1	0.8234	3.2577
20	YTHDC2	1.2720	2.6497	64	UBAP2L	0.8228	2.4411
21	FXR2	1.2631	2.6908	65	DDX52	0.8174	2.2821
22	PAIP2	1.2483	2.4163	66	EIF4G1	0.8131	2.1946
23	HNRNPR	1.2415	3.8242	67	PATL1	0.8000	2.4657
24	TIMM50	1.2409	2.0455	68	NUP205	0.7837	3.2316
25	TM9SF3	1.2390	2.3339	69	STT3B	0.7823	3.1737
26	NUFIP2	1.2369	2.0671	70	ZC3H15	0.7572	2.7284
27	STAU1	1.2348	2.2456	71	MAD2L1	0.7305	3.5226
28	PHB	1.2294	2.1218	72	EIF4B	0.7266	2.6607
29	GNAI1	1.2105	2.1141	73	PRRC2A	0.7256	2.0471
30	STT3A	1.1695	2.3154	74	AQR	0.7102	2.2301
31	PCBP1	1.1653	2.6686	75	MPP6	0.7082	2.0168
32	SLC25A1	1.1467	2.8454	76	YWHAZ	0.6994	2.7816
33	LMF2	1.1326	3.4129	77	PKLR	0.6986	2.6461
34	RAB1A	1.1311	2.6430	78	ZNF326	0.6836	1.9599
35	SLC25A31	1.1290	2.6149	79	TVP23B	0.6762	2.3538
36	ACTA1	1.1280	2.2963	80	RHOA	0.6655	2.1924
37	POFUT1	1.1246	2.0213	81	NXF1	0.6341	3.5419
38	GNAI3	1.1033	2.0376	82	CNBP	0.6332	2.2705
39	TUFM	1.1020	2.4613	83	RNPS1	0.6277	2.0435
40	SLC25A11	1.1011	1.9911	84	HK1	0.6104	2.2408
41	ATXN2L	1.0839	3.6677	85	RPL12	0.6081	4.1514
42	PPIB	1.0669	2.9175	86	DDX39A	0.6079	2.7843
43	SSR4	1.0562	2.6999	87	CLTC	0.5924	3.1210
44	ACTA1	1.0537	2.1014				

Pur-alpha affinity capture-MS analysis using fNS cells and Oli-neu cells

Table A.2.: Significantly enriched protein groups in fetal neural stem (fNS) cells, identified using an affinity capture-mass spectrometry approach. The evidence files (MaxQuant) of three replicates were processed using Perseus. Potential contaminants, positive reverse sequences and proteins, which featured valid values in less than two replicates were removed. Target IP (Pur-alpha antiserum) to control IP (preimmune serum) ratios were calculated, log2 transformed and normalized to the median per replicate. The one-sample t-test against 0 in combination with the Benjamini Hochberg correction was applied. Proteins featuring a false discovery rate adjusted p-value ≤ 0.05 and a log2 fold change ≥ 0.585 were considered as interaction partner and arranged according to the log2 fold changes, starting with the highest value. Proteins involved in viral genome replication regulation are labeled in red (determined by GOrilla). Always one protein of a protein group is mentioned in the list. The protein rang no 43, UPF0568 protein C14orf166 homolog was not assigned to a gene yet. FC = fold change; IP = immunoprecipitation.

No	Gene	log2 fold change	-log10 p-value
1	Pura	4.5644	3.3275
2	Ybx1	3.8184	2.5719
3	Ikbkg	3.4192	2.4118
4	Chuk	3.4002	2.4189
5	Ikbkb	3.1568	1.8311
6	Ncl	3.0083	1.8287
7	Hnrnpab	2.9791	1.7459
8	Hnrnpdl	2.8973	2.5253
9	Upf1	2.8892	1.9760
10	Elavl1	2.5820	1.9843
11	Ilf2	2.5506	2.2601
12	Ssb	2.3810	2.5369
13	Larp1	2.3790	2.3066
14	Prkar2a	2.2838	2.8890
15	Ddb1	2.2492	4.0952
16	Ncbp1	2.2317	2.1936
17	Hnrnpa0	2.2107	1.9957
18	Syncrip	2.1246	2.2947
19	Purb	2.0958	2.3794
20	Larp4	1.9912	3.0212
21	Rbmx	1.8563	2.8392
22	Sec13	1.8328	2.4719
23	Igf2bp3	1.7522	2.2202
24	Fmr1	1.7200	3.0476
25	Myef2	1.6405	3.8744
26	Tardbp	1.6098	1.7426
27	Rps4x	1.5572	1.9912
28	Rps3a	1.4983	2.4753
29	Hnrnpu	1.4924	2.1740
30	Elavl2	1.4706	2.3336
31	Rpn2	1.4595	2.3586
32	Cltc	1.4462	1.9217
33	Stau1	1.4334	2.3665
34	Fip1l1	1.3575	3.2511
35	Jup	1.3300	2.2964
36	Pabpc1	1.3069	2.9380
37	Hnrnpf	1.2411	1.8909
38	Ddx17	1.1922	1.8252
39	Ddx3x	1.1870	3.2624
40	Hnrnpc	1.1083	1.9466
41	Map1b	1.0920	1.8643
42	Ilf3	1.0861	2.7728
43	N/A	0.9929	2.0989
44	Rpl23a	0.9918	1.9632
45	Rps11	0.9838	2.4801
46	Hspa8	0.9313	1.9115
47	Rpl11	0.9126	2.2095
48	Lars	0.8898	1.8434
49	Rps20	0.8498	2.3810
50	Ddx5	0.8346	2.5722
51	Rpl17	0.7948	1.8905
52	Mcm3	0.6896	1.7424
53	Hnrnpm	0.6539	2.6157

Table A.3.: Significantly enriched protein groups in Oli-neu cells, identified using an affinity capture-mass spectrometry approach. The evidence files (MaxQuant) of three replicates were processed using Perseus. Potential contaminants, positive reverse sequences and proteins, which featured valid values in less than two replicates, were removed. Target IP (Pur-alpha antiserum) / control IP (preimmune serum) ratios were calculated, log2 transformed and normalized to the median of every replicate. The one-sample t-test against 0 in combination with the Benjamini Hochberg correction was applied. Proteins featuring a false discovery rate adjusted p-value ≤ 0.05 and a log2 fold change ≥ 0.585 were considered as interaction partner and arranged in the table according to the log2 fold changes, starting with the highest value. Proteins involved in viral genome replication regulation are labeled in red (determined using GOrilla). Always one protein of a protein group is mentioned in the list. The protein rang no 2, uncharacterized protein C2orf71 homolog, can not be assigned to a gene yet.

No	Gene	log2 fold change	-log10 p-value	No	Gene	log2 fold change	-log10 p-value
1	Pura	4.4607	4.1553	16	Twf1	2.0102	1.7467
2	C2orf71	3.5721	2.4447	17	Ilf2	2.0022	3.6080
3	Hnrnpab	3.0401	2.9186	18	Acta1	1.9790	1.9710
4	Ncl	2.9395	1.8117	19	Elavl1	1.9710	2.8894
5	Hnrnpa1	2.8629	2.4418	20	Capzb	1.9563	1.9241
6	Fmr1	2.7624	2.2847	21	Syncrip	1.9293	2.0121
7	Ilf3	2.5376	3.0186	22	Capza1	1.9215	1.9829
8	Hnrnpa0	2.4815	3.0567	23	Myef2	1.9096	2.0613
9	Ces1f	2.3618	2.6191	24	Chuk	1.8855	2.1196
10	Upf1	2.3330	2.4355	25	Pabpc1	1.8571	3.0306
11	Fxr1	2.3194	3.4838	26	Hnrnpu	1.8439	1.7470
12	Mov10	2.2995	2.8239	27	Hnrnpa2b1	1.8300	2.4039
13	Ncbp1	2.2265	2.3895	28	Coro1c	1.8133	1.7773
14	Hnrnpd	2.2085	2.0209	29	Lgals8	1.8110	1.8685
15	Purb	2.0420	2.1845	30	Rps9	1.7878	2.1098

GO term enrichment analysis of HEK293 cell interaction partner analysis

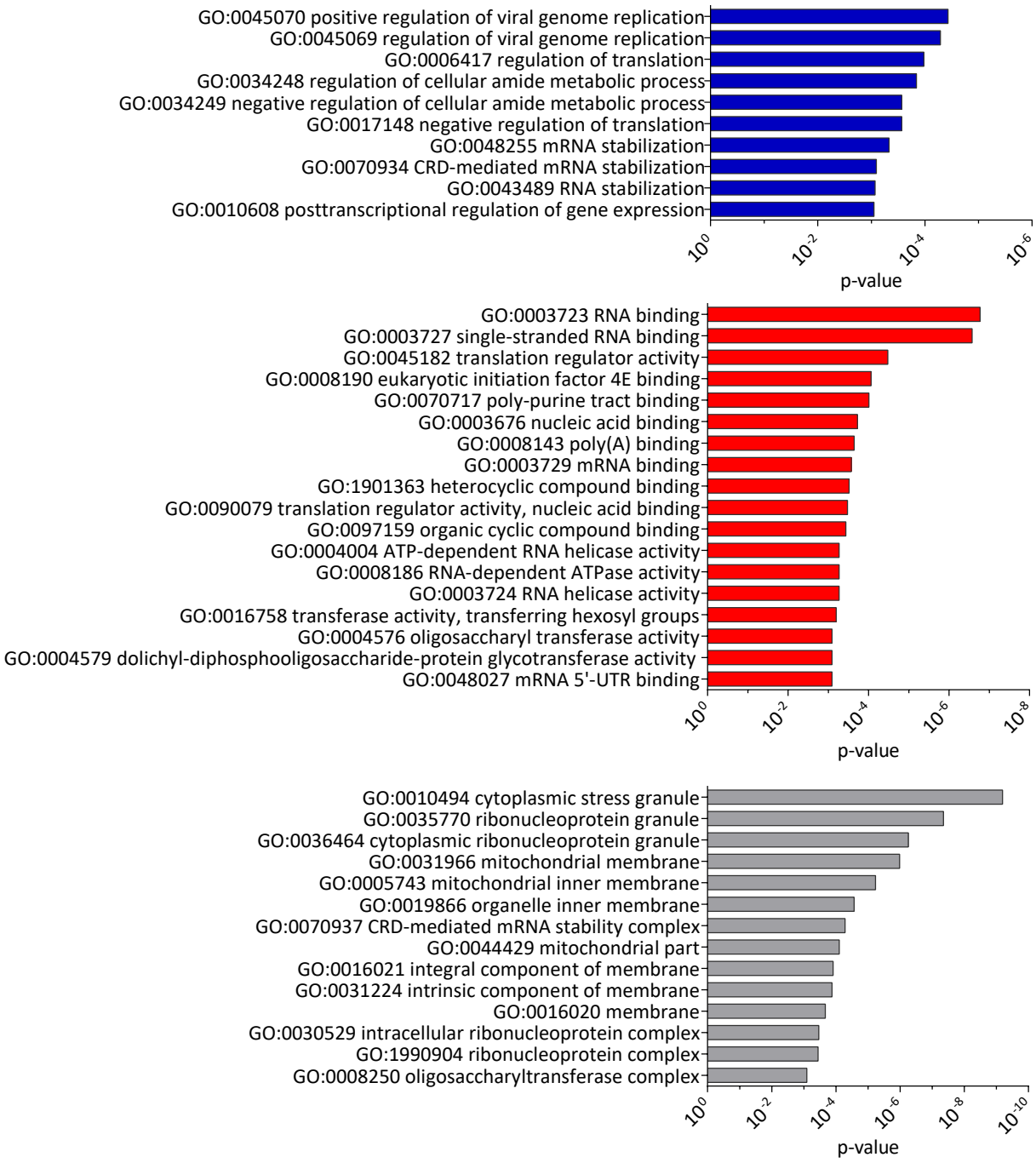

Fig. A.8.: GO term enrichment analysis of BirA*-Pura assay, including the ontologies (a) biological process, (b) molecular function and (c) cellular component. All 87 significantly enriched proteins, identified using the BirA*-Pura assay, were analyzed for enriched GO terms using GOrilla. The search was implemented with a reference set of proteins, containing all 2,080 detected proteins (identified using MaxQuant), whereof 1,952 proteins could finally be associated with a GO term. As identifier, the leading razor protein was used. The bar charts represent the uncorrected enrichment p-value of GO terms, calculated by hypergeometric testing and GO terms are ranked in ascending order, according to their p-values. The threshold was set to a p-value of 0.001. GO = gene ontology

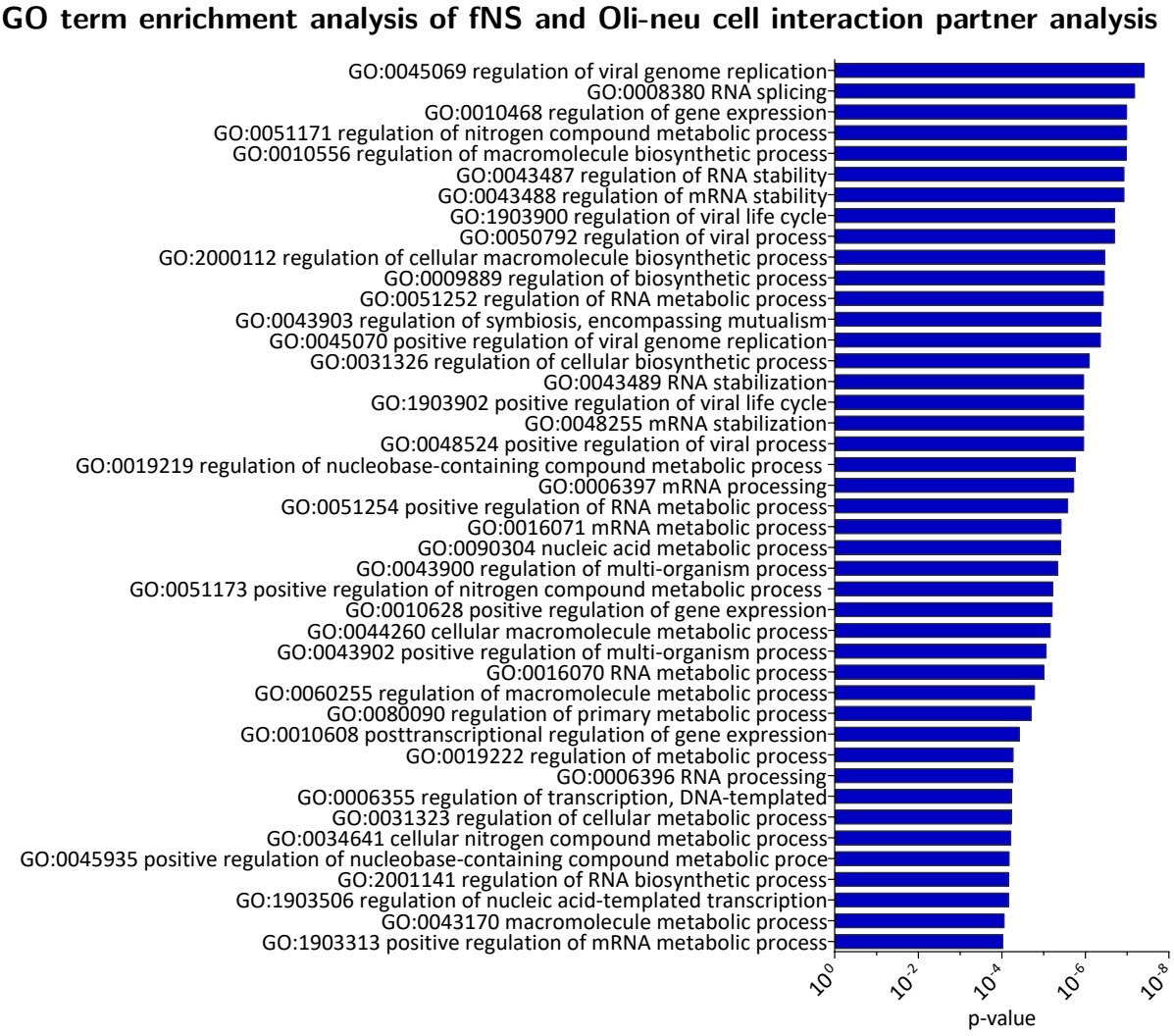

(a) Enriched GO terms - Biological process

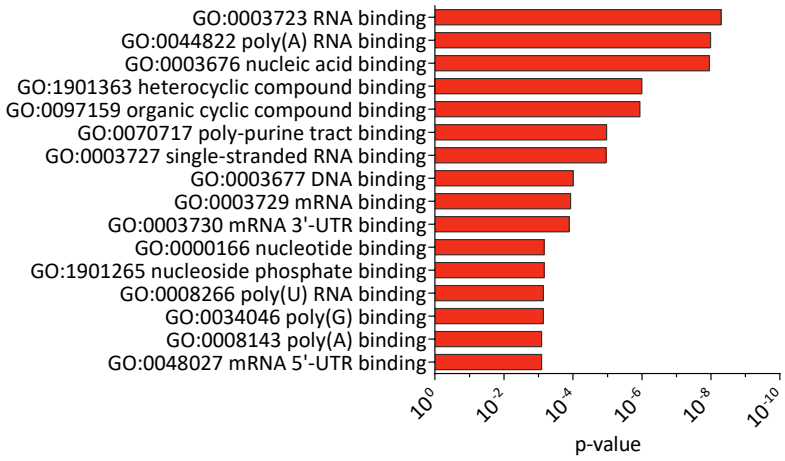

(b) Enriched GO terms - Molecular functions

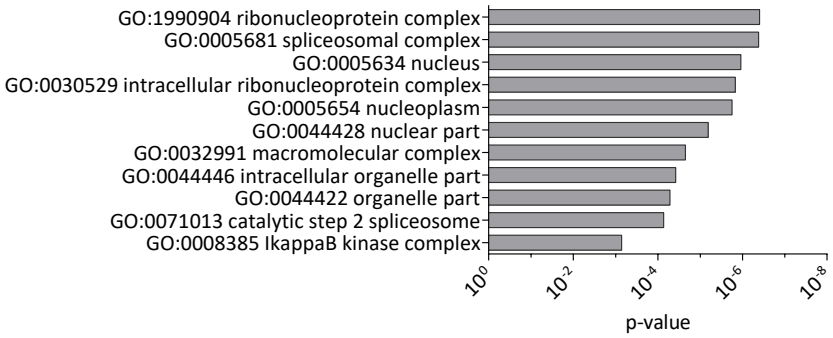

(c) Enriched GO terms - Cellular components

Fig. A.9.: GO enrichment analysis of proteins identified by fetal neural stem (FNS) cell co-immunoprecipitation assay. The GO enrichment analysis was performed with 53 significantly enriched proteins against all 583 (651 implemented) identified proteins (MaxQuant), which served as background proteins. As identifier the leading razor protein was used and the p-value threshold was set to 0.001, removing all GO terms exhibiting a greater p-value. GOrilla finally calculated the enrichment p-value of each GO term by hypergeometric testing and the results were blotted in a bar chart with p-values in ascending order. The histogram (a) depicts the top 43 enriched biological processes. It should be noted that the significance threshold of the ontology biological processes was changed to a p-value of 0.0001 in order to reduce the protein list to the most enriched ones. The complete list can be found in the electronic supplement (Supplementary Data S22) (b) depicts all enriched molecular function; (c) depicts all enriched cellular components.

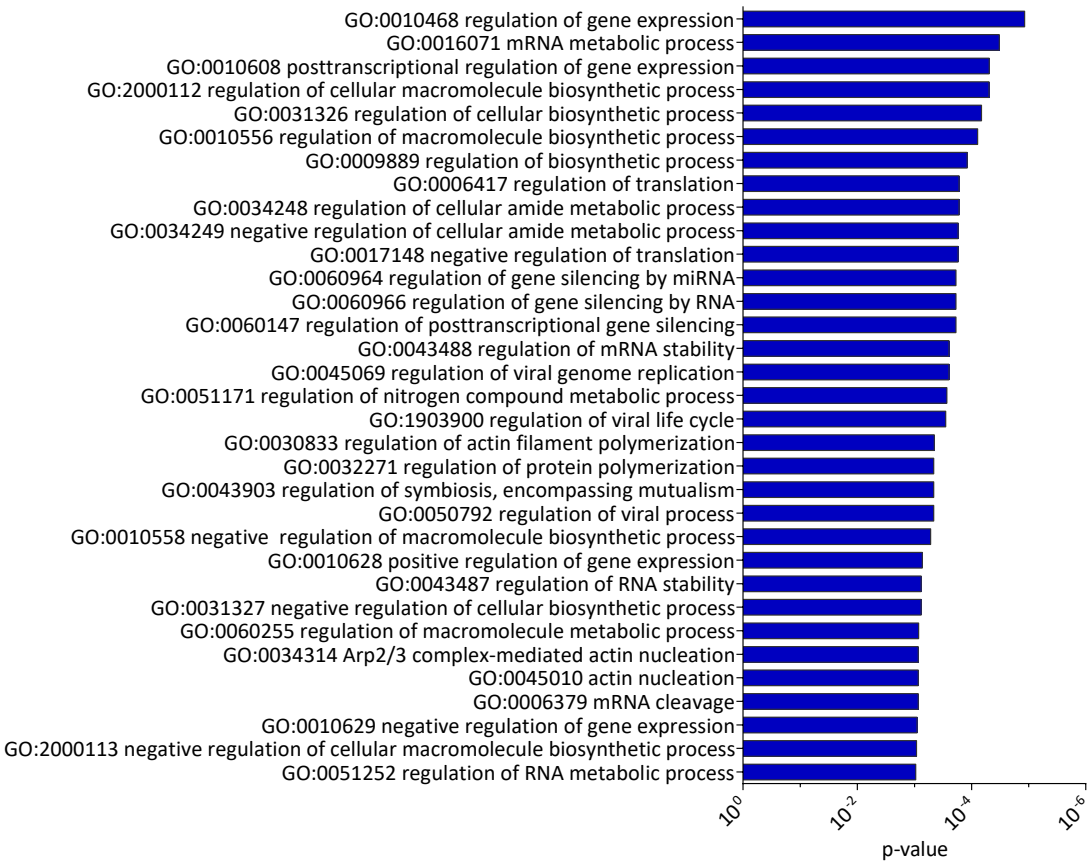

(a) Enriched GO terms - Biological process

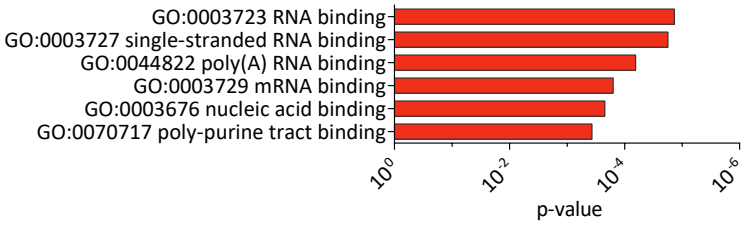

(b) Enriched GO terms - Molecular functions

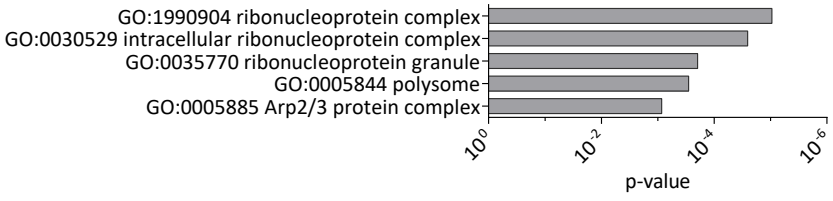

(c) Enriched GO terms - Cellular components

Fig. A.10.: GO enrichment analysis of enriched proteins identified by Oli-neu co-IP assay. The GO enrichment analysis was performed with 76 significantly enriched proteins against all 630 (726 implemented) identified proteins (MaxQuant), which served as background proteins. As identifier the leading razor protein was used and the p-value threshold was set to 0.001, removing all GO terms exhibiting a greater p-value. GOrilla calculated the enrichment p-value of each GO term by hypergeometric testing and the results were blotted in a bar chart with p-values in ascending order. GO = gene ontology; co-IP = co-immunoprecipitation.

Potential Pur-alpha interaction partner

Experiment	Gene name	Protein name
Hek Bio-ID	SETD7	Histone-lysine N-methyltransferase SETD7
	CCDC54	Coiled-coil domain-containing protein 54
	COPZ1	Coatomer subunit zeta-1
	YIPF4	Protein YIPF4
	LMAN2	Vesicular integral-membrane protein VIP36
	PDHB	Pyruvate dehydrogenase E1 component subunit beta
	EXOSC7	Exosome complex component RRP42
	LONP1	Lon protease homolog, mitochondrial
	BRAP	BRCA1-associated protein
	PLXNB2	Plexin-B2
	ZRANB2	Zinc finger Ran-binding domain-containing protein 2
FNS Co-IP	Fxr2	Fragile X mental retardation syndrome-related protein 2
	Mov10	Putative helicase MOV-10
	Ddx6	Probable ATP-dependent RNA helicase DDX6
	Ythdf1	YTH domain-containing family protein 1
	Cul5	Cullin-5
Oli-neu Co-IP	Ikbkg	NF-kappa-B essential modulator
	Actr2	Actin-related protein 2
	Dbn1	Drebrin
	Srsf1	Serine/arginine-rich splicing factor 1
	Matr3	Matrin-3

Fig. A.11.: List of proteins without valid data in control samples Using the Perseus software every interaction partner analysis was searched for proteins which exhibited valid values in at least two of three target-IP samples but no valid values or only one valid value in the control-IP samples. If a protein in the control-IP sample was detected with an intensity value, only proteins with a log2 target to control ratio of ≥ 0.585 were considered. The remaining proteins were finally listed according to their experimental detection. Additionally, all proteins that have already been identified as significantly enriched proteins in other interaction partner analyses (BioID or co-IP) were labeled with red color.

B. List of Figures

C. List of Tables

D. Uniform Resource Locator (URL)

- URL1: `http://www.thermofisher.com/de/de/home/life-science/protein-biology/protein-biology-learning-center/protein-biology-resource-library/pierce-protein-methods/quantitative-proteomics.html` (01/2017)
- URL2: `http://bioinformatics.psb.ugent.be/webtools/Venn/`

E. Abbreviations

ab	antibody
ACN	acetonitrile
ADP	adenosine diphosphate
APC/C	anaphase-promoting complex/cyclosome
ASA	arylsulphatase A
ATP	adenosine triphosphate
B104 CM	B104 conditioned medium
bFGF	basic fibroblast growth factor
BioID	proximity-dependent biotinylation and identification of proteins
BirA*	constitutively active E.coli biotin ligase
BMP	bone morphogenetic protein
bp	base pair
BSA	bovine serum albumin
cDNA	complementary DNA
CNS	central nervous system
CNTF	ciliary neurotrophic factor
DAPI	4',6-diamidin-2-phenylindol
ddH2O	double destilled water
DMEM	Dulbecco's Modified Eagle's Medium
DMSO	dimethyl sulfoxide
DNA	deoxyribonucleic acid
DTT	dithiothreitol
E	embryonic
ECL	enhanced chemiluminescence
ECM	extracellular matrix
EDTA	ethylenediaminetetraacetic acid
EGF	epidermal growth factor
ER	endoplasmatic reticulum
EYFP	enhanced yellow fluorescent protein
ESC	embryonic stem cell
FA	formic acid
FACS	fluorescence-activated cell sorting
FASP	filter aided sample prep
FC	fold change
FCS	fetal calf serum
FDR	false discovery rate
FNS	fetal neural stem cell
GAPDH	glyceraldehyde-3-phosphate dehydrogenase

GO	gene ontology
gp	guinea pig
GST	glutathione S-transferase
HDAC	histone deacetylases
HEK293T	human embryonic kidney cells
HeLa	Henrietta Lacks cells (immortal cell line)
HEPES	4-(2-hydroxyethyl)-1-piperazineethanesulfonic acid
HPLC	high pressure liquid chromatography
HRP	horseradish peroxidase
i.a.	inter alia
ICC	immunocytochemistry
IGF	insuline like growth factor
IP	immunoprecipitation
IPC	intermediate progenitor cell
iTRAQ	isobaric tags for relative and absolute quantitation
kDa	kilodalton
MAPK	mitogen-activated protein kinase
MG132	carbobenzoxy-Leu-Leu-leucinal
MLD	metachromatic leukodystrophy
mRNA	messenger RNA
MS	mass spectrometry
MS	multiple sclerosis
MWCO	molecular weight cut-off
NaCl	sodium chloride
NG2	chondroitin sulfate proteoglycan NG2
NGF	nerve growth factor
NGM	neurospheres growth medium
NGS	normal goat serum
NH4HCO3	ammonium bicarbonate
NIH3T3	mouse embryonic fibroblast cells
NRG1	neuregulin 1
NSC	neural stem cell
NPC	neural progenitor cell
NSPCs	neural stem and progenitor cells
ON	overnight
OPC	oligodendrocyte precursor cell
P	perinatal
PAGE	polyacrylamide gel electrophoresis
PBS	phosphate buffered saline
PCR	polymerase chain reaction
PDGF	platelet derived growth factor
PFA	paraformaldehyde
PI	propidium iodide
Pi3K	phosphoinositide 3-kinase
ppm	parts per million

qPCR	real-time quantitative PCR
rb	rabbit
RNA	ribonucleic acid
rpm	revolutions per minute
RT	room temperature
RT-PCR	reverse transcriptase PCR
SAX	strong anion exchange
SDS	sodium dodecyl sulfate
SHH	sonic hedgehog
SILAC	stable isotope labeling by amino acids in cell culture
SPE	solid phase extraction
StageTips	stop-and-go-extraction tips
VZ	ventricular zone
T3	triiodothyronine
TBS	Tris-buffered saline
TEAB	triethylammonium bicarbonate
TF	transcription factor
TFA	trifluoroacetic acid
TMT	tandem mass tag
Tris-HCl	Tris(hydroxymethyl)-aminomethan hydrochloride
UA	Urea and Hepes buffer
WB	western blot
WT	wild type
SVZ	subventricular zone

F. Supplements

F.1. Plasmid maps

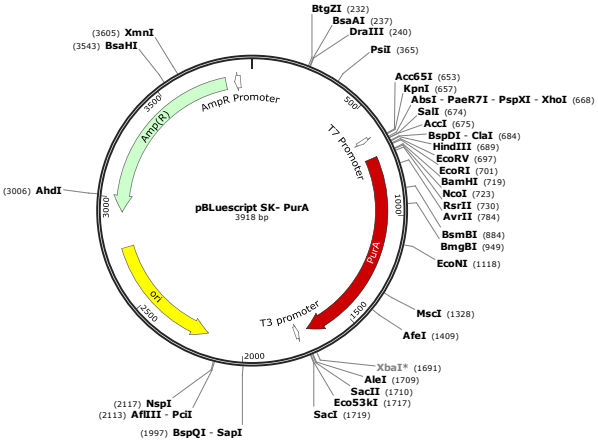

(a) pBluescript SK-(-)-Pura

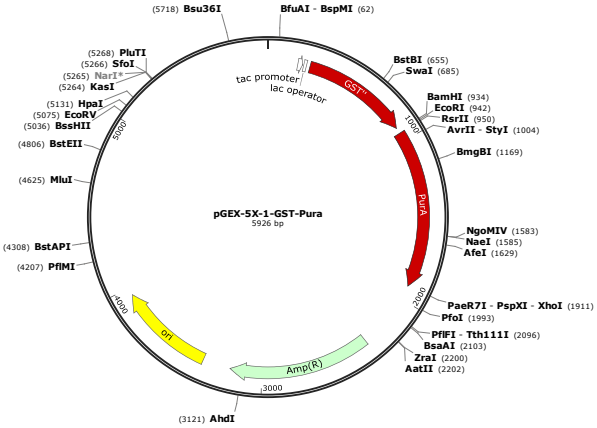

(b) pGEX-5X-1-GST-Pura

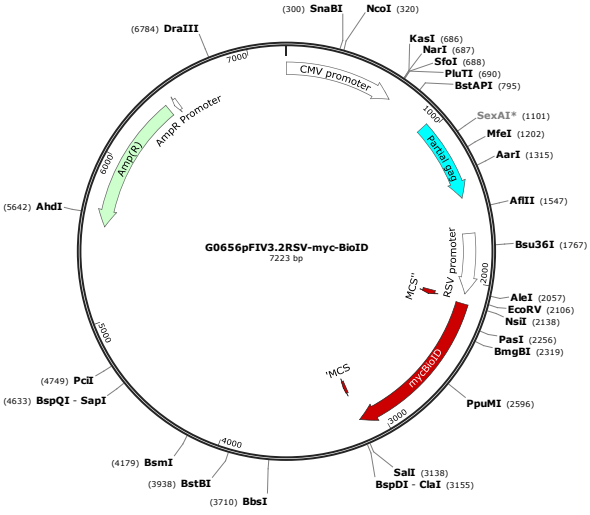

(c) G0656pFIV3.2RSV-myc-BioID

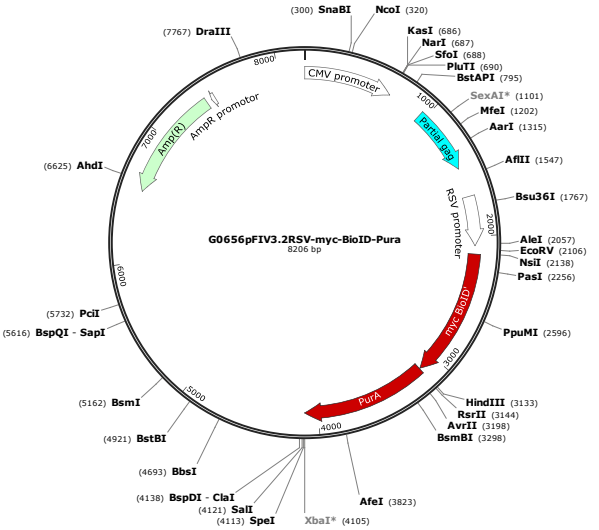

(d) G0656pFIV3.2RSV-myc-BioID-Pura

F.2. Data files (DVD)

In the printed version of this thesis an envelope containing a DVD with data media can be found on the last page of the book. It contains the following supplemental data files:

Differentiation of multipotent progenitor cells (NPCs) to oligodendrocyte precursor cells (OPCs)

- Supplementary Data S1: Hierarchical clustering analysis (Cluster 4) including normalized intensities (txt)
- Supplementary Data S2a: Hierarchical clustering analysis (Cluster 4) - Gene ontology enrichment analysis - Biological processes (txt)
- Supplementary Data S2b: Hierarchical clustering analysis (Cluster 4) - Gene ontology enrichment analysis - Cellular components (txt)
- Supplementary Data S3: Significantly upregulated proteins from day 6 until day 15 of neurosphere differentiation (txt)
- Supplementary Data S4: Significantly upregulated proteins from day 9 until day 15 of neurosphere differentiation (txt)
- Supplementary Data S5: Significantly upregulated proteins from day 12 until day 15 of neurosphere differentiation (txt)
- Supplementary Data S6a: Significantly upregulated proteins from day 9 until day 15 and day 12 until day 15 of neurosphere differentiation - Gene ontology enrichment analysis - Biological processes (txt)
- Supplementary Data S6b: Significantly upregulated proteins from day 9 until day 15 and day 12 until day 15 of neurosphere differentiation - Gene ontology enrichment analysis - Cellular components (txt)
- Supplementary Data S7: Transcription regulating factors identified during neurosphere differentiation (txt)
- Supplementary Data S8: Receptors and receptor interacting proteins identified during neurosphere differentiation (txt)
- Supplementary Data S9: Kinases identified during neurosphere differentiation (txt)
- Supplementary Data S10: Significantly downregulated proteins from day 6 until day 15 of neurosphere differentiation (txt)
- Supplementary Data S11a: Significantly downregulated proteins from day 6 until day 15, from day 9 until day 15 and from day 12 until day 15 of neurosphere differentiation - Gene ontology enrichment analysis - Biological processes (txt)
- Supplementary Data S11b: Significantly upregulated proteins from day 6 until day 15, from day 9 until day 15 and from day 12 until day 15 of neurosphere differentiation - Gene ontology enrichment analysis - Cellular components (txt)

- Unprocessed MaxQuant result text files: Neurospheres evidence and Neurospheres ProteinGroups (txt)
- Processed Neurospheres differentiation data set (log2 fold changes of significantly regulated proteins) (txt)
- Supplementary Images S1: Immunocytochemistry images of neurosphere differentiation (jpg)

Differentiation of rat oligodendrocyte precursor cells (OPCs) to oligodendrocytes

- Supplementary Data S12: Gene ontology enrichment analysis of proteins significantly upregulated at day 3 of oligodendrocyte precursor cell differentiation (txt)
- Supplementary Data S13: Gene ontology enrichment analysis of proteins significantly upregulated at day 6 of oligodendrocyte precursor cell differentiation (txt)
- Supplementary Data S14: Gene ontology enrichment analysis of proteins significantly upregulated at day 9 of oligodendrocyte precursor cell differentiation (txt)
- Supplementary Data S15: Transcription regulating factors and histone modifiers identified during oligodendrocyte precursor cell differentiation (txt)
- Supplementary Data S16: Receptors and receptor interacting proteins identified during oligodendrocyte precursor cell differentiation (txt)
- Supplementary Data S17: Kinases identified during oligodendrocyte precursor cell differentiation (txt)
- Supplementary Data S18: Significantly downregulated proteins in all time points of oligodendrocyte precursor cell differentiation (txt)
- Supplementary Data S19: Gene ontology enrichment analysis of proteins significantly downregulated at day 3 of oligodendrocyte precursor cell differentiation (txt)
- Supplementary Data S20: Gene ontology enrichment analysis of proteins significantly downregulated at day 6 of oligodendrocyte precursor cell differentiation (txt)
- Supplementary Data S21: Gene ontology enrichment analysis of proteins significantly downregulated at day 9 of oligodendrocyte precursor cell differentiation (txt)

- Unprocessed Proteom Discoverer result text files: OPC PSM and OPC ProteinGroup (txt)
- Processed OPC differentiation data set (log2 fold changes of significantly regulated proteins) (txt)

Investigation of transcriptional activator protein Pur-alpha - Interaction partner analyses

- Supplementary Data S22: Gene ontology enrichment analysis of fNS cell interaction partner analysis (txt)

- Unprocessed Maxquant result text files (evidence and ProteinGroups) for HEK293T BioID approach, fNS CoIP approach and Olineu CoIP approach (txt)
- Processed protein groups lists for HEK293T BioID approach, fNS CoIP approach and Olineu CoIP approach (txt)

F.3. Acknowledgements

First of all, I would particularly like to thank Prof. Dr. V. Gieselmann for the opportunity to conduct my doctoral thesis in the IBMB and for being my primary thesis supervisor. Furthermore, I especially thank him for his support and advice regarding my project.

In addition, I also feel grateful to Prof. Dr. G. M. König, from the Institute for Pharmaceutical Biology, for being my secondary thesis supervisor.

Particularly, I want to thank my direct supervisor Dr. Dominic Winter for his steady support and his suggestions during the last years as his Ph.D. student and of course for giving me the opportunity to work on my thesis subjects in his working group. In cases of questions and problems I could always ask for his advice.

Furthermore, I would like to give special thanks to the Faculty of Medicine of the University of Bonn for the generous funding of my research provided through BONFOR Forschungsförderprogramm.

I especially thank Dr. Marc Sylvester for his time to answer all my questions in-depth and Dr. Nahal Brocke-Ahmadinejad for her support in evaluation of computerized data. In this regard, I also want to thank Ralph and Albert for introducing me to the LaTeX system and for providing solutions for every problem that occurred.

I certainly want to thank all my colleagues of the AG Winter group, Alireza Dehghani, Shiva Ahmadi, Srigayatri Ponnaiyan, Fatema Akter and especially our technical assistant Norbert Rösel for his unrestricted support and for always having time. My gratitude also goes to Claudia Yaghootfam, Heidi Simonis and Karola Ragout for their technical and administrative support. In this regard I feel grateful to all my other colleagues of the AG Eckhardt, AG Thelen and AG Matzner for the funny time spend together during lunch, coffee breaks and after work.

Finally, my gratitude goes to Ralph, my friends and my family, who supported me throughout my entire life, through ups and downs.